Influence of hydrothermal activity and substrata nature on faunal colonization processes in the deep sea

Joan Manel Alfaro Lucas

THESE DE DOCTORAT DE

L'UNIVERSITE
DE BRETAGNE OCCIDENTALE
COMUE UNIVERSITE BRETAGNE LOIRE

ECOLE DOCTORALE N° 598
Sciences de la Mer et du littoral
Spécialité : Ecologie Marine

Par

Joan M. ALFARO-LUCAS

Influence of hydrothermal activity and substrata nature on faunal colonization processes in the deep sea.

Thèse présentée et soutenue à Brest le 10 décembre 2019
Unité de recherche : Unité Etude des Ecosystèmes Profonds (EEP) au laboratoire LEP (Ifremer)

Rapporteurs avant soutenance :

Dr François LALLIER
Professeur, Sorbonne Université

Dr Jeroen INGELS
Research Faculty, Florida State University

Composition du Jury :

Dr Sabine GOLLNER
Tenure Scientist, Royal Netherlands Institute for Sea Research

Dr Eric THIEBAUT
Professeur, Sorbonne Université

Dr Gérard THOUZEAU (Président du Jury)
Research Director, CNRS

Dr François LALLIER
Professeur, Sorbonne Université

Dr Jeroen INGELS
Research Faculty, Florida State University

Dr Jozée SARRAZIN (Directrice de thèse)
Cadre de Recherche, Ifremer Brest

Invités :
Dr Daniela ZEPPILLI   Cadre de Recherche, Ifremer Brest

Dr Florence PRADILLON   Cadre de Recherche, Ifremer Brest

Dr Olivier GAUTHIER   Maître de Conférence, Université Bretagne Occidentale

"It is this contingency that makes it difficult, indeed virtually impossible, to find patterns that are universally true in ecology. This, plus an almost suicidal tendency for many ecologists to celebrate complexity and detail at the expense of bold, first-order phenomena. Of course the details matter. But we should concentrate on trying to see where the woods are, and why, before worrying about the individual tree."

John H. Lawton (1999)

Als meus pares Anna i Manel, per tot el que ens heu donat,
a la meva germana Anna
i a la meva companya de vida Romina,
per tot el que hem fet i els reptes que encara ens queden.

Index

General discussion, conclusions and perspectives

General References

*In French

List of figures

lake. Colonized substratum blocks at B. active, C. intermediate, D. periphery and E. far sites. Also visible in the photos are the other types of substratum used in parallel experiments.

List of tables

Résumé étendu

Résumé étendu

La chimiosynthèse microbienne forme la base du réseau trophique des assemblages faunistiques des sources hydrothermales. Ces assemblages se caractérisent par de fortes abondances et biomasses contrastant fortement avec la majorité des habitats des écosystèmes marins profonds (200-300 m de profondeur). Les sources hydrothermales se distinguent aussi par la grande variabilité physico-chimique de l'environnement, directement liée aux processus géologiques. Au cœur de cette variabilité spatio-temporelle, de grands invertébrés symbiotiques prospèrent. Ils habitent des niches distinctes, formant une zonation d'assemblages correspondant à des gradients physico-chimiques. Ces organismes se distribuent en fonction de leur tolérance à la toxicité des fluides, aux fortes variations de températures et de leurs besoins nutritionnels. D'autres facteurs, moins connus, comme les apports larvaires, les interactions biologiques et les facteurs stochastiques affectent également la diversité et la structure des communautés.

Les sources hydrothermales en milieu océanique profond ont été historiquement considérées comme des écosystèmes insulaires, spatialement discrets et restreints. Cette vision ne prenait pas en compte les zones d'interactions et de transition entre ces écosystèmes chimiosynthétiques et ceux situés en périphérie. En fait, les études sur les zones périphériques sont rares et se concentrent généralement sur la mégafaune benthique. Depuis récemment, un nombre croissant de publications suggèrent que les sources ne sont pas isolées et auraient une « sphère d'influence » dans l'espace et le temps. Aussi, peu après la découverte des sources hydrothermales, d'autres communautés

basées sur la chimiosynthèse ont été répertoriées dans le milieu océanique profond telles que les communautés associées aux sources froides (seeps) ou celles associées aux grands débris organiques comme les carcasses de baleines et les bois coulés. L'hypothèse que certaines espèces des sources hydrothermales auraient pu coloniser les communautés associées aux débris organiques, attirés par les conditions environnementales particulières qui s'y développent, a grandement motivé les études de ces milieux. Ainsi, la présence de ces îlots organiques pourrait permettre leur dispersion vers de nouveaux habitats éloignés : c'est l'hypothèse de la « pierre de gué » ou « stepping-stone hypothesis ». Bien qu'elle ne soit pas universelle, cette hypothèse a été validée pour certaines espèces, en particulier chez les polychètes. Cependant, peu d'études ont comparé la composition des communautés et la redondance entre les espèces colonisant les habitats des sources hydrothermales (sources actives et périphérie) avec celles des bois coulés.

Or, dans un contexte où les communautés des grands fonds sont de plus en plus confrontées aux impacts anthropiques, il devient essentiel de mieux comprendre les facteurs qui contrôlent la structure de ces communautés. De nouvelles approches écologiques innovantes, permettant la caractérisation des communautés, sont apparues au cours des dernières décennies, dont celle basée sur les traits fonctionnels. Dans le milieu océanique profond, ces approches ont rarement été mises en œuvre mais elles présentent un certain intérêt pour des écosystèmes caractérisés par de forts gradients environnementaux comme ceux associés aux sources hydrothermales. Ces approches

peuvent être mises en œuvre pour mieux comprendre les facteurs qui influencent la structure des communautés. En raison de la zonation des espèces ingénieures le long du gradient de stress, on a supposé que les communautés associées aux sources hydrothermales étaient analogues à celles des écosystèmes intertidaux. Cependant, d'autres facteurs rendent les sources hydrothermales des écosystèmes uniques. Conceptuellement, les habitats hydrothermaux peuvent être considérés comme un continuum se distribuant entre les fumeurs noirs à haute température jusqu'aux zones d'émission diffuses et aux zones périphériques inactives. En raison de la dépendance des producteurs primaires pour les composés réduits, les sources hydrothermales présentent un gradient de productivité primaire qui est positivement corrélé avec le stress environnemental. La corrélation positive entre le stress environnemental et la productivité est à son tour partiellement corrélée avec une importance croissante des interactions biologiques en raison de l'augmentation de l'abondance des espèces.

La composition des espèces d'une communauté est déterminée par un ensemble de facteurs biotiques et abiotiques. Les modèles conceptuels actuels perçoivent les communautés locales comme des sous-ensembles d'un pool régional d'espèces. Les pools d'espèces régionales sont « tamisés » par différents filtres interagissant à plusieurs échelles spatio-temporelles. Les processus qui se produisent à des échelles temporelles de millions d'années déterminent la distribution des lignées, les processus de diversification et d'extinction des espèces et déterminent finalement les « pools » régionaux d'espèces. La dispersion et l'environnement sélectionnent certains traits qui permettent aux taxons de

coloniser des habitats optimaux. À des échelles plus petites, les interactions biotiques inter- et intra-spécifiques affinent cette distribution et déterminent la composition spécifique locale. La biodiversité est donc un résultat direct ces processus de structuration des communautés. La façon dont les assemblages changent en termes d'identité des espèces et de leur abondance dans l'espace et le temps est l'une des questions fondamentales de l'écologie. Non seulement la biodiversité locale (α-diversité) mais surtout ses dissemblances spatio-temporelles (β-diversité) reflètent les processus qui génèrent et maintiennent la mosaïque d'assemblages trouvée dans la nature.

L'un des facteurs les plus étudiés pour expliquer la structuration des communautés est l'énergie et son extension : la productivité. Les perturbations et le stress environnemental sont également reconnus depuis longtemps comme des principaux moteurs de la structure des communautés et des patrons de biodiversité. Pendant des décennies, l'écologie des communautés s'est concentrée sur les espèces et leurs relations avec les facteurs environnementaux. Par conséquent, contrairement à d'autres disciplines, ce domaine a produit d'innombrables études de cas spécifiques, empêchant l'énoncé de généralités et de théories écologiques. Pourtant, la biodiversité est un concept complexe à multiples facettes qui englobe également, par exemple, les performances des espèces, c'est-à-dire leur fonctionnement aussi appelée « diversité fonctionnelle ». L'analyse de la diversité fonctionnelle est une alternative qui permet de proposer des hypothèses sur le plan écologique ainsi que de mieux comprendre les processus et les mécanismes qui sous-tendent la distribution des espèces.

L'objectif de cette thèse était de mieux comprendre les processus de colonisation qui structurent les communautés au niveau des sources hydrothermales actives du champ Lucky Strike, situé sur la dorsale médio-Atlantique. Cette étude s'est intéressée à un gradient s'échelonnant des zones hydrothermales actives, aux zones périphériques inactives faiblement sédimentées jusqu'aux zones de basaltes nus. Sur la base d'un modèle conceptuel des gradients qui caractérisent les habitats des sources hydrothermales des grands fonds, liés au stress environnemental et à la productivité, une approche moderne a été appliquée afin d'explorer les modèles de biodiversité au cours du processus de colonisation. Cette approche était basée sur trois facettes différentes, à savoir la richesse en espèces, les traits fonctionnels et les isotopes stables. Cette thèse est entièrement basée sur une expérience de colonisation de 2 ans. Quatre « sites » représentant différents niveaux d'activité hydrothermale et représentatifs de l'hétérogénéité des habitats du champ Lucky Strike ont été sélectionnés. Ces sites étaient situés sur et en périphérie plus ou moins proche de l'édifice de la Tour Eiffel (1700 m). Ils correspondent aux sites décrits au sein d'autres études pilotes fait par le Laboratoire Environnement Profond de l'Ifremer. Sur chaque site, trois substrats standardisés d'ardoise et de chêne (~ 10 cm^3) ont été déployés en 2013 lors de la campagne MoMARSAT et ont été récupérés deux ans plus tard lors de la campagne MoMARSAT 2015 à bord du R / V *Pourquoi pas* ? avec le ROV *Victor6000*. Afin d'atteindre les objectifs de la thèse, un grand effort a été investi dans la construction d'une base de données unique qui rassemble les trois aspects différents mais complémentaires de la biodiversité : la richesse en espèces, les traits fonctionnels de ces

espèces et leurs valeurs isotopiques. L'ensemble de données a ensuite été utilisé, partiellement ou complètement, pour répondre aux questions spécifiques.

Chapitre 1

L'objectif principal de ce chapitre était de mieux comprendre les interactions entre le stress environnemental et la disponibilité de l'énergie sur la structuration des communautés des sources hydrothermales. Pour ce faire, la colonisation de substrats d'ardoise par la faune a été analysée sur quatre sites échelonnés le long d'un gradient d'activité hydrothermale. Les espèces, la biodiversité fonctionnelle et la composition de la méio- et de la macrofaune colonisatrice ont été comparées. Afin de mieux comprendre la structuration des communautés, un modèle nul a été appliqué afin de déterminer l'effet de l'environnement sur la richesse fonctionnelle au niveau de chacun des sites étudiés. La diversité β de ces espèces et la diversité fonctionnelle ont été quantifiées et décomposées en « turnover » et « nestedness » et des indices de Contributions Locales à la Diversité β (LCBD en anglais) ont été calculés afin d'évaluer 1) l'influence de l'environnement sur les assemblages faunistiques, 2) la composante de la diversité β conduisant aux patrons observés et 3) les sites de l'étude contribuant plus que prévu à la dissimilarité globale. Des analyses d'isotopes stables ont été réalisées sur la faune de chaque site pour déterminer l'origine de la matière organique consommée et examiner le gradient énergétique de productivité primaire d'origine chimiosynthétique le long du gradient. Nous avons posé comme hypothèses (1) que l'activité hydrothermale devrait restreindre la diversité

fonctionnelle et (2) qu'une grande similarité en termes de composition et de traits fonctionnels devrait être observée entre les sites actifs et inactifs.

Les espèces trouvées sur les ardoises des deux sites les plus actifs étaient des habitants typiques des sources hydrothermales, tandis que celles trouvées sur les substrats des sites périphériques appartenaient principalement à des groupes de taxons représentatifs des substrats durs des fonds marins du champ Lucky Strike. Contrairement à ce que qui était attendu, nos résultats montrent que la richesse fonctionnelle augmente le long du gradient d'activité, en étant plus forte sur les sites actifs. Ainsi, les conditions environnementales des sites inactifs contribueraient à filtrer des caractéristiques spécifiques, réduisant ainsi la richesse fonctionnelle malgré une diversité d'espèces similaire. La présence d'espèces et de traits fonctionnels exclusifs a entraîné un fort « turnover » entre les deux sites inactifs, produisant les plus fortes β-diversités. En conséquence, certains sites inactifs ont contribué plus que prévu à la β-diversité totale des espèces et à la diversité des traits fonctionnels.

Globalement, le changement de composition et de fonctions a conduit à une plus grande dissimilarité au sein du compartiment de la méiofaune, suggérant un degré de spécialisation inférieur à celui de la macrofaune. Nous suggérons que la productivité élevée des sites actifs contribue au soutien d'une richesse fonctionnelle plus élevée. Cette hypothèse était appuyée par la distribution des traits fonctionnels entre les sites. Ainsi, les sites actifs soutiennent des caractéristiques plus coûteuses en énergie, telles que les

grandes tailles et une proportion plus élevée d'espèces prédatrices. Les communautés des sources hydrothermales ne sont donc pas seulement des « points chauds ou hot spots » de biomasse et d'abondance, mais aussi de richesse fonctionnelle. Les analyses isotopiques ont montré qu'une partie de cette productivité est exportée vers les assemblages des zones inactives périphériques. Les liens énergétiques et la redondance de la faune suggèrent que les environnements actifs et inactifs peuvent être considérés comme des entités interconnectées. Ces résultats assureront la reconnaissance et la protection des habitats périphériques historiquement négligés. En effet, ils représentent des composantes importantes de l'écosystème car ils abritent des assemblages taxonomiquement et fonctionnellement riches, diversifiés et uniques qui contribuent à augmenter la diversité β de ces milieux. Dans ce contexte, la faible richesse fonctionnelle des zones inactives suggère que la faune qui y vit pourrait être particulièrement vulnérable aux changements environnementaux liés aux impacts naturels et anthropiques, tels que l'exploitation minière.

Chapitre 2

L'objectif principal de ce chapitre était de comparer la diversité des espèces, la diversité fonctionnelle et la structure des communautés de méio- et macrofaune entre les sources hydrothermales et les bois coulés et d'identifier les principaux facteurs d'influence. Pour ce faire, les substrats d'ardoise et de bois ont été analysés en quatre groupes différents comprenant : 1) l'ardoise et 2) les bois placés au sein d'un édifice hydrothermal actif et 3) l'ardoise et 4) les bois placés au sein d'une zone périphérique

inactive. Trois facettes complémentaires de la biodiversité ont été analysées dans ce chapitre soit la richesse spécifique, les traits fonctionnels et les isotopes stables suivant un cadre similaire pour la diversité α et β. Pour la diversité fonctionnelle, un modèle nul a été appliqué afin de déterminer les effets de l'environnement et du type de substrat sur chacun des quatre groupes et d'identifier les facteurs structurant les communautés. Les isotopes stables et leurs indices ont été utilisés pour construire des espaces isotopiques en utilisant le même cadre de diversité fonctionnelle, ce qui a permis d'analyser les chevauchements entre niches fonctionnelles et isotopiques. Une extension de ce cadre pour l'étude de la diversité β a été privilégiée.

Les résultats montrent que les substrats minéraux (ardoises) dans les zones actives possèdent une richesse isotopique et fonctionnelle supérieure à ceux situés en périphérie. Ceci suggère que, malgré le stress environnemental associé, la présence de diverses ressources chimiosynthétiques permet le soutien de diverses stratégies écologiques et la formation d'assemblages de densités plus élevées pour la méio- et la macrofaune. Les substrats de bois des sites inactifs étaient colonisés par un nombre plus important d'espèces et d'individus que les ardoises des conditions hydrothermales actives et périphériques, respectivement. Ces assemblages colonisant les bois étaient largement dominés par des spécialistes des communautés de bois coulé. Les valeurs élevées de diversité isotopique estimées sur les bois mettent en évidence des voies à double énergie, c'est-à-dire chimiosynthétiques et photosynthétiques (matière organique du bois). La présence de ressources de diverses origines (chimiosynthétiques/photosynthétiques)

aurait probablement favorisé le développement de nombreuses stratégies écologiques différentes (richesse fonctionnelle élevée) permettant aux espèces d'exploiter des ressources très variées dans le même habitat et de diminuer la pression de compétition.

Tout comme ce qui est observé au niveau des zones hydrothermales actives, ces résultats étendent le concept de « points chauds ou hotspots» de diversité associés aux habitats de bois coulés à la facette fonctionnelle. La forte redondance des espaces isotopiques et fonctionnels souligne l'importance des substrats bois dans les grands fonds marins en tant que « pierres de gué ou stepping stones » potentielles pour la dispersion de la méio- et macrofaune, non seulement pour les espèces des zones hydrothermales actives, mais également pour celles qui se trouvent en périphérie.

Les résultats et les conclusions de cette thèse ouvrent la voie à de futures études et représentent une référence solide d'où dériver des hypothèses écologiques qui permettront d'accroître notre compréhension de l'écologie des écosystèmes chimiosynthétiques, des milieux marins profonds et plus largement, sur les facteurs qui influencent la structure des communautés. Cette thèse est basée sur la plus importante expérience de colonisation réalisée sur les sources hydrothermales de la dorsale médio-Atlantique. Cependant, cette dernière était « restreinte » à 4 sites différents représentant deux environnements -sites hydrothermaux actifs et périphériques- et deux habitats -sources hydrothermales et bois coulés-. Elle permet donc de comparer les schémas de biodiversité de façon double en considérant des sites hydrothermaux actifs (stressants et

productifs) et des zones périphériques inactives (stables et improductives). Plus d'informations sont nécessaires pour caractériser la relation à plus petite échelle entre les espèces, la richesse fonctionnelle et différents niveaux d'activité hydrothermale. Cette thèse est l'une des premières tentatives de se concentrer sur l'écologie des sources en appliquant une approche contemporaine d'étude des communautés, y compris l'utilisation d'indices fonctionnels et de diversité β récemment développés. Les résultats de cette thèse pourraient avoir une implication importante pour la compréhension des écosystèmes de sources hydrothermales et leur protection contre les activités industrielles imminentes. Plus largement, cette thèse met également en évidence le potentiel des sources hydrothermales peu profondes comme laboratoires naturels permettant de tester d'importantes hypothèses écologiques.

Introduction

The deep sea

The deep sea is defined as the environment below ~200 m depth constituting the largest biome on Earth, yet the most unexplored (Ramirez-Llodra et al. 2010). It is a dark and cold environment with an average depth of about 4000 m, low temperatures (<4°C) and high hydrostatic pressures (reviewed in Danovaro et al. 2014). Most of the deep sea (~50%) lies at abyssal depths between 3 and 6 km and is a relatively flat muddy habitat interrupted and subdivided by hills, seamounts, island arcs, trenches and mid-ocean ridges (Smith et al. 2008). Due to these characteristics, many authors have given to the deep sea the status of a remote "extreme habitat". Arguably though the most extreme ecological feature of the deep sea is the scarcity of energy (Smith et al., 2008). Photosynthesis is usually not supported at waters deeper than 200-300 m. Deep-sea communities thus, largely depend on the sinking organic matter produced thousands of meters above in photosynthetic surface layers (Ramirez-Llodra et al., 2010; Smith et al., 2008; Danovaro et al., 2014). For instance, only 0.5 to 2% of the surface primary production reach the deep sea below 2000 m depth (Smith et al. 2008). Before reaching the seafloor, microorganisms attach on the sinking detritus and degrade the most labile compounds producing a rain of very refractory organic particles (Campanyà-Llovet et al. 2017). Thus, not only the scarce but also the low-quality food is available to the deep-sea benthos (Campanyà-Llovet et al., 2017).

Paradoxically, this vast, energy-deprived and low-quality-food environment is home to communities with remarkable species richness, albeit extremely low biomass and densities (Snelgrove and Smith, 2002; Smith et al. 2008). As many as 100 species of macrofauna, and many more of meiofauna, may be found per 0.25 m² of seafloor (Snelgrove and Smith, 2002). In addition, the deep sea is an apparently temporal and spatial stable environment that lacks the 3-dimensional biogenic structures that characterize other species-rich habitats on Earth (Snelgrove and Smith, 2002). Not only richness but the high evenness, or lack of dominance, characterizes most of the abyss with Pielou's index (J') values varying between 0.7 and 1 (Ramirez-Llodra et al., 2010). Several hypotheses, some of them mutually exclusive, have been proposed in order to explain the origin of such a high diversity (reviewed in Snelgrove and Smith (2002); McClain and Schlacher (2015) and references therein):

- The "stability-time hypothesis" (Hessler & Sanders 1967; Sanders, 1968) states that the temporal stability of the deep-sea environment has allowed evolutionary processes driven by competition that have resulted in a fine niche partitioning among species allowing coexistence.

- The "biological cropping hypothesis" (Dayton & Hessler, 1972) states that small-scale disturbances by sediment-feeders species or "croppers" produce constant top-down control on benthic assemblages preventing competitive exclusion of the otherwise better competitor species.

- The "patch-mosaic hypothesis" (Grassle & Sanders, 1973) states that the deep sea supports microhabitats with very long temporal duration impacted by very small-scale disturbances producing a diversity of successional stages between patches and at the landscape scale. High diversity results from the very fine adaptations of species to these microhabitats and stages.

Mixed evidences documented over years support and/or contradict some of these hypotheses (reviewed in Snelgrove and Smith, 2002; McClain and Schlacher, 2015) but it is now clear that the deep sea is not as homogenous as earlier thought, neither spatially nor temporally (e.g., Durden et al., 2015; Zeppilli et al., 2016; Bates et al., 2018). Aside of the exciting and unresolved debate on its high species richness, energy availability is recognized as a capital driver of deep-sea biodiversity, biomass patterns, community structure and ecosystem functioning (Smith et al., 2008; McClain and Barry, 2014; Wooley et al., 2016) (Figure 1). Given that productivity at shallow waters is heterogeneous, changing with latitude and distance to the coast, deep-sea biodiversity patterns also change along latitudinal, bathymetric and horizontal gradients (Wei *et al.* 2010; Brault *et al.* 2013a, b; Wagstaff *et al.* 2014; McCallum *et al.* 2015; McClain & Rex 2015; Stuart *et al.* 2016; Woolley *et al.* 2016). Due to the allochtonous energy nature this relationship has been termed as a "food-supply-diversity" relationship (sensu McClain and Schlacher, 2015) instead than a productivity-diversity relationship.
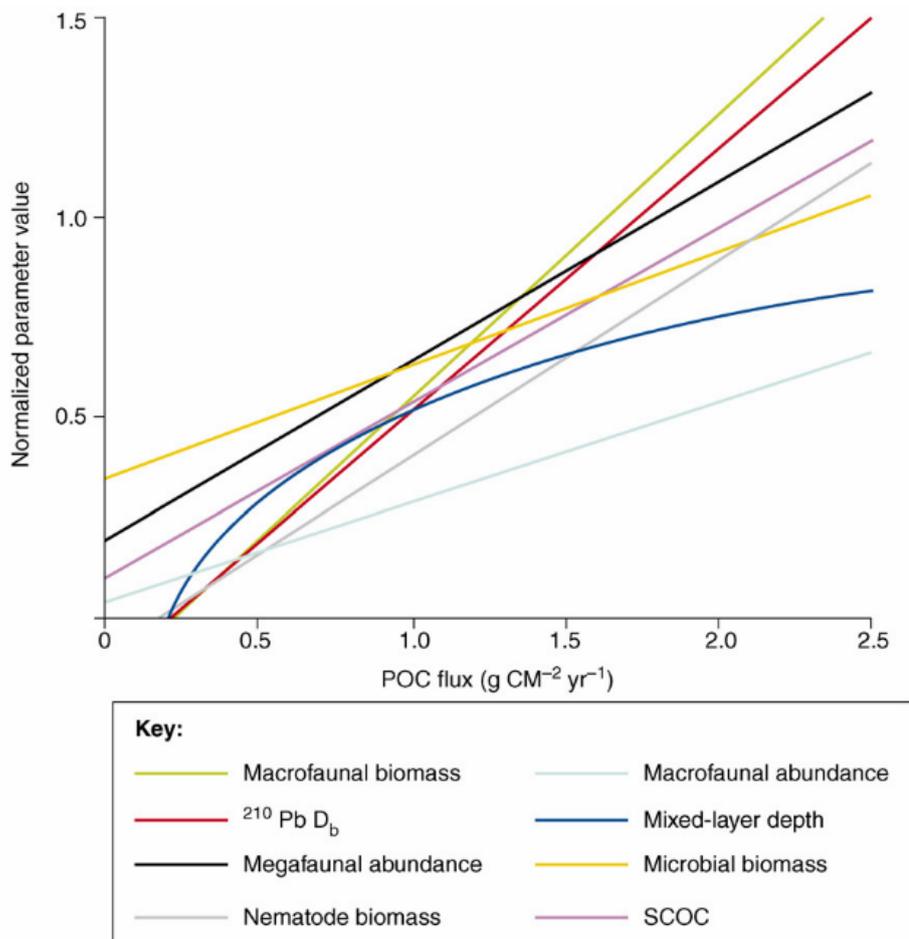
Figure 1.1. Relationships of energy measured as particulate organic carbon (POC flux) and ecosystem structure and function in the deep sea. ^{210}Pb D_b= Bioturbation intensity. SCOC= sediment community oxygen consumption. Figure from Smith et al. (2008).

At large scales, three big patterns of deep-sea biodiversity arise linked to different forms of energy (McClain and Barry, 2014; Woolley et al., 2017). Firstly, particulate organic carbon and depth present an exponential-negative relationship and diversity usually decreases from the slope, between 200 and 2000 m depth, to the abyss (McClain and Barry, 2014). Secondly, more species are found on tropical slopes than those located on temperate or polar latitudes due to the higher thermal energy (Woolley et al., 2017). Thirdly, between 2000 and 6500 m depth however, diversity peaks at high latitudes (30-

50°) and closer to continental margins due to the higher organic matter export linked to both the high seasonal primary production of temperate seas and margins (Woolley et al., 2017). Biodiversity patterns tend to be more pronounced along bathymetric than along horizontal gradients (McClain & Rex 2015). Exceptions are found along horizontal gradients created by strong coastal influences, oxygen minimum zones and topographic features such as canyons and chemosynthetic-based habitats like hydrothermal vents (Sancho *et al.* 2005; Cordes *et al.* 2010; Wei *et al.* 2010; Leduc *et al.* 2012; Smith *et al.* 2014; McClain & Rex 2015).

A striking discovery that broke the rule: deep-sea chemosynthetic-based ecosystems

Forty years ago, scientists observed for the very first time hydrothermal vents (at that time "hot springs") at the Galapagos Spreading Center (Lonsdale 1977; Corliss et al., 1979). The discovery of lush and unique communities, associated to vents, broke several major deep-sea ecological paradigms and still represents one of the most relevant discoveries of the past century (German et al., 2011). Vent ecosystems are mainly found at active tectonic plate boundaries along mid-ocean spreading centers and in back-arc basins (Figure 2 and 3) (Beaulieu et al., 2013, 2015). There, seawater percolates through cracks and fissures and reacts with the ocean crust forming the anoxic hydrothermal fluids that are characterized by high temperatures, and elevated concentrations of chemically reduced compounds and heavy metals (Figure 2) (Le Bris et al., 2019). Free-living or invertebrate-symbiont microorganisms obtain their energy through the

oxidation of the reduced compounds found in the fluids. This process is known as chemosynthesis and forms the trophic base of various faunal assemblages with high abundances and biomass strikingly contrasting with those living on the majority of the widespread deep-sea soft-bottom habitats (Corliss et al.; 1979; Sievert and Vetriani, 2015). The recognition of vents as hotspots of productivity completely challenged the idea of a total dependence on photosynthetic primary productivity of surface waters (German et al., 2011).

Hydrothermal vents also differentiate from the majority of the deep sea due to their high physicochemical variability directly linked to geological processes (Bates et al., 2010; reviewed in Levin et al., 2016; Mullineaux et al., 2017 and Le Bris et al., 2019). Fluids are emitted either as undiluted focused vents at temperatures up to 400°C, with low pH and oxygen concentrations, or after their interaction with ambient seawater creating lower-temperature emissions called diffuse flows (Figure 2) (Le Bris et al., 2019). At the interface of undiluted focused fluxes and cold seawater the precipitation of metals forms black smoker chimneys (Karson et al., 2015). The accumulation of precipitate metals with time may produce large hydrothermal "edifices" and metal deposits (Figure 2) (e.g., Boschen et al., 2013; Van Dover, 2019). Sulfide edifices are characterized by a high physicochemical and spatiotemporal variability with continuous processes of activation, inactivation and reactivation of fluid exits, chimney collapses, and gradual changes in edifice porosity (Sarrazin et al., 1997, 2002). All of these phenomenons and dynamics occur during species life spans and at spatial scales of < 1m. Within this spatiotemporal variability, large

symbiotic invertebrates thrive, inhabiting distinct niches along the environmental gradient forming a zonation or mosaic-like pattern, dominating biomass and acting as foundation species (e.g., Sarrazin *et al.* 1997; Shank *et al.* 1998; Luther III *et al.* 2001; Govenar 2010; Husson *et al.* 2017; Bris *et al.* 2019).
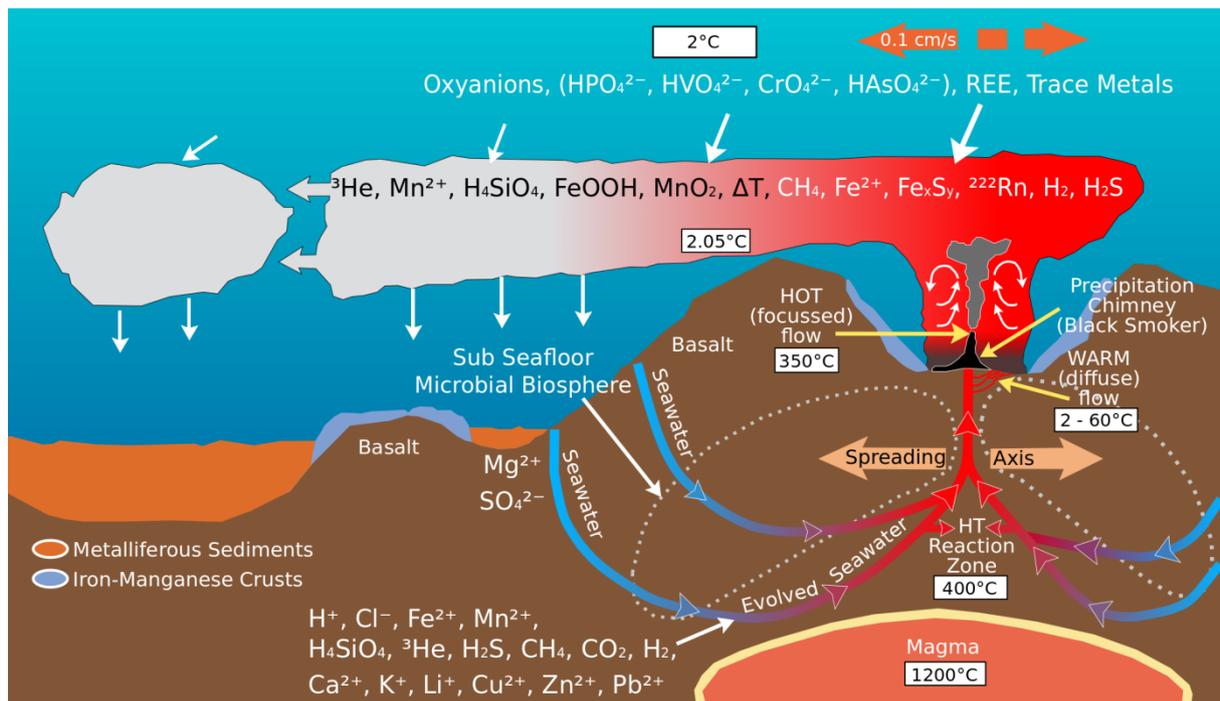
Figure 1.2. Diagram illustrating the formation and circulation of hydrothermal vents and fluids at an ocean spreading center. Image from NOAA.

Diversity in space and time: from basin to local scales

Currently, 572 deep-sea vents are known: 344 at mid-ocean ridges, 117 at back-arc spreading centers, 106 at volcanic arcs, and 5 at intraplate hotspots (Figure 3; Beaulieu, 2015). Inactive seafloor in between these discrete patches of vent activity is not suitable for the establishment of chemosynthetic microorganisms and symbiotic foundation

species. Furthermore, the majority of the associated heterotrophic vent fauna has not been observed on other habitats. Thus, dispersal of larvae and initial habitat colonization (settlement and recruitment) are critical factors for population viability at these patchily and restricted habitats (Van Dover et al., 1988; Mullineaux et al., 2000; Marsh et al. 2001; Adams et al. 2012). However, several studies have shown that vent fauna rapidly colonize nascent sites (e.g., Shank et al., 1998; Tunnicliffe et al., 1997; Marcus et al., 2008).

The temporal and spatial heterogeneity at local and regional scales certainly shape vent biodiversity patterns and composition of communities. Indeed, hydrothermal vents are patchily distributed and separated by a few to hundreds of kilometers, depending of their geographic locations (Figure 3). Vents present distinct faunal composition and diversity at different ocean basins, or parts of them, forming several biogeographic provinces (Moalic et al., 2012). Vents of a given region however may greatly differ in their composition due to specific environmental characteristics, such as the nature of substrata or the chemical composition of vent fluids (Desbruyeres et al., 2001; Goffredi et al., 2017). Furthermore, spreading centers are characterized by different spreading rates and classified as fast, intermediate, slow and ultraslow (Figure 3) (Karson et al., 2015; Mullineaux et al., 2017; Le Bris et al., 2019). Fast spreading centers are associated to a larger supply of magma, which enhances disturbances such as catastrophic volcanic eruptions (<10 years), and harbor clusters of close-distant (10's km) vents with low longevities. On the other hand, at slow spreading centers and many back-arc systems, vents are more spaced between them (10-100's km), long-lived (1000's years) and volcanic

eruptions are rare. These characteristics interact to shape the observed species diversity and composition at local and regional scales with disturbance rates and habitat heterogeneity contributing on ecological time scales and tectonic on evolutionary scales (Mullineaux et al., 2017). For instance, frequent volcanic eruptions may decrease diversity locally but may create a mosaic of successional stages among vent increasing the regional diversity (Mullineaux et al., 2010). Vents distance, major geographic barriers in between and depth may limit dispersal between active vents reducing recovery and thus diversity (Mullineaux et al., 2017).
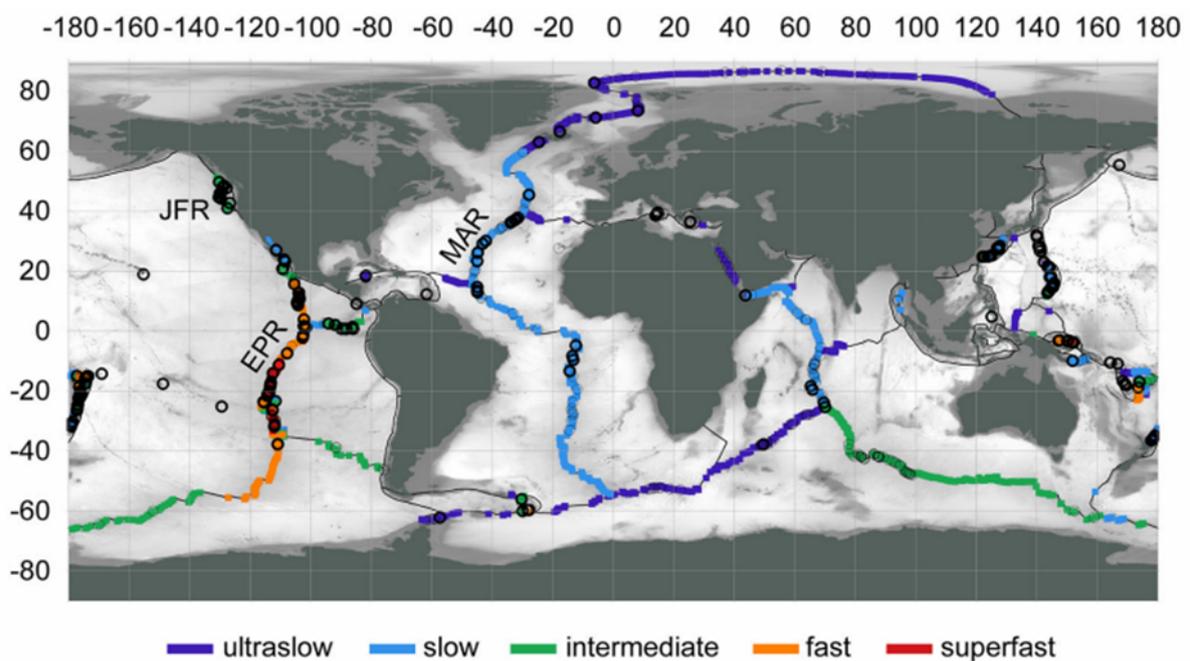
Figure 1.3. Global distribution of vent hydrothermal vents (circles) along mid-ocean ridges and back-arc basins, denoting different spreading rates. Image from Mullineaux et al. (2017).

Dispersal plays a key role in maintaining and structuring vent communities (Mullineaux et al., 2010). Larval supply can dramatically be altered after the depletion of local source populations, allowing colonization by species from distant sites (Mullineaux et al., 2010). At the edifice scale, vent fauna form a zonation of assemblages, matching gradients in physicochemical conditions depending on their tolerance to toxicity and temperature and their nutritional requirements (see biological interactions below) (Figure 4) (Sarrazin et al., 1997; Luther et al., 2001; Govenar et al., 2005; Govenar et al., 2007; Sarrazin et al., 2015). Larval supply, stochasticity and biological interactions also affect diversity patterns and community assembly although they are much less understood (Micheli et al. 2002; Mullineaux et al. 2003; Mullineaux et al. 2010; Mullineaux et al. 2012). These assemblages are usually dominated in terms of abundance and biomass by symbiotic foundation invertebrate species. Macro- and meiofauna also exhibit zonation with higher diversity at intermediate regimes or at inactive peripheral areas (Gollner et al., 2010; Gollner et al., 2015; Sarrazin et al., 2015).
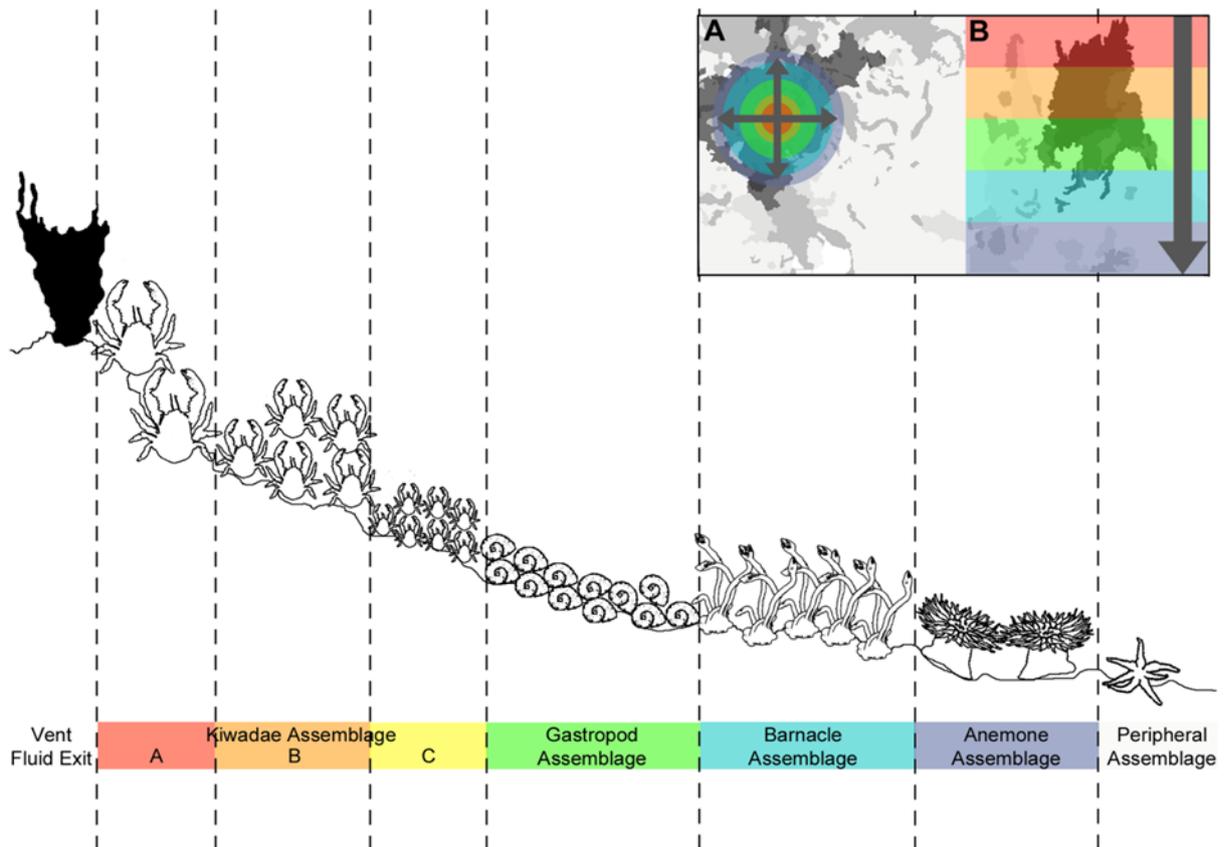
Figure 1.4. Zonation of species along a hydrothermal vent gradient at the East Scotia Ridge (Southern Ocean). Patterns of zonation in both horizontal (A) and vertical (B). Image from Marsh et al. (2012).

Temporal variations of faunal assemblages are usually associated to the natural geologic variability of vents and biological succession (Figure 5). Although different, both processes are driven by changes in the environment that are difficult to disentangle (Mullineaux et al., 2017). Sulfide edifices are characterized by a high physicochemical and spatiotemporal variability. Thus, compositional changes in fauna follow the continuous processes of activation, inactivation and reactivation of fluid exits, chimney collapses, and gradual changes in edifice porosity (Sarrazin et al., 1997, 2002; Cuvelier et al., 2011). Primary succession starts after catastrophic volcanic eruptions that eradicate established faunal communities. Succession at vents has been studied only at the fast-spreading East

Pacific (9.50′ N) in 1991 and 2006 (Figure 5), and at the intermediate-spreading Juan de Fuca Ridge on the Axial Volcano and on the Co-Axial Segment in 1998 and 1993, respectively (Shank et al., 1998; Gollner et al., 2010; Tunnicliffe et al., 1997; Marcus et al., 2009). The lack of catastrophic events at vents on the slow spreading Mid-Atlantic Ridge and back-arc Lau Basin have shown a remarkable global stability of communities for periods longer than a decade (Cuvelier et al., 2014; Du Preez and Fisher, 2018).

The East Pacific Rise (EPR) succession after the eruption in 1991 has become the textbook example of vent succession (Figure 5). There, succession occurs in ~5 years and starts with the establishment of microbial mats followed successively by the settlement of the siboglinid tubeworm *Tevnia jerichonana*, the giant tubeworm *Riftia pachyptila*, and ultimately by the mussel *Bathymodiolus thermophilus* (Figure 5) (Shank et al., 1998). The waning of fluid corresponds to the colonization of *R. pachyptila* suggesting that *T. jerichonana* is an early colonizer although it may also promote *R. pachyptila* settlement through biogenic settlement cues (Mullineaux et al., 2000). Ultimately, *B. thermophilus* outcompetes *R. pachyptila* by reducing fluid fluxes due to engineering effects (Johnson et al., 1988; Shank et al., 1998). Following succession, macro- and meiofaunal species richness increases with time (Shank et al., 1998; Gollner et al., 2015). During the succession process, other biological interactions may also exert an effect through predation (see below) (Micheli et al., 2000; Mullineaux et al., 2003; Sancho et al., 2005). Although succession at vents may seem deterministic, that observed after the eruption of 2006 showed that the time of arrival of larvae from distant communities had a strong and persistent effect on

vent succession suggesting that pioneer effects are relevant and that vents may follow

alternative successional trajectories (Mullineaux et al., 2010; Mullineaux et al., 2012).
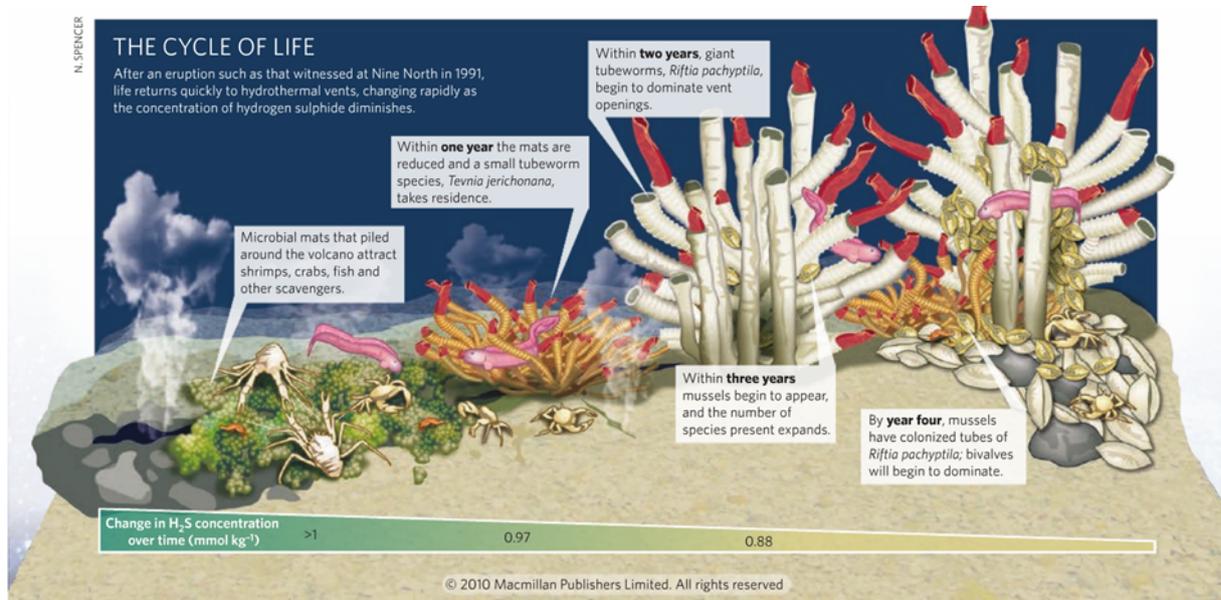
Figure 1.5. Conceptual model of faunal succession on the East Pacific Rise hydrothermal vents after the volcanic eruption. Image from Qiu (2010).

Are vents discrete patches? The vent sphere of influence

Due to their particularities, vents have been historically considered as island-like,

spatially discrete and restricted, ecosystems in the deep sea (Levin et al., 2016). This point

of view ignores the interactions and transitions zones between vents and surrounding

environments (Levin et al., 2016; Le Bris et al., 2019). A growing body of literature strongly

suggests that vents are not isolated and have a "sphere of influence" in space and time

(Figure 6; *sensu* and reviewed in Levin et al., 2016). Evidence suggests a supply of

biological and chemical materials and energy from high-productivity vent habitats to the

contrasting food-deprived deep-sea background habitats (Erickson *et al.* 2009; Levin *et al.* 2016; Ardyna *et al.* 2019; Bris *et al.* 2019). Indeed, it has been estimated that the contribution of vents to the available organic carbon of the deep sea may represent up to 3% (Levin et al., 2016). Hydrothermal vent plumes migrate over long distances (hundreds of kms) vertically and laterally, creating bio-geochemical heterogeneity into the water column and affecting pelagic and benthic environments even at the basin scale (Resing *et al.* 2015; Ardyna *et al.* 2019). Other mechanisms may also represent continuous links with the surrounding deep sea such as: a) export of vent particulate organic carbon (Erickson *et al.* 2009; Bell *et al.* 2017), b) trophic transfer by vagrant predators and scavengers (Micheli *et al.* 2002; Sancho *et al.* 2005), c) release of vent species gametes into the water column (Mullineaux *et al.* 2010) and d) settlement of vent species in surrounding environments beyond the limits of established adult populations (Dover *et al.* 1988; Mullineaux *et al.* 1998).
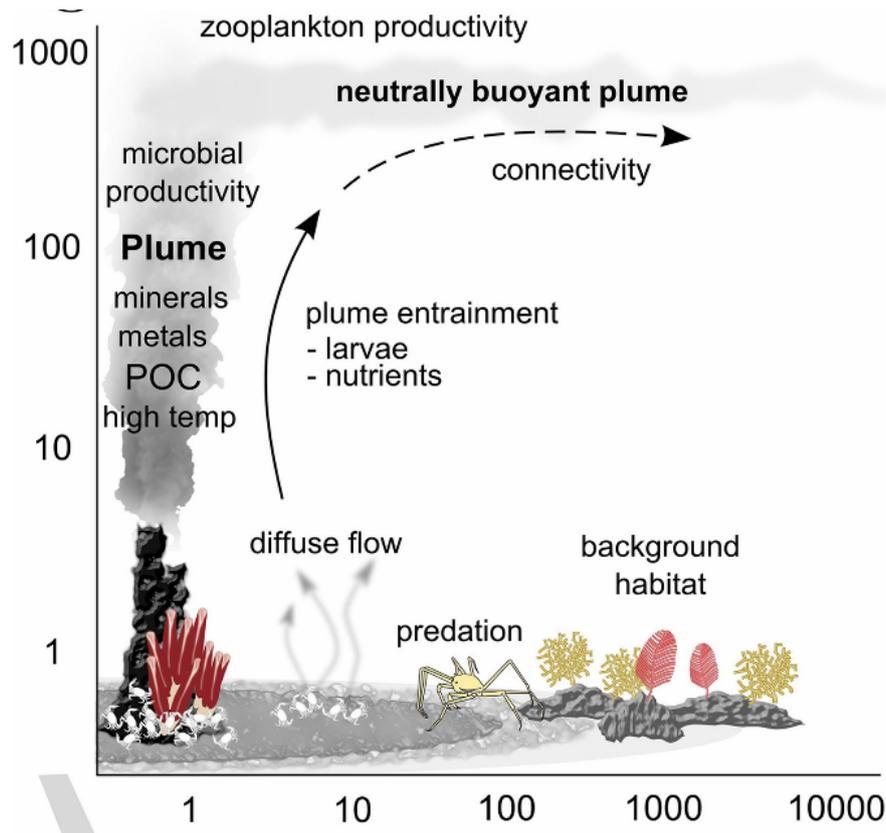
Figure 1.6. Interaction of hydrothermal vent and deep-sea background habitats. Image from Levin et al. (2016).

Some authors have hypothesized that transition zones from vents to background habitats may represent ecotones (Levin et al., 2016). Ecotones, from the Greek "oikos" (home) and "tonus" (tension), are boundaries, transitional or tension areas between ecological systems, i.e., communities, ecosystems, biomes, etc. (Kark and Rensburg, 2006). Edges between systems are widespread worldwide and early prompted the attention of scientist due to their effects on fauna. Ecotones may be areas that harbor critical ecosystem services by regulating flows of organisms, materials, and energy across landscapes (Rise et al., 2004). Both theoretical and empirical research suggest that edge effects may increase, reduce, or have no effect on species richness and abundance, both in plants and

animals, and thus are key zones for understanding ecosystem functions at the landscape

scale (Murcia, 1995; Rise and Sisk, 2004; Rise et al., 2004; Magnago et al., 2014).

However, sampling at peripheries of vents is scarce despite the fact that they may

offer critical ecosystem services (Govenar et al., 2007; Sen et al., 2016). Peripheries are

diverse and represent a mosaic of physicochemical and geological-rich habitats (Figure 7;

e.g., Ferrini et al., 2008). These inactive areas may support important functions serving,

for instance, as vent species nursery zones (e.g., Dittel et al., 2008; Marsh et al., 2015).

Analyses of megafauna suggests that sessile or highly-mobile non-vent

predators/scavengers taxa, such as sponges, hydroids, squat lobsters and fishes, usually

inhabit inactive habitats (Figure 7) (e.g., Desbruyères et al., 2001; Kim and Hammerstorm,

2012; Sen et al., 2015). These taxa are commonly found on the deep sea but at peripheries

they may sometimes attain higher abundances presumably supported by the

consumption of organic matter of chemosynthetic origin (Erickson et al., 2009; Sen et al.,

2016). Less information is available for the macrofaunal and meiofaunal compartments.

Some studies however suggest that rich assemblages of meiofauna may inhabit inactive

areas (Gollner et al., 2010a; 2010b; 2015). Due to their limited dispersal capabilities these

tiny animals may be especially susceptible to natural and anthropogenic impacts (Gollner

et al., 2010a).

Figure 1.7. Pillow lava in hydrothermal vent peripheral areas in the Galapagos Ridge. Image from NOAA.

Cognate habitats, the stepping-stone hypothesis and the continuum of reducing environments

Soon after the discovery of vents in 1977, other cognate communities were found in distinct reducing environments such as those created in cold seeps (Paull et al., 1984). The discovery of inhabitants of the same linages but with a limited overlap at species level in cold seeps created the perception of two distinct, although evolutionary-related, ecosystems (Paull et al. 1984). Furthermore, large wood logs and whale carcasses, also named wood and whale falls, were found to sustain chemosynthetic productivity and faunal overlap with vents and seeps (Smith et al., 1989; Baco et al., 1999; Smith and Baco, 2003; Smith, 2006; Fujiwara et al., 2007; Lundsten et al., 2010a, b; Bernardino et al., 2010; Bienhold et al., 2013; Kiel, 2016; Smith et al., 2017; Shimabukuro et al., 2019). Organic falls are interesting habitats because they represent an eco-evolutionary link between the

shallow and deep sea (whale carcasses) and the land and the ocean (woods) (Smith et al., 2015; Judge and Barry, 2016).

Hydrothermal vents and organic fall are eco-evolutionarily related habitats (Smith et al., 2016). The discovery of whales falls showed that similar linages inhabit organic falls and vents (Smith et al., 1989). Smith et al. (1989) proposed the Stepping-stones Hypothesis that states that organic falls may act as stepping stones for the dispersal of some vent fauna to new and distant habitats. Soon after, evidences suggest that some of the most iconic vent foundation species, such as chemosynthetic mussels, likely evolved from shallow waters to the deep sea using organic falls in a stepping stone fashion (Distel et al., 2000; Jones et al., 2006; Miyazaki et al., 2010; Lorion et al., 2012, 2013; Thubaut et al., 2013). A side of the evolutionarily implications of this theory, two fundamental question are if organic falls are actually colonized by vent fauna, and if so, if organic falls are key for the dispersal of these fauna to reach vent sites separated by large distances.

In the recent years, several studies have shown that organic falls do share some fauna with vents and other chemosynthetic-based ecosystems such as seeps (Feldman et al., 1998; Smith et al., 2015; Sumida et al., 2016; Smith et al., 2017; Shimabukuro et al., 2019). This fauna mainly consists in sulfide tolerant generalists polychaetes rather than the iconic vent chemosymbiotic foundation species (e.g., Smith et al., 2017; Shimabukuro et al., 2019). Regarding if organic falls connect distant vents is still to be answered but genetic approaches may shed light on by analyzing populations of species colonizing these environments.

Certainly, wood is widely distributed in the deep sea but probably more abundant in deep areas closer to rivers and densely forested coasts (Turner et al., 1973). Wood forms patches of organic enrichment in an extremely food-limited environment. The degradation of wood passes through several overlapping successional stages, hosting unique and diverse communities (Figure 8; Bienhold et al., 2013). These energy-rich habitats have three main sources of energy: a) wood organic matter, b) chemosynthetic primary productivity from the microbial oxidation of reduced compounds produced from the anaerobic decomposition of wood and c) typical deep-sea organic matter from photosynthetic origin (Bernardino et al., 2010; Bienhold et al., 2013; Kalenitchenko et al., 2016; Kalenitchenko et al., 2018). Consequently, wood falls are colonized by a suit of wood specialists, chemosymbiotic, sulfide generalists and opportunistic background fauna constituting both hotspots of evolutionary novelty and diversity in the deep sea (Bernardino et al., 2010; Bienhold et al., 2010; Judge and Barry, 2016; Saeedi et al., 2019).

The discovery of habitats with intermediate physico-chemical characteristics, such as sedimented vents and hydrothermal seeps, led some authors to hypothesize that chemosynthetic-based ecosystems may constitute a "continuum of reducing ecosystems" (Levin et al. 2012; Portail et al. 2015; Portail et al., 2016; Kiel 2016). Contradicting this idea however, recent evidence suggest that close vents may present highly dissimilar faunal compositions due to local physical (substratum type) and chemical (fluid nature) conditions (Goffredi et al. 2017). Thus, the continuum of reducing habitats may not apply

universally and relevant eco-evolutionary processes driving differentiation between and among systems may be due to system-specific characteristics (Goffredi et al. 2017).
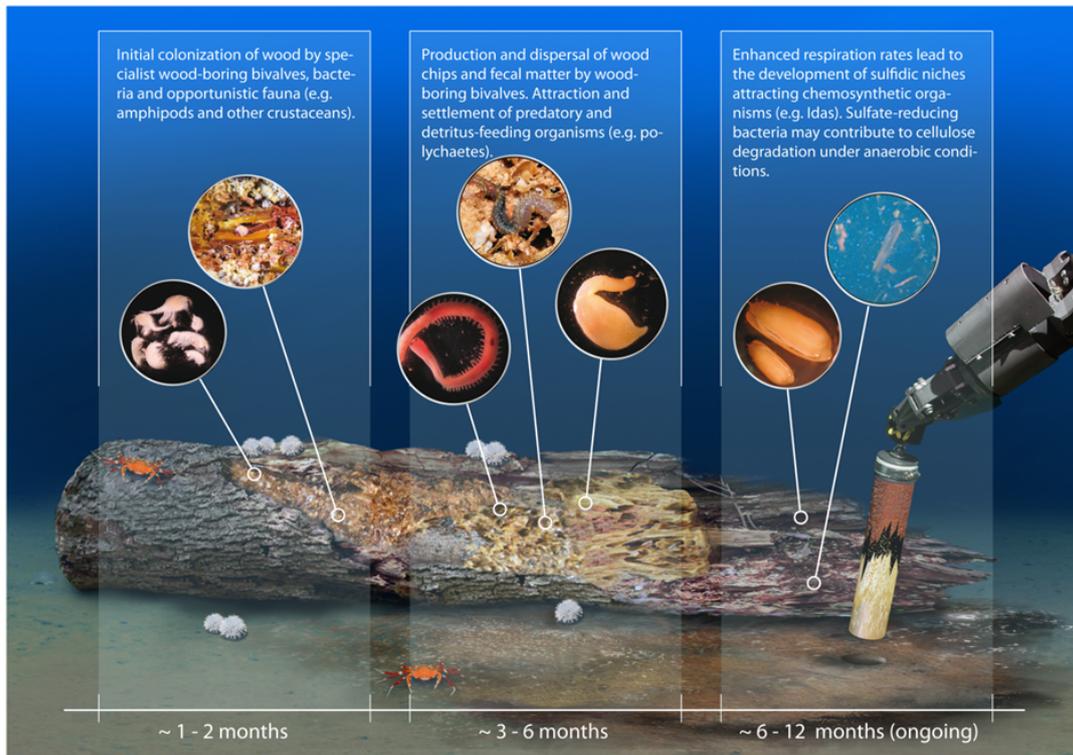
Figure 1.8. Conceptual model of faunal succession on deep-sea wood falls showing the different energy-based assemblages and their faunal compositions. Image from Bienhold et al. (2013).

Problematic

Heterogeneous conditions and high dissimilarity of fauna between and among spatially discrete communities such as vents create challenges for managing and conservation issues (Goffredi et al. 2017). Certainly, each chemosynthetic habitat show unique characteristics that may interact with other factors, such as depth and geographic distance. Depth and distance have long been recognized as strong structuring factors among and between chemosynthetic habitats (e.g., Desbruyères et al., 2001; Van Dover et

al., 2002). It is becoming essential to better understand these aspects, especially in an era in which these communities are facing serious direct and indirect anthropogenic impacts.

In fact, despite its remoteness, the deep-sea is not isolated and has already received impacts of anthropogenic origin (Figure 9) (Ramirez-Llodra et al., 2011; Levin and Le Bris, 2015). Vents may not be an exception (Boschen et al., 2013). Hydrothermal activity eventually ceases and the massive sulfide deposits generated after years of venting are becoming attractive for the developing deep-sea mining industry (Boschen et al., 2013; Van Dover, 2019). As such, understanding vent ecological aspects such as dispersal, colonization and resilience is more than ever of main importance. Although rarely considered, the relationships of vents with other chemosynthetic communities should also be addressed. For instance, it is fundamental for management and conservation strategies to test not only if whale and wood falls act as suitable habitats for vent fauna of active and inactive environments but also to determine for which specific taxa they act as stepping stones and why.
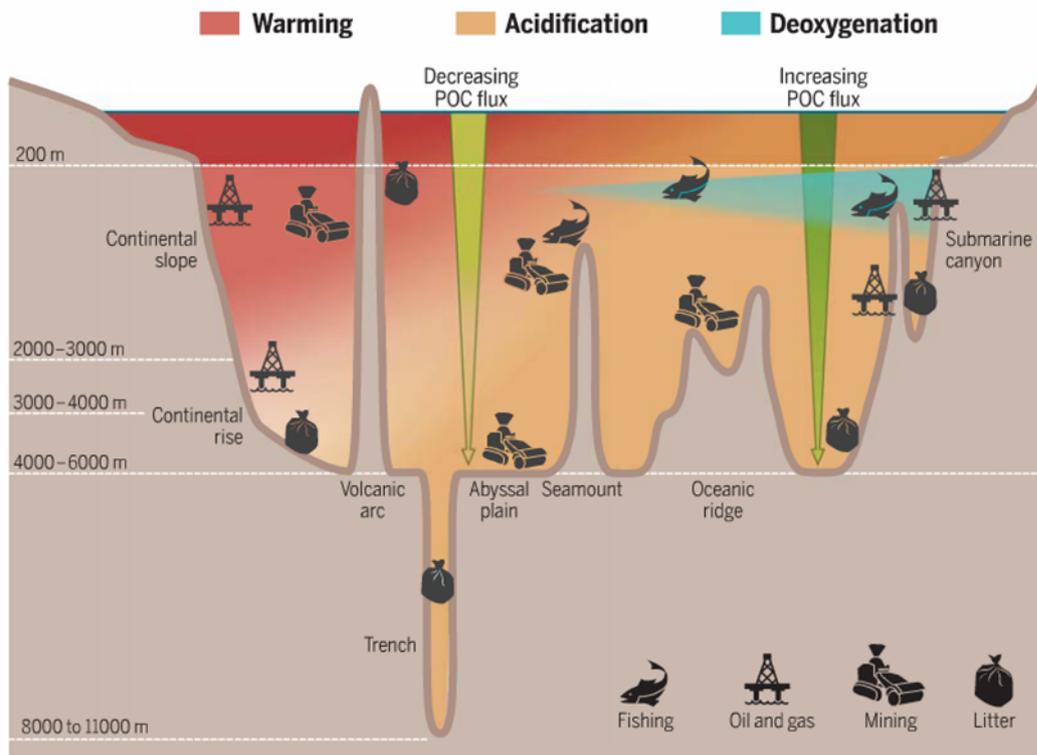
Figure 1.9. Current impacts facing deep-sea ecosystems at different depths. Image from Levin and Le Bris (2015).

Promising opportunities and new approaches: hydrothermal vents as natural laboratories

As illustrated above, vents are heterogeneous even within the same, or close, geological settings. The statement of generalities instead of local specificities is thus difficult, something common not only in "vent ecology", but in community ecology in general (Lawton, 1999; McGill et al., 2006). To overcome this issue, some new and innovative approaches have emerged in the recent decades, such as trait-based approaches (McGill et al., 2006). In vents, and the deep sea in general, these approaches have rarely been implemented (but see McClain et al., 2018; Chapman et al., 2019; Portail et al., 2019). These approaches may be of special interest for systems with marked

environmental gradients (McGill et al., 2006) and may help to elucidate gaps in community assemblage processes at vents (see below).

Deep-sea vents are of special interest because they constitute systems in which the main drivers of biodiversity such as disturbance, productivity and biotic interactions correlate and interact in a short space (see below). In fact, vents may be seen as natural laboratories (Hall-Spencer et al. 2008). For instance, shallow water vents have been used as systems to test acidification impacts on species diversity, faunal and trophic structure and ecosystem functioning (e.g., Hall-Spencer et al. 2008; Kroeker et al. 2011; Fabricius et al. 2014; Garrard et al. 2014; Vizzini et al. 2017; Teixidó et al. 2018). Due to the rapid colonization of vents, colonization experiments have been widely used and proven to be useful to disentangle some key questions in vent ecology such as colonization and succession (e.g., Van Dover et al., 1988; Mullineaux et al., 1998; Micheli et al., 2000; Mullineaux et al., 2003; Van Dover and Lutz et al., 2004; Pradillon et al., 2005; Kelly and Metaxas, 2006, 2007, 2008; Lenihan et al., 2008; Pradillon et al., 2009; Cuvelier et al., 2014; Zeppilli et al., 2015; Plum et al., 2017; Baldrighi et al., 2018; Nakamura et al., 2018). Vents are therefore ideal systems to test hypotheses and better understand the drivers and constraints of biodiversity not only at vents but also in the surrounding deep sea.

Nothing but gradients: productivity, environmental stress and biological interactions

Due to the zonation of foundation species along the stress gradient, vents have been hypothesized to be analogous of intertidal zone systems (Johnson *et al.* 1994). Other factors, however, make hydrothermal vents unique systems (Johnson *et al.* 1994; Micheli *et al.* 2002; Mullineaux *et al.* 2003; Levesque *et al.* 2006). Conceptually, vents may be viewed as systems varying from high-temperature black smokers to diffuse flow areas and inactive peripheries. As a direct extension of the extraordinary geological activity, arguably three partially correlated gradients mainly govern the assembly of communities: environmental stress, productivity, and biological interactions (Figure 10).
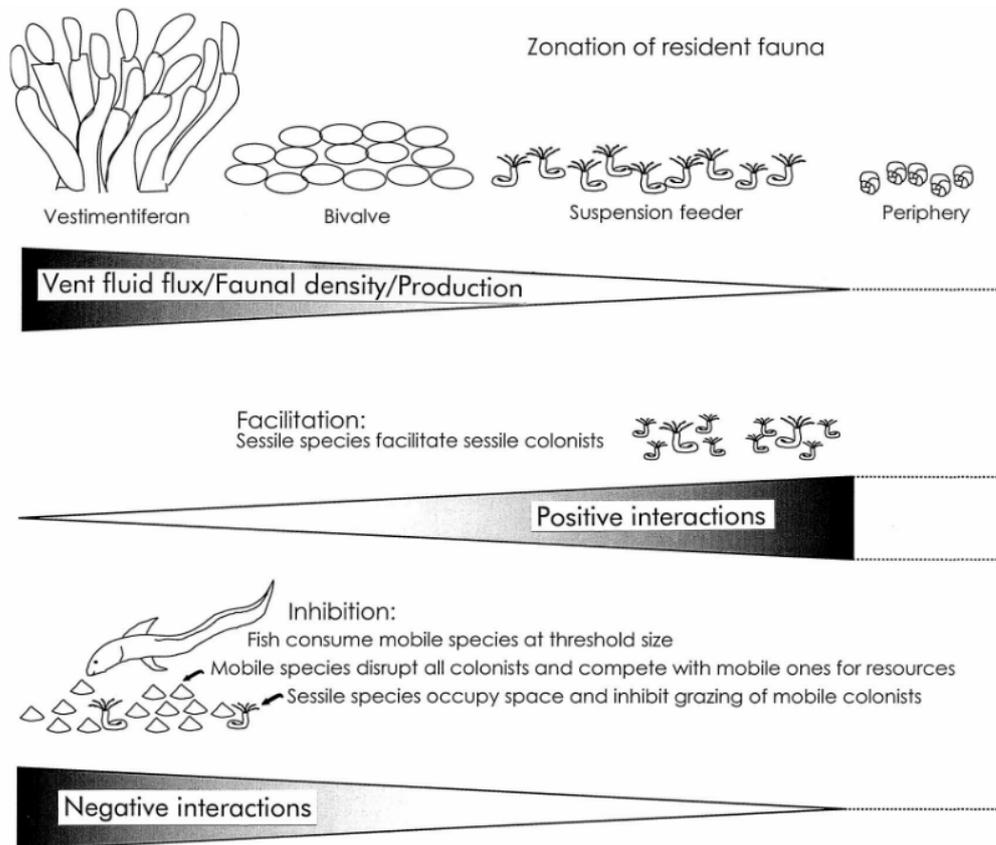
Figure 1.10. Conceptual model of the main gradients found along a deep-sea hydrothermal vent gradient based on successional studies in the East Pacific Rise. Image from Mullineaux et al. (2003).

Determinants and patterns of environmental stress

The upper end of the environmental stress spectrum is characterized by a rapid fluctuating nature making hydrothermal vents one of the most stressful habitats for life (Bates et al., 2010). Main stressful factors include the presence of reduced chemical compounds, low pH, high temperature and high concentrations of heavy metals. Sulfide is arguably the main reduced compound found in vent fluids. Sulfide compounds inhibit cellular respiration and spontaneously react with, and diminish, oxygen concentrations (Scott and Fisher, 1995). Higher temperatures are usually positively correlated with

higher concentrations of reduced chemical compounds. Temperature itself affects vent organisms from enzymes to behaviors (Bates et al., 2010). Higher heavy metals concentrations are also usually associated with both higher fluxes of reduced compounds and high temperatures, and may cause oxidative stress to vent animals (Scott and Fisher, 1995). Indeed, several authors have shown that the spatial distribution of faunal assemblages at vents was strongly correlated with the gradient of physico-chemical conditions (e.g., Luther III et al., 2001).

Productivity, primary producers and its distribution

Due to the reliance on reduced compounds by vent primary producers, hydrothermal vents show a primary productivity gradient that is positively correlated with environmental stress (Micheli et al., 2000; Mullineaux et al., 2003; Le Bris et al., 2019). Primary producers at vents include chemosynthetic bacteria and archea (Sievert and Vetrianni, 2015). The symbiotic associations of these microorganisms with large invertebrates form the main primary producer entities, similar to corals in tropical reefs (Le Bris et al., 2019). At most vent sites, the biomass is largely dominated by these large "holobionts" (*sensu* Le Bris et al. 2019; e.g., Bergquist et al., 2003; Husson et al., 2017) that act as foundation species, creating biogenic habitats that modify the environment (Govenar, 2010). Due to physiological constraints both microorganisms and symbiotic invertebrates do not inhabit the hottest parts where the availability of reduced compound is maximal. So far, the upper thermal limit for prokaryotes is ~122 °C and ~50–55 °C for

invertebrates (Kashefi, 2003; Girguis and Lee, 2006). Conversely, due to the absence of reduced compounds, holobionts are not able to live far away from sources. The most favorable niches for symbiotic invertebrates are located in areas of high oxygen availability where the temperatures vary between 15°C and 25°C (reviewed in Le Bris et al., 2019). Therefore, it is expected to find a productivity peak at intermediate regimes, with lower productivities at both extremes.

Biological interactions

The positive correlation between environmental stress and productivity is in turn correlated with an increasing importance of biological interactions (Micheli et al., 2000; Mullineaux et al., 2002, Govenar, 2010). The positive correlation between productivity and abundance of individuals promote biological interactions within and among species. Foundation species at vents inhabit microhabitats where different fluid fluxes mix with cold well-oxygenated seawater (Govenar, 2010). Foundation species morphologies and physiologies are usually unique in many aspects (Fisher and Childress 1992), which allow them to persist under and exploit the stressful conditions and toxic reduced compounds, respectively (Govenar, 2010). Foundation species create biogenic habitats that physically and chemically modify the environment and provide new spaces for colonization and shelter from predation and contribute to increase environmental heterogeneity (Govenar and Fisher, 2007; Kelly and Metaxas, 2008; Govenar, 2010). Moreover, foundation species may facilitate the settlement of other species including other foundation species (Shank

et al., 1998; Mullineaux et al., 2000). At the periphery of vents, positive biological interactions may be also important for colonization processes. For instance, Mullineaux et al. (2003) found that serpulid polychaetes and foraminifers facilitate the establishment of other sessile colonists.

Heterotrophic vent species (not foundation species) usually attain high densities at intermediate fluid flux habitats and all of them ultimately rely on the same resources (reduced compounds/chemosynthetic organic matter) suggesting high competition for space and nutrients (Micheli et al., 2000; Levesque et al., 2003; Govenar, 2010; Govenar et al., 2015). Negative biological interactions, such as predation, are also important in structuring vents assemblages (Governar, 2010). Zoarcid fishes, vent endemic predators, favor the settlement of foundation species in high fluid flow habitats by actively predating limpets and limiting their bulldozing effect (Micheli et al., 2002; Sancho et al., 2005). Moreover, although their roles have been historically overlooked, predator species at vents are common and include octopods, bythograeid crabs, several families of polychaetes and snails (Governar, 2010). In fact, most common taxa at vents, such as bivalves, gastropods, tube-dwelling and scale-covered polychaetes, and crustaceans, present physical protection structures from both exposure to environment and predation (Tunnicliffe 1992; Govenar, 2010).

Community assembly

Community assembly is the process by which species composition and patterns of a community are determined (Mittlebach and Schemske, 2015). Determinants of community assembly can be articulated into four main processes, namely selection, drift, speciation and dispersal (Vellend, 2010; Mittelbach, 2012). Developments in coexistence theory (Chesson, 2000) helped to reconcile both niche-based, i.e., species niche differences, and neutral-based mechanisms, i.e., dispersal random variation, and stated that both mechanisms interact to define how communities are assembled (Hubbel, 2005; Adler et al., 2007) (Figure 11). Current conceptual models perceive local communities as subsets of a regional species pool (Figure 11). Regional species pools are "sieved" by different filters interacting at multiple spatiotemporal scales (Weiher et al., 2011; Mittlebach and Schemske, 2015). Processes occurring at temporal scales of millions of years drive lineage distributions, diversification and extinction processes of species and ultimately determine regional species pools (Vellend, 2010; Mittlebach and Schemske, 2015). Dispersal and environment select for certain species traits that allow taxa to reach suitable habitats (Weiher et al., 2011; Kraft et al., 2015; Cadotte et al., 2017). At smaller scales, inter- and intraspecific biotic interactions further determine the local composition of species, influencing through demographic stochasticity, the dispersal of species, the environment, speciation and extinction rates and ultimately the regional species pool (Figure 11; Chesson, 2000; Adler, 2007; Vellend, 2010; HilleRisLambers et al., 2012).

Community assembly may be deterministic, historically contingent or both (Fukami, 2010). When deterministic processes act, similar environments in a given region may reach a single stable equilibrium because environmental specificities and interspecific interactions govern the assembly of the communities (Chase, 2003). In other cases, the history of the assembly may lead to dissimilar communities in similar environments due to priority effects (Chase, 2003, Fukami, 2010). A priority effect is the process by which the early arrival of a species influences negatively or positively the performances of the later arrivals leading to different successional outcomes depending on the order of arrival of species (Fukami, 2010). Thus, in historically contingent communities, stochastic processes related to dispersal are of capital importance and several alternative stable states may be possible. Single stable equilibrium states are likely reached in systems with small regional species pools, high rates of connectivity, low productivity and high disturbance (Chase, 2003). Alternative stable states are more likely in systems with large regional species pools, low rates of connectivity, high productivity and low disturbance (Chase, 2003).
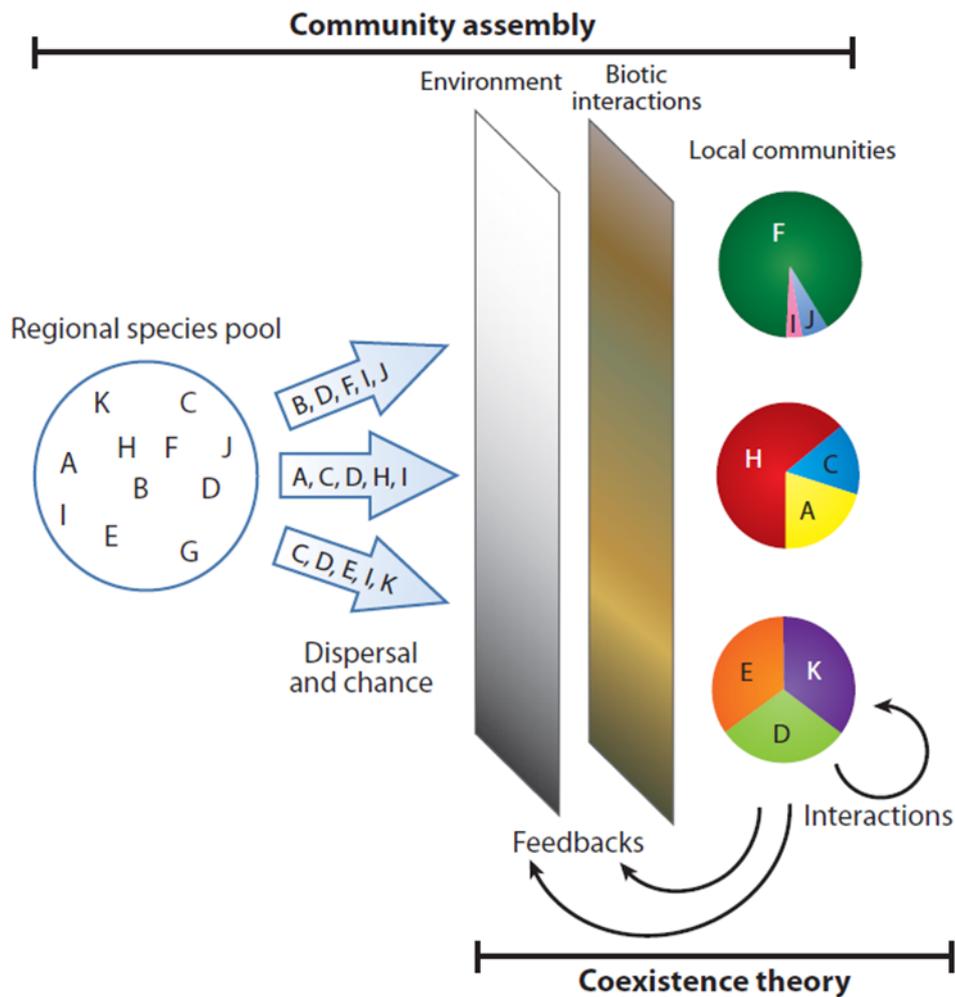
Figure 1.11. Conceptual model of community assembly. Image from HillRisLambers et al. (2010).

Biodiversity and community assembly

Biodiversity and its patterns are direct outcomes of the assembly of communities (Weiher et al., 2011). How assemblages change in species identities and abundances in space and time is one of the fundamental questions in ecology (Gaston, 2000; McGill *et al.* 2006; Vellend, 2010; Kraft *et al.* 2011; Anderson et al., 2011). Not only local biodiversity (α-diversity) but especially its spatiotemporal dissimilarities (β-diversity) reflect the

processes that generate and maintain the mosaic of assemblages found in nature (Anderson et al., 2011; Villéger *et al.* 2011; Legendre and De Càceres, 2013; Myers *et al.* 2013). β-diversity is defined as the variation in species compositions among sites and provides a direct link between local and regional diversity (Whittaker 1960, 1972; Anderson et al., 2011). Several frameworks and indexes exist in order to measure β-diversity (Baselga, 2010; Anderson et al., 2011; Legendre and De Caceres, 2013; Legendre et al., 2014). Of particular interest is the recognition that β-diversity may be produced by two different mechanisms: turnover and species loss, or its special case nestedness (reviewed in Legendre et al., 2014). Turnover is the replacement of some species by others (Figure 12) as a consequence of environmental filtering or historical constraints, whereas nestedness refers to the process by which species of lower richness sites are strict subsets of those of richer sites highlighting a non-random process of species loss (Baselga, 2010; Legendre, 2014).
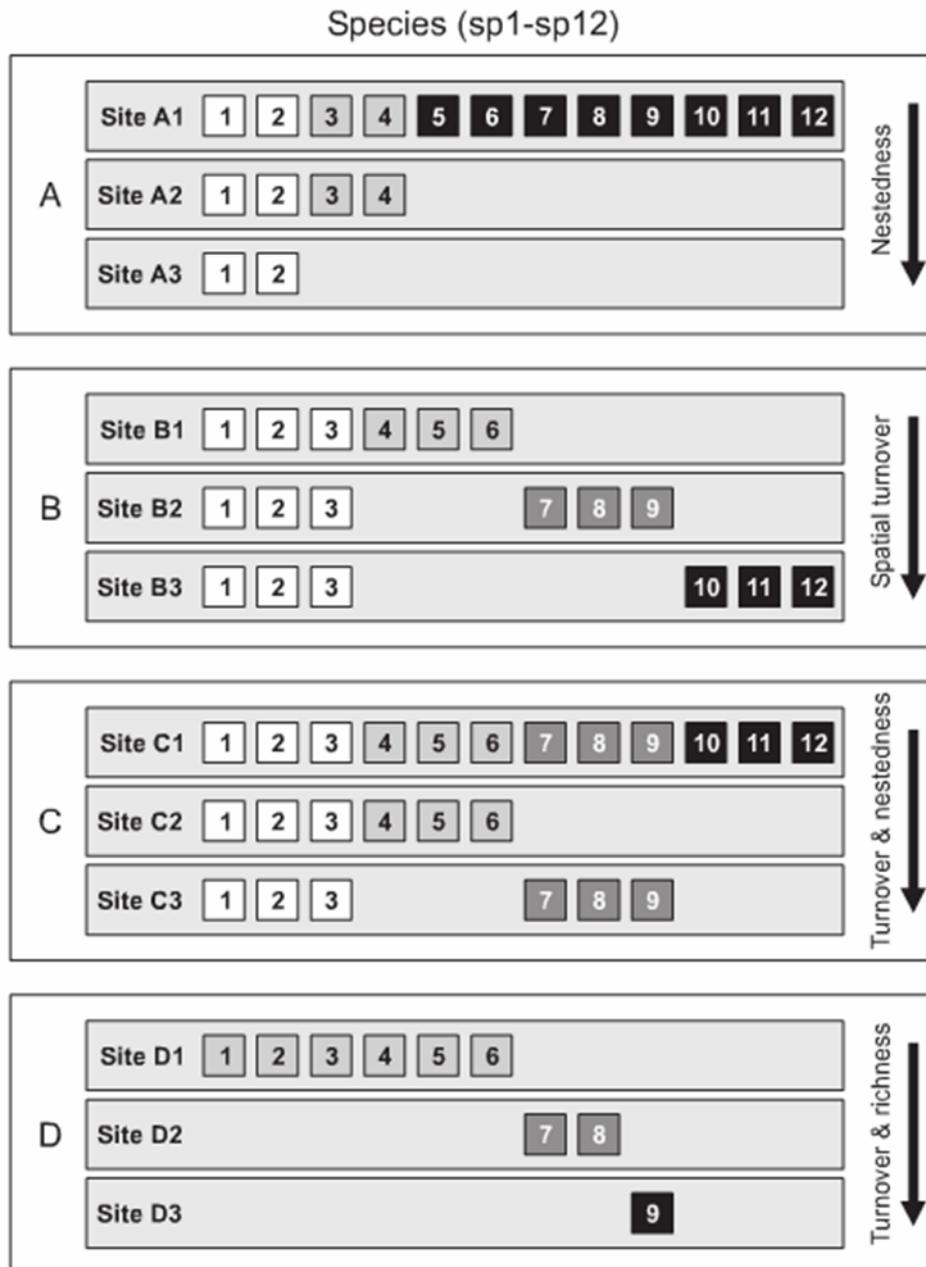
Figure 1.12. The different components of the β-diversity. β-diversity may be caused by nestedness only (A), turnover only (B), nestedness and turnover (C) or turnover and species loss (D). Image from Baselga (2010).

Energy, environmental stress and their interaction on biodiversity

One of the most studied drivers of community assembly is energy and its extension: productivity (Mittelbach et al., 2001). Productivity is defined as the rate of energy flow to

a system, for instance as in mg $C \cdot m^{-2} \cdot yr^{-1}$. Despite its straightforward definition, it is rarely measured directly and instead indirect measures are used such as radiance, rainfall and biomass among others (Mittlebach et al., 2001). The availability of radiation, kinetic and chemical energy deeply shapes biodiversity patterns on Earth and is referred as the productivity-diversity relationship (PDR) (Gaston, 2000; Mittelbach et al., 2001; Woolley et al., 2017). Highly-productive habitats usually support more biodiversity (eg., Gaston, 2000; Mittlebach et al., 2001; Chase and Leibold, 2002; Chase, 2010). The shape of the productivity-diversity relationship and its causes have been a matter of discussion for decades (Mittelbach et al., 2001; Chase & Leibold, 2002; Gillman and Wright, 2006; Pärtel et al., 2007; Whittaker, 2010a, b; Gillman and Wright, 2010; Pärtel et al., 2010). The relationship is thought to be scale-dependent and more frequently, albeit not always, positive-humped or positive-linear at local, regional and global scales (Mittelbach et al., 2001; Chase & Leibold, 2002). Dozens of hypotheses have been formulated in order to explain the productivity-diversity relationship. At more local scales (including the scale of the present thesis) some of the most debated hypothesis are:

- **More-Individual hypothesis** (Wright, 1983; Srivastava and Lawton, 1998): energy availability limits the total number of individuals that a community harbors, which in turn restricts the number of species with viable populations (see Storch et al. (2018) for a review). A monotonic increase of the number of individuals and diversity is expected with increasing energy.

- **Resource competition theory** (Tilman, 1977): this theory departs from the assumption that no single species can be competitively dominant for all resources.

A positive hump-shape PDR is expected due to competitive exclusion of different dominant species at high and low productivity, respectively, and their coexistence at intermediate regimes.

- **More specialization theory** (Schoener, 1976; and sensu McClain and Schlacher (2015)): at high productivities, some resources may be abundant enough to both allow specialist species to exploit specific resources and to prevent competitive exclusion. At low productivities, resources are too scarce so that specialist species may not be able to exploit them. A positive linear PDR is expected.

- **Productive space hypothesis** (Post, 2002): since energy-transfer efficiency is low between basal and higher trophic levels, high productivities promote higher diversity by supporting more trophic levels.

Disturbance and environmental stress also have been long recognized as main drivers of community structure and biodiversity patterns (e.g., Mouillot et al., 2013). One of the most influential models is the *Intermediate Disturbance Hypothesis* of Connell (1978). This hypothesis predicts that along an increasing gradient of stress, diversity will be low at both extremes due to the extinction of poorly-adapted species at higher stress levels and the exclusion of poorly-competitive species at lower stress levels. Diversity thus is predicted to peak at intermediate level of disturbance due to the coexistence of stress-tolerant and competitive dominant species. Literally hundreds of studies have given either support, partial support or refute the theory (Violle et al., 2007, Svensson et al., 2012;

Fox, 2013a, 2013b; Sheil and Burslem, 2013), although one of the main issues are the many different measures of biodiversity used in tests, especially those integrating richness and abundance (Svensson et al., 2012). Of special interest is the dynamic equilibrium hypothesis of Huston (1979) which integrates productivity and stress to predict diversity. This model shows that at high productivity regimes strong disturbances are required to counteract competitive exclusions, whereas at lower productivity, weak disturbances are enough to prevent competitive exclusion. Interestingly, at intermediate productivity regimes, the predictions of Connell (1978) and Huston (1979) overlap because highest diversity is predicted at intermediate levels of disturbance.

Current community assembly approaches

For decades, community ecology focused on species and their relationships with environmental factors (Lawton, 1999; McGill et al., 2006). In consequence, unlike other disciplines, community ecology produced uncountable case-specific studies preventing the statement of generalities and ecological theories (Lawton, 1999; McGill et al., 2006). Yet, biodiversity is a multifaceted complex concept that also embraces, for instance, species performances, i.e., the functioning of species or the functional diversity (Diaz and Cabido, 2001). The analysis of functional diversity is an alternative to produce more ecological meaningful statements and to better understand the processes and mechanisms underlying species distributions (McGill et al., 2006). Functional diversity is defined as the value and range of functional traits of organisms (Diaz and Cabido, 2001). Functional

traits are organism features that reflect responses to the environment (response traits), effects on ecosystem functioning (effect traits) or a mixture of both (Diaz and Cabido, 2001) (Figure 13). In other words, as Petchey and Gaston (2006) wrote "*functional diversity generally involves understanding communities and ecosystems based on what organisms do, rather than on their evolutionary history*". Thus, functional diversity is for obvious reasons of particular interest for the study of community assembly (McGill et al., 2006) and the linkage between community and ecosystem ecology (Weiher, 2011; Mittlebach, 2012).

Conventional wisdom holds that if niche-based processes, such as competition or environmental filtering, are mainly driving the assembly of a given community a non-random distribution of species and/or traits would be expected (Figure 13) (e.g., Mouchet et al., 2010; Mouillot et al., 2013; Weiher et al., 2011). A higher co-occurrence of dissimilar traits than that expected by chance, i.e., trait over-dispersion, is expected when competition is structuring assemblages. This is explained by the competitive exclusion and limiting similarity principles where co-existence between species is reached due to their different ecological niches (Hardin, 1960). On the contrary, a higher co-occurrence of very similar traits than expected by chance, i.e., trait under-dispersion, is expected under the effect of environmental filtering due to selection for similarly adapted species. Finally, random distribution of traits may point out on the role of neutral-based mechanisms in driving community assemblage (Hubbel, 2005; however see Kraft et al. (2015) and Cadotte and Tucker (2017) for a critical revision of niche-based assumptions). The importance of each mechanism is, in many cases, scale-dependent: environmental filtering has higher influence at regional scale whilst biotic interactions govern local

assembly of community (e.g., Chase, 2014). Arguably the main question nowadays is not *"which mechanism is valid in ecology but which mechanism has the strongest influence on communities* (Mouchet et al. 2010). This is true because communities mainly structured by competition are considered to be more stable under environmental stress than those structured by the environment (e.g., Didham et al., 2005; Ashford et al., 2018). A complementary approach may be applied using phylogenies to further support the patterns tested with traits (Webb et al., 2002).
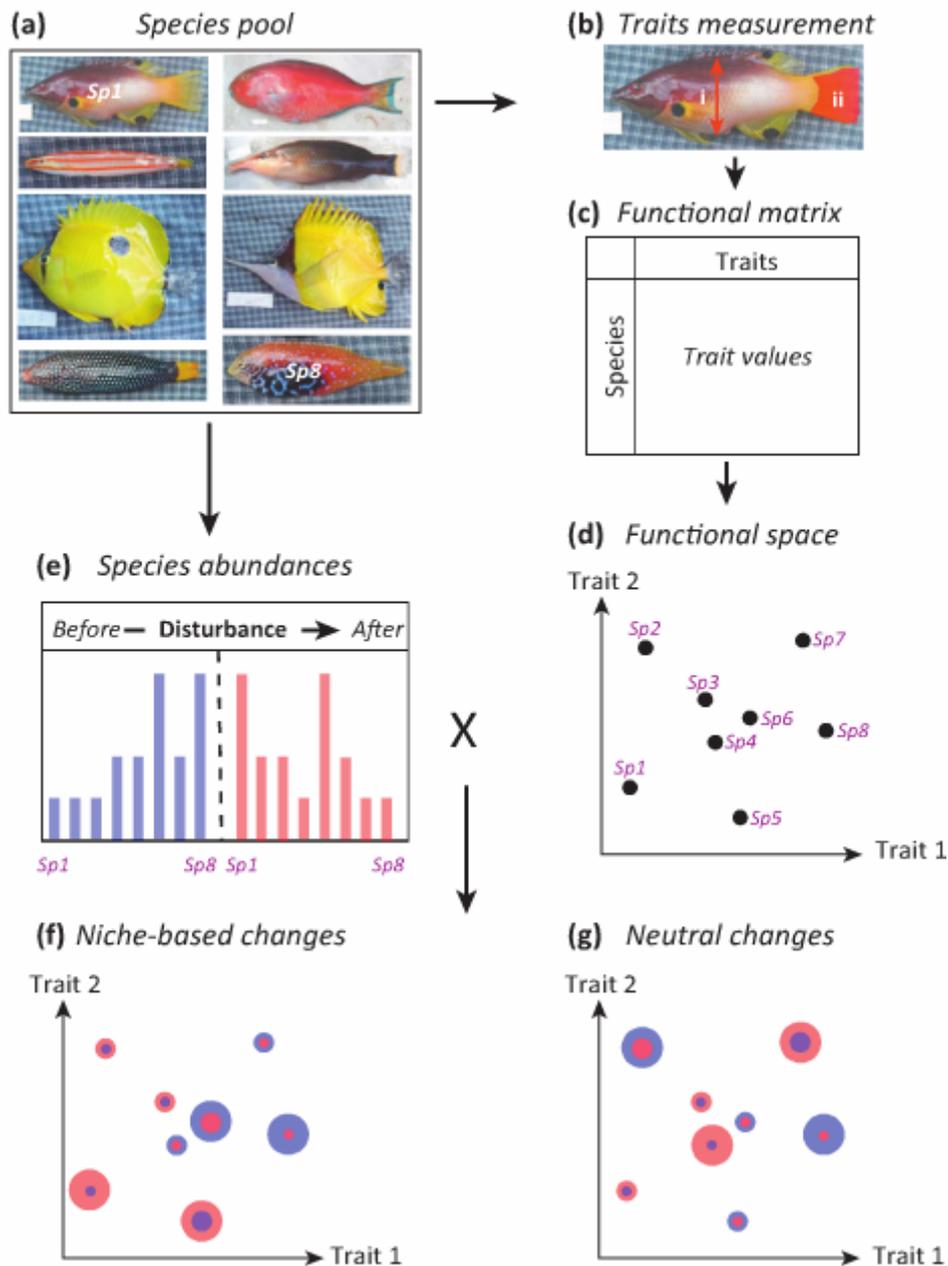
Figure 1.13. Putative changes of the functional structure (2-dimensional functional space) of an 8-species assemblage to a hypothetical disturbance. Image from Mouillot et al. (2013).

By analogy to the Hutchinsons's niche concept (1957), a powerful approach to determine functional diversity is to estimate the distribution of functional units in a n-dimensional trait space (Figure 13) (Villéger et al., 2008; Mouchet et al., 2010; Moulliot et al., 2013). Within this multifunctional space, several facets of functional diversity can be

estimated using functional indices with the potential to reveal the processes that structure assemblages (Mouchet et al., 2010). Arguably, most used indices are functional richness, divergence and evenness (Villéger et al., 2008). Conversely, the same approach was used with stable isotopes (e.g., Newsome et al., 2007; Rigolet et al., 2015; Cuchurusset et al., 2015). In ecology, stable isotopes have been traditionally used to reconstruct diets and gain insights into taxa diets (Layman et al., 2007; reviewed in Layman et al., 2012). Nevertheless, isotopes, generally $\delta^{13}C$ and $\delta^{15}N$, may also represent an integrated value with information on the physical habitat and trophic features, i.e, two main axes of the ecological niche of species (Newsome et al., 2007; Rigolet et al., 2015; Cuchurusset et al., 2015). Thus, in generating an scaled isotopic δ-space, analogous indices to those used for functional diversity, may be estimated. In the recent years, this powerful common framework for the study of functional and isotopic diversity has been extended to the functional and isotopic dissimilarity of communities, i.e., the functional and isotopic β-diversity, turnover and nestedness (Villéger et al., 2011; Villéger et al., 2013; Cuchurusset et al., 2015).

Thesis objectives

The main objective of the present thesis was to investigate the early processes driving community assembly in hydrothermally active habitats and vent periphery of the Lucky Strike vent field on the northern Mid-Atlantic Ridge. This was done by deploying an integrated colonization experiment along an environmental gradient, from stressful active to stable inactive peripheral areas, during two years. To complete the picture, the interactions with cognate communities, namely wood falls, were also investigated. In order to achieve these goals, a modern multifaceted framework of community assembly based on species, functional traits and stable isotopes was applied. Aside of local patterns of species distribution, dissimilarities (β-diversity) were investigated taxonomically and functionally using different complementary frameworks. This thesis is organized in two main result chapters (chapters 3 & 4) preceded by one methodological chapter (chapter 2) explaining the construction of the detailed dataset that includes taxonomic, functional and isotopic biodiversity found in colonizing substrata. The last chapter (chapter 4) is a general discussion, including some conclusions and perspectives.

Chapter 1:

This chapter explains the colonization experiment, the faunal sorting/identification phase and the construction of the extensive dataset that was produced during this thesis. Three different but complementary aspects of biodiversity were analyzed: species richness, species functional traits and species isotopic values.

Chapter 2:

The main objective of this chapter was to better understand the interactions between environmental stress and energy availability on early community assembly in vents. In order to do so, the colonization of taxa on slate substrata at four contrasting active and inactive sites representing a gradient of hydrothermal activity within the Lucky Strike vent field was analyzed. Species and functional biodiversity patterns and composition of the colonizing fauna were compared. In order to gain insight into community assembly processes, I applied a null model to determine the effect of environment to functional richness in each of the studied sites. Applying the Legendre and De Caceres (2013) framework, species and functional β-diversity were quantified, decomposed into turnover and nestedness components and the Local Contributions to β-Diversity indices were calculated to evaluate 1) the influence of the environment on faunal assemblages, 2) the component of β-diversity leading to the observed patterns and 3) the sites of the study contributing more than expected to the global dissimilarity. Functional β-diversity was estimated at each site, which constitutes an innovative approach in these environments. In this chapter, stable isotope analyses were analyzed on the fauna at each deployment site to determine the origin of the consumed organic matter and examine the energetic gradient of primary productivity of chemosynthetic origin from active to peripheral sites.

Chapter 3:

The main objective of this chapter was to compare species and functional biodiversity patterns and the structure of early-stage communities between vents and woods and identify the main influencing drivers. In order to do so, colonizing slate and wood substrata were analyzed in four different groups consisting of: 1) slate and 2) wood substrata placed in hydrothermal vent conditions and 3) slate and 4) wood substrata placed at inactive periphery. Three complementary biodiversity facets were analyzed in this chapter based on species richness, functional traits and stable isotopes following a similar framework for α- and β-diversity. For functional diversity, I applied a null model to determine the effects of environment and substrata type on functional richness in each of the four groups to gain insights into the drivers structuring communities. Stable isotopes were used to construct isotopic spaces and their derived isotopic indices using the same framework for functional diversity as Villéger et al. (2008), which allowed the analyses of functional and isotopic niche overlaps. I also used an extension of this framework based on Baselga (2010) for the study of β-diversity (extended for functional and isotopic β-diversity after Villéger et al. (2011) and Cuchurusset et al., 2015) to quantify and decompose the assemblage dissimilarities into the turnover and nestedness components.

Chapter 1

A multifacet database

A multifacet database

In order to achieve the thesis goals, an important investment was done on the construction of a unique dataset that includes three different but complementary aspects of biodiversity: species richness, species functional traits and species isotopic values. The dataset was used afterwards, partially or completely, to answer the specific questions of the two result chapters. All of these data were obtained by myself during the thesis with the help/supervision of experts in different fields (taxonomy, traits, isotopes), that are either coauthors of the papers to be submitted or acknowledged within them.

Study area: the Lucky Strike hydrothermal vent and the Eiffel Tower edifice

The Lucky Strike hydrothermal vent field (47º13′30′′ N, 32º16′30′′ W) was discovered serendipitously during the French-American Ridge Atlantic program (FAZAR) when scientists obtain sulfide material with vent fauna from a dredge (Karson et al., 2015). The Lucky Strike hydrothermal vent field is located at ~1700 m depth on the Mid-Atlantic Ridge (MAR) at approximately 400 km south from the Azores (Karson et al., 2015). Hydrothermal activity at Lucky Strike is mainly located within the summit depression of Lucky Strike Seamount at ~1700 m depth in, and along, the sides of a solidified lava lake. Lucky Strike Seamount represents one the largest axial volcanoes within the MAR. The magma chamber fueling venting activity is located at ~3.5 km depth beneath the seafloor and is 3 to 4 km wide (Karson et al., 2015). Active and inactive hydrothermal deposits are distributed along an area of ~1km^2 in about 30 vent sites.

Hydrothermal venting is mainly located on extensive deposits of sulfide both east and west of the lava lake. In the eastern zone, black smoker chimneys can be up to 20 m in height, and deposits have complex morphologies of up to 20 m in diameter, such as those found in the Eiffel Tower edifice.

The Eiffel Tower is a 11 m-high edifice situated at the southeast of a fossil lava lake. The structure harbors several black smokers with temperature up to 324 °C and extensive diffuse flow areas (Charlou et al., 2009; Cuvelier et al., 2009) (Figure 2.1A). Bottom seawater temperature in the area is around 4.4°C (Cuvelier et al., 2009; Sarrazin et al., 2015). The Eiffel Tower edifice harbor communities that are representative of the entire Lucky Strike vent field (Desbruyères et al., 2001). Eiffel Tower is dominated by two faunal assemblages: one associated to the shrimp *Mirocaris fortunata* in the more restricted and "warmer" microhabitats, and the other associated to the ecosystem engineer mussel *Bathymodiolus azoricus* in "colder" microhabitats (Desbruyères et al., 2001; De Busserolles et al., 2009; Cuvelier et al., 2009; Cuvelier et al., 2010; Sarrazin et al., 2015; Husson et al., 2017).

Despite small scale variations inherent to changes in the fluid fluxes, temporal studies showed a remarkable global stability of assemblages on the edifice for over a decade (Cuvelier et al., 2011). Warmer microhabitats, with mean temperatures of 9.5°C, are areas of very porous anhydrite substrata and highly variable environmental conditions. *M. fortunata* is a highly mobile species, able to tolerate temperatures up to 36°C

(Shillito et al., 2006). These two characteristics may be key to explain the dominance of this species in warmer, more unstable, habitats. On the other hand, *B. azoricus* individuals are attached between them and to the substratum by their byssus. They form extensive beds in areas where mean temperature range from 4.8 to 8.8°C. Anhydrite substratum may be unsuitable for sessile invertebrate due to its physical instability (Tunnicliffe & Juniper, 1990). In addition, environmental conditions on anhydrite substrata may be too harsh to allow the establishment of *B. azoricus* (Cuvelier et al., 2009). Kelly & Metaxas (2006) in a colonization experiment at anhydrite chimneys on the Juan de Fuca ridge (NE Pacific) found low colonization on substrata placed at anhydrite chimneys. Thus, the environmental conditions rather than substratum properties may explain the absence of the mussel in anhydrite substrata.

B. azoricus assemblages are segregated by their sizes, producing a zonation-like pattern (Comtet & Desbruyères, 1998; Desbruyères et al., 2001). Larger mussels (>6 cm) are associated to the upper end of the environmental gradient with peaks of ~14 °C (Desbruyères et al., 2001; De Busserolles et al., 2009; Cuvelier et al., 2009; Cuvelier et al., 2010; Husson et al., 2017). Medium-size mussels (1.5-6 cm) colonize microenvironments belonging to the intermediate environmental gradient, whereas small mussels (0.5-1.5 cm) colonize the end of the gradient with temperatures close to ambient seawater (De Busserolles et al., 2009; Cuvelier et al., 2009; Cuvelier et al, 2010; Husson et al., 2016). The forces driving these patterns remain a topic of discussion and several non-exclusive explanations have been proposed.

Along the hydrothermal gradient, some patterns on the distribution of associated heterotrophic species have also been reported (Sarrazin et al., 2015; Husson et al., 2017). Polychaetes and copepods tend to dominate warmer habitats, whereas gastropods and nematodes are more abundant in colder habitats (Sarrazin et al., 2015; Zeppilli et al., 2015; Husson et al., 2017; Plum et al., 2017). Overall densities and species richness of both meio- and macrofauna tend to be higher in colder habitats (Sarrazin et al., 2015; Husson et al., 2017).

Peripheries around active areas are poorly known habitats and the information comes from visual observations and/or colonizing experiments (Desbruyères et al., 2001; Zeppilli et al., 2015; Plum et al., 2017; Baldrighi et al., 2018). Fauna consist of filter-feeding and small sessile carnivore species scattered around, such as cirripeds and hydroids, and highly mobile ichthyofauna, which make frequent intrusions into active areas (Desbruyères et al., 2001). Despite low densities, results of previous colonization experiments around Eiffel Tower showed that diverse assemblages of copepods and nematodes, with numerous "rare" species, also inhabit the poorly-sedimented and bare-basalt substrata found at peripheries (Zeppilli et al., 2015; Plum et al., 2017; Baldrighi et al., 2018). Many of these copepods have appendix structures, such as claw-like setae, suggesting their adaptations to hard substrata (Plum et al., 2017). Towards active environments some generalist species become dominant, while sensitive "rare" species disappear (Zeppilli et al., 2015). This is somehow opposed to what is observed for

macrofauna, which increase the dominance and density but also the degree of specialization from periphery to active areas.

The experiment

This thesis is entirely based on a colonizing experiment of 2 years of duration. Four "sites" representing different hydrothermal vent regimes and the heterogeneity of habitats of the Lucky Strike vent field were selected (Figure 2.1, B-E). Sites were located along and away the Eiffel Tower edifice and correspond to those of other previous pilot studies (Cuvelier et al., 2014; Zeppilli et al., 2015; Plum et al., 2016; Baldrighi et al., 2018). The "active" site is located on the north-west side of Eiffel Tower and is the most active site of this experiment, with the presence of microbial mats and a small high-temperature chimney in the vicinity (few cm) (Figure 2.1B, Figure 2.2A). The "intermediate" site is located on the western side of the edifice, in an area of diffuse flow (Figure 2.1C, Figure 2.2B). Both sites are colonized by dense assemblages of *B. azoricus*. The "periphery" site is located in a poorly sedimented area with no visible hydrothermal activity between the Eiffel Tower (~50 m) and Montségur edifices (~85 m) (Figure 2.1D, Figure 2.2C). The "far" site is located on a basaltic seabed on the west side of the lava lake with no visible hydrothermal vent activity, at ~90, ~120 and ~470 m away from Helen, Pico and ET active edifices, respectively (Figure 2.1F, Figure 2.2D).

At each site, three slate and oak wood size-standardized substrata (~10 cm^3) were deployed in 2013 during the MoMARSAT cruise (https://doi.org/10.17600/13030040) on board of the R/V *Pourquoi pas?*, using the ROV *Victor6000*. Slates were chosen due to their basalt-like smooth and inert characteristics (Cuvelier et al., 2014; Zeppilli et al., 2015; Plum et al., 2017), whereas woods were chosen due to their potential for sustaining chemosynthesis and colonization by hydrothermal vent taxa (e.g., Bienhold et al., 2013). Temperature at each site was recorded for 9 months every 15 minutes with an autonomous NKE ST 6000 temperature probe attached to wood substrata (Figure 2.3). All substrata were recovered after two years with the ROV Victor6000, during the MoMARSAT 2015 cruise (https://doi.org/10.17600/15000200).
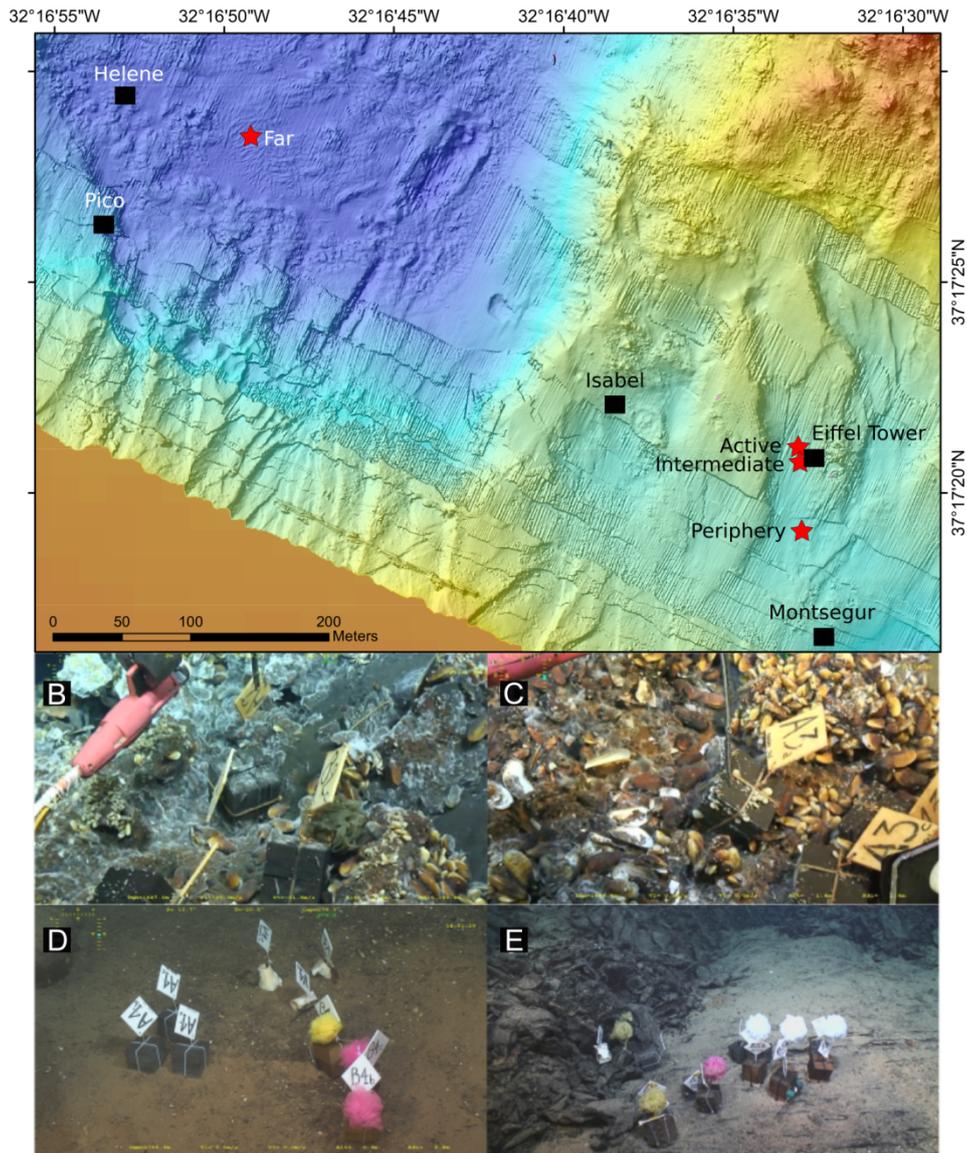
Figure 2.1. The southeast region of the Lucky Strike vent field located at 1700 m depth on the Mid-Atlantic Ridge, south of the Azores. A. Locations of the four deployment sites (red stars) and surrounding main active edifices (black squares). Note that the far site is located further west, in the fossil lava lake. Colonized substratum blocks at B. active, C. intermediate, D. periphery and E. far sites. Also visible in the photos are the other types of substratum used in parallel experiments.
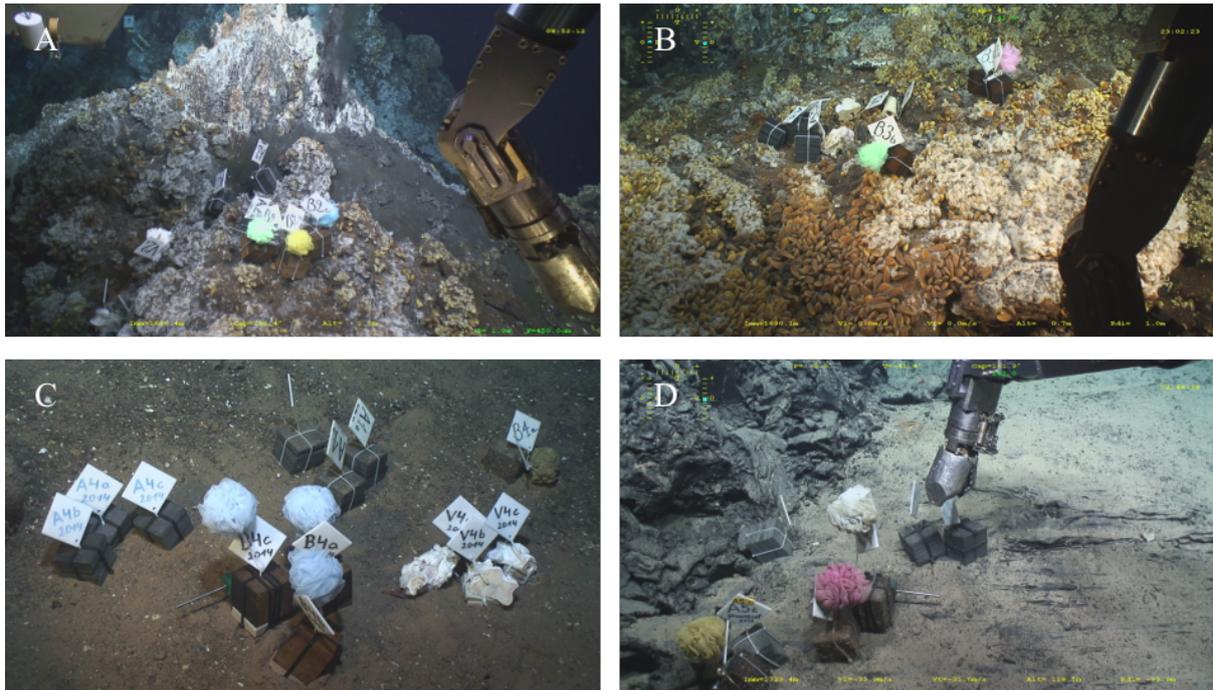
Figure 2.2. Pictures of the different sites. A. Active site. B. Intermediate site. C. Periphery site. D. Far site. Note the in A and B the by dense assemblages of B. azoricus mussel. The periphery and the far sites located in an area with no visible hydrothermal activity and in a poorly sedimented and on a basaltic seabed, respectively.
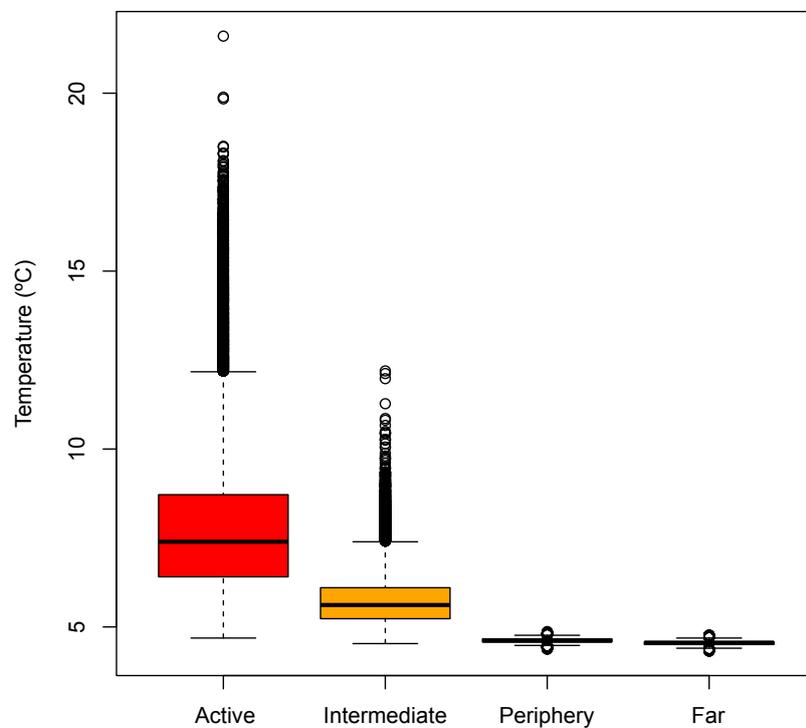
Figure 2.3. Box plots of temperatures registered during 9 months at the different sites along (Active & Intermediate) and away (Periphery & Far) the Eiffel Tower edifice in the Lucky Strike.

Sample processing and faunal sorting

Once on board, each substratum was carefully washed with filtered seawater and sieved through 300-µm and 20-µm mesh sieves to separate the meio- and macrofaunal compartments. Due to the small size of benthos, the use of 300 and/or 500 µm mesh sieves to sample macrofauna has become common in the deep sea (e.g., Montagna et al., 2017). Meiofauna is defined as the fraction of taxa that pass through a 1 mm sieve (Gière, 2007). In this thesis, I refer to meiofauna and macrofauna to the taxa found in 20-µm and 300-µm mesh sieves, respectively, acknowledging that they do not correspond to the strict definitions of meio- and macrofauna, and that typical groups of both compartments will be present in the 300-µm compartment. Meiofaunal samples were placed in 4% seawater-buffered formalin while macrofaunal samples were preserved in 96° ethanol. Two substratum of each site were individually preserved in 96° ethanol while the third was individually preserved in 4% seawater-buffered formalin for further examination in the laboratory.

The taxonomic facet: species and morphospecies

Once in the laboratory, sieved samples were sorted manually under a stereomicroscope and all taxa was counted and classified to the lowest taxonomical level possible. Larvae and individuals without head were discarded and not considered further. Some groups of taxa were classified with the help of experts, either coauthors or acknowledged in chapters. In the specific case of slate substrata, *B. azoricus* individuals

were gently placed horizontally in Petri dishes under the stereo microscope and sized

using the software Leica Application Suit (LAS) version 4.9.0 for preliminary (see below).

Large *B. azoricus* individuals (>1 cm) were sized manually using calipers. Meiofaunal

samples were transferred to 200 ml beakers and 3 subsamples of 5 ml each were taken

from the original volumes and stained with Phloxine. A maximum of 100 randomly-

collected individuals of the different meiofaunal groups were mounted on slides and

classified to the lowest taxonomical level possible. Prior to be mounted on slides,

nematodes were passed through a formalin-ethanol-glycerol treatment to prevent

dehydration (see Zeppilli et al., 2015). Nematodes and copepods from meiofaunal

samples were identified under the microscope. Due to the difficulty of confidently

determine the species or morphospecies, juveniles of macrofaunal taxa found in 20-µm

samples were not considered in the present study.

After sampling on hydrothermally active areas, to the best of my knowledge

Sarrazin et al. (2015) as well as Husson et al. (2017) reported the highest number of species,

a total of 70 and 79 species (Table 2.1). In this thesis, 6845 and 29013 individuals found in

the meio- and macrofauna compartments were classified in a total of 116 species and/or

morphospecies in hydrothermally active and periphery conditions along and away of the

edifice in slate and wood substrata (Table 2.3). Considering slate substrata only, a proxy

of natural vent substrata, 77 taxa were identified in hydrothermally active and inactive

conditions (see Chapter 3). Many taxa were found exclusively on wood placed at

periphery and far site. Indeed, several species were wood-fall specialists and are further

discussed in Chapter 4.

Table 2.1. Studies of natural assemblages or colonizing experiments and the biodiversity found. *Only mineral substrata (e.g., slate) mimicking vent environment is considered.

Study	Edifice	Taxa	Sampling methods	Sampling zone	Identified taxa
Van Dover et al. (1996)	Eiffel Tower, Sintra and Statue	Not specified, presumably mega- and macrofauna	In situ observations, sampling of biota	Vent and the surrounding seafloor habitat.	25
Van Dover & Trask (2000)	Eiffel Tower and Sintra	Macrofauna and meiofauna (>63 μm)	ROV manipulator (5 replicates)	Mussel beds	28
Cuvelier et al. (2014)*	Eiffel Tower	Macrofauna (>250 μm) and meiofauna (250-63 μm)	2-years colonization experiment, 3 sites, no replicates	Mussel beds	45
Sarrazin et al. (2015)	Eiffel Tower	Macrofauna (>250 μm) and meiofauna (250-63 μm)	ROV grabs and slurp gun (12 replicates)	Mussel beds	70
Zeppilli et al. (2015)*	Eiffel Tower	Meiofauna (250-20 μm) (nematods only)	9-months colonization experiment; 4 sites, no replicates	Mussel beds and inactive peripheries	23
Plum et al. (2016)*	Eiffel Tower	Meiofauna (>20 μm) (copepods only)	2-years colonization experiment, no replicates	Mussel beds and inactive peripheries	45
Husson et al. (2017)	Eiffel Tower	Macrofauna (>250 μm) and meiofauna (250-63 μm)	ROV grabs and slurp gun	Mussel beds	79
This thesis	Eiffel Tower	Macrofauna (>300 μm) and meiofauna (>20 μm)	2-years colonization experiment; 4 sites, 3 replicates per site	Mussel beds and inactive peripheries	77

Slate substrata at hydrothermally active sites (active and intermediate sites) were

placed directly on *Bathymodiolus azoricus* mussel beds. It can be argued that taxa found in

colonizing substrata could be immigrants rather than colonizers thus questioning the validity of using this experiment to study colonization and early community assembly processes in vents. Observations during recovery however, evidenced that substrata at both sites were not entirely covered by mussels although they were placed directly on their beds (Figure 2.1 and 2.2). Furthermore, the small individual sizes of mussels strongly suggest that *B. azoricus* assemblages on substrata were the result of colonization rather than immigration from nearby beds (Figure 2.4) (Comtet and Desbruyères, 1998). In fact, large mussels (> 1 mm) were rare on colonizing substrata (Figure 2.4). Although immigration from surroundings for other species cannot be neglected based on *B. azoricus* data, I confidently address thesis goals. To disentangle the drivers of *B. azoricus* zonation along the hydrothermal vent gradient was not a goal of this thesis. Nevertheless, size analyses provided some interesting insights that are discussed below.

B. azoricus forms extensive beds in the Lucky Strike field at hydrothermally active areas ranging from almost background temperatures to up to 30°C (Van Dover et al., 2005; Comtet and Desbruyères, 1998; Cosel et al., 1999; Sarrazin et al., 2015). However, larger mussels (>6 cm) usually dominate areas with warmer and more variable temperatures, whereas small mussels (0.5-1.5 cm) dominate the end of the gradient with more stable temperatures close to ambient seawater (Comtet and Desbruyères, 1998; de Busserolles et al., 2009; Cuvelier et al., 2009; Cuvelier et al, 2010; Sarrazin et al., 2015; Husson et al., 2016). Results of this experiment suggest that *B. azoricus* is able to settle at environments with peaks of over 20°C even in the absence of abundant adult assemblages. Of all hypotheses

proposed to explain *Bathymodiolus* zonation, these results strongly support the early hypothesis of Comtet and Desbruyères (1998) that intra- and inter-specific competition at warmer environments, and not the harsh environment itself, are the main factors driving zonation. Nevertheless, the intermediate site was more colonized by *B. azoricus* and the recruits were larger than at active sites (Figure 1) suggesting that post-larvae and juveniles may suffer higher mortality rates at harsher environments.
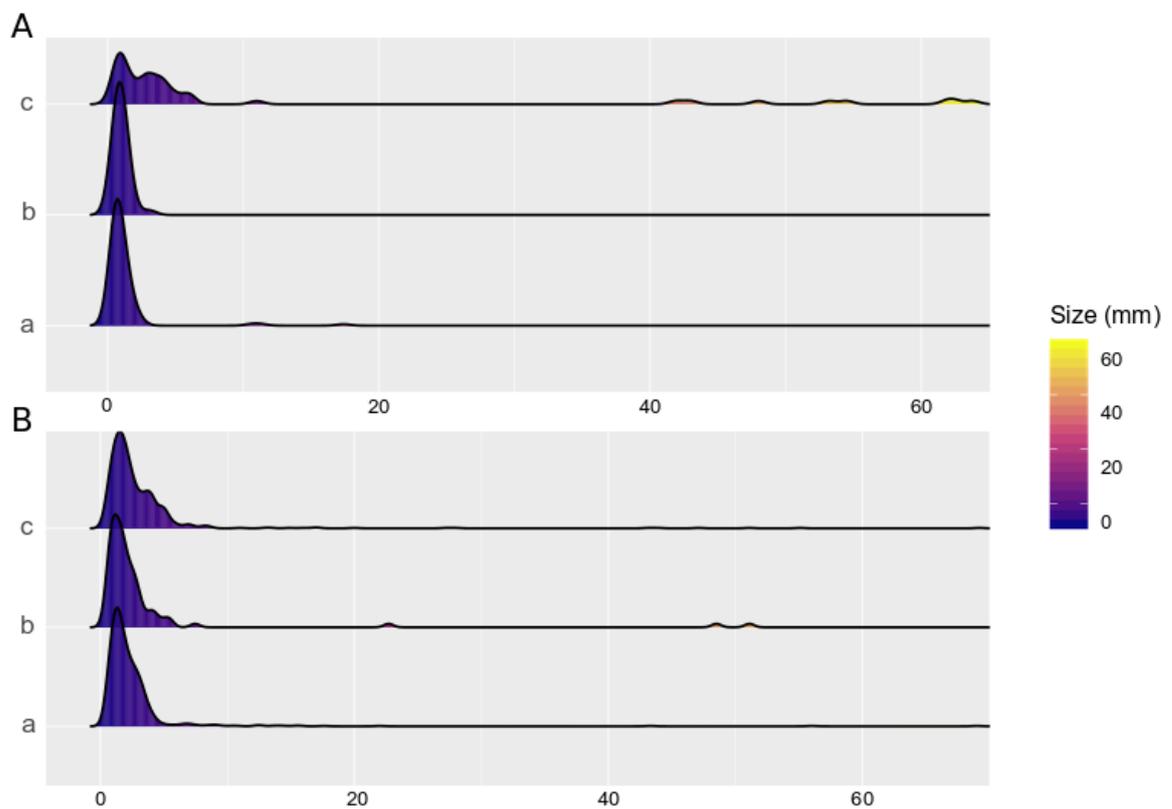
Figure 2.4. Histograms of size of *Bathymodiolus azoricus* colonizing the three (a-c) slate substrata at (A) the active and (B) the intermediate site.

The functional facet: species functional traits

Three functional response traits putatively related to productivity and stress were attributed to the different sampled species (total of 116 species). They include "adult mobility", "adult body size" and "feeding mechanism" (Tables 2 and 3). Traits were obtained from direct measurements and/or literature, including the sFDVent database (Chapman *et al.* 2019). For missing data, experts were consulted or the information was obtained from close-relative species inhabiting similar habitats, if possible.

The three functional response traits were selected due to their relationship with productivity and stress. Adult mobility affects the ability of a species to access suitable habitat and nutritional sources (Chapman et al., 2019). More mobile species may be less vulnerable to the environment stress and predation (Bates et al., 2010). Size is fundamentally related to energy flow and nutrient cycling (McGill et al., 2006). It affects the physiological tolerance of organisms (thermal mass, barriers to diffusion, and limits anatomical, physiological or behavioral options) and it is also tightly related to dispersal and reproduction (Gollner et al., 2015; McClain et al., 2018a). Feeding mechanism are indicators of ecosystem productivity or energy availability (Post, 2002; McClain et al., 2018b).

These traits were also chosen because were easily derived from morphological analyses of fauna and/or bibliography. Other traits were also of interest for answering the questions addressed in this thesis but none information was available or were difficult to obtain for many taxa. Among these traits, the type of larvae was of particular interest due to its relationship with the dispersion of the species and the energetic investment of

adults. This information was available for several gastropods but virtually for none of the

polychaete species founded (Desbruyeres et al., 2006).

Table 2.2. Functional traits, definition and modalities, analyzed in fauna of this thesis.

Trait	Modalities	Definition	Rationale	References
Adult motility	1 (Sessile)	Non-mobile	This trait affects the ability of a species to access suitable habitat and nutritional sources. More mobile species may be less vulnerable to the environment stress and predation.	Bates et al. (2010); Chapman et al. (2019)
	2 (Facultative)	Regularly non-mobile and only moving when necessary.		
	3 (Slow)	Regularly free slow swimmer, walker or crawler.		
	4 (Fast)	Regularly free fast swimmer and/or walker.		
Adult body size	0	0,02 - <0,3 mm	Size is fundamentally related to energy flow and nutrient cycling. It affects the physiological tolerance of organisms (thermal mass, barriers to diffusion, and limits anatomical, physiological or behavioral options). It is also tightly related to dispersal and reproduction.	McGill et al. (2006); Gollner et al. (2015); McClain et al. (2018a)
	1	≥0,3 - <1 mm		
	2	≥1 - <5 mm		
	3	≥5 - <10 mm		
	4	≥10 - <15 mm		
	5	≥15 - <20 mm		
	6	≥20 mm		
Feeding mechanism	Symbiotic	Obtain energy from a symbiotic relationship	Feeding mechanisms are indicators of ecosystem productivity or energy availability. A diverse community will likely harbor species with diverse feeding mechanisms and trophic levels.	Post (2002); McClain et al. (2018b)
	Filter feeder	Obtain food particles mainly from filtering the water column		
	Deposit feeder	Mainly obtain food particles from the surface or buried food particles from the subsurface		
	Grazing	Scrap or nibble food from substrate.		
	Predator	Mainly capture animals capable of resistance.		

The isotopic facet: $\delta^{13}C$, $\delta^{15}N$ and $\delta^{34}S$ stable isotopes

I analyzed the $\delta^{13}C$, $\delta^{14}N$ and $\delta^{34}S$ of 326 samples belonging to 42 species found on 300 μm samples (Table 3). Some of these species were found in 300 μm samples as well. These three stable isotopes were chosen due to their ability to express distinct values depending on the energy pathways and origin. Previous studies have shown that in vent systems, including the Eiffel Tower, the input of organic matter from photosynthetic origin may be neglected since these systems are largely based on *in situ* chemosynthetic production (e.g., de Busserolles et al., 2009; Portail et al., 2018). The 300 $\delta^{13}C$ is a very useful isotope because it may reflect several chemosynthetic pathways. For instance, $\delta^{13}C$ values from -15‰ to -10‰, -12.9±3.4‰, and from –36‰ to -30‰ reflect methanotrophy, reductive tricarboxylic acid (rTCA) and Calvin-Benson-Bassham (CBB) cycles, respectively (e.g., Reid et al., 2013; Portail *et al.* 2018). Nitrogen in vent systems may reflect two distinct sources of inorganic N acquisition by primary producers (microorganisms and *B. azoricus*) with very different signatures, i.e., nitrates ($\delta^{15}N$= 5-7‰) and ammonium ($\delta^{15}N$<0‰) (Lee and Childress, 1994; Riekenberg et al., 2016). $\delta^{34}S$ may present very distinct values depending on its origin with values around and below 10‰ for organic matter of chemosynthetic origin and values around or over 19‰ for photosynthetic origin (e.g., Reid et al., 2013).

The $\delta^{13}C$ and $\delta^{14}N$ values were estimated for all the 42 species whereas $\delta^{34}S$ was estimated for 32 species due to low tissue masses. For larger taxa, muscle tissue was used. Guts and calcareous structures were removed whenever possible manually. Inorganic

carbon present in samples can be a source of bias in carbon stable isotope analysis. "Champagne tests" were used to highlight the presence of carbonates in tissues (Jaschinski et al. 2008) and, when positive, samples were acidified by exposing them to HCl vapours for 48h in an airtight container (Hedges & Stern 1984). After acidification, a second "champagne test" series were run. When the second test was still positive we proceeded with direct acidification (0.2 ml of 10% HCl added directly to the sample in a silver cup) (Jaschinski et al 2008). Isotopic analyses were done at the University of Liège (Belgium) by Dr L Michel (LEP, Ifremer) using a vario MICRO cube (Elementar, Germany) elemental combustion system coupled to an IsoPrime100 (Elementar, United Kingdom) isotope ratio mass spectrometer. Isotopic ratios were expressed using the widespread δ notation (Coplen 2010), in ‰ and relative to the international references Vienna Pee Dee Belemnite (for carbon), Atmospheric Air (for nitrogen) and Vienna Canyon Diablo Troilite (for sulfur). IAEA (International Atomic Energy Agency, Vienna, Austria) certified reference materials sucrose (IAEA-C-6; $\delta^{13}C$ = -10.8 ± 0.5‰; mean ± SD), ammonium sulphate (IAEA-N-1; $\delta^{15}N$ = 0.4 ± 0.2‰; mean ± SD) and silver sulfide (IAEA-S-1 $\delta^{34}S$ = -0.3‰) were used as primary analytical standards. Sulfanilic acid (Sigma-Aldrich; $\delta^{13}C$ = -25.6 ± 0.4‰; $\delta^{15}N$ = -0.13 ± 0.4‰; $\delta^{34}S$ = 5.9 ± 0.5‰; means ± SD) was used as secondary analytical standard. Standard deviations on multi-batch replicate measurements of secondary and internal lab standards (seabass muscle) analysed interspersed with samples (one replicate of each standard every 15 analyses) were 0.2‰ for both $\delta^{13}C$, 0.3‰ for $\delta^{15}N$ and 0.5‰ for $\delta^{34}S$.

Table 2. 3. Species sorted and identified in the present thesis, with their functional traits and the stable isotopes analyzed and the compartment found. M= macrofauna, m= meiofauna. See definition of traits modalities in Table 2.2.

Taxonomy				Functional traits				Stable isotope			Compartment	
Phylum	Class	Subclass	Species	Mobility	Size	Feeding	Reference	δ13C	δ15N	δ34S	m	M
Mollusca	Bivalvia	Pteriomorphia	*Bathymodiolus azoricus*	2	6	symbiotic	Desbruyères et al. (2006) and references therein	√	√	√		X
			Idas spp.	1	3	filter feeding	Rodrigues et al. (2015)	√	√	√		X
		Heterodonta	*Xyloredo* sp.	1	3	symbiotic	Voight (2015); authors pers. obs.	√	√	√		X
			Xylophaga sp.	1	3	symbiotic	Voight (2015); authors pers. obs.	√	√	√		X
	Gastropoda	Vetigastropoda	*Lepetodrilus atlanticus*	3	2	grazer	Desbruyères et al. (2006) and references therein	√	√	√		X
			Pseudorimula midatlantica	3	3	grazer	Desbruyères et al. (2006) and references therein	√	√	√		X
		Cocculiniformia	*Coccopigya spinigera*	3	3	grazer	Jeffreys (1883); Dantart and Luque (1994)	√	√	√		X
		Patellogastropoda	*Paralepetopsis ferrugivora*	3	5	grazer	Desbruyères et al. (2006) and references therein	√	√	√		X
		Vetigastropoda	*Protolira valvatoides*	3	2	grazer	Desbruyères et al. (2006) and references therein	√	√	√		X
		Heterobranchia	*Lurifax vitreus*	3	2	grazer	Desbruyères et al. (2006) and references therein	√	√	√		X
			Xylodiscula analoga	3	2	grazer	Desbruyères et al. (2006) and references therein					X
		Neomphalina	*Lirapex costellata*	3	2	grazer	Desbruyères et al. (2006) and references therein	√	√	√		X
		Neritimorpha	*Divia briandi*	3	3	grazer	Desbruyères et al. (2006) and references therein	√	√	√		X
		Neomphalina	*Peltospira smaragdina*	3	4	grazer	Desbruyères et al. (2006) and references therein					X
		Caenogastropoda	*Laeviphitus debruyeris*	3	2	grazer	Desbruyères et al. (2006) and references therein					X
			Phymorhynchus sp.	3	6	predator	Van Dover (1995)	√	√	√		X
Annelida	Polychaeta	Sedentaria	*Amphisamytha lutzi*	2	5	deposit feeder	Desbruyères et al. (2006) and references therein	√	√	√		X

	Taxon			Feeding	Reference				
	Paramytha sp.	2	5	deposit feeder	Jumars et al. (2015); Shimabukuro pers. obs.	√	√	√	X
	Acrocirridae sp.	3	3	deposit feeder	Jumars et al. (2015); authors pers. obs.				X
	Prionospio unilamellata	2	5	deposit feeder	Desbruyères et al. (2006) and references therein	√	√		X
	Laonice asaccata	2	6	deposit feeder	Desbruyères et al. (2006) and references therein	√	√		X
	Spionidae sp. 1	2	3	deposit feeder	Shimabukuro pers. obs.				X
	Capitella sp. 1	3	3	deposit feeder	Alfaro-Lucas et al. (2018); Shimabukuro pers. obs.	√	√	√	X
	Capitella sp. 2	3	4	deposit feeder	Alfaro-Lucas et al. (2018); Shimabukuro pers. obs.	√	√		X
	Opheliidae sp.	3	3	deposit feeder	Jumars et al. (2015)				X
	Flabelligeridae sp.	3	2	deposit feeder	Desbruyères et al. (2006) and references therein				X
Errant	*Glycera tesselata*	3	4	predator	Desbruyères et al. (2006) and references therein	√	√	√	X
	Sirsoe sp.	3	3	deposit feeder	Shimabukuro pers. obs.	√	√	√	X
	Hesionidae sp. 3	3	2	deposit feeder	Shimabukuro pers. obs.	√	√	√	X
	Hesionidae sp. 4	3	2	deposit feeder	Shimabukuro pers. obs.	√	√		X
	Hesionidae sp. 5	3	2	deposit feeder	Shimabukuro pers. obs.				X
	Pleijelius sp.	3	2	deposit feeder	Alfaro-Lucas et al. (2018)				X
	Branchipolynoe seepensis	4	6	deposit feeder	Desbruyères et al. (2006) and references therein	√	√	√	X
	Branchinotogluma sp. 1	4	3	predator	Jumars et al. (2015); authors pers. obs.				X
	Branchinotogluma sp. 2	4	4	predator	Jumars et al. (2015); authors pers. obs.				X
	Bathykermadeca sp.	4	4	predator	Jumars et al. (2015); authors pers. obs.				X
	Lepidonotopodium sp.	4	4	predator	Jumars et al. (2015); authors pers. obs.	√	√	√	X
	Harmothoe sp. 1	4	4	predator	Jumars et al. (2015); authors pers. obs.				X
	Harmothoe sp. 2	4	4	predator	Jumars et al. (2015); authors pers. obs.				X

			Malmgrenia sp.	4	4	predator	Jumars et al. (2015); authors pers. obs.				X
			Macellicephala sp.	4	2	predator	Jumars et al. (2015); authors pers. obs.	√	√		X
			Polynoidae sp. 1	4	4	predator	Jumars et al. (2015); authors pers. obs.				X
			Ophryotrocha cf. *platykephale*	3	2	grazer	Desbruyères et al. (2006) and references therein	√	√	√	X
			Ophryotrocha sp. 2	3	2	grazer	Desbruyères et al. (2006) and references therein				X
			Ophryotrocha fabriae	3	2	grazer	Desbruyères et al. (2006) and references therein	√	√		X
			Dorvilleidae sp. 1	3	2	grazer	Jumars et al. (2015); Shimabukuro pers. obs.				X
			Strepternos sp.	3	3	predator	Jumars et al. (2015); Shimabukuro pers. obs.	√	√	√	X
			Phyllodocidae sp.	3	3	predator	Jumars et al. (2015); authors pers. obs.				X
			Tomopteris sp. 1	4	2	predator	Jumars et al. (2015)				X
			Tomopteris sp. 2	4	2	predator	Jumars et al. (2015)				X
			Nereididae sp.	4	3	predator	Jumars et al. (2015), Shimabukuro pers. obs.				X
			Archinome sp.	3	3	predator	Desbruyères et al. (2006) and references therein				X
Cnidaria			Cnidaria sp.	2	2	predator	Desbruyères et al. (2006) and references therein				X
Arthropoda	Malacostraca	Eumalacostraca	*Mirocaris fortunata*	4	6	predator	Desbruyères et al. (2006) and references therein	√	√	√	X
			Alvinocaris sp.	4	6	predator	Desbruyères et al. (2006) and references therein	√	√	√	X
			Luckia striki	3	3	deposit feeder	Desbruyères et al. (2006) and references therein	√	√	√	X
			Liljeborgiidae sp.	3	3	deposit feeder	Authors pers. obs	√	√	√	X
			Stegocephalidae sp.	3	3	deposit feeder	Authors pers. obs				X
			Phoxocephalidae sp.	3	3	deposit feeder	Authors pers. obs				X
			Bonnierella sp.	3	3	deposit feeder	Authors pers. obs				X
			cf. *Storthyngura* sp.	3	3	deposit feeder	Desbruyères et al. (2006) and references therein	√	√	√	X

Class	Order	Species			Feeding	Reference					
		Heteromesus sp.	3	3	deposit feeder	Authors pers. obs	√	√			X
		Asellota sp. 2	3	3	deposit feeder	Authors pers. obs					X
		Asellota sp. 3	3	3	deposit feeder	Authors pers. obs					X
		Asellota sp. 4	3	3	deposit feeder	Authors pers. obs					X
		Haploniscidae sp.	3	2	deposit feeder	Desbruyères et al. (2006) and references therein					X
		Obesutanais sigridae	2	2	deposit feeder	Desbruyères et al. (2006) and references therein					X
		cf. *Typhlotanais incognitus*	3	2	deposit feeder	Desbruyères et al. (2006) and references therein					X
		Cumacea sp.	4	4	deposit feeder	Authors pers. obs					X
Ostracoda	Podocopa	*Thomontocypris excussa*	4	1	grazer	Desbruyères et al. (2006) and references therein; Chapman et al. (2019); Tanaka pers. Obs.	√	√	√	X	X
		Xylocythere sp.	4	1	grazer	Desbruyères et al. (2006) and references therein; Chapman et al. (2019); Tanaka pers. Obs.				X	
Hexanauplia	Copepoda	Dirivultidae sp.	4	0	grazer	Heptner & Ivanenko (2002), Limén et al. (2008), Gollner et al. (2015), Senokuchi et al. (2018)				X	
		Aphotopontius sp.	4	1	grazer	Heptner & Ivanenko (2002); Limén et al. (2008); Gollner et al. (2015), Senokuchi et al. (2018)	√	√		X	X
		Rimipontius sp.	4	1	grazer	Heptner & Ivanenko (2002); Limén et al. (2008); Gollner et al. (2015), Senokuchi et al. (2018)				X	X
		Siphonostomatoida sp.	4	1	grazer	Heptner & Ivanenko (2002); Limén et al. (2008); Gollner et al. (2015), Senokuchi et al. (2018)					X
		Bathylaophonte azorica	3	1	grazer	Heptner & Ivanenko (2002)	√	√	√	X	X
		Tegastidae sp.	3	0	grazer	Heptner & Ivanenko (2002)				X	
		Smacigastes micheli	3	1	grazer	Desbruyères et al. (2006) and references therein, Chapman et al. (2019)	√	√		X	X
		Miraciidae sp.	3	1	grazer	Heptner & Ivanenko (2002)				X	X
		Tisbe sp. 1	4	0	grazer	Heptner & Ivanenko (2002)				X	

			Tisbe sp. 2	4	1	grazer	Heptner & Ivanenko (2002)		X
			Ameiridae sp. 1	3	1	grazer	Heptner & Ivanenko (2002)	X	X
			Ameiridae sp. 2	3	1	grazer	Heptner & Ivanenko (2002)	X	X
			Ameiridae sp. 3	3	0	grazer	Heptner & Ivanenko (2002)	X	
			Ameiridae sp. 4	3	0	grazer	Heptner & Ivanenko (2002)	X	
			Archesola typhlops	3	0	grazer	Heptner & Ivanenko (2002)	X	X
			Haifameira sp.	3	1	grazer	Heptner & Ivanenko (2002)		X
			Mesochra sp.	3	0	grazer	Heptner & Ivanenko (2002)	X	
			cf. *Ambilimbus* sp.	3	0	grazer	Heptner & Ivanenko (2002)	X	
			cf. Kelleriidae sp.	4	0	grazer	Heptner & Ivanenko (2002)	X	
			Heptnerina confusa	4	1	grazer	Heptner & Ivanenko (2002)	X	X
			Ectinosomatidae sp. 1	3	0	grazer	Heptner & Ivanenko (2002)	X	X
			Ectinosomatidae sp. 2	3	1	grazer	Heptner & Ivanenko (2002)		X
			Donsiellinae sp.	3	1	grazer	Heptner & Ivanenko (2002)	X	X
			Cyclopina sp.	4	1	grazer	Heptner & Ivanenko (2002)	X	X
			Cyclopoida sp.	4	1	grazer	Heptner & Ivanenko (2002)	X	X
			Calanoida sp.	4	1	grazer	Heptner & Ivanenko (2002)	X	X
	Arachnida	Acari	Halacaridae sp.	3	1	predator	Desbruyères et al. (2006); Authors pers. obs	X	X
	Pycnogonida		Pycnogonida sp.	3	6	predator	Desbruyères et al. (2006); Authors pers. obs		X
Echinodermata	Ophiuroidea		Ophiuroidea sp.	3	3	deposit feeder	Desbruyères et al. (2006); Authors pers. obs		X
Nematoda	Chromadorea	Chromadoria	*Halomonhystera* sp.	3	0	deposit feeder	Wieser (1953); Zeppilli et al. (2015)	X	
			Xyalidae sp.	3	0	deposit feeder	Wieser (1953); Zeppilli et al. (2015)	X	
			Theristus sp.	3	0	deposit feeder	Wieser (1953); Zeppilli et al. (2015)	X	
			Paracanthonchus sp.	3	0	predator	Wieser (1953); Zeppilli et al. (2015)	X	
			Chromadorita sp.	3	0	deposit feeder	Wieser (1953); Zeppilli et al. (2015)	X	
			Cephalochaetosoma sp.	2	0	deposit feeder	Wieser (1953); Zeppilli et al. (2015)	X	

			Microlaimus sp.	3	0	grazer	Wieser (1953); Zeppilli et al. (2015)				X	
			Desmodora sp.	3	0	deposit feeder	Wieser (1953); Zeppilli et al. (2015)					X
			Epsilonema sp.	3	0	deposit feeder	Wieser (1953); Zeppilli et al. (2015)				X	
			Desmoscolex sp.	3	0	deposit feeder	Wieser (1953); Zeppilli et al. (2015)				X	
	Enoplea	Enoplia	*Oncholaimus dyvae*	3	3	predator	Wieser (1953); Zeppilli et al. (2015)	√	√	√	X	X
		Unknown	Nematoda sp. 1	3	0	deposit feeder	Wieser (1953); Zeppilli et al. (2015)				X	
Chaetognatha			Chaetognatha sp.	2	3	predator	Authors pers. obs					X
Platyhelmintes			Turbellaria sp.	3	2	predator	Authors pers. obs	√	√	√		X
Nemertea			Nemertea sp.	3	2	predator	Authors pers. obs	√	√	√		X

Chapter 2

Low environmental stress and productivity regime reduces functional

richness along a deep-sea hydrothermal vent gradient*

Low environmental stress and productivity regime reduces functional richness along a deep-sea hydrothermal vent gradient

*Authors***:** JM Alfaro-Lucas[1,4,5], F Pradillon[1], D Zeppilli[1], LN Michel[1], P Martinez-Arbizu[2], H Tanaka[3], M Foviaux[1], J Sarrazin[1]

[1] Institut Français de Recherche pour l'Exploitation de la Mer (IFREMER), Centre Bretagne, Plouzané, France

[2] Senckenberg am Meer, German Center for Marine Biodiversity Research, Wilhelmshaven, Germany

[3] Ocean Literacy Group, Graduate School of Science, The University of Tokyo, Tokyo, Japan

[4] Corresponding author: joanmanel.alfaro@e-campus.uab.cat

[5] Orcid ID: 0000-0001-5725-3218

Abstract

Little is known on the interacting effects of primary productivity and environmental stress on early community assembly processes in the deep sea (>200 m), the largest environment on Earth. Here, we studied the colonization of mineral substrata deployed along a deep-sea hydrothermal vent gradient at four hydrothermally active and inactive areas at 1700 m depth in the Lucky Strike vent field (Mid-Atlantic Ridge). We examined in detail the composition of the meio- and macrofaunal communities established after two years and evaluated diversity and functional patterns along the vent gradient. Our hypotheses were that (1) hydrothermal activity would constrain functional diversity and (2) we should observe a high similarity in composition and functional entities between the active and inactive sites. However, our observations did not match our hypotheses. Contrary to what was expected, our results show that functional richness increased along the vent activity gradient, being higher at active sites. Environmental conditions at inactive sites appear to filter for specific traits, thereby contributing to reduce functional richness despite a high species diversity. The presence of exclusive species and functional entities led to a high turnover between inactive sites, producing the highest β-diversities. As a result, some inactive sites contributed more than expected to the total species and functional β-diversities for both meio- and macrofauna. Overall, compositional and functional turnover drove the total dissimilarity for meio- and macrofauna, but nestedness was more important in meiofauna suggesting a lower degree of specialization compared with macrofauna. We suggest that the high productivity at active sites supports higher functional richness, more energetically expensive traits and that some of this productivity may be exported to inactive assemblages. The faunal overlap and energy links suggest that rather than operating as separate entities, active and inactive environments may be considered as interconnected entities. In the context of this network of environments, low functional richness suggests that inactive areas may be especially vulnerable to environmental changes related to natural and anthropogenic impacts, such as deep-sea mining.

Résumé :

Il existe peu de connaissances sur les effets combinés de la productivité primaire et du stress environnemental sur la structure des assemblages de faune dans les environnements marins profonds (> 200 m) ; ces derniers représentant de loin le plus large biome de la planète. Au sein de cette étude, nous avons analysé la colonisation de différents substrats minéraux déployés le long d'un gradient d'activité hydrothermale au sein de quatre sites situés à 1700 m de profondeur dans le champ Lucky Strike (dorsale médio-Atlantique). Nous avons examiné en détail la composition des communautés de la méio- et de la macrofaune établies sur les substrats d'ardoise après deux ans et avons évalué la diversité et les traits fonctionnels le long du gradient. Nous avons posé comme hypothèses (1) que l'activité hydrothermale devrait restreindre la diversité fonctionnelle et (2) qu'une grande similarité en termes de composition et d'entités fonctionnelles devrait être observée entre les sites actifs et inactifs. Cependant, nos observations ne correspondent pas à ces hypothèses. Contrairement à ce que nous attendions, nos résultats montrent que la richesse fonctionnelle augmente le long du gradient d'activité, en étant plus forte sur les sites actifs. Ainsi, les conditions environnementales présentes sur les sites inactifs contribueraient à filtrer des caractéristiques spécifiques, réduisant ainsi la richesse fonctionnelle malgré une plus grande diversité d'espèces. La présence d'espèces et d'entités fonctionnelles exclusives a entraîné un fort « turnover » entre les différents sites inactifs, produisant les plus fortes β-diversités. En conséquence, certains sites inactifs ont contribué plus que prévu à la β-diversité totale des espèces et des entités fonctionnelles pour la méio- et la macrofaune. Globalement, le changement de composition et de fonctions a conduit à une plus grande dissimilarité au niveau de la méiofaune, suggérant un degré de spécialisation inférieur à celui de la macrofaune. Nous suggérons que la productivité élevée sur les sites actifs contribue au soutien d'une richesse fonctionnelle plus élevée, de traits fonctionnels plus coûteux, et qu'une partie de cette productivité est exportée vers les assemblages des zones inactives. Les liens énergétiques et la redondance de la faune suggèrent que les environnements actifs et

inactifs peuvent être considérés comme des entités interconnectées. Dans ce contexte, la faible richesse fonctionnelle des zones inactives suggère que ces dernières pourraient être particulièrement vulnérables aux changements environnementaux liés aux impacts naturels et anthropiques, tels que l'exploitation minière en environnements marins profonds.

Mots-clés: communautés; colonisation; filtre environnemental; β-diversité, diversité fonctionnelle; méiofaune; macrofaune

Introduction

Productivity and environmental stress are the main drivers of colonization, biodiversity patterns and community structure (Chase & Leibold 2002; Chase 2010; Weiher *et al.* 2011). Locally, species richness is often positively correlated with primary productivity (Mittelbach *et al.* 2001; Chase 2010), whereas the relationship between functional richness and productivity remains more elusive (Lamanna *et al.* 2014; McClain *et al.* 2018). High increases in environmental stress "filter" for suitable species traits, therefore limiting colonization and reducing species and functional diversity (Weiher *et al.* 2011; Mouillot *et al.* 2013; Teixidó *et al.* 2018). Studies on marine shallow-water gradients (~3 m) have shown that stress has negative effects on colonization, species and functional richness, and assemblage structural, and trophic complexity (e.g., Hall-Spencer *et al.* 2008; Fabricius *et al.* 2014; Vizzini *et al.* 2017; Teixidó *et al.* 2018), but concomitant increases in productivity may in some cases attenuate some effects through higher food supply (e.g., Kroeker *et al.* 2011; Garrard *et al.* 2014). Despite their importance, the interaction effects of these drivers on the structure of communities in the deep sea (>200 m), the largest environment on Earth, remain poorly understood (McClain & Rex 2015; McClain & Schlacher 2015; Ashford et al. 2018).

The rich communities in the relatively homogenous and stable deep sea (Smith and Snelgrove, 2002) largely depend on an intermittent supply of organic matter produced in shallower photosynthetically active waters (Ruhl and Smith, 2004; Ruhl et al., 2008). In this context, deep-sea hydrothermal vents (HV) are hotspots of chemoautolithotrophic-

based productivity and biomass where productivity correlates, at least partially, with environmental stress (Le Bris *et al.* 2019). At HVs, oxygenated cold seawater percolates through and reacts with the ocean crust, forming oxygen-depleted, acidic, toxic vent fluids (Le Bris *et al.* 2019). Their dilution with oxygenated water create gradients home to microbial communities that obtain their energy through the oxidation of chemical compounds, which makes up the trophic basis of dense invertebrate assemblages (Sievert & Vetriani 2012). HV assemblages are often dominated by large chemosymbiotic invertebrates considered major primary producers (Le Bris et al., 2019) that inhabit distinct niches along the gradient, forming mosaic-like patterns and acting as foundation/engineer species (Sarrazin *et al.* 1997; Shank *et al.* 1998; Luther III *et al.* 2001; Govenar 2010).

Smaller invertebrates are associated with these foundation species forming low-diversity assemblages compared with the surrounding deep sea (e.g., Govenar *et al.* 2005; Gollner *et al.* 2010; Zeppilli *et al.* 2015; Plum et al., 2017). The majority of vent taxa exhibit behavioral and/or physiological adaptations to deal with environmental stress, explaining the low number of species present in HV fields (Bates *et al.* 2010; Govenar 2010; Gollner *et al.* 2015; Zeppilli et al., 2018). The stress/productivity gradients strongly structure faunal communities (Luther III *et al.* 2001; Bates *et al.* 2010; Gollner *et al.* 2015). Areas of higher fluid flux are characterized by low macrofaunal diversities, whereas areas of lower emissions exhibit higher diversities (e.g., Sarrazin et al. 2015), but functional diversity patterns remain largely unexplored. Furthermore, HVs have been historically considered

as island-like habitats and much less attention has thus been given to the putative gradient and to interactions with adjacent inactive environments (Levin *et al.* 2016). Adjacent inactive areas are characterized by a mosaic of physico-chemical and geological conditions (e.g., Boschen *et al.* 2016), but little is known about their associated biodiversity and drivers of community structure. Inactive habitats adjacent to vents may harbor diverse assemblages and share taxa with active habitats (Govenar *et al.* 2005; Gollner *et al.* 2010, 2015b; Zeppilli *et al.* 2015; Sen et al., 2015; Plum et al., 2017). They may play an important ecological role by, for example, serving as nursery zones for vent species (e.g., Marsh *et al.* 2012). Conversely, the fauna of inactive habitats may take advantage of the pool of organic matter of chemosynthetic origin from nearby habitats (Erickson *et al.* 2009; Bell *et al.* 2017).

The objective of the present study was to examine the colonization processes of meio- and macrofauna on a series of mineral substratum blocks that were deployed for 2 years along a gradient of hydrothermal activity. We investigated four contrasting active and inactive habitats, representative of the heterogeneity found within the Lucky Strike vent field, to examine and compare the composition, diversity and functional traits of the colonizing fauna. Species and functional β-diversity were quantified to evaluate the influence of the environment on faunal assemblage structure and we identified which component of β-diversity (turnover/nestedness) better explained the observed patterns. Finally, we performed stable isotope analyses on the fauna at each deployment site to determine the origin of consumed organic matter and examine the energetic gradient of

primary productivity of chemosynthetic origin from active to inactive sites. We hypothesize that (H1) functional diversity is lower at active vent sites due to environmental constraints on species physiology and, (H2) the structure of the faunal assemblages is more similar in sites within the hydrothermally active (respectively inactive) habitats than between hydrothermally active and inactive habitats.

Materials and methods

Study area, experimental setup and sample processing

We deployed size-standardized slate blocks (10 cm^3) to use as artificial substrata for 2 years at four different "sites" characterized by a decreasing level of hydrothermal activity, hereafter referred to as the "active", "intermediate", "periphery" and "far" sites relative to the hydrothermally active Eiffel Tower edifice (ET) (Lucky Strike vent field, ~1700 m depth, Mid-Atlantic Ridge) (Table 3.1) (Appendix S3.1). Based on previous pilot studies, slate blocks were chosen for their basalt-like, smooth and inert surface (Cuvelier et al., 2014; Zeppilli et al., 2015; Plum et al., 2017). Located on the north-west side of the ET edifice, the active site is the most active one in the vent field, with the presence of microbial mats and a small high-temperature chimney within the vicinity (few cm) of the deployed substrata. The intermediate site is located further down on the western side of the edifice, in an area of diffuse flow. The active and intermediate sites are colonized by dense assemblages of the foundation species mussel *Bathymodiolus azoricus*. The periphery site is a poorly sedimented area with no visible hydrothermal activity located between the ET (~50 m) and Montsegur edifices (~85 m). The far site is situated on an inactive

basaltic seabed on the west side of the lava lake, at ~90, ~120 and ~470 m away from the

Helen, Pico and ET active edifices, respectively (Table 3.1).

Table 3.1. Location of the substratum blocks and temperatures registered at the four study sites. All temperatures are in °C.

Site	Distance to closest active vent (m)	Mean ± sd temperature	Minimum temperature	Maximum temperature	Temperature range
Active	0	7.93±2.13	4.69	21.6	16.91
Intermediate	0	5.79±0.77	4.53	12.2	7.67
Periphery	~50	4.62±0.07	4.38	4.87	0.49
Far	~90	4.55±0.07	4.32	4.77	0.44

Slate blocks were deployed during the MoMARSAT 2013 (https://doi.org/10.17600/13030040) cruise on board the R/V *Pourquoi pas?*, using the ROV *Victor6000*. Three blocks were deployed at each of the four sites. Temperature was recorded for 9 months every 15 minutes using an autonomous NKE ST 6000 temperature probe attached to wood blocks from a parallel experiment running at each site (Table 3.1). All substrata were recovered two years after deployment using *Victor6000*, during the MoMARSAT 2015 cruise (https://doi.org/10.17600/15000200). Each slate block was placed in an individual isotherm sampling box and, once on board, was carefully washed with filtered seawater and sieved through 300 μm and 20 μm mesh sieves. The use of 300 and/or 500 μm mesh sieves to sample macrofauna has become common in the deep sea (e.g., Montagna et al., 2017), although meiofauna is defined as the fraction of taxa that pass through a 1 mm sieve (Gière, 2007). In this study we refer to meiofauna and

macrofauna to the taxa found in 20 μm and 300 μm mesh sieves, respectively, acknowledging that are not the actual definitions of meio- and macrofauna, and that typical groups of both compartments will be present in the 300-μm compartment. Meiofaunal samples were preserved in 4% seawater-buffered formalin and macrofaunal samples were preserved in 96° ethanol. Two slate blocks from each site were individually preserved in 96° ethanol, and the third was individually preserved in 4% seawater-buffered formalin for further examination in the laboratory. Once in the laboratory, sieved samples were sorted manually under a stereo microscope and all taxa were counted and identified to the lowest taxonomical level possible. Larvae and individuals without heads were discarded and not considered further. Meiofaunal samples were transferred to 200 ml beakers and three subsamples of 5 ml each were taken from the original volumes and stained with phloxine. A maximum of 100 randomly collected individuals of the various meiofaunal groups were mounted on slides and identified to the lowest taxonomical level possible. Prior to mounting, nematodes underwent a formalin-ethanol-glycerol treatment to prevent dehydration (see Zeppilli et al., 2015). Juveniles of macrofaunal taxa found in 20 μm samples were not considered.

Taxonomical and functional biodiversity indices

B. azoricus is the main foundation species of the Lucky Strike vent field and the ET, forming dense mussel-bed habitats (Desbruyères *et al.* 2001). Because its inclusion would certainly drive the main trends in biodiversity metrics, we excluded it from our analyses. We estimated the total and mean species richness (S), and the mean abundance (N) and

evenness (J') per site for meio- and macrofauna, respectively. We estimated meiofaunal abundances as the total and mean number of individuals found in each of the three subsamples (5 ml each) for each block at each site.

In addition, we analyzed three functional response traits that are related to productivity and stress. They include "adult mobility" (hereafter "mobility"), "maximum adult body size" (hereafter "size") and "feeding mechanism", for meio- and macrofauna taxa (see trait definitions, modalities, references, and datasets in Appendix S3.2). Traits were obtained from direct measurements and/or literature, including the sFDVent database (Chapman *et al.* 2019). We estimated the total and mean functional richness (FRic) per site as the percentage of functional volume at each site derived from a multidimensional functional space (Mouchet *et al.* 2010). This space was constructed using synthetic components of a principal coordinate analysis (PCoA) encapsulating the variation of functional entities (FEs), i.e., the unique trait combinations, of meio- and macrofauna at each site. The FE coordinates on the first three (98.7% of inertia) and four (93.87% of inertia) PCoA axes were used to estimate FRic for meiofauna and for macrofauna. We also calculated the total and mean number of FEs and the mean functional evenness (FEve) at each site. The low meiofaunal species richness, and thus the low number of FEs, at the periphery site prevented calculation of mean FRic and FEve for all substrata at this site.

Additionally, we ran a null model to test if the observed FRic at different sites differed significantly from random distributions of species into FEs. Specifically, we tested if HV activity in active and intermediate sites or deep-sea environment in periphery and far sites filter for certain traits reducing less than expected. Null models were run 4999 times for each site to generate 95% confidence intervals of expected FRic values, simulating a random sorting of species from the total pool of FEs, and maintaining the observed number of species per site. Observed FRic values did not deviate from null expectations if they fell within confidence intervals. Due to the low number of FEs generated from our selected traits in meiofauna, to run the null models, we were forced to estimate FRic with a very low number of dimensions (2). This generated FRic volumes from functional axes with little information and we therefore did not run null models for meiofauna.

To estimate the total taxonomic and functional β-diversity (BD$_{Total}$ and fBD$_{Total}$) and the mechanisms driving overall β-diversity for meio- and macrofauna, we estimated the total variance of the presence-absence species-by-site and FEs-by-site tables using the Jaccard dissimilarity coefficient (Legendre & Cáceres 2013; Legendre 2014). BD$_{Total}$ computed from Jaccard dissimilarity coefficient reaches its maximum value (1) when all sites exhibit totally different species compositions (Legendre and De Caceres, 2013). BD$_{Total}$ was decomposed into species turnover and nestedness to assess the mechanisms generating β-diversity for both macro- and meiofauna (Baselga 2010; Legendre 2014). The degree of uniqueness of each site in terms of species and FE composition was estimated

by the local contribution to β-diversity (LCBD) indices (Legendre & Cáceres 2013). LCBD indices were tested for significance using random permutations assuming the null hypothesis that species and FEs were randomly distributed among sites. Furthermore, to estimate the dissimilarity between each site and the processes driving dissimilarities, β-diversity between each pair of sites (D) was estimated and decomposed into turnover and nestedness.

Analyses of community structure with respect to species and FEs

We ran distance-based redundancy analyses (db-RDA) of Hellinger-transformed species abundances and abundance-weighted FEs constrained by a "site" factor to test if species assemblages and FEs, respectively, were differently structured by the conditions of each site. Additionally, we performed multiple factor analyses (MFAs), i.e., symmetric correlative analyses, to visualize and compare the taxonomic and FE structures of the meio- and macrofaunal assemblages and to characterize species and FE associations with sites. We used the RV coefficient, which measures the relatedness of two datasets derived from separate ordinations (Robert & Escoufier 1976), to assess the correlation of the taxonomic and functional meio- and macrofaunal community structure, respectively, and tested significances using permutations (Josse *et al.* 2008). The RV coefficient ranges from 0 (independent datasets) to 1.

Isotope analyses

The ᵀᴹ13C, ᵀᴹ14N and ᵀᴹ34S of 19 taxa identified in the macrofaunal compartment were analyzed (Appendix S3.3). For qualitative comparison values of ᵀᴹ13C from -15‰ to -10‰, -12.9±3.4‰, and from -36‰ to -30‰ were considered representative of organic matter derived from chemosynthesis: methanotrophy, reductive tricarboxylic acid (rTCA) and Calvin-Benson-Bassham (CBB) cycles, respectively (e.g., Portail *et al.* 2018 and references therein). Values of ᵀᴹ34S between ~16‰ and 19‰ were considered representative of organic matter of photosynthetic origin, whereas values around and below 10‰ were considered of chemosynthetic origin (Reid *et al.* 2013). Values of ᵀᴹ15N were used to qualitatively discuss the trophic position of taxa. Due to the low number of samples (1), the periphery site was excluded from statistical analyses.

Statistical analyses

All indices and statistical tests were computed in R v. 3.5.3 (R Core Team, 2019). Taxonomic indices were computed using the package *vegan* (Oksanen et al., 2019). Functional indices, null models and Figure 1 were computed modifying the script provided by Teixido et al. (2018) and the *dbFD* function in the *FD* package (Laliberté & Legendre 2010). Differences in mean taxonomic and functional metrics, as well as stable isotope ratios were tested using ANOVAs or Kruskal-Wallis tests. Assumptions of normality and homogeneity of variances were tested using Shapiro-Wilk and Bartlett tests, respectively. Inter-site post-hoc comparisons were performed using Tukey honest significant difference tests or Dunn's test of multiple comparisons using rank-sum tests

with Bonferroni correction. ®-diversity analyses and LCBD indices were calculated using the *beta.div* and *beta.div.com* functions in the *adespatial* package (Dray et al., 2019). db-RDAs were run with the *capscale* function in *vegan* after check for multivariate homogeneity of variances with the *betadisper* function coupled with permutations tests. MFAs and RV coefficients were computed using the *FactoMineR* package (Lê et al., 2008).

Results

Taxonomic and functional biodiversity metrics

We identified 1690 and 7708 specimens belonging to meio- and macrofauna, respectively (Appendix S3.4). In the macrofaunal compartment, *Bathymodiolus azoricus* was only found at the active and intermediate sites (total of 2563 individuals). With the exception of *B. azoricus*, we identified 77 taxa. Nineteen and 46 taxa belonged exclusively to the meio- and macrofaunal compartments, respectively, and 12 species were shared. Our detailed species identification exceeds the most extensive studies undertaken at the Lucky Strike vent field and the ET to date (Dover & Series 2000; Cuvelier *et al.* 2014; Sarrazin *et al.* 2015; Zeppilli *et al.* 2015; Plum *et al.* 2017; Baldrighi *et al.* 2018). Shared taxa were large meiofaunal individuals of copepods, nematodes and halacarids.

The total number of species, FE and FRic per site are shown in Table 2 and Figure 3.1A and B. Overall, the highest values for all indices were found in both hydrothermally active sites and the far site, whereas the periphery site was the least rich in meio- and macrofauna (Figure 3.1A-B). Total FRic in the far site however, was as low as in the

periphery site. For meiofauna, all FEs were found in the active and intermediate sites, but for macrofauna some exclusive FEs were found in inactive and active sites (Figure 3.1C-D). Significant statistical differences were found in mean diversity indices comparisons between sites (Appendix S3.4). Both hydrothermally active sites showed higher number of mean species and abundances of meio- and macroinvertebrates than the inactive sites (Table 3.2). Evenness showed contrasting patterns between meio- and macrofauna. J' was relatively high at all sites for meiofauna and peaked at the periphery site, whereas the macrofauna increased constantly from the hydrothermally active sites to the far site, peaking in the latter (Table 3.2). The mean number of FEs and mean FRic were higher in both hydrothermally active sites for meio- and macrofauna. Functional evenness did not exhibit clear patterns, but was higher at the periphery site for both meio- and macrofauna. Macrofaunal null models revealed that the observed FRic at the far site was lower than expected by chance, whereas FRic values at other sites fell within the expected values (Figure 3.2).

Table 3.2. Taxonomic and functional α- and β–diversity indices of meio- and macrofauna assemblages at the four study sites. High values are highlighted in bold. S_{Total}= total species richness per site; S= mean species richness; N= abundance; J'= evenness; $FRic_{Total}$= total functional richness per site; FRic= mean functional richness; FE_{Total}= total functional entities per site; FE= mean functional entities; FEve= functional evenness; BD_{Total}= total beta diversity; LCBD= local contribution to β-diversity. Additionally, some indices are given as percentages (%). p_{adj}= adjusted p-value. *Estimated from one sample only.

		Meiofauna				Macrofauna			
	Index	Active	Intermediate	Periphery	Far	Active	Intermediate	Periphery	Far
Taxonomic α-diversity	S_{Total} (%)	**24** (77.42)	18 (58.06)	7 (22.58)	17 (54.84)	29 (50)	**31** (53.45)	15 (25.86)	27 (46.55)
	S	**17±2.65**	13±2.65	3.67±1.15	11.33±1.53	**21.33±1.15**	**21.33±2.89**	7.67±0.58	13±2.65
	N	**363.67±165.9**	125±6.24	14±1.73	60.67±26.69	**1032.33±586.14**	639.33±264.85	16±2.65	27.33±12.5
	J'	0.81±0.05	0.72±0.09	**0.87±0.05**	0.85±0.09	0.47±0.18	0.7±0.09	0.84±0.03	**0.88±0.08**
Functional α-diversity	$FRic_{Total}$ (%)	**100**	**100**	10.19	6.4	**49.81**	42.52	16.53	21
	FRic	**90.67±16.5**	**90.67±16.5**	10.19*	6.4±0	**39.25±9.77**	31.8±7.07	3.78±5.01	8.82±7.7
	FE_{Total} (%)	**8** (100)	**8** (100)	4 (50)	5 (62.5)	13 (68.42)	**14** (73.68)	8 (42.11)	12 (63.16)
	FE	**7.67±0.58**	7.34±0.58	2.67±1.15	5±0	11.34±0.58	**11.67±1.53**	6±1	6.67±1.53
	FEve	0.39±0.1	0.49±0.06	**0.60***	0.33±0.05	0.32±0.03	0.34±0.04	**0.61±0.07**	0.39±0.1
Taxonomic β–diversity	BD_{Total}	0.33				0.37			
	Turnover (%)	0.22 (66)				0.33 (90.7)			
	Nestedness (%)	0.11 (33)				0.034 (9.3)			
	LCBD (p_{adj})	0.18 (1.00)	0.23 (1.00)	**0.32** (0.04)	0.26 (0.93)	0.2 (1.00)	0.2 (1.00)	**0.3** (0.02)	0.29 (0.02)
Functional β–diversity	β–diversity	0.19				0.24			
	Turnover (%)	0.03 (18)				0.18 (75)			
	Nestedness (%)	0.15 (82)				0.06 (25)			
	LCBD (p_{adj})	0.14 (1)	0.14 (1)	**0.42** (0.1)	0.31 (0.46)	0.21 (1)	0.16 (1)	**0.4** (0.01)	0.23 (1)
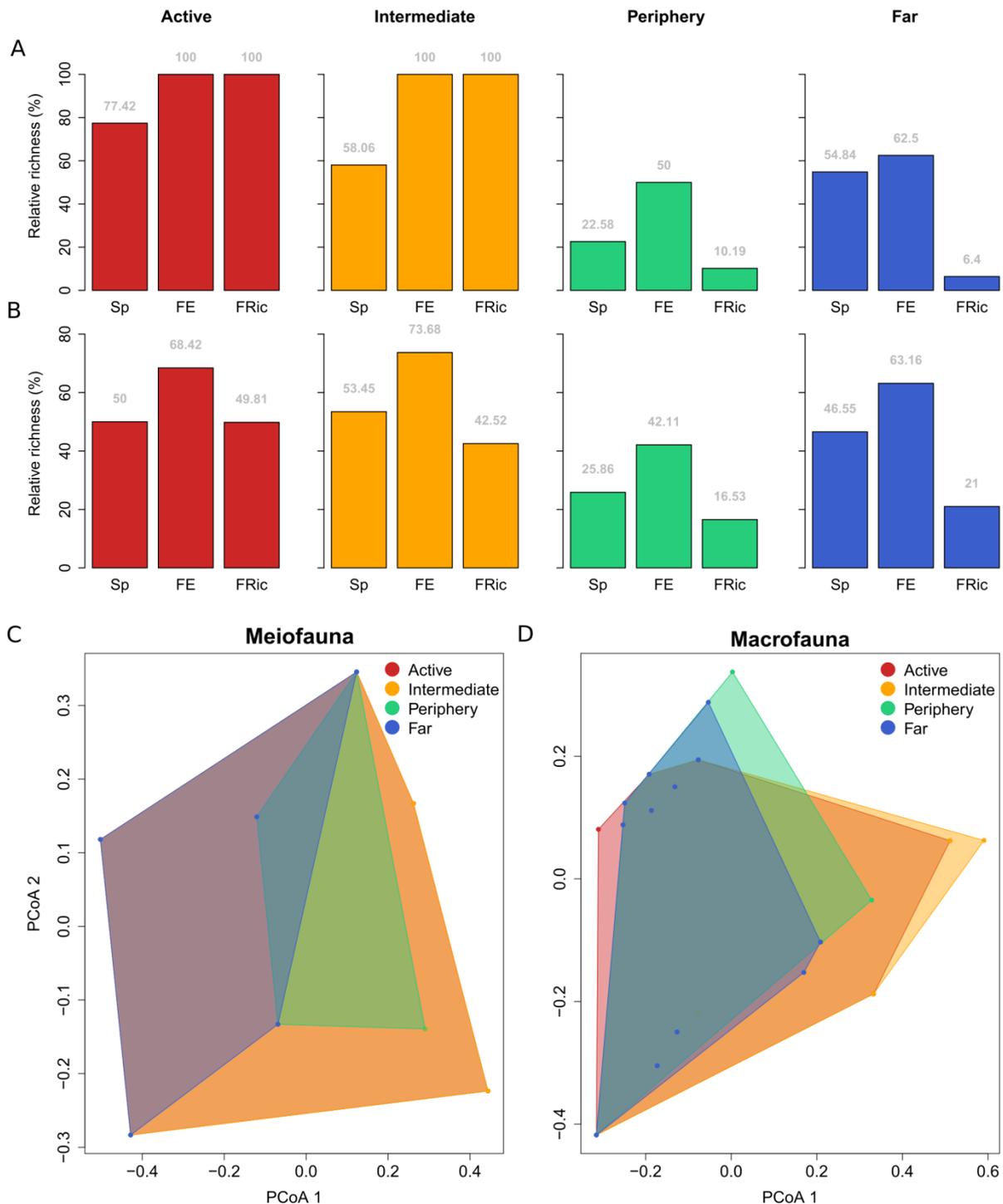
Figure 3.1. Percentage of species (Sp), functional entities (FE) and richness (FRic) per site for (A) meio- and (B) macrofauna. Functional richness (volume) represented as the area in a two-dimensional PCoA space for (C) meio- and (D) macrofauna. Note that the functional spaces for meiofauna in the periphery and the far sites are fully contained in the functional spaces of the active and the intermediate sites; they are not between them. For macrofauna, although they overlap substantially, the functional volume of the periphery and far sites are not fully contained in the volumes of the hydrothermally active sites, nor are they situated between them.
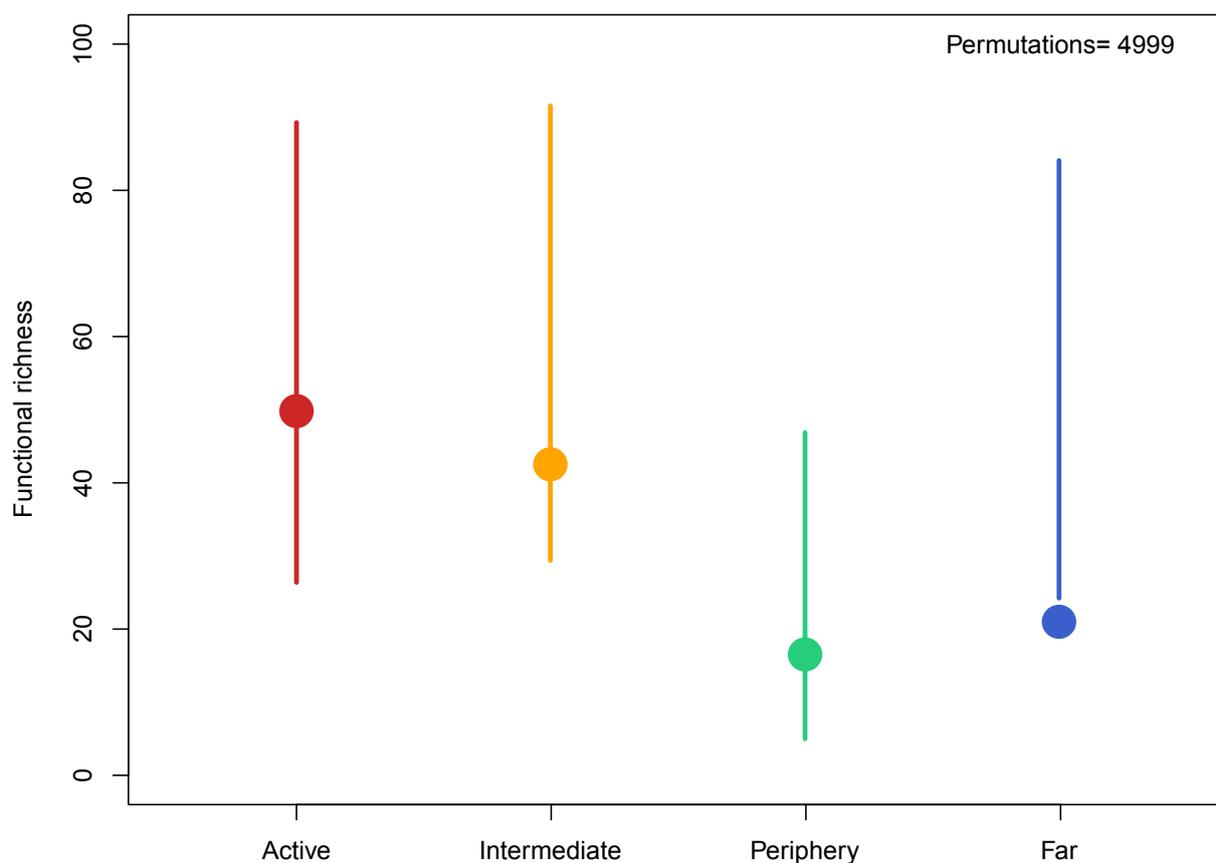
Figure 3.2. Null model of functional richness (FRic) (percentage volume of the total functional space) among sites for macroinvertebrates. Points are the observed values of FRic and bars represent the 95% confidence interval of expected values generated by simulating random species sorting from the total pool of functional entities (19 functional entities), based on the observed number of species at each site.

Species β-diversity among sites was lower for meio- (BD_{Total}= 0.33) than for macrofauna (BD_{Total}= 0.37) (Table 3.2). Turnover contributed more to BD_{Total} for both meio- (66%) and macrofauna (90.7%). Nestedness nevertheless contributed roughly three times more to BD_{Total} for meiofauna (33%) than for macrofauna (9.3%). The periphery site was the most dissimilar site for both compartments and contributed significantly more to BD_{Total} than the other sites ($p_{adjusted}$= 0.04 and 0.02, respectively). The far site was also quite

dissimilar compared with the other sites for both meio-and macrofauna and contributed significantly more to BD_{Total} for the latter ($p_{adjusted}$= 0.02) (Table 3.2). Pairwise comparisons of sites revealed low β-diversity dissimilarity (D) between the active and intermediate sites, which was mainly driven by turnover in both compartments (Appendix S3.5). Unexpectedly, the periphery and far sites were more dissimilar, or as dissimilar as they were to the active and the intermediate sites for meio- and macrofauna (Appendix S3.5). Turnover in both compartments drove the differences observed between the periphery and far sites.

Functional β-diversity among sites was lower for meio- (fBD_{Total}= 0.19) than for macrofauna (fBD_{Total}= 0.24) (Table 3.2). Contrasting mechanisms were driving dissimilarity in both compartments: nestedness contributed more than four times more to fBD_{Total} than turnover for meiofauna, whereas turnover contributed three times more than nestedness to fBD_{Total} for macrofauna (Table 3.2). In both compartments, the periphery and far sites contributed more to fBD_{Total} than the two hydrothermally active sites (Table 3.2), and in the case of macrofauna this difference was significant in the periphery site ($p_{adjusted}$= 0.01) (Table 3.2). Pairwise comparison of sites revealed that there was no functional β-diversity dissimilarity (D) between the active and intermediate sites for meiofauna, because both sites contained the same FEs (Appendix S3.5). The low β-diversity dissimilarity between active and intermediate sites for macrofauna was largely driven by turnover (Appendix S3.5). Again, the far and periphery sites were more dissimilar, or as dissimilar as they were to the active and the intermediate sites for meio- and macrofauna (Appendix S3.5).

Dissimilarity between periphery and far sites was largely driven by turnover in both compartments.

Meiofauna and macrofauna taxonomic and functional community structure

The relative abundance of taxonomic groups and traits showed that some groups/traits were more abundant at some sites, suggesting structural differences along the gradient for meio- and macrofauna (Figure 3.3A and B). Supporting these observations, the dbRDA model with "sites" as a predictor variable explained 66.41 and 56.91% of the total inertia in meio- and macrofauna species assemblage structures (p<0.001 in both models). These results were well-illustrated in the MFA ordinations, which showed that different taxa characterized each site and that both compartments were similarly structured in the four groups (Figure 3.4A-B). The RV coefficient (the relatedness of the two datasets derived from separate ordinations) between the meio- and macrofaunal compartments was 0.92 (p-value= 9.04^{e-05}), further supporting this observation. The first axis of the global PCA (42.51% of the global inertia) separated hydrothermally active blocks from the inactive blocks (Figure 3.4A). The second axis (18.08% of the global variance) separated the periphery and far site blocks (Figure 3.4A). The third axis (12.38% of the global variation) further separated active site blocks from the intermediate site blocks (Figure 3.4B). Both meio- and macrofaunal compartments contributed similarly to the three axes. The taxonomic groups and 20 species contributing the most to the ordination of blocks in the first three axes of the global PCA are shown in Figure 3.4C-D.
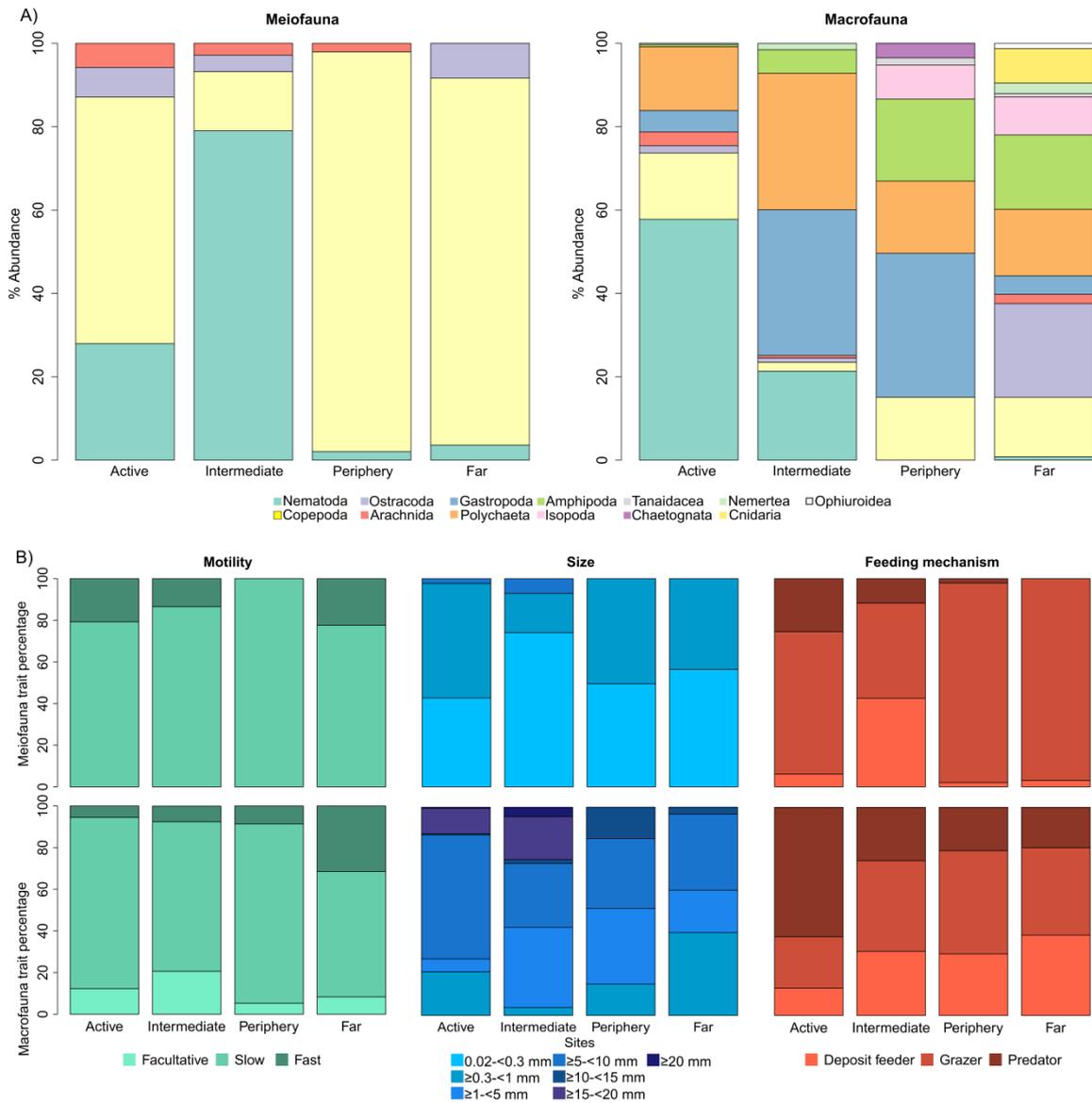
Figure 3.3. Proportion of meio- and macrofauna groups (A) and trait categories (B) at the four study sites.
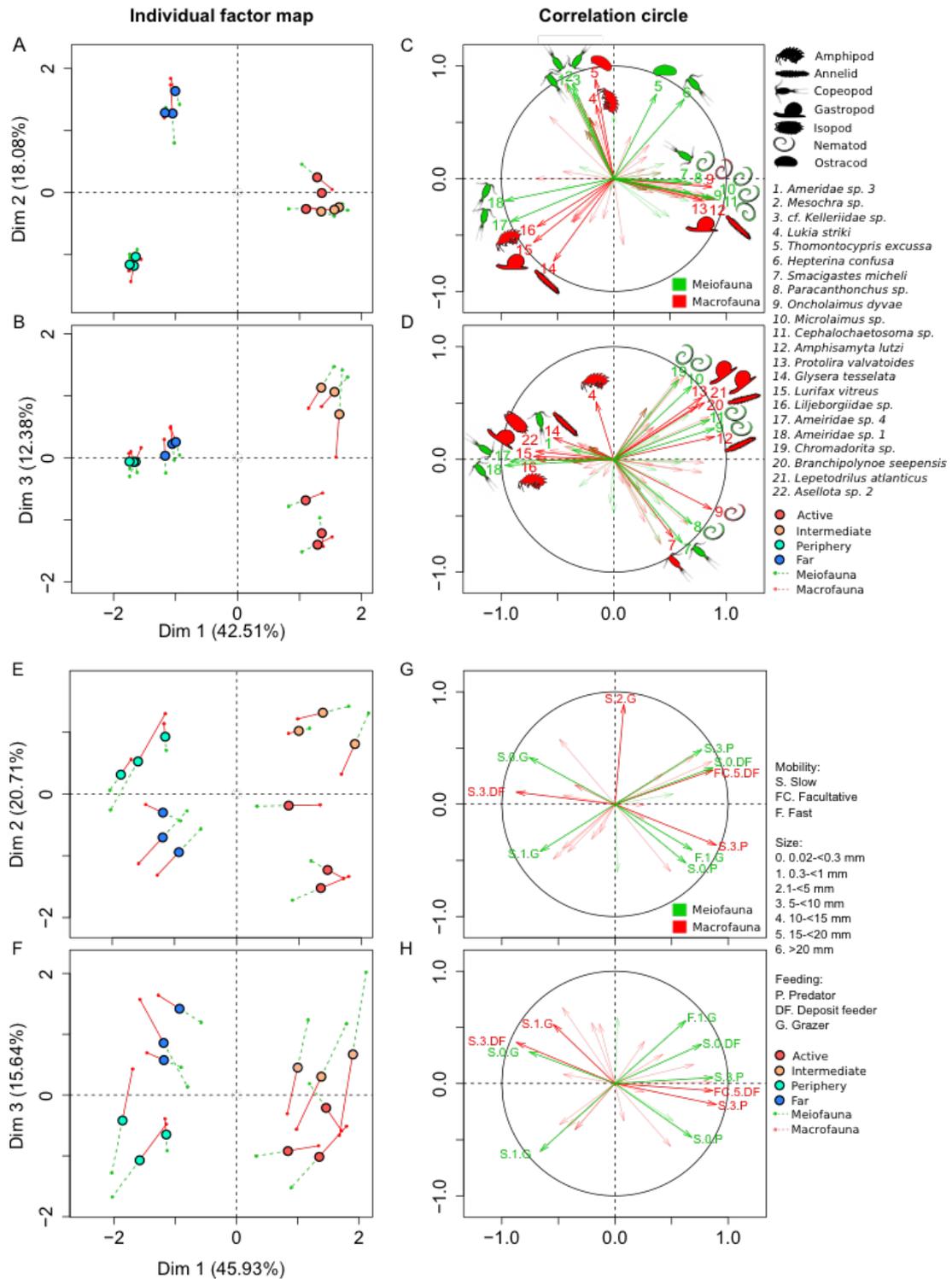
Figure 3.4. Multiple factor analysis (MFA) of meio- and macrofauna taxa and traits. **A-D**. Species-based MFA. **E-H**. Functional-entities-based MFA. **A, B, E and F**. Individual factor map showing block positions for meiofauna (green) and macrofauna (red) partial PCAs, and the Global PCA (black dots) along the first, second, and third axes. **C, D, G and H**. Correlation circle highlighting the main taxa/functional entities contributing to the ordination of sites for meiofauna and macrofauna along the first, second, and third axes. Copepoda, Ostracoda, Gastropoda, Polychaeta and Isopoda silhouettes were freely downloaded from PhyloPic under Public Domain Dedication 1.0 License.

The dbRDA model for FE community structure explained 70.02 and 63.96% of the total inertia in meio- and macrofauna, respectively (p<0.001 for both models). Trait MFA ordinations yielded a similar picture as that observed for species. The meio- and macrofauna of the sites harbored different FE assemblages and both compartments were similarly structured into four groups (Figure 3.4E and F). The RV coefficient for the FEs of the meio- and macrofauna compartments was 0.62 (p-value= 0.002), further supporting this finding. The first axis of the global PCA (45.93% of the global inertia) differentiated the hydrothermally active substrata from the inactive substrata (Figure 3.4E). The second axis (20.71% of the global variance) separated the active and intermediate site blocks (Figure 3.4E). The third axis (15.64% of the global variation) further separated the periphery site blocks from the far site blocks (Figure 3F). The 10 FEs contributing the most to the ordination of blocks in the first three axes of the global PCA are shown in Figure 3.4G-H.

Stable isotopes

Mean species isotope values are shown in Appendix S3.3. Mean $\delta^{13}C$ values ranged from -34.57‰ for *Smacigastes micheli* at the active site to -17.39‰ for the polychaete *Lepidonotopodium* sp. at the far site. Mean $\delta^{15}N$ values ranged from -7.05‰ for the polychaete *Branchipolynoe seepensis* at the active site to 9.89‰ for *Lepidonotopodium* sp. at the far site. Mean $\delta^{34}S$ values ranged from 2.65‰ in *B. seepensis* at the active site to 14.03‰ in *Lepidonotopodium* sp. at the far site. Active and intermediate sites did not show any differences in mean $\delta^{13}C$, $\delta^{15}N$ and $\delta^{34}S$ values. Compared with active and intermediate

sites, the far site had a significantly less negative mean $\delta^{13}C$ ($p_{adjusted}$= 0.004 and 0.03,

respectively), higher mean $\delta^{15}N$ (only compared to the intermediate site (p= 0.003), and

higher mean $\delta^{34}S$ ($p_{adjusted}$= 23^{e-05} and 11^{e-05}, respectively). Although the periphery site was

not included in the analyses, the only available sample belonged to the amphipod

Liljeborgidae sp. and its isotopic values were similar to that of the same species at the far

site.

Discussion

Contrary to our first hypothesis (H1), the highest values in total and mean

functional richness for the meio- and macroinvertebrate assemblages were found in the

two hydrothermally active sites. The opposite trend has been observed in shallow-water

vents (<0.5-3 m depth, Teixidó *et al.* 2018). Deep-sea vents are not only hotspots of primary

production, but also of evolutionary novelty, thereby differing from their shallower

counterparts, which have a very low degree of unique species (Tarasov et al., 2005). Our

results suggest that even under strong environmental stress, high productivity can lead

to the evolution of not only well-adapted, but functionally rich assemblages. Despite

stress, high-energetic deep-sea vents may support more functional strategies (FRic)

relaxing the effect of competition and allowing for a relatively high number of species to

coexist in high densities in reduced spaces.

Furthermore, null models in macrofauna revealed that FRic was only lower than

expected by chance at the far site (~90 m away of hydrothermal fluid influence),

suggesting strong trait convergence. Macroinvertebrates at the far site had a similar number of species and FEs as, for instance, the intermediate site, but roughly half the FRic. Although null models were not run for meiofaunal assemblages, the similar observed species-FEs-FRic relationship also suggests strong trait convergence at this site. Lower FRic values than expected by chance provide evidence for assemblages structured by environmental filtering (Chase & Leibold 2002; Chase 2010; Weiher *et al.* 2011a). Assemblages structured predominantly by the physical environment are typically more sensitive to disturbances than those structured by random and interspecific competition processes (e.g., Didham et al., 2005; Ashford et al., 2018). However, competition between species may potentially produce similar patterns as those observed here, and we did not undertake any phylogenetic analyses to support trait patterns (Mayfield and Levine, 2010). Our results however are concordant with recent deep-sea studies that have shown that peracarid assemblages in sediments and octocoral communities are also structured by the environment (Quattrini *et al.* 2017; Ashford *et al.* 2018). Thus, it is likely that the physical environment structures faunal assemblages on inactive bare-basalts at the early stages of community assembly. This evidence for environmental structuring agrees with previous studies that have suggested that these assemblages may be vulnerable to environmental disturbances (Gollner *et al.* 2015a).

Despite their lower FRic, inactive areas showed similar total species richness as those observed at active areas (see the far site) and previous studies suggested that they can be colonized by diverse assemblages (Gollner et al., 2015; Zeppilli *et al.* 2015; Plum *et*

al. 2017). Furthermore, pairwise comparisons of species and FE assemblages show that dissimilarity between periphery and far sites was mainly driven by turnover in both compartments. This turnover indicates that exclusive species and FEs, not their absence, drive dissimilarity between these sites. In concordance, LCBD indices identified the periphery (meio- and macrofauna) and far (macrofauna) sites as contributing more than expected to total taxonomic β-diversity. These two sites also greatly contributed to the functional β-diversity in meiofauna. However, in this case, the species-poor FE assemblage — rather than uniqueness — was the cause of such contribution, as highlighted by the complete functional overlap with active sites. For macrofauna, the far and periphery sites greatly contributed to the functional β-diversity due to exclusive FEs. Contrary to our hypothesis, the inactive sites were as dissimilar, or even more dissimilar, as they were to the two hydrothermally active sites highlighting the high heterogeneity of assemblages at adjacent inactive vent habitats.

As hypothesized, we found low species and FE dissimilarities between hydrothermally active sites, which led to their non-significant LCBD for both meio- and macrofauna. However, dissimilarities were driven by turnover in both compartments showing that exclusive species were found at both sites and that the environment plays a strong structural role (Luther III *et al.* 2001). Some taxa characterizing the inactive sites were also commonly found at actives sites including the gastropod *Lurifax vitreus*, the polychaete *Glycera tesselata*, the amphipod *Luckia 98oloni*, the ostracod *Thomontocypris excussa* and the copepod *Hepterina 98oloniz*, among others. This lack of specificity was

more obvious for meiofauna, and may explain the lower β-diversity for this compartment. Supporting other studies, our results suggest that β-diversity is higher for macrofauna than for meiofauna, because larger species are better adapted to specific environments (Gollner et al., 2010; Gollner et al., 2015a; Gollner et al., 2015b). Further support was provided by the fact that functional β-diversity was mainly driven by nestedness in meiofauna and turnover in macrofauna, suggesting that although meio- and macrofauna were taxonomically similarly structured, the underlying mechanisms driving differences in species and FEs compositions along the gradient differed in magnitude.

The functional structures of meio- and macrofauna were also congruent. Some striking commonalities and trends further suggest strong links between traits and vent productivity/stress for both compartments. Among the traits, predators and larger species characterized the meio- and macrofauna of hydrothermally active sites. Large size may be advantageous in the vent environment, because it may help increase the animal's physiological tolerance to cope with a rapidly changing environment, especially in meiofauna (see Vanreusel et al., 2010; Gollner et al., 2015 and references therein). The high motility of the meiofaunal species at active sites also supports adaptations that can mitigate non-optimal conditions (Bates et al., 2010; Gollner et al., 2015). In addition, the largest-sized meio- and macrofauna species were only found at hydrothermally active sites, whereas very small sizes characterized the inactive sites for macrofauna. Size also represents a direct link with energy (e.g., McGill *et al.* 2006), as does predation. In fact, the number of predator species strongly decreased from the active to the far sites. In

agreement with food-web ecology theory (Post 2002), this decrease strongly suggests that vent primary productivity sustains complex trophic assemblages with high trophic levels (Govenar 2012).

In the context of potential mining of vent systems (Van Dover *et al.* 2018; Van Dover 2019), our results strongly advocate precautionary measures. Rather than separate entities, active and inactive areas should be considered as a continuum of biologically and trophically interconnected assemblages. Values of ^{TM34}S around 16‰ and 19‰ are generally considered as representatives of organic matter of photosynthetic origin, whereas values around and below 10‰ are considered of chemosynthetic origin (Erickson *et al.* 2009; Reid *et al.* 2013). ^{TM34}S values of species at far sites varied between 11‰ and 14‰. Thus, our stable isotope analysis suggests that vent primary chemosynthetic production may be exported as far as ~90 m (minimum distance to an active edifice of the far site) in the Lucky Strike vent field. This energy may be used by taxa not normally found at active sites, establishing spatial subsidies that may extend the vent's "sphere of influence" (*sensu* Levin *et al.* 2016) far from active areas (Reid *et al.* 2013; Bell *et al.* 2017; Ardyna *et al.* 2019; Bris *et al.* 2019). Much effort has been done in raising awareness on the largely under-sampled and poorly studied inactive sulfide deposits, the main mining industry target (Van Dover 2019). Insights of this study however, strongly suggest that historically overlooked heterogeneous areas as close as <100 m harbor diverse assemblages with unique species and functional entities that may be affected by

environmental changes such as those produced by anthropogenic activities (Van Dover *et al.* 2018).

References

Ardyna, M., Lacour, L., Sergi, S., d'Ovidio, F., Sallée, J.-B., Rembauville, M., et al. (2019). Hydrothermal vents trigger massive phytoplankton blooms in the Southern Ocean. Nat Commun, 10, 2451.

Ashford, O.S., Kenny, A.J., Froján, C.R., Bonsall, M.B., Horton, T., Brandt, A., et al. (2018). Phylogenetic and functional evidence suggests that deep-ocean ecosystems are highly sensitive to environmental change and direct human disturbance. Proc. R. Soc. B, 285, 20180923.

Baldrighi, E., Zeppilli, D., Crespin, R., Chauvaud, P., Pradillon, F. & Sarrazin, J. (2018). Colonization of synthetic sponges at the deep-sea Lucky Strike hydrothermal vent field (Mid-Atlantic Ridge): a first insight. Marine Biodiversity, 48, 89–103.

Baselga, A. (2010). Partitioning the turnover and nestedness components of beta diversity. Global Ecology and Biogeography, 19, 134–143.

Bates, A.E., Lee, R.W., Tunnicliffe, V. & Lamare, M.D. (2010). Deep-sea hydrothermal vent animals seek cool fluids in a highly variable thermal environment. Nature Communications, 1, ncomms1014.

Bell, J.B., Reid, W.D., Pearce, D.A., Glover, A.G., Sweeting, C.J., Newton, J., et al. (2017). Hydrothermal activity lowers trophic diversity in Antarctic hydrothermal sediments. Biogeosciences, 14, 5705–5725.

Boschen, R.E., Rowden, A.A., Clark, M.R., Pallentin, A. & Gardner, J. (2016). Seafloor massive sulfide deposits support unique megafaunal assemblages: Implications for seabed mining and conservation. Marine Environmental Research, 115, 78–88.

Lê S., Josse J., Husson F. (2008). FactoMineR: An R Package for Multivariate Analysis. Journal of Statistical Software, 25(1), 1-18.

Le Bris, N., Yücel, M., Das, A., evert, S., LokaBharathi, P. & Girguis, P.R. (2019). Hydrothermal Energy Transfer and Organic Carbon Production at the Deep Seafloor. Frontiers in Marine Science, 5, 531.

Chapman, A.S., Beaulieu, S.E., Colaço, A., Gebruk, A.V., Hilario, A., Kihara, T.C., et al. (2019). sFDvent: A global trait database for deep-sea hydrothermal-vent fauna. Global Ecology and Biogeography.

Chase, J.M. (2010). Stochastic Community Assembly Causes Higher Biodiversity in More Productive Environments. Science, 328, 1388–1391.

Chase, J.M. & Leibold, M.A. (2002). Spatial scale dictates the productivity–biodiversity relationship. Nature, 416, 427–430.

Cuvelier, D., Beesau, J., Ivanenko, V.N., Zeppilli, D., Sarradin, P.-M. & Sarrazin, J. (2014). First insights into macro- and meiofaunal 103olonization patterns on paired wood/slate substrata at Atlantic deep-sea hydrothermal vents. Deep Sea Research Part I: Oceanographic Research Papers, 87, 70–81.

Desbruyères, D., Biscoito, M., Caprais, J.-C., Colaço, A., Comtet, T., Crassous, P., et al. (2001). Variations in deep-sea hydrothermal vent communities on the Mid-Atlantic Ridge near the Azores plateau. Deep Sea Research Part I: Oceanographic Research Papers, 48, 1325–1346.

Didham R.K., Watts C.H., Norton D.A. (2005). Are systems with strong underlying abiotic regimes more likely to exhibit alternative stable states? Oikos 110, 409–416.

Dray S., Bauman D., Blanchet G., Borcard D., Clappe S., Guenard G., Jombart T., Larocque G., Legendre P., Madi N., Wagner H.H. (2019). Adespatial: Multivariate Multiscale Spatial Analysis. R package version 0.3-4. https://CRAN.R-project.org/package=adespatial

Erickson, K.L., Macko, S.A. & Dover, C.L. (2009). Evidence for a chemoautotrophically based food web at inactive hydrothermal vents (Manus Basin). Deep Sea Research Part II: Topical Studies in Oceanography, 56, 1577–1585.

Fabricius, K., De'ath, G., Noonan, S. & Uthicke, S. (2014). Ecological effects of ocean acidification and habitat complexity on reef-associated macroinvertebrate communities. Proceedings of the Royal Society B: Biological Sciences, 281, 20132479.

Garrard, S.L., Gambi, C.M., ipione, B., Patti, F.P., Lorenti, M., Zupo, V., et al. (2014). Indirect effects may buffer negative responses of seagrass invertebrate communities to ocean acidification. Journal of Experimental Marine Biology and Ecology, 461, 31–38.

Gollner, S., Govenar, B., Arbizu, P., Mills, S., Bris, N., Weinbauer, M., et al. (2015a). Differences in recovery between deep-sea hydrothermal vent and vent-proximate communities after a volcanic eruption. Deep Sea Research Part I: Oceanographic Research Papers, 106, 167–182.

Gollner, S., Govenar, B., Fisher, C.R. & Bright, M. (2015b). Size matters at deep-sea hydrothermal vents: different diversity and habitat fidelity patterns of meio- and macrofauna. Marine Ecology Progress Series, 520, 57–66.

Gollner, S., Riemer, B., Arbizu, P., Bris, N. & Bright, M. (2010). Diversity of Meiofauna from the 9°50′N East Pacific Rise across a Gradient of Hydrothermal Fluid Emissions. PloS ONE, 5, e12321.

Govenar, B. (2010). The Vent and Seep Biota, Aspects from Microbes to Ecosystems. Springer, 33, 403–432.

Govenar, B. (2012). Energy Transfer Through Food Webs at Hydrothermal Vents: Linking the Lithosphere to the Biosphere. Oceanography, 25, 246–255.

Govenar, B., Bris, N., Gollner, S., Glanville, J., erghis, A., Hourdez, S., et al. (2005). Epifaunal community structure associated with Riftia pachyptila aggregations in chemically different hydrothermal vent habitats. Marine Ecology Progress Series, 305, 67–77.

Hall-Spencer, J.M., Rodolfo-Metalpa, R., Martin, S., Ransome, E., Fine, M., Turner, S.M., et al. (2008). Volcanic carbon dioxide vents show ecosystem effects of ocean acidification. Nature, 454, 96.

Luther III, G.W., Rozan, T.F., Taillefert, M., Nuzzio, D.B., Meo, C., ank, T., et al. (2001). Chemical speciation drives hydrothermal vent ecology. Nature, 410, 813.

Josse, J., Pagès, J. & Husson, F. (2008). Testing the significance of the RV coefficient. Computational Statistics & Data Analysis, 53, 82–91.

Kroeker, K.J., Micheli, F., Gambi, M. & Martz, T.R. (2011). Divergent ecosystem responses within a benthic marine community to ocean acidification. Proc National Acad Sci, 108, 14515–14520.

Laliberté, E. & Legendre, P. (2010). A distance-based framework for measuring functional diversity from multiple traits. Ecology, 91, 299–305.

Lamanna, C., Blonder, B., Violle, C., Kraft, N.J., Sandel, B., Šímová, I., et al. (2014). Functional trait space and the latitudinal diversity gradient. Proceedings of the National Academy of Sciences, 111, 13745–13750.

Legendre, P. (2014). Interpreting the replacement and richness difference components of beta diversity. Global Ecology and Biogeography, 23, 1324–1334.

Legendre, P. & Cáceres, M. (2013). Beta diversity as the variance of community data: dissimilarity coefficients and partitioning. Ecology Letters, 16, 951–963.

Levin, L.A., Baco, A.R., Bowden, D.A., Colaco, A., Cordes, E.E., Cunha, M.R., et al. (2016). Hydrothermal Vents and Methane Seeps: Rethinking the Sphere of Influence. Frontiers in Marine Science, 3, 72.

Mayfield M.M., Levine J.M. (2010) Opposing effects of competitive exclusion on the phylogenetic structure of communities. Ecol. Lett. 13, 1085–1093

Marsh, L., Copley, J.T., Huvenne, V.A., Linse, K., Reid, W.D., Rogers, A.D., et al. (2012). Microdistribution of Faunal Assemblages at Deep-Sea Hydrothermal Vents in the Southern Ocean. PloS ONE, 7, e48348.

McClain, C.R., Nunnally, C., Chapman, A.S. & Barry, J.P. (2018). Energetic increases lead to niche packing in deep-sea wood falls. Biology Letters, 14, 20180294.

McClain, C.R. & Rex, M.A. (2015). Toward a Conceptual Understanding of β-Diversity in the Deep-Sea Benthos. Annual Review of Ecology, Evolution, and Systematics, 46, 623–642.

McClain, C.R. & Schlacher, T.A. (2015). On some hypotheses of diversity of animal life at great depths on the seafloor. Marine Ecology, 36, 849–872.

McGill, B.J., Enquist, B.J., Weiher, E. & Westoby, M. (2006). Rebuilding community ecology from functional traits. Trends in Ecology & Evolution, 21, 178–185.

Micheli, F., Peterson, C.H., Mullineaux, L.S., Fisher, C.R., Mills, S.W., Sancho, G., et al. (2002). Predation structures communities at deep-sea hydrothermal vents. Ecol Monogr, 72, 365–382.

Mittelbach, G.G., Steiner, C.F., heiner, S., Gross, K.L., Reynolds, H.L., Waide, R.B., et al. (2001). What is the observed relationship between species richness and productivity? Ecology, 82, 2381–2396.

Mouchet, M.A., Villéger, S., Mason, N.W. & Mouillot, D. (2010). Functional diversity measures: an overview of their redundancy and their ability to discriminate community assembly rules. Functional Ecology, 24, 867–876.

Mouillot, D., Graham, N., Villéger, S., Mason, N. & Bellwood, D.R. (2013). A functional approach reveals community responses to disturbances. Trends in Ecology & Evolution, 28, 167–177.

Oksanen J., Blanchet F.G., Friendly M., Kindt R., Legendre P., McGlinn D., Minchin P.R., O'Hara R.B., Simpson G.L., Solymos P., Stevens M.H.H., Szoecs E., Wagner H. (2019). Vegan: Community Ecology Package. R package version 2.5-4. https://CRAN.R-project.org/package=vegan

Plum, C., Pradillon, F., Fujiwara, Y. & Sarrazin, J. (2017). Copepod colonization of organic and inorganic substrata at a deep-sea hydrothermal vent site on the Mid-Atlantic Ridge. Deep Sea Research Part II: Topical Studies in Oceanography, 137, 335–348.

Portail M., Brandily C., Cathalot C., Colaço A., Gelinas Y., Husson B., Sarradin P.M., Sarrazin J. (2018). Food-web complexity across hydrothermal vents on the Azores triple junction. Deep Sea Research Part I: Oceanographic Research Papers, 131, 101-120

Post, D.M. (2002). The long and short of food-chain length. Trends in Ecology & Evolution, 17, 269–277.

Quattrini, A.M., Gómez, C.E. & Cordes, E.E. (2017). Environmental filtering and neutral processes shape octocoral community assembly in the deep sea. Oecologia, 183, 221–236.

R Core Team (2019). R: A language and environment for statistical computing. R Foundation for Statistical Computing, Vienna, Austria. URL https://www.R-project.org/

Reid, W.D., Sweeting, C.J., Wigham, B.D., Zwirglmaier, K., Hawkes, J.A., McGill, R.A., et al. (2013). Spatial Differences in East Scotia Ridge Hydrothermal Vent Food Webs: Influences of Chemistry, Microbiology and Predation on Trophodynamics. PloS ONE, 8, e65553.

Robert, P. & Escoufier, Y. (1976). A Unifying Tool for Linear Multivariate Statistical Methods: The RV-Coefficient. Journal of the Royal Statistical Society: Series C (Applied Statistics), 25, 257–265.

Ruhl H.A. & Smith Jr. K.L. (2004). Shifts in deep-sea community structure linked to climate and food supply. Science, 305, 513-515.

Ruhl H.A., Ellena J.A., Smith Jr. K.L. (2008). Connections between climate, food limitation, and carbon cycling in abyssal sediment communities. PNAS, 105, 17006-17011

Sarrazin, J., Legendre, P., de Busserolles, F., Fabri, M.-C., Guilini, K., Ivanenko, V.N., et al. (2015). Biodiversity patterns, environmental drivers and indicator species on a high-temperature hydrothermal edifice, Mid-Atlantic Ridge. Deep Sea Research Part II: Topical Studies in Oceanography, 121, 177–192.

Sarrazin, J., Robigou, V. & Progress …, J.S. (1997). Biological and geological dynamics over four years on a high-temperature sulfide structure at the Juan de Fuca Ridge hydrothermal observatory.

Sen, A., Kim, S., Miller, A.J., Hovey, K.J., Hourdez, S., Luther, G.W., et al. (2016). Peripheral communities of the Eastern Lau Spreading Center and Valu Fa Ridge: community composition, temporal change and comparison to near-vent communities. Marine Ecology, 37, 599–617.

Shank, T.M., Fornari, D.J., Damm, K.L., Lilley, M.D., Haymon, R.M. & Lutz, R.A. (1998). Temporal and spatial patterns of biological community development at nascent deep-

sea hydrothermal vents (9°50′N, East Pacific Rise). Deep Sea Res Part II Top Stud Oceanogr, 45, 465–515.

Sievert, S. & Vetriani, C. (2012). Chemoautotrophy at Deep-Sea Vents: Past, Present, and Future. *Oceanography*, 25, 218–233.

Smith, C. & Snelgrove, P. (2002). Oceanography and Marine Biology: An Annual Review, 40, 311–342.

Teixidó, N., Gambi, M., Parravacini, V., Kroeker, K., Micheli, F., Villéger, S., et al. (2018). Functional biodiversity loss along natural CO2 gradients. Nature Communications, 9, 5149.

Van Dover, C.L. (2019). Inactive Sulfide Ecosystems in the Deep Sea: A Review. Frontiers in Marine Science, 6, 461.

Van Dover, C.L., Arnaud-Haond, S., Gianni, M., Helmreich, S., Huber, J.A., Jaeckel, A.L., et al. (2018). Scientific rationale and international obligations for protection of active hydrothermal vent ecosystems from deep-sea mining. Marine Policy, 90, 20–28.

Van Dover, C.L. & Series, T.J. (2000). Diversity at deep-sea hydrothermal vent and intertidal mussel beds.

Vanreusel, A., Groote, A., Gollner, S. & Bright, M. (2010). Ecology and Biogeography of Free-Living Nematodes Associated with Chemosynthetic Environments in the Deep Sea: A Review. PloS ONE, 5, e12449.

Vizzini, S., Martínez-Crego, B., Andolina, C., Massa-Gallucci, A., Connell, S. & Gambi, M. (2017). Ocean acidification as a driver of community simplification via the collapse of higher-order and rise of lower-order consumers. Sci Rep-uk, 7, 4018.

Weiher, E., Freund, D., Bunton, T., Stefanski, A., Lee, T. & Bentivenga, S. (2011). Advances, challenges and a developing synthesis of ecological community assembly theory. Philosophical transactions of the Royal Society of London. Series B, Biological sciences, 366, 2403–13.

Zeppilli, D., Leduc, D., Fontanier, C., Fontaneto, D., Fuchs, S., Gooday, A.J., et al. (2018). Characteristics of meiofauna in extreme marine ecosystems: a review. Marine Biodiversity, 48, 35–71.

Zeppilli, D., Vanreusel, A., Pradillon, F., Fuchs, S., Mandon, P., James, T., et al. (2015). Rapid 109olonization by nematodes on organic and inorganic substrata deployed at the deep-sea Lucky Strike hydrothermal vent field (Mid-Atlantic Ridge). Marine Biodiversity, 45, 489–504.
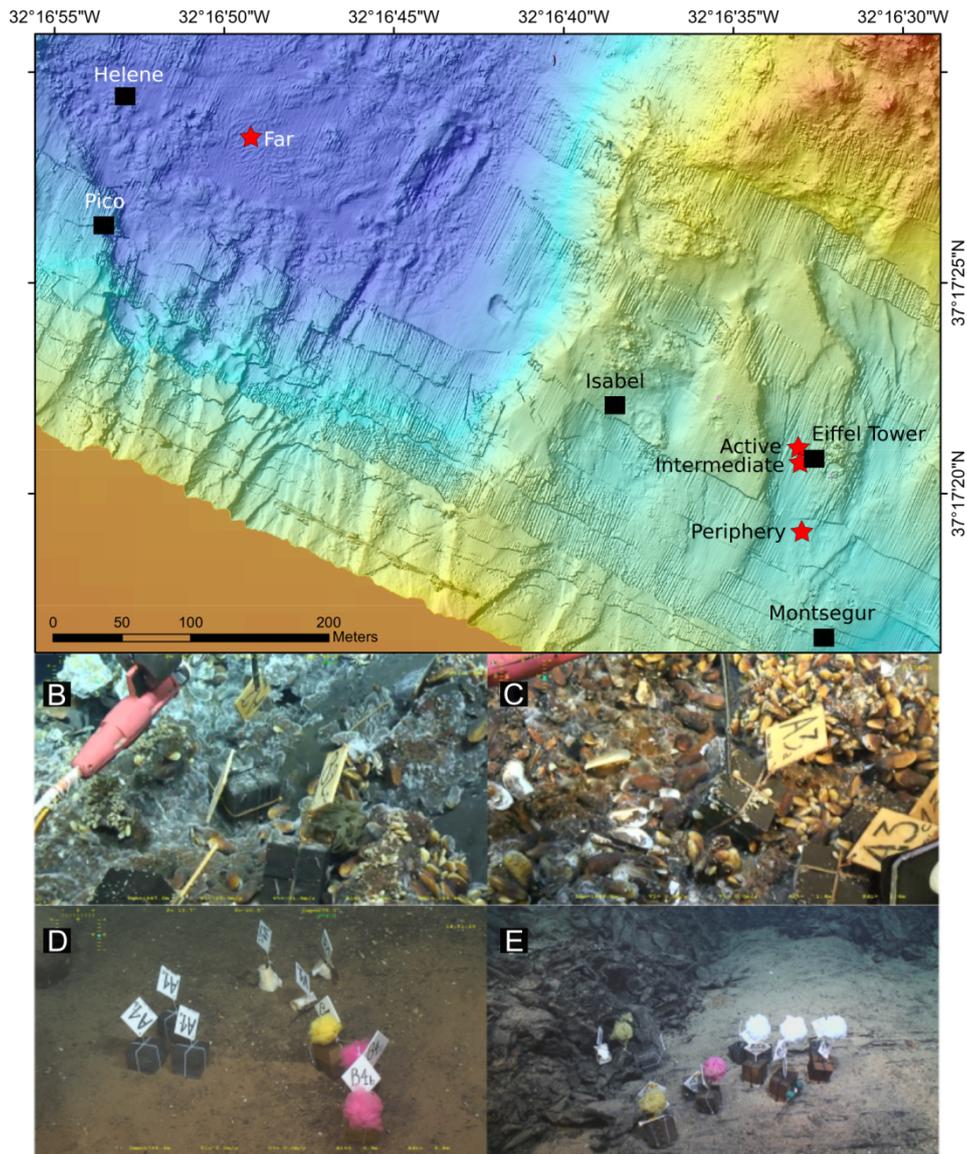
Figure S3.1.1. The southeast region of the Lucky Strike vent field located at 1700 m depth on the Mid-Atlantic Ridge, south of the Azores. A. Locations of the four deployment sites (red stars) and surrounding main active edifices (black squares). Note that the far site is located further west, in the fossil lava lake. Colonized substratum blocks at B. active, C. intermediate, D. periphery and E. far sites. Also visible in the photos are the other types of substratum used in parallel experiments.

Appendix S3.2

Table S3.2.1. Functional indices used to measure functional diversity. Formulas for index computation, index relationships, properties, and interpretations can be found in the given references.

Measure	Goal	Properties	Interpretation	References
Functional richness (FRic)	FRic measures the volume of functional space.	FRic is very sensitive to the number of species and outliers. It does not consider species abundance.	High FRic values equal to high functional richness	Villéger et al., 2008; Mouchet et al., 2010
Functional entities (FEs)	FEs measures the number of unique trait combinations.	FEs is very sensitive to the number of species. It does not consider species abundances.	High FEs may indicate high functional richness	Teixido et al. 2018
Functional evenness (FEve)	FEve measures the regularity of the distribution of species and abundances in the functional space.	FEve determines the distribution of species in the functional space independently of its volume. It considers species abundance. It is only weakly affected by species richness. Bounded between 0 and 1.	FEve is high when species and species abundance are regularly distributed in the functional space. Low values of FEve correspond to uneven of species and their abundance in the functional space.	Villéger et al., 2008; Mouchet et al., 2010

Table S3.2.2. Species trait definitions for meio- and macrofauna species.

Trait	Categories	Definition	Rationale	References
Adult motility	1 (Facultative)	Regularly non-mobile and only moving when necessary	This trait affects the ability of a species to access suitable habitat and nutritional sources. Species with high mobility may be less vulnerable to the environment stress and predation.	Bates et al. (2010)
	2 (Slow)	Regularly vagile slow swimmer, walker, or crawler		
	3 (Fast)	Regularly vagile fast swimmer and/or walker		
Maximum adult body size	0	0.02 - <0,3 mm	Size is fundamentally related to energy flow and nutrient cycling. It affects the physiological tolerance of organisms (thermal mass, barriers to diffusion, and limits anatomical, physiological or behavioral options). It is also closely related to dispersal and reproduction.	McGill et al. (2006); Gollner et al. (2015); McClain et al. (2018a)
	1	≥0.3 - <1 mm		
	2	≥1 - <5 mm		
	3	≥5 - <10 mm		
	4	≥10 - <15 mm		
	5	≥15 - <20 mm		
	6	≥20 mm		
Feeding mechanism	Deposit	Mainly obtains food particles from the surface or buried food particles from the subsurface	Feeding mechanisms are indicators of ecosystem productivity or energy availability. A diverse community will likely harbor species with diverse feeding mechanisms and trophic levels.	Post (2002); McClain et al. (2018b)
	Grazing	Scrapes or nibbles food from substrate		
	Predator	Mainly captures prey capable of resistance		

Table S.3.2.3. Functional traits of meiofauna species.

Species	Adult mobility	Max adult body size	Feeding mechanism	References
Halomonhystera sp.	2	0	Deposit feeder	Wieser (1953); Zeppilli et al. (2015)
Oncholaimus dyvae	2	3	Predator	Wieser (1953); Zeppilli et al. (2019)
Paracanthonchus sp.	2	0	Predator	Wieser (1953); Zeppilli et al. (2015)
Microlaimus sp.	2	0	Grazer	Wieser (1953); Zeppilli et al. (2015)
Cephalochetosoma sp.	2	0	Deposit feeder	Wieser (1953); Zeppilli et al. (2015)
Chromadorita sp.	2	0	Deposit feeder	Wieser (1953); Zeppilli et al. (2015)
Theristus sp.	2	0	Deposit feeder	Wieser (1953); Zeppilli et al. (2015)
Epsilonema sp.	2	0	Deposit feeder	Wieser (1953); Zeppilli et al. (2015)
Tegastidae sp.	2	0	Grazer	Heptner & Ivanenko (2002)
Smacigastes micheli	2	1	Grazer	Heptner & Ivanenko (2002)
Hepterina confusa	3	1	Grazer	Heptner & Ivanenko (2002)
Calanoida sp.	3	1	Grazer	Heptner & Ivanenko (2002)
Bathylaophonte azorica	2	1	Grazer	Heptner & Ivanenko (2002)
Tisbidae sp. 1	3	0	Grazer	Heptner & Ivanenko (2002)
Donsiellinae sp.	2	1	Grazer	Heptner & Ivanenko (2002)
Miraciidae sp.	2	1	Grazer	Heptner & Ivanenko (2002)
Ameiridae sp. 1	2	1	Grazer	Heptner & Ivanenko (2002)
Ameiridae sp. 2	2	1	Grazer	Heptner & Ivanenko (2002)
Ameiridae sp. 3	2	0	Grazer	Heptner & Ivanenko (2002)
Ameiridae sp. 4	2	0	Grazer	Heptner & Ivanenko (2002)
Ectinosomatidae sp. 1	2	0	Grazer	Heptner & Ivanenko (2002)
Ectinosomatidae sp. 2	2	1	Grazer	Heptner & Ivanenko (2002)
Archesola typhlops	2	0	Grazer	Heptner & Ivanenko (2002)
Mesochra sp.	2	0	Grazer	Heptner & Ivanenko (2002)
Aphotopontius sp.	3	1	Grazer	Heptner & Ivanenko (2002) ; Limén et al. (2008) ; Gollner et al. (2015), Senokuchi et al. (2018)
Rimipontius sp.	3	1	Grazer	Heptner & Ivanenko (2002) ; Limén et al. (2008) ; Gollner et al. (2015), Senokuchi et al. (2018)
cf. *Ambilimbus* sp.	2	0	Grazer	Heptner & Ivanenko (2002)
cf. Kelleiriidae sp.	3	0	Grazer	Heptner & Ivanenko (2002)
Thomontocypris excussa	3	1	Grazer	Desbruyères et al. (2006) and references therein; Chapman et al. (2019); Tanaka pers. Obs.
Xylocythere sp.	3	1	Grazer	Desbruyères et al. (2006) and references therein; Chapman et al. (2019); Tanaka pers. Obs.
Halacaridae sp.	2	1	Predator	Desbruyères et al. (2006) and references therein

Table S.3.2.4. Functional traits of macrofauna species.

Species	Adult motility	Max body size	Feeding mechanism	References
Lepetodrilus atlanticus	2	2	Grazer	Desbruyères et al. (2006) and references therein
Pseudorimula midatlantica	2	3	Grazer	Desbruyères et al. (2006) and references therein
Protolira valvatoides	2	2	Grazer	Desbruyères et al. (2006) and references therein
Lurifax vitreus	2	2	Grazer	Desbruyères et al. (2006) and references therein
Xylodiscula analoga	2	2	Grazer	Desbruyères et al. (2006) and references therein
Lirapex costellata	2	2	Grazer	Desbruyères et al. (2006) and references therein
Shinkailepas briandi	2	3	Grazer	Desbruyères et al. (2006) and references therein
Laeviphitus debruyeresi	2	2	Grazer	Desbruyères et al. (2006) and references therein
Amphisamytha lutzi	1	5	Deposit feeder	Desbruyères et al. (2006) and references therein
Glycera tesselata	2	4	Predator	Desbruyères et al. (2006) and references therein
Branchipolynoe seepensis	3	6	Deposit feeder	Desbruyères et al. (2006) and references therein
Branchinotogluma sp. 1	3	3	Predator	Jumars et al. (2015); authors pers. obs.
Bathykermadeca sp.	3	4	Predator	Jumars et al. (2015); authors pers. obs.
Lepidonotopodium sp.	3	4	Predator	Jumars et al. (2015); authors pers. obs.
Macelliphaloides sp.	3	2	Predator	Jumars et al. (2015); authors pers. obs.
Polynoid sp. 1	3	4	Predator	Jumars et al. (2015); authors pers. obs.
Prionospio unilamellata	1	5	Deposit feeder	Desbruyères et al. (2006) and references therein
Laonice athecata	1	6	Deposit feeder	Desbruyères et al. (2006) and references therein
Ophryotrocha cf. *platykephale*	2	2	Grazer	Desbruyères et al. (2006) and references therein
Ophryotrocha fabriae	2	2	Grazer	Desbruyères et al. (2006) and references therein
Phyllodocidae sp.	2	3	Predator	Jumars et al. (2015); authors pers. obs.
Acrocirridae sp.	2	3	Deposit feeder	Jumars et al. (2015); authors pers. obs.
Tomopteris sp. 1	3	2	Predator	Jumars et al. (2015)
Tomopteris sp. 2	3	2	Predator	Jumars et al. (2015)
Opheliidae sp.	1	3	Deposit feeder	Jumars et al. (2015)
Nereididae sp.	3	3	Predator	Jumars et al. (2015), Shimabukuro pers. obs.
Flabelligeridae sp.	2	2	Deposit feeder	Desbruyères et al. (2006) and references therein
Cnidaria sp.	1	2	Predator	Desbruyères et al. (2006) and references therein
Luckia striki	2	3	Deposit feeder	Desbruyères et al. (2006) and references therein
Liljeborgiidae sp.	2	3	Deposit feeder	Desbruyères et al. (2006), Authors pers. obs
Stegocephalidae sp.	2	3	Deposit feeder	Desbruyères et al. (2006), Authors pers. obs
cf. *Storthyngura* sp.	2	3	Deposit feeder	Desbruyères et al. (2006) and references therein

Asellota sp. 1	2	3	Deposit feeder	Desbruyères et al. (2006)
Asellota sp. 2	2	3	Deposit feeder	Desbruyères et al. (2006)
Asellota sp. 4	2	3	Deposit feeder	Desbruyères et al. (2006)
Obesutanais sigridae	1	2	Deposit feeder	Desbruyères et al. (2006) and references therein
cf. *Typhlotanais incognitus*	2	2	Deposit feeder	Desbruyères et al. (2006) and references therein
Thomontocypris excussa	3	1	Grazer	Desbruyères et al. (2006) and references therein; Chapman et al. (2019); Tanaka pers. Obs.
Aphotopontius sp.	3	1	Grazer	Heptner & Ivanenko (2002); Limén et al. (2008); Gollner et al. (2015), Senokuchi et al. (2018)
Rimipontius sp.	3	1	Grazer	Heptner & Ivanenko (2002); Limén et al. (2008); Gollner et al. (2015), Senokuchi et al. (2018)
Bathylaophonte azorica	2	1	Grazer	Heptner & Ivanenko (2002)
Smacigastes micheli	2	1	Grazer	Desbruyères et al. (2006) and references therein, Chapman et al. (2019)
Miraciidae sp.	2	1	Grazer	Heptner & Ivanenko (2002)
Tisbe sp. 2	3	1	Grazer	Heptner & Ivanenko (2002)
Ameiridae sp. 1	2	1	Grazer	Heptner & Ivanenko (2002)
Ameiridae sp. 2	2	1	Grazer	Heptner & Ivanenko (2002)
Lobopleura sp.	2	1	Grazer	Heptner & Ivanenko (2002)
Haifameira sp.	2	1	Grazer	Heptner & Ivanenko (2002)
Hepterina confusa	3	1	Grazer	Heptner & Ivanenko (2002)
Donsiellinae sp.	2	1	Grazer	Heptner & Ivanenko (2002)
Cyclopina sp.	3	1	Grazer	Heptner & Ivanenko (2002)
Cyclopoida sp.	3	1	Grazer	Heptner & Ivanenko (2002)
Halacaridae sp.	2	1	Predator	Desbruyères et al. (2006)
Ophiuroidea sp.	2	3	Deposit feeder	Desbruyères et al. (2006)
Oncholaimus dyvae	2	3	Predator	Wieser (1953); Zeppilli et al. (2019)
Desmodora sp.	2	1	Grazer	Wieser (1953); Zeppilli et al. (2015)
Chaetognatha sp.	1	3	Predator	Desbruyères et al. (2006)
Nemertea sp.	2	2	Predator	Desbruyères et al. (2006)

References:

1. Chapman, A. S. et al. sFDvent: A global trait database for deep-sea hydrothermal-vent fauna. Global Ecology and Biogeography. https://doi.org/10.1111/geb.12975 (2019).

2. Bates, A. E., Lee, R. W., Tunnicliffe, V. & Lamare, M. D. Deep-sea hydrothermal vent animals seek cool fluids in a highly variable thermal environment. *Nature Communications* **1,** 14 (2010).

3. Chapman, A. S., Tunnicliffe, V. & Bates, A. E. Both rare and common species make unique contributions to functional diversity in an ecosystem unaffected by human activities. *Diversity and Distributions* **24,** 568–578 (2018).

4. Desbruyères, D. *et al.* Variations in deep-sea hydrothermal vent communities on the Mid-Atlantic Ridge near the Azores plateau. *Deep Sea Research Part I: Oceanographic Research Papers* **48,** 1325–1346 (2001).

5. Gollner, S., Govenar, B., Fisher, C. R. & Bright, M. Size matters at deep-sea hydrothermal vents: different diversity and habitat fidelity patterns of meio- and macrofauna. *Marine ecology progress series* **520,** 57–66 (2015).

6. Heptner M. V. & Ivanenko V. N. Copepoda (Crustacea) of hydrothermal ecosystems of the World Ocean. *Arthropoda Selecta* **11**, 117-134 (2002).

7. Jumars, P. A., Dorgan, K. M. & Lindsay, S. M. Diet of Worms Emended: An Update of Polychaete Feeding Guilds. *Annu Rev Mar Sci* **7,** 497–520 (2015).

8. Laliberté, E. & Legendre, P. A distance-based framework for measuring functional diversity from multiple traits. *Ecology* **91,** 299–305 (2010).

9. Levesque, C., Juniper, K. S. & Limén, H. Spatial organization of food webs along habitat gradients at deep-sea hydrothermal vents on Axial Volcano, Northeast Pacific. *Deep Sea Research Part I: Oceanographic Research Papers* **53,** 726–739 (2006).

10. McClain, C. R., Barry, J. P. & Webb, T. J. Increased energy differentially increases richness and abundance of optimal body sizes in deep-sea wood falls. *Ecology* **99,** 184–195 (2018).

11. McGill, B. J., Enquist, B. J., Weiher, E. & Westoby, M. Rebuilding community ecology from functional traits. *Trends in Ecology & Evolution* **21,** 178–185 (2006).

12. Mouchet, M. A., Villéger, S., Mason, N. W. & Mouillot, D. Functional diversity measures: an overview of their redundancy and their ability to discriminate community assembly rules. *Functional Ecology* **24,** 867–876 (2010).

13. Senokuchi, R. *et al.* Chemoautotrophic food availability influences copepod assemblage composition at deep hydrothermal vent sites within sea knoll calderas in the northwestern Pacific. *Marine Ecology Progress Series* **607,** 37–51 (2018).

14. Villéger, S. *et al*. New multidimensional functional diversity indices for a multifaceted framework in functional ecology. *Ecology* **89**, 2290-2301 (2019).

15. Wieser, W. Die Beziehung zwischen Mundhoehlengestalt, Ernaehrungsweise und Vorkommen bei freilebenden marinen Nematoden. *Arkiv for Zoologi* 2, 439–484 (1953).

16. Zeppilli, D. *et al.* Rapid colonisation by nematodes on organic and inorganic substrata deployed at the deep-sea Lucky Strike hydrothermal vent field (Mid-Atlantic Ridge). *Marine Biodiversity* **45,** 489–504 (2015).

17. Zeppilli D. *et al*. Ecology and trophic role of *Oncholaimus dyvae* sp. nov. (Nematoda: Oncholaimidae) from the lucky strike hydrothermal vent field (Mid-Atlantic Ridge*). BMC Zoology* **4**: 6 (2019).

Appendix S3.3

Isotope analyses:

For relatively large taxa, muscle tissue was used. Guts and calcareous structures were removed manually whenever possible. Inorganic carbon present in samples can be a source of bias in carbon stable isotope analysis. "Champagne tests" were used to highlight the presence of carbonates in tissues (Jaschinski et al. 2008) and, when positive, samples were acidified by exposing them to HCl vapors for 48 h in an airtight container (Hedges & Stern 1984). After acidification, a second "champagne test" series was run. When the second test was still positive, we proceeded with direct acidification (0.2 ml of 10% HCl added directly to the sample in a silver cup) (Jaschinski et al 2008). Isotope analyses were done at the University of Liege (Belgium) using a vario MICRO cube (Elementar, Germany) elemental combustion system coupled to an IsoPrime100 (Elementar, United Kingdom) isotope ratio mass spectrometer. Isotope ratios were expressed using the widespread δ notation (Coplen 2010), in ‰ and relative to the international references Vienna Pee Dee Belemnite (for carbon), Atmospheric Air (for nitrogen) and Vienna Canyon Diablo Troilite (for sulfur). IAEA (International Atomic Energy Agency, Vienna, Austria) certified reference materials sucrose (IAEA-C-6; $\delta^{13}C$ = -10.8 ± 0.5‰; mean ± SD), ammonium sulphate (IAEA-N-1; $\delta^{15}N$ = 0.4 ± 0.2‰; mean ± SD), and silver sulfide (IAEA-S-1 $\delta^{34}S$ = -0.3‰) were used as primary analytical standards. Sulfanilic acid (Sigma-Aldrich; $\delta^{13}C$ = -25.6 ± 0.4‰; $\delta^{15}N$ = -0.13 ± 0.4‰; $\delta^{34}S$ = 5.9 ± 0.5‰; means ± SD) was used as a secondary analytical standard. Standard deviations on multi-batch replicate measurements of secondary and internal lab standards (seabass muscle) were interspersed with samples (one replicate of each standard every 15 analyses) were 0.2‰ for both $\delta^{13}C$, 0.3‰ for $\delta^{15}N$ and 0.5‰ for $\delta^{34}S$.

Table S3.3.1. Stable isotope mean (X) and standard deviations (sd) values for δ¹³C, δ¹⁵N and δ³⁴S for active, intermediate (Interm.), periphery (Periph.) and far sites. N= number of samples. Code= number representing species at Figure S2A and S2B.

Species	N	Site	Code	X δ¹³C	sd δ¹³C	X δ¹⁵N	sd δ¹⁵N	X δ³⁴S	sd δ³⁴S
Amphisamytha lutzi	12	Active	10	-24.37	2.68	4.87	0.45	3.54	0.76
Bathymodiolus azoricus	3	Active	-	-32.09	0.28	-7.69	1.43	5.99	2.43
Branchipolynoe seepensis	1	Active	4	-29.34		-7.05		2.65	
Glycera tesselata	1	Active	6	-28.41		7.18		5.25	
Lepetodrilus atlanticus	1	Active	5	-28.92		1.76			
Protolira valvatoides	2	Active	7	-27.24	0.21	1.96	0.16	6.35	1.21
Pseudorimula midatlantica	2	Active	2	-31.92	0.67	0.81	1.31	4.21	
Smacigastes micheli	1	Active	1	-34.57		3.24			
Oncholaimus dyvae	1	Active	11	-22.73		5.02		3.58	
Lirapex costellata	1	Active	9	-24.78		4.11		6.76	
Sipuncula sp.	1	Active	12	-18.97		4.83			
Prionospio unilamellata	1	Active	8	-27.24		3.20			
Ophryotrocha sp. 3	1	Active	3	-31.47		3.38			
Amphisamytha lutzi	12	Interm.	10	-24.79	0.77	0.75	1.46	6.71	1.14
Bathymodiolus azoricus	23	Interm.	-	-32.01	1.30	-8.04	5.70	5.09	1.74
Branchipolynoe seepensis	18	Interm.	4	-30.56	1.52	-6.65	1.50	3.40	1.45
Glycera tesselata	5	Interm.	6	-24.18	0.63	4.95	0.32	4.74	0.13
Lepetodrilus atlanticus	1	Interm.	5	-26.94		1.86		3.55	
Protolira valvatoides	7	Interm.	7	-26.25	0.38	1.60	0.24	5.31	0.91
Pseudorimula midatlantica	3	Interm.	2	-29.46	1.35	1.08	0.57	2.82	0.49
Sipuncula *sp.*	2	Interm.	12	-21.39	1.06	3.72	1.06	4.05	
Aphotopontius sp.	1	Interm.	13	-23.10		1.23			
Ophryotrocha sp. 3	1	Interm.	3	-28.24		0.90			
Oncholaimus dyvae	1	Interm.	11	-23.30		3.08		3.82	
Liljeborgiidae sp.	1	Periph.	18	-21.35		8.33			
Lepidonotopodium sp.	1	Far	17	-17.39		9.89		14.03	
Luckia striki	1	Far	15	-20.89		6.26		11.91	
Storthyngura sp.	1	Far	14	-22.77		6.94		11.25	
Heteromesus sp. 1	1	Far	16	-19.32		5.70			
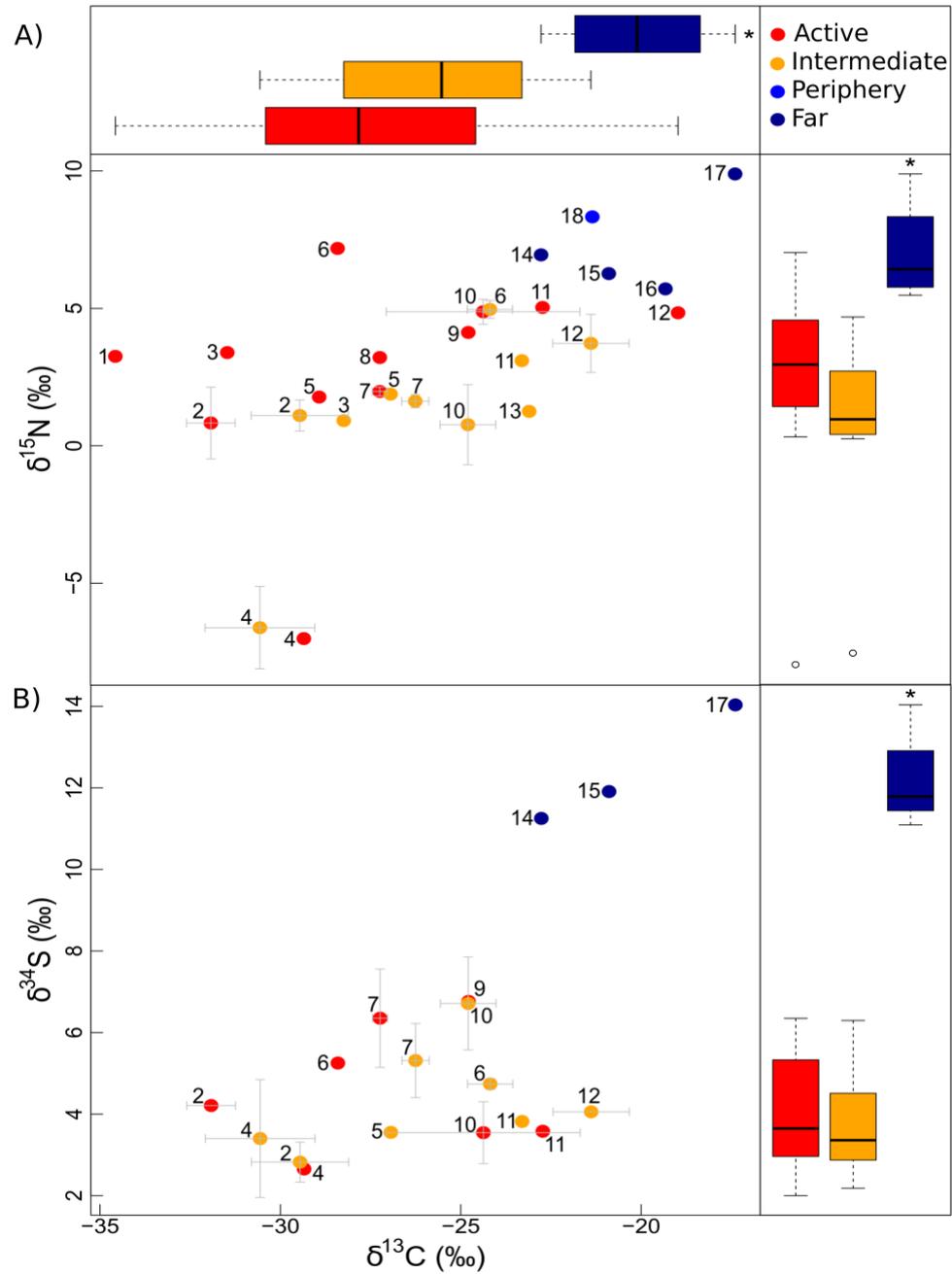
Figure S3.3.1. Stable isotope biplots of taxa at the sites included in this study. A. Biplot of ™¹³C and ™¹⁴N values with boxplots showing the distribution of the ™¹³C (upper boxplots) and ™¹⁴N (right boxplots) values at each site. B. Biplots of the ™¹³C and ™³⁴S values with boxplots of the distribution of the ™³⁴S (right boxplots) values at each site. Asterisks indicate sites with statistically different means (p>0.05). 1. *Smacigastes micheli*. 2. *Pseudorimula midatlantica*. 3. *Ophryotrocha* cf. *fabriae*. 4. *Branchipolynoe seepensis*. 5. *Lepetodrilus atlanticus*. 6. *Glycera tesselata*. 7. *Protolira valvatoides*. 8. *Prionospio unilamellata*. 9. *Lirapex costellata*. 10. *Amphisamytha lutzi*. 11. *Oncholaimus dyvae*. 12. Sipuncula sp. 13. *Aphotopontius* sp. 14. cf. *Storthyngura* sp. 15. *Luckia striki*. 16. Assellota sp. 1. 17. *Lepidonotopodium* sp. 18. Liljeborgiidae sp.

Appendix S3.4

Table S3.4.1. Mean percentage abundance (± standard deviation) of meiofaunal taxa (<300->20 µm) on the slate blocks at the four sites. Higher values are highlighted in bold.

Phylum	Class	Order	Species	Active	Intermediate	Periphery	Far
Nematoda	Chromadorea	Monhysterida	*Halomonhystera* sp.	0.17±0.16	0	0	0
		Monhysterida	*Theristus* sp.	0	0	2.08±3.61	0.93±1.60
		Chromadorida	*Paracanthonchus* sp.	17.28±12.24	1.85±1.18	0	0
		Chromadorida	*Chromadorita* sp.	0.65±1.12	12.10±6.24	0	1.75±3.04
		Desmodorida	*Cephalochaetosoma* sp.	5.30±2.76	**30.51±20.65**	0	0
		Desmodorida	*Microlaimus* sp.	2.20±2.91	27.45±15.17	0	0.58±1.01
		Desmodorida	*Epsilonema* sp.	0	0	0	0.37±0.65
	Enoplea	Enoplida	*Oncholaimus dyvae*	2.35±1.31	7.07±4.66	0	0
Arthropoda	Hexanauplia	Cyclopoida	*Heptnerina confusa*	6.54±1.99	6.80±4.53	0	7.32±3.42
			cf. *Ambilimbus* sp.	0	0	0	1.85±3.21
			cf. Kelleriidae sp.	0	0	0	6.36±4.00
		Calanoida	Calanoida sp.	0.22±0.37	0	0	0
		Harpacticoida	Tegastidae sp.	8.53±9.11	0	5.13±8.88	2.34±4.05
			Smacigastes micheli	**18.59±4.51**	1.03±1.78	0	0
		Harpacticoida	*Bathylaophonte azorica*	6.37±8.32	0	0	8.72±7.60
			Tisbidae sp. 1	3.96±6.49	0.54±0.47	0	0.37±0.65
			Donsiellinae sp.	0.06±0.10	0.26±0.45	0	0
			Miraciidae sp.	5.30±3.85	1.08±0.53	2.56±4.44	0
			Ameiridae sp. 1	2.05±2.71	0.26±0.45	**45.83±8.18**	18.61±5.25
			Ameiridae sp. 2	0	0.52±0.91	0	0
			Ameiridae sp. 3	0.65±1.12	0	0	**22.50±19.08**
			Ameiridae sp. 4	0.22±0.37	0	36.06±4.16	6.48±3.67
			Ectinosomatidae sp. 1	2.65±2.50	0.26±0.45	6.25±10.83	2.84±0.63
			Ectinosomatidae sp. 2	0	0	0	0.58±1.01
			Archesola typhlops	0.86±1.49	1.31±0.86	0	0
			Mesochra sp.	0.29±0.50	0	0	10.02±8.01
		Siphonostomatoida	*Aphotopontius* sp.	2.40±3.61	2.12±2.97	0	0
			Rimipontius sp.	0.45±0.45	0	0	0
	Ostracoda	Podocopida	*Thomontocypris excussa*	7.15±6.26	3.72±0.79	0	8.34±5.37
			Xylocythere sp.	0	0.26±0.44	0	0
	Arachnida	Trombidiformes	Halacaridae sp.	5.77±5.23	2.84±2.71	2.08±3.61	0

Table S.3.4.2. Mean raw abundance (± standard deviation) of macrofaunal taxa (≥300 µm) on the slate blocks at the four sites. High values are highlighted in bold. Abundances of *Bathymodiolus azoricus* are shown, although this species was not included in statistical analyses (see Materials and Methods).

Phylum	Class	Order	Species	Active	Intermediate	Periphery	Far
Mollusca	Bivalvia	Mytilida	*Bathymodiolus azoricus*	78±57.58	776.33±179.63	0	0
	Gastropoda	Lepetellida	*Lepetodrilus atlanticus*	10.33±11.93	40.33±14.64	0	0
			Pseudorimula midatlantica	8.67±10.02	22.00±8.89	0	0
		Trochida	*Protolira valvatoides*	21.00±17.09	124.00±14	0	0
			Lurifax vitreus	0.67±0.58	3.33±4.04	**5.67±3.51**	0.67±1.15
			Xylodiscula analoga	0	3.33±1.53	0	0
			Lirapex costellata	1.33±0.58	1.00±1.73	0	0
		Cycloneritida	*Divia briandi*	1.67±2.08	0	0	0
		Littorinimorpha	*Laeviphitus debruyeresi*	0	6.33±4.93	0	0
Annelida	Polychatea	Terebellida	*Amphisamytha lutzi*	95.00±87.64	133.00±71.44	0	0
			Acrocirridae sp.	0	0.33±0.58	0	0.67±0.58
			Flabelligeridae sp.	0	0	0	1.00±0.00
		Phyllodocida	*Glycera tesselata*	4.33±6.66	11.67±4.93	2.33±0.58	0.33±0.58
			Branchipolynoe seepensis	4.33±2.31	29.33±28.92	0	0
			Branchinotogluma sp. 1	0	1.33±2.31	0	0
			Bathykermadeca sp.	0	0	0	0.67±1.15
			Lepidonotopodium sp.	0.33±0.58	0	0	0.33±0.58
			Macellicephala sp.	0.33±0.58	0	0	0
			Polynoidae sp. 1	0	0.67±1.15	0	0
			Phyllodocidae sp.	0	0	0	0.33±0.58
			Tomopteris sp. 1	0.33±0.58	0	0	0
			Tomopteris sp. 2	0.33±0.58	0	0	0
			Opheliidae sp.	0	0	0	0.33±0.58
			Nereididae sp.	0	0	0.33±0.58	0.33±0.58
		Spionida	*Prionospio unilamellata*	1.67±2.89	0.33±0.58	0	0
			Laonice athecata	0	0.33±0.58	0	0
		Eunicia	*Ophryotrocha* cf. *platykephale*	0	13.00±22.52	0	0
			Ophryotrocha fabriae	22.33±20.53	24.00±29.55	0	0
Cnidaria			Cnidaria sp.	0	0	0	3.33±5.77
Arthropoda	Malacostraca	Amphipoda	*Luckia striki*	3.33±2.89	31.33±12.34	0.33±0.58	3.33±0.58
			Liljeborgiidae sp.	0	0	2.67±2.89	0.67±1.15
			Stegocephalidae sp.	0	0	0	0.33±0.58
		Isopoda	cf. *Storthyngura* sp.	0	0	0	1.33±1.53
			Heteromesus sp. 1	0	0	0	0.67±1.15
			Asellota sp. 2	0	0	1.00±1.00	1.33±1.53
			Asellota sp. 4	0	0	0.33±0.58	0
		Tanaidacea	*Obesutanais sigridae*	0	0	0.33±0.58	0
			cf. *Typhlotanais incognitus*	0	0	0	0.33±0.58
	Ostracoda	Podocopida	*Thomontocypris excussa*	20.33±20.26	7.33±6.03	0	**6.67±5.13**
	Hexanauplia	Siphonostomatoida	*Aphotopontius* sp.	33.67±49.69	8.67±9.29	0.67±0.58	0

			Rimipontius sp.	3.00±3.00	1.67±0.58	0	0
		Harpacticoida	*Bathylaophonte azorica*	1.00±1.73	0.33±0.58	0.33±0.58	1.33±0.58
			Smacigastes micheli	95.00±45.90	1.00±1.73	0	0
			Miraciidae sp.	7.33±1.15	1.00±1.00	0	0.33±0.58
			Tisbe sp. 2	4.67±8.08	0	0	0.67±0.58
			Ameiridae sp. 1	0	0	0.33±0.58	0
			Ameiridae sp. 2	0	0	0.33±0.58	0
			Lobopleura sp.	9.67±16.74	0.67±1.15	0.33±0.58	0
			Haifameira sp.	0	0	0	0.33±0.58
			Donsiellinae sp.	0	0.33±0.58	0	0
		Cyclopoida	*Heptnerina confusa*	1.00±1.00	0.67±1.15	0.33±0.58	0
			Cyclopina sp.	0	0	0	0.33±0.58
			Cyclopoida sp.	1.00±0.0	0.33±0.58	0	0
	Arachnida	Trombidiformes	Halacaridae sp.	27.67±34.78	5.00±5.57	0	0.33±0.58
Echinodermata	Ophiuroidea		Ophiuroidea sp.	0	0	0	0.33±0.58
Nematoda	Enoplea	Enoplida	*Oncholaimus dyvae*	**648.67±581.74**	**157.67±162.93**	0	0
	Chromadorea	Desmodorida	*Desmodora* sp.	0	0	0	0.33±0.58
Chaetognatha			Chaetognatha sp.	0	0	0.67±1.15	0
Nemertea			Nemertea sp.	3.33±2.89	9.00±6.08	0	0.67±1.15

Table S3.4.3. Tukey multiple comparisons of means (95% family-wise confidence level of variances) and Dunn tests after significant analyses of variances (ANOVAs) or Kruskal-Wallis rank-sum test between sites for taxonomical and functional indices for meio- and macrofauna. Significant p-values are shown in bold. Diff= means difference. * p-values<0.01

	Macrofauna		Meiofauna	
Species richness	**diff**	**p**	**diff**	**p**
Intermediate - Active	0.00*	1.00	-4.00	0.17
Periphery - Active	-13.67	**0.00***	-13.33	**0.00***
Far - Active	-8.33	**0.00***	-5.67	**0.04**
Periphery - Intermediate	-13.67	**0.00***	-9.33	**0.00***
Far - Intermediate	-8.33	**0.00***	-1.67	0.77
Far - Periphery	5.33	0.05	7.67	**0.01**
Log(Abundance)	**diff**	**p**	**diff**	**p**
Intermediate - Active	-0.44	0.60	-1.00	**0.02**
Periphery - Active	-4.02	**0.00***	-3.13	**0.00***
Far - Active	-3.57	**0.00***	-1.78	**0.00***
Periphery - Intermediate	-3.57	**0.00***	-2.13	**0.00***
Far - Intermediate	-3.12	**0.00***	-0.78	0.07
Far - Periphery	0.45	0.60	1.35	**0.00***
Evenness	**diff**	**p**	**diff**	**p**
Intermediate - Active	0.23	0.13	-4.00	0.17
Periphery - Active	0.37	**0.01**	-13.33	**0.00***
Far - Active	0.41	**0.01**	-5.67	**0.04**
Periphery - Intermediate	0.14	0.42	-9.33	**0.00***
Far - Intermediate	0.18	0.24	-1.67	0.77
Far - Periphery	0.04	0.97	7.67	**0.01**
Functional richness	**diff**	**p**	**diff**	**p**
Intermediate - Active	-7.45	0.64	-0.16	0.87
Periphery - Active	-35.47	**0.00***	-	-
Far - Active	-30.43	**0.00***	2.06	**0.04**
Periphery - Intermediate	-28.03	**0.00***	**-**	**-**
Far - Intermediate	-22.99	**0.02**	2.22	**0.03**
Far - Periphery	5.04	0.84	-	-
Functional eveness	**diff**	**p**		
Intermediate - Active	0.03	0.95		
Periphery - Active	0.29	**0.00***		
Far - Active	0.08	0.50		
Periphery - Intermediate	0.26	**0.00***		
Far - Intermediate	0.05	0.79		
Far - Periphery	-0.21	**0.02**		

Appendix S3.5

Table S3.5.1. Pairwise dissimilarity between sites (D) using the Jaccard dissimilarity coefficient and its decomposition into the nestedness and turnover components for meio- and macrofauna species and the functional entity assemblages found at each site.

Taxonomic β-diversity							
Meiofauna				**Macrofauna**			
D				**D**			
	Active	Intermediate	Periphery		Active	Intermediate	Periphery
Intermediate	0.38			Intermediate	0.38		
Periphery	0.76	0.81		Periphery	0.81	0.82	
Far	0.59	0.75	0.74	Far	0.78	0.82	0.8
Nestedness				**Nestedness**			
	Active	Intermediate	Periphery		Active	Intermediate	Periphery
Intermediate	0.18			Intermediate	0.06		
Periphery	0.51	0.21		Periphery	0.11	0.12	
Far	0.13	0.01	0.3	Far	0.01	0.02	0.1
Turnover				**Turnover**			
	Active	Intermediate	Periphery		Active	Intermediate	Periphery
Intermediate	0.2			Intermediate	0.34		
Periphery	0.25	0.6		Periphery	0.7	0.7	
Far	0.45	0.74	0.44	Far	0.77	0.8	0.7
Functional β-diversity							
Meiofauna				**Macrofauna**			
D				**D**			
	Active	Intermediate	Periphery		Active	Intermediate	Periphery
Intermediate	0			Intermediate	0.2		
Periphery	0.5	0.5		Periphery	0.69	0.62	
Far	0.37	0.37	0.5	Far	0.44	0.37	0.57
Nestedness				**Nestedness**			
	Active	Intermediate	Periphery		Active	Intermediate	Periphery
Intermediate	0			Intermediate	0.06		
Periphery	0.5	0.5		Periphery	0.14	0.22	
Far	0.37	0.37	0.1	Far	0.04	0.09	0.17
Turnover				**Turnover**			
	Active	Intermediate	Periphery		Active	Intermediate	Periphery
Intermediate	0			Intermediate	0.14		
Periphery	0	0		Periphery	0.55	0.4	
Far	0	0	0.4	Far	0.4	0.28	0.4
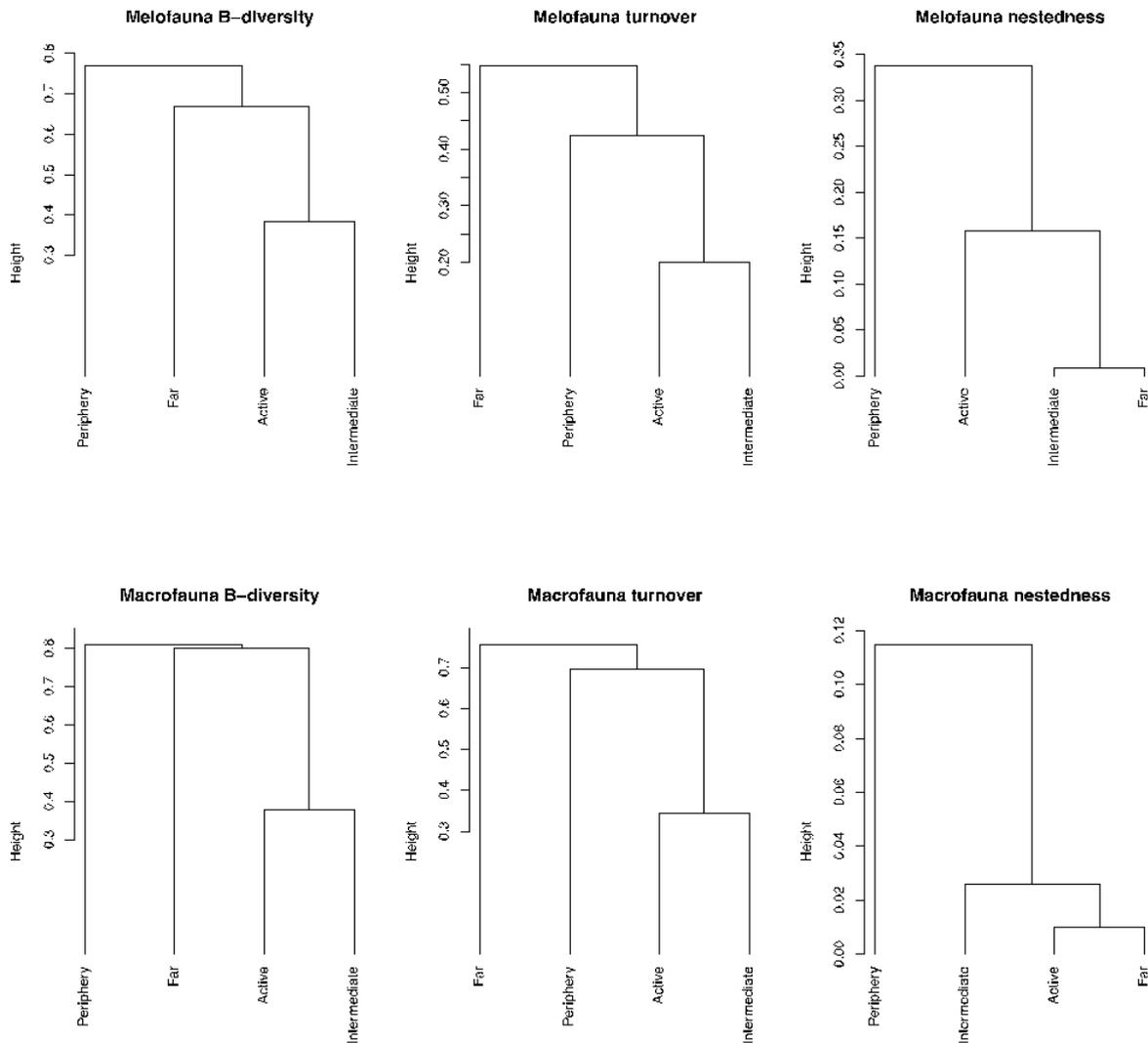
Figure S3.5.1. Clustering using average linkage of the pairwise dissimilarity (β-diversity), and its decomposition into the turnover and nestedness components of species assemblages of meio- and macrofauna found at each site.
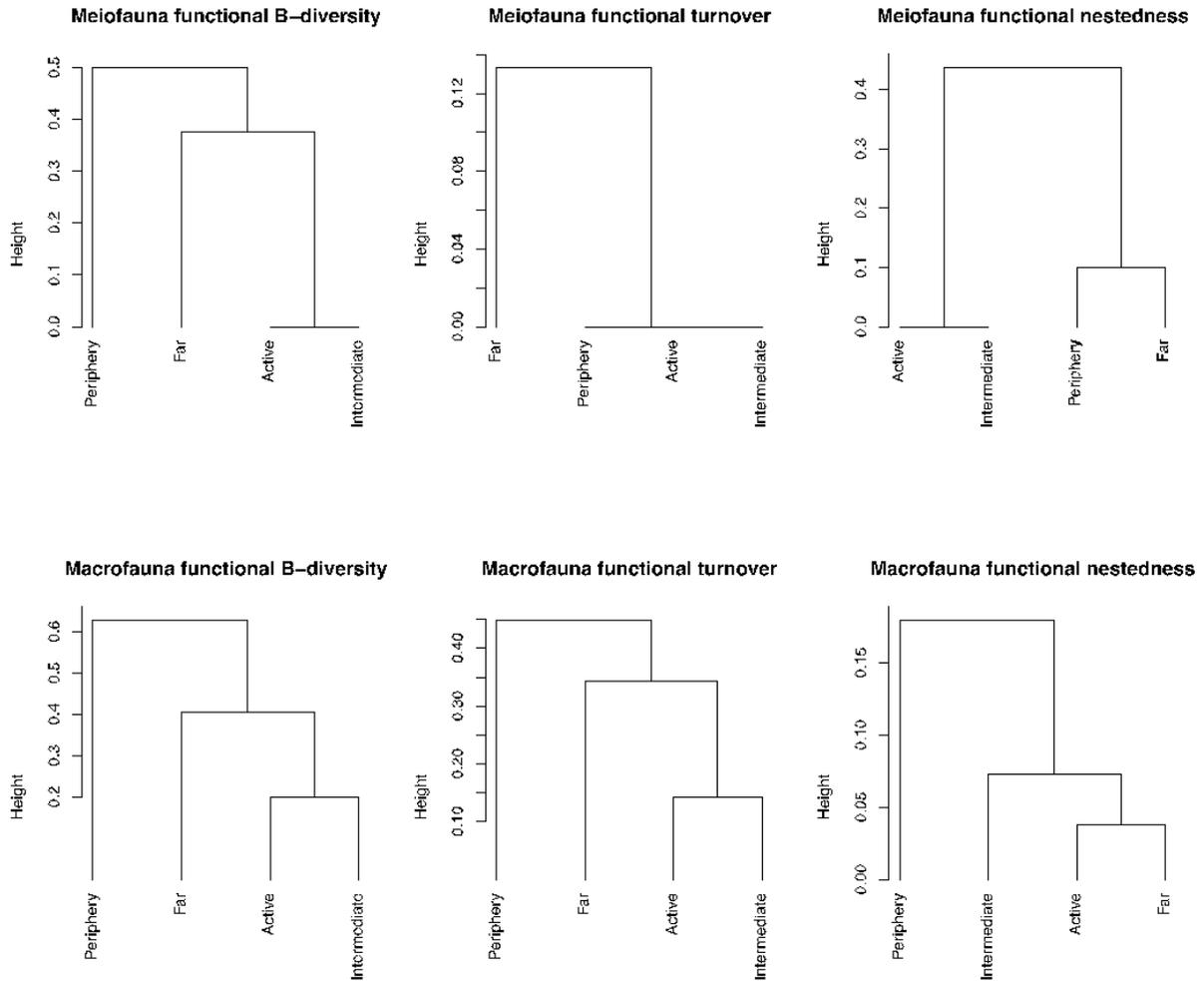
Figure S3.5.2. Clustering using average linkage of the pairwise dissimilarity (β-diversity), and its decomposition into the turnover and nestedness components of functional entity assemblages of meio- and macrofauna found at each site.

Chapter 3

Environment and diversity of ressources structure biodiversity and

assemblage composition at deep-sea hydrothermal vents and wood falls*

Environment and diversity of ressources structure biodiversity and assemblage composition at deep-sea hydrothermal vents and wood falls

Running title: Community assembly of vents and wood falls

Authors: JM Alfaro-Lucas[1, 5, 6], D Zeppilli[1], F Pradillon[1], LN Michel[1], P Martinez-Arbizu[2], H Tanaka[3], M Shimabukuro[1], G Schaal[4], M Foviaux[1], J Sarrazin[1]

[1] Institut Français de Recherche pour l'Exploitation de la Mer (IFREMER), Centre Bretagne, Plouzané, France

[2] Senckenberg am Meer, German Center for Marine Biodiversity Research, Wilhelmshaven, Germany

[3] Ocean Literacy Group, Graduate School of Science, The University of Tokyo, Tokyo, Japan

[4] Institut Universitaire Européen de la Mer, Université de Bretagne Occidentale, Plouzané, France

[5] Corresponding author: joanmanel.alfaro@e-campus.uab.cat

[6] Orcid ID: 0000-0001-5725-3218

Abstract

Multiple drivers including energy availability interact to shape the assembly of communities but little is known about this topic in the deep sea (>200 m), the largest environment on Earth. Eco-evolutionarily-related chemosynthetic-based habitats, such as hydrothermal vents and wood falls, constitute natural labs to study such processes. Here, we perfomed a 2-year experiment to study in detail the colonization of mineral and wood substrata on hydrothermal active and inactive areas at 1700 m depth in the Lucky Strike vent field (Mid-Atlantic Ridge). We examined the biodiversity patterns using an integrated framework of functional and isotopic α- and β-diversity and compared the community composition and structure. Mineral substrata in active regimes presented higher isotopic and functional richness than mineral substrata in inactive periphery suggesting that the presence of various chemosynthetic ressources in active areas support more diverse ecological strategies allowing for denser species-rich assemblages despite the associated environmental stress. Despite the species-poor assemblages observed for the smaller fauna, the presence of resources of different origins (chemosynthesis and photosynthesis) rather than the diversity of resources of one single energy source, as observed in mineral substrata in active regimes, boost the functional richness as well as the species richness and abundances at woods in periphery. These findings extend the concept of "hotspots of diversity" of wood habitats to the functional facet. The eco-evolutionary processes linked to environmental conditions and substratum type significantly drive the species and functional structures of assemblages. The high isotopic and functional space overlap highlights the role of woods in the deep-sea as potential stepping stones for meio- and macrofauna, not only for "vent" inhabitants but also for other species such as those found on the periphery.

Keywords: community assembly; energy; functional diversity; isotopic diversity; β-diversity; functional overlap

Résumé

Plusieurs facteurs, incluant la disponibilité d'énergie, interagissent sur la structure des communautés de faune, mais il existe peu de connaissances sur ce sujet dans les environnements marins profonds (> 200 m), qui représentent tout de même le plus grand biome de notre planète. Les habitats dont la chaîne alimentaire repose sur la chimiosynthèse, tels que les sources hydrothermales et les bois coulés, constituent des laboratoires naturels pour etudié de tels processus. Dans la présente étude, nous avons réalisé une expérience de deux ans pour étudier en détail la colonisation de substrats minéraux et de bois sur des zones hydrothermales actives et inactives, situées à 1 700 m de profondeur sur le champ Lucky Strike (dorsale médio-Atlantique). Nous avons examiné la biodiversité en utilisant un cadre intégré de α et de β-diversité fonctionnelles et isotopiques et comparé la composition et la structure des communautés. Nos résultats montrent que les substrats minéraux dans les zones actives possèdent une richesse isotopique et fonctionnelle supérieure à ceux situés en périphérie. Ceci suggère que la présence de diverses ressources chimiosynthétiques permet le soutien de diverses stratégies écologiques et la formation d'assemblages de densités plus élevées et ce, malgré le stress environnemental associé. Malgré la présence d'assemblages pauvres en espèces pour la faune de petites tailles, la présence de ressources de diverses origines (chimiosynthétiques et photosynthétiques) plutôt que la diversité des ressources d'une source d'énergie unique, comme observé sur les substrats minéraux des zones actives, a permis d'accroître la richesse fonctionnelle et l'abondance des espèces sur les substrats bois situés en périphérie. Ces résultats étendent le concept de «points chauds » ou hotspots de diversité» associés aux habitats « bois » à la facette fonctionnelle. Les processus éco-évolutifs, liés aux conditions environnementales et au type de substrat, joueraient un rôle important sur la composition et la structure fonctionnelle des assemblages. La forte redondance des espaces isotopiques et fonctionnels souligne l'importance des substrats bois dans les grands fonds marins en tant que potentiels « pierres de gué » ou « stepping stones » pour la meio- et la macrofaune, non seulement

pour les habitants des zones hydrotermales actives, mais également pour d'autres espèces telles que celles qui se trouvent à la périphérie.

Mots-clés : assemblages de faune ; énergie ; diversité fonctionnelle, diversité isotopique ; β-diversité ; redondance fonctionnelle

Introduction

Speciation and extinction mainly determine regional species pools, which are "sieved" by different interacting "filters" leading to the formation of local communities (Vellend, 2010; Weiher et al., 2011; Mittlebach and Schemske, 2015). Along broad gradients, dispersal and environment select for certain species traits, and inter- and intraspecific biotic interactions further determine the composition and abundances of species at local scales (Chesson, 2000; Adler, 2007; HilleRisLambers et al., 2012, Weiher et al., 2011; Kraft et al., 2015; Cadotte et al., 2017). Energy is also recognized as a main driver structuring communities with high-productive habitats usually supporting more biodiversity (e.g. Mittlebach et al., 2001; Chase and Leibold, 2002; Chase, 2010). Understanding patterns and processes driving biodiversity needs an assessment of not just the taxonomic but also the functional facet of biodiversity (Petcheley and Gaston, 2006; McGill et al., 2006; Weiher et al., 2011). The interplay of multiple filters and drivers in shaping both community assembly and different facets of biodiversity have been examined in terrestrial and shallow water systems (e.g., Micheli and Halpern, 2005; Weiher et al., 2011) but they remain less understood in the deep sea (>200m), the largest environment on Earth (e.g., McClain and Barry, 2014; Judge and Barry, 2016; Ashford et al., 2018).

Hydrothermal vents and wood logs create eco-evolutionary-related habitats considered hotspots of energy that contrast with the majority of energy-deprived deep-sea habitats (Distel et al., 2000; Bienhold et al., 2013; Le Bris et al., 2019). Rather than

shallow-water photosynthetic productivity, vent assemblages are yclop by the microbial oxidation of chemically reduced compounds of volcanic origin (reviewed in Le Bris et al., 2019). In wood habitats, the energy comes from 1) wood organic matter and 2) the microbial oxidation of reduced compounds produced from its anaerobic decomposition (Bernardino et al., 2010; Bienhold et al., 2013; Kalenitchenko et al., 2016; Kalenitchenko et al., 2018). Chemosynthetic niches in wood falls, and other organic falls, are exploited by some vent taxa, which may use wood as "stepping stones" to colonize new distant vent habitats (e.g., Smith et al., 1989; Feldman et al., 1998; Baco et al., 1999; Smith et al., 2015; Sumida et al., 2016; Smith et al., 2017; Kiel, 2017; Shimabukuro et al., 2019). Moreover, some vent iconic taxa likely originated in shallow waters and used organic falls to colonize deep-sea vents (e.g., Distel et al., 2000; Jones et al., 2006; Fujiwara et al., 2010; Miyazaki et al., 2010; Lorion et al., 2013; Thubaut et al., 2013). Fundamental differences also exist between these two systems (Kiel et al., 2016). Vents are mainly associated to tectonic plate boundaries (e.g., Van Dover et al., 2002) whereas wood is widespread but more commonly concentrated in canyons, trenches, and continental margins near large rivers and forested regions (Wolff, 1979; Bienhold et al., 2013; Romano et al., 2013). Vents create spatially larger habitats than wood logs and present substantial supply of energy mainly governed by geological processes (Johnson et al., 1988; Luther III et al., 2001; Tivey et al., 2002; Barreyre et al., 2014). Wood is directly exploited by specialist taxa, such as wood-boring bivalves, that contribute to significantly reduce habitat longevity but at the same time allow access to non-specialist taxa to wood energy, including chemosynthetic producers (Turner, 1973; Voight, 2015; Bienhold et al., 2013).

It is well known that larger and higher productivity systems support higher biodiversity (Wright, 1983; Wiens, 1989; Mittlebach et al., 2001). Increases in species richness may translate into higher functional richness facilitating species coexistence, or alternatively, lead to an increase in niche packing (Micheli and Halpern, 2002; Hooper et al., 2005; Lamanna et al., 2014; McClain et al., 2018). Thus, it would be expected that vents support higher biodiversity than wood falls. Vent energy sources however, are emitted with fluids at temperatures up to 400°C, creating low-oxygen and acidic environments with high concentrations of heavy metals. Metazoan life is therefore absent at highest fluid regimes (Johnson et al., 1986; Childress and Fisher, 1992; Le Bris et al., 2019). Vents are colonized by specific pools of species resulting in high abundance and biomass but low-richness compared to the rich surrounding deep sea. At local scales and at comparable level of species richness however, the high availability of energy at vents supports higher functional diversity than peripheral areas facilitating the coexistence of such high densities of species (see Chapter 3). The heterogeneity of habitats, the presence of multiple energy sources and the positive effects of engineering species enhance biodiversity in both vents and woods (Govenar, 2010; Bienhold et al., 2013; Alfaro-Lucas et al., 2016, 2018). Evidence suggests that wood falls are hotspots of diversity in the deep-sea. They harbor faunal assemblages that are composed by a mixture between wood-specialists, chemosymbiotic fauna, generalists and sulfide-tolerant background fauna (Bienhold et al., 2013). Standardized comparisons between vents and woods however, are difficult to achieve as they rarely co-occur in nature (but see experiments in Gaudron et al., 2012; Cunha et al., 2013). To understand the drivers of biodiversity and community

assembly in chemosynthetic-based communities may shed light on fundamental processes regulating chemosyntahtic and deep-sea ecosystems.

The main objective of this study was to identify and compare the drivers of species and functional biodiversity patterns as well as community structure between deep-sea vents and wood falls. The multiple gradients along short distances in vents including environmental stress, productivity and energy sources, make these systems ideal natural laboratories where manipulative experiments may be easily settle up (Van Dover and Lutz, 2004; Hall-Spencer et al., 2006; McClain et al., 2016). Furthermore, recent approaches suggest that stable isotopes may provide integrated values reflecting habitat features, system energy flows, feeding strategies, among others, providing new and complementary perspectives on community drivers and structures to those given by functional traits (Bearhop et al., 2004; Newsome et al., 2007; Rigolet et al., 2015; Cucheurosset et al., 2015). Here, we use an experimental design to compare the colonization of meio- and macroinvertebrates on mineral and wood substrata deployed over 2-years in contrasting vent environmental conditions. Using an integrated multifacet framework, we derived and compared the taxonomic, functional and isotopic α- and β-diversity patterns, and estimated their functional and isotopic niche overlap.

Material and Methods

Study area, experimental set-up and sample processing

Slate and wood substrata (~10 cm^3) were deployed at the vicinity and away of the hydrothermally active Eiffel Tower (TE) edifice (Lucky Strike vent field, ~1700 m depth, Mid-Atlantic Ridge) (Table 4.1) during the MoMARSAT 2013 cruise (https://doi.org/10.17600/13030040) on board of the R/V *Pourquoi pas?*, using the ROV *Victor6000*. We placed a triplicate series of slate and wood substrata on two sites of hydrothermal activity and two others on vent periphery (no hydrothermal activity) in order to represent the high environmental heterogeneity found in the vent field (Appendix S4.1). Hydrothermally active sites were colonized by dense assemblages of the chemosymbiotic mussel *Bathymodiolus azoricus* and were in (a) an area situated at the north-west side of the TE edifice in the vicinity of a small high-temperature chimney and visible microbial mats and (b) an area of diffuse-flow venting at the western side of TE. Periphery areas were not colonized by *B. azoricus* and were in (a) a poorly sedimented area between the TE (~50 m) and Montsegur edifices (~85 m) and (b) a bare-basalt seabed within a fossilized lava lake at ~90, ~120 and ~470 m away from Helen, Pico and TE active edifices, respectively.

To characterize environmental conditions, temperature was recorded for 9 months every 15 minutes with an autonomous NKE ST 6000 temperature probe attached the wood substrata at each site (Table 4.1). Substrata were individually recovered two years after their deployment, placed in isotherm sampling boxes and brought to the surface

with the ROV Victor6000 during the MoMARSAT 2015 cruise (https://doi.org/10.17600/15000200). Each substratum was washed with filtered seawater and sieved through 20-μm and 300-μm mesh. Meiofauna is defined as the fraction of taxa that pass through a 1 mm sieve (Gière, 2007) but the use of 300 and/or 500 μm mesh sieves to sample macrofauna has become common in the deep sea (e.g., Montagna et al., 2017). Here we refer to meiofauna and macrofauna the taxa found in 20-μm and 300-μm mesh sieves, respectively, although they do not correspond to the strict definitions of meio- and macrofauna. We acknowledge that typical groups of both compartments will be present in the 300-μm compartment. Preservation, sorting, count and identification procedures for both faunal compartments are described in Chapter 3.

Table 4.1. Sites where substrata were placed and temperature registered at the different sites of this study. All temperatures are in °C.

Site	Distance to closest active vent (m)	Mean ± sd temperature	Minimum temperature	Maximum temperature	Temperature range
NW Eiffel Tower	0	7.93±2.13	4.69	21.6	16.91
W Eiffel Tower	0	5.79±0.77	4.53	12.2	7.67
Sedimented area	~50	4.62±0.07	4.38	4.87	0.49
Lava lake	~90	4.55±0.07	4.32	4.77	0.44

Biodiversity measures and community structure analyses

In order to compare the effects of environmental conditions and substrata on the structure of assemblages, we analyzed slate and wood substrata in 4 groups: (a) slate

substrata in hydrothermally active conditions (considered as vent assemblages), (b) wood substrata in hydrothermally active conditions (considered as wood fall habitats under hydrothermally active conditions), (c) slate substrata at peripheral sites (considered as vent peripheral assemblages) and (d) wood substrata at peripheral sites (considered as wood fall assemblages). Thus, a total of six substrata (2 sites x 3 substrata/site) were analyzed in each of the four groups. For each of group, we estimated the total group and their mean species richness (S), mean abundance (N) and mean evenness (J') for both the 20-µm and 300-µm compartments.

Three functional response traits related with energy/productivity and environmental stress were analyzed for meio- and macrofaunal taxa. Selected traits were (a) "adult mobility", (b) "max adult body size" and (c) "feeding mechanism" (see trait definitions, modalities, references and datasets in Appendix S4.2). Traits were directly measured on individuals and/or obtained from the literature including the sFDVent database (Chapman *et al.* 2019). Using trait combinations, species were classified in groups of unique combinations, i.e., functional entities (FEs). Total and mean functional richness (FRic), represented by the percentage of functional volume derived from the total multidimensional functional space, were estimated per group for both faunal compartments (Mouchet *et al.* 2010). This space was constructed using the synthetic components of a Principal Coordinate Analysis (PcoA) encapsulating the variation of FEs. The FEs coordinates on the first 3 and 6 PcoA axes were used to estimate FRic in meio- and macrofauna. These axes represented 98.7% and 95.31% of inertia in meio- and

macrofauna assemblages, respectively. We also calculated the mean number functional evenness (Feve) for each group. Due to the low number of FEs on some slates from periphery in meiofauna, the mean FRic and Feve values of this group was estimated in only four out of six substrata.

Additionally, we applied a null model to test if environmental conditions or substrata nature filtered for certain traits. Null models were run 4999 times for each group to generate 95% confidence intervals of expected FRic values simulating a random sorting of species from the total pool of FEs while maintaining the total observed number of species per group (Teixidó et al., 2018). Observed FRic values did not deviate from null expectations if within confidence intervals. The low number of FEs in some meiofaunal groups impeded running the models with FRic estimated from 3 PcoA forcing us to estimate FRic with less axes. Such FRic values would represent an important loss of information and we thus decided to run null models only in the macrofaunal compartment.

Total isotopic richness (Iric) of each group was derived from the $\delta^{13}C$, $\delta^{15}N$ and $\delta^{34}S$ isotopic values obtained from 326 samples belonging to 42 species of macroinvertebrates (see Appendix S4.3 and Chapter 3 for the complete isotopic analyses methods and values). $\Delta^{13}C$ and $\delta^{15}N$ values were estimated for all 42 species whereas $\delta^{34}S$ was estimated for 33 species due to insufficient tissue material. Following the methodological framework

applied to create a functional space (Cucherousset and Villéger, 2015), we developed 2 isotopic spaces to estimate Iric based on $\delta^{13}C$ and $\delta^{15}N$, and $\delta^{13}C$ and $\delta^{34}S$ separately.

We run distance-based Redundancy Analyses (db-RDA) of Hellinger-transformed species abundances and abundance-weighted FEs constrained by the factors "environmental conditions", i.e., hydrothermal active and inactive conditions, and substrata nature, i.e., slate and wood substrata, with interactions to test if assemblages of species and FEs, respectively, were differently structured by one or the other factor in each group of meio- and macrofauna.

Taxonomic, functional and isotopic dissimilarities and niche overlap

In order to quantify dissimilarity between faunal compartments, we computed the taxonomic and functional β-diversity among the four groups with a common conceptual framework using the Jaccard dissimilarity coefficient (Baselga et al., 2012; Villéger et al., 2011; Villéger et al., 2013). This coefficient reaches its maximum value (1) when compared groups exhibit totally different species composition or, in the case of functional β-diversity, when functional spaces do not overlap. On the contrary, it equals 0 when compared groups exhibit the same species composition or exhibit a perfect overlap in functional space. To assess the mechanisms generating β-diversity, we decomposed dissimilarities into its two components: turnover and nestedness. Turnover accounts for species or functional differences due to species replacement, whereas nestedness accounts for differences due to the loss of species, leading to strict subsets of the richer sample

(Baselga et al., 2012). Furthermore, to investigate dissimilarities in isotopic spaces, we estimated the Isotopic Similarity (Isim) and Isotopic Nestedness (Ines) indices (Cucherousset and Villéger, 2015). For two groups, Isim estimates the ratio between the volume of the intersection and that of the union of the two groups. It equals 0 when there is no overlap in the isotopic space and 1 when there is a perfect overlap of the two groups. Ines estimates the ratio between the volume of the intersection and that of the smallest group. It equals 0 when there is no overlap and 1 when the group with the smallest isotopic space entirely overlaps with the larger. The overlap of functional (meio- and macrofauna) and isotopic (macrofauna only) spaces between groups were also estimated.

Statistical analyses

All indices, statistical analyses and tests were computed in R v. 3.5.3 (R Core Team, 2019). Taxonomic indices were computed using the package *vegan* (Oksanen et al., 2019). Functional indices and null models of FRic were computed using the script provided by Teixidó et al. (2018) and the *dbFD* function of the package *FD* (Laliberté & Legendre 2010). Differences in mean taxonomic and functional metrics, as well as stable isotope ratios were tested with ANOVAs or Kruskal-Wallis tests. Assumptions of normality and homogeneity of variances were tested with Shapiro-Wilk and Bartlett tests, respectively. Inter-group post-hoc comparisons were performed using Tukey Honest Significant Difference tests or Dunn's test of multiple comparisons using Rank Sum with Bonferroni correction. Db-RDAs were run with the *capscale* function in *vegan* after checking for multivariate homogeneity of variances with the *betadisper* function coupled to

permutations tests. Taxonomic and functional dissimilarity analysis indices were calculated using the *beta.pair* and *functional.beta.per* functions from the package *betapart* (Baselga et al., 2018). Isim and Ines metrics were computed using the R script provided by Cucherousset and Villéger (2015). Functional and isotopic space overlap was estimated using the scripts provided by Teixidó et al. (2018) and Cucherousset and Villéger (2015), respectively.

Results

Biodiversity patterns

We identified a total of 6845 and 29 013 individuals belonging to 38 and 95 species of meio- and macroinvertebrates, respectively (Appendix S4.4). Thirteen species were shared between the two faunal compartments and mainly belonged to large nematodes, copepods and ostracods. The characterization of species in functional entities (FEs) yielded a total of 8 and 19 FEs of meio- and macroinvertebrates, respectively. Mean taxonomic and functional indices showed several significant differences suggesting that colonization was heterogeneous among substratum types and environmental conditions in both compartments (Table 4.2 and Appendix S4.4). Slate meio- and macroinvertebrate assemblages in periphery were less rich in species, individuals, FEs and FRic but were more taxonomically and functionally evenly colonized than substrata on active sites. Wood substrata in periphery were densely colonized and highly dominated by a few species with low species richness, FEs and FRic in meiofauna but very high species

richness, abundance, FEs and FRic in macrofauna. Total number of species, FEs, FRic found in each group illustrated more clearly these trends (Figure 4.1): meiofaunal species, FEs, FRic were higher in hydrothermally active conditions independently of the substratum type, whereas for macrofaunal richness species, FEs, FRic were higher on wood substrata independently of the environmental conditions (Figure 4.1). Null models for macrofaunal assemblages revealed that FRic was only lower than expected by chance in slate located at the periphery (Appendix S4.5). Interestingly, isotopic richness changed dramatically whether it was measured from the isotopic space generated by $\delta^{13}C$ and $\delta^{15}N$ or by $\delta^{13}C$ and $\delta^{34}S$ values (Figure 4.1). Iric $_{C:N}$ was higher in substrata at hydrothermally active conditions especially in wood substrata. Iric $_{C:S}$ was higher on wood substrata especially at the periphery (Figure 4.1).

Table 4.2. Taxonomic, functional and isotopic indices of meio- and macrofauna assemblages. Highest values are highlighted in bolt. S= species richness. N= abundance. J'= evenness. FRic: function richness. FE: functional entities. Feve: functional evenness. $Iric_{cn}$: isotopic richness ($\delta^{13}C/ \delta^{15}N$). $Iric_{cs}$: isotopic richness ($\delta^{13}C/ \delta^{34}S$).

Macrofauna	Slate/Active	Slate/Periphery	Wood/Active	Wood/Periphery
S	22.33±1.97	10.67±3.78	**28.17**±7.78	27.50±2.88
N	1263.00±459.94	22.00±10.66	981.67±398.69	**2569.00**±793.21
J	0.51±0.11	**0.86**±0.06	0.61±0.08	0.59±0.05
FRic	23.90±3.93	2.49±2.64	**54.89**±18.22	22.56±6.62
FE	12.50±1.05	6.67±1.37	**15.67**±2.73	13.67±1.37
Feve	0.31±0.04	**0.52**±0.12	0.30±0.04	0.19±0.06
$Iric_{cn}$	0.25	0.03	**0.42**	0.04
$Iric_{cs}$	0.096	0.004	0.25	**0.41**
Meiofauna	**Slate/Active**	**Slate/Periphery**	**Wood/Active**	**Wood/Periphery**
S	**15.00**±3.22	7.50±4.37	14.67±3.88	10.17±1.60
N	244.33±167.67	37.33±30.65	203.17±104.83	**657.50**±549.25
J	0.76±0.08	**0.86**±0.07	0.72±0.08	0.55±0.13
FRic	**90.67**±14.45	7.35±1.90	70.44±18.23	3.01±1.66
FE	**7.5**±0.55	4.75±0.5	6.5±0.83	4.17±0.41
Feve	0.35±0.10	**0.39**±0.14	0.30±0.04	0.20±0.13
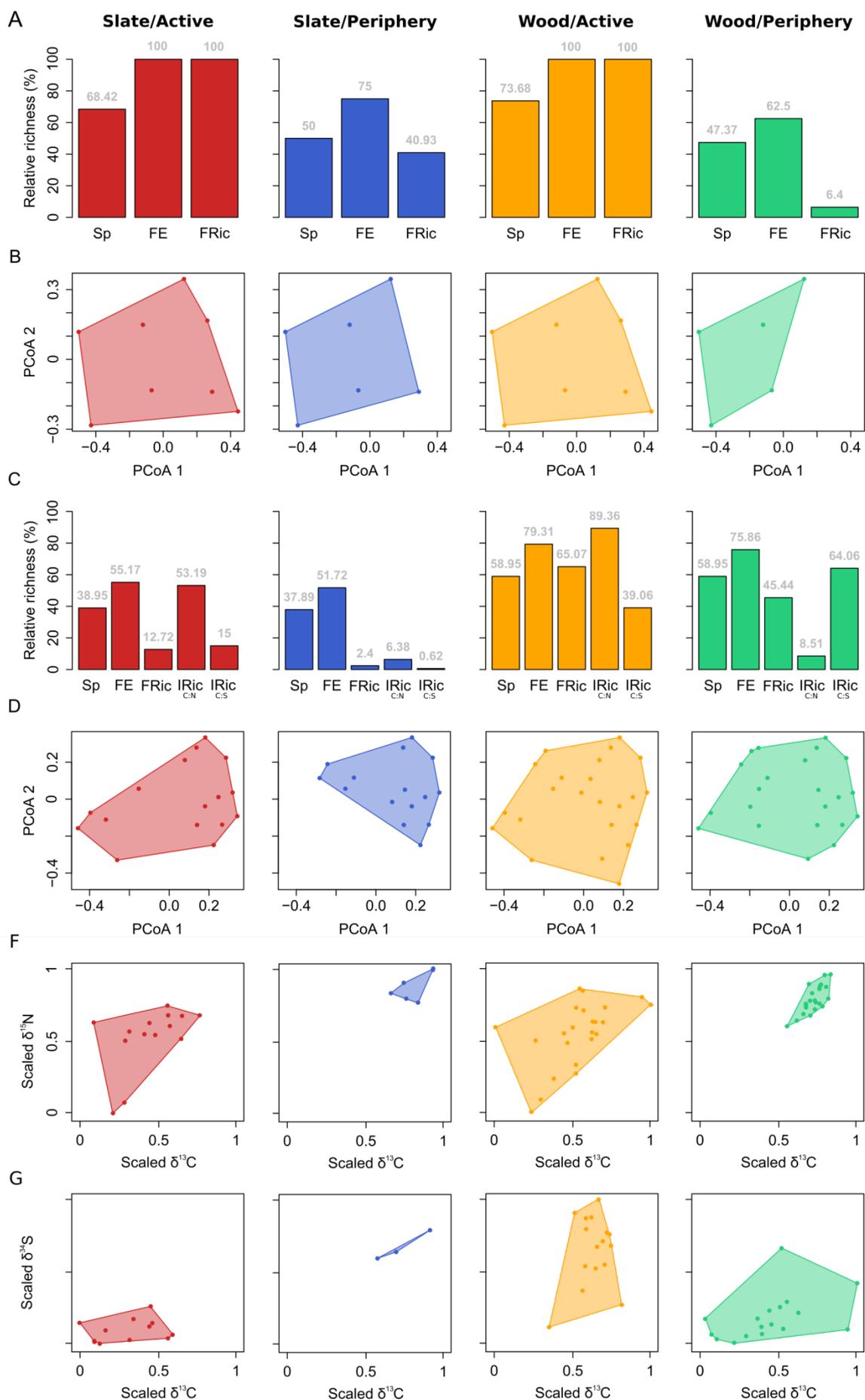
Figure 4.1. Percentage of total species (Sp), functional entities (FE), functional richness (FRic), and isotopic richness (Iric C:N, Iric C:S) in meio- (A) and macrofauna (C). Functional spaces of each assemblages of meio- (B) and macrofauna (D). The $\delta^{13}C/\delta^{15}N$ (F) and $\delta^{13}C/\delta^{34}S$ (G) isotopic spaces.

Community structure

Constrained multivariate analyses showed that the interactions between substratum nature and environment significantly structured assemblages in terms of species (meiofauna: $r^2= 0.47$, P=0.001; macrofauna: $r^2= 0.53$, P=0.002) and FEs (meiofauna: $r^2= 0.4$, P=0.003; macrofauna: $r^2= 0.53$, P=0.001) revealing that the effect of one factor depends on the nature of the other. In both cases, ordination model plots showed that substrata were clustered by environment along the first ordination axis separating hydrothermally active and peripheral conditions (Figure 4.2). The second axis revealed that substratum nature was the main community structural factor at the periphery (Figure 4.2). Thus, species assemblages and FEs tend to converge in hydrothermally active conditions, and to diverge in wood and slate in periphery (Figure 4.2).

For meiofauna, hydrothermally active substrata were mainly colonized by slow predatory and deposit feeders, mainly nematodes and copepods, some of them of largest sizes (Figure 4.2). Substrata at periphery were mainly colonized by fast and small grazer copepods on slates and slow and small copepods on woods. For macrofauna, typical vent taxa colonized substrata at hydrothermally active conditions, while typical deep-sea hard substrata and wood-fall taxa colonized slate and wood substrata in inactive conditions.

Bivalves of the subfamily Bathymodiolinae, *B. azoricus* and *Idas* spp., were respectively closely associated with hydrothermally active conditions or wood substrata in periphery. Nematodes and copepods were also tightly associated with hydrothermal conditions whereas amphipods and isopods were characteristic of slates at periphery. Hydrothermally active conditions were characterized by slow/mobility-reduced (facultative), large/very large taxa with a variety of feeding strategies (e.g., symbiosis, grazer, deposit feeder and predators) (Figures 4.2). Although less abundant, large sizes were also found on woods in the periphery but not on slates (Figure 4.2). Macro-invertebrates in slate inactive conditions were mainly slow medium deposit feeders, whereas woods were colonized by sessile/slow and small/medium taxa with a variety of feeding strategies (e.g., deposit and suspension feeding and grazing).
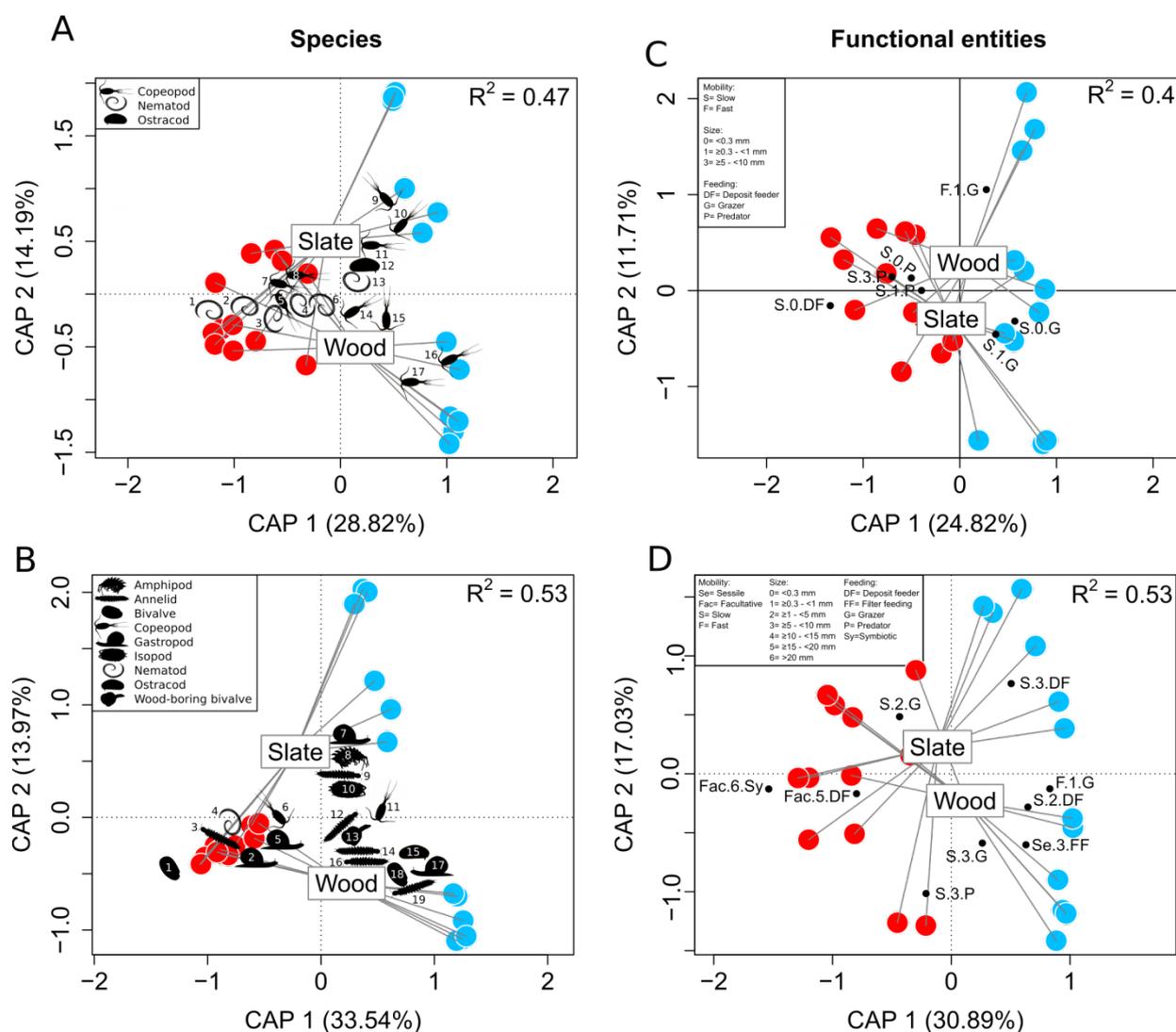
Figure 4.2. Ordination plots of db-RDA models Hellinger-transformed abundances of species and functional entities for meio- (A and C) and macrofauna (C and D). Red dots are substrata placed in hydrothermally active conditions whereas blue dots are substrata placed in inactive conditions. For meiofauna (A): 1. *Cephalochaetosoma* sp. 2. *Paracanthonchus* sp. 3. *Microlaimus* sp. 4. *Oncholaimus dyvae*. 5. *Smacigastes micheli*. 6. *Chromadorita* sp. 7. Tegastidae sp. 8. *Hepnerina confusa*. 9. Ameridae sp. 4. 10. Amereidae sp. 1. 11. Amereidae sp 3. 12. *Thomontocypris excussa*. 13. *Theristus* sp. 14. Ameiridae sp. 2. 15. *Bathylaophonte azorica*. 16. *Mesochra* sp. 17. Cf. Kelleiiridae sp. For macrofauna (B): 1. *Bathymodiolus azoricus*. 2. *Protolira valvatoides*. 3. *Amphisamytha lutzi*. 4. *Oncholaimus dyvae*. 5. *Lepetodrilus atlanticus*. 6. *Smacigastes micheli*. 7. *Lurifax vitreus*. 8. Liljeborgiidae sp. 9. *Glycera tesselata*. 10. Assellota sp. 2. 11. *Bathylaophonte azorica*. 12. Hesionidae sp. 5. 13. *Xyloredo* sp. 14. *Capitella* sp 1. 15. *Thomontocypris excussa*. 16. Hesionidae sp. 3. 17. *Coccopygia spinifera*. 18. *Idas* spp. 19. *Strepternos* sp.

Assemblage dissimilarities

Due to the higher number of shared species between groups (23.8% of the total), dissimilarities in assemblages were lower in meio- than in macrofauna (Figure 4.3A and B; Appendix S4.6). In both compartments, turnover was the main driver of variance between faunal assemblages, although nestedness was higher in meiofauna (Appendix S4.6). As expected from results of multivariate ordination, β-diversity of meio- and macrofaunal assemblages was lower between woods and slates in hydrothermally active conditions (meiofauna: 0.31, macrofauna: 0.52) (Appendix S4.6). Assemblages on woods at periphery were highly dissimilar although they shared many species with other groups (Figure 4.3A and B). About 50% and ~58% of the total meio- and macrofaunal species on slates at active and peripheral conditions, respectively, were found on woods at the periphery (Figure 4.3A and B). This apparently contradiction between the high dissimilarities and great species overlap can be explained by the high exclusive species found on woods at the periphery, which led to high turnover and β-diversity values (Figure 4.3A and B, Appendix S4.6). A similar phenomenon occurred between woods in hydrothermally active conditions and slates and woods at periphery.
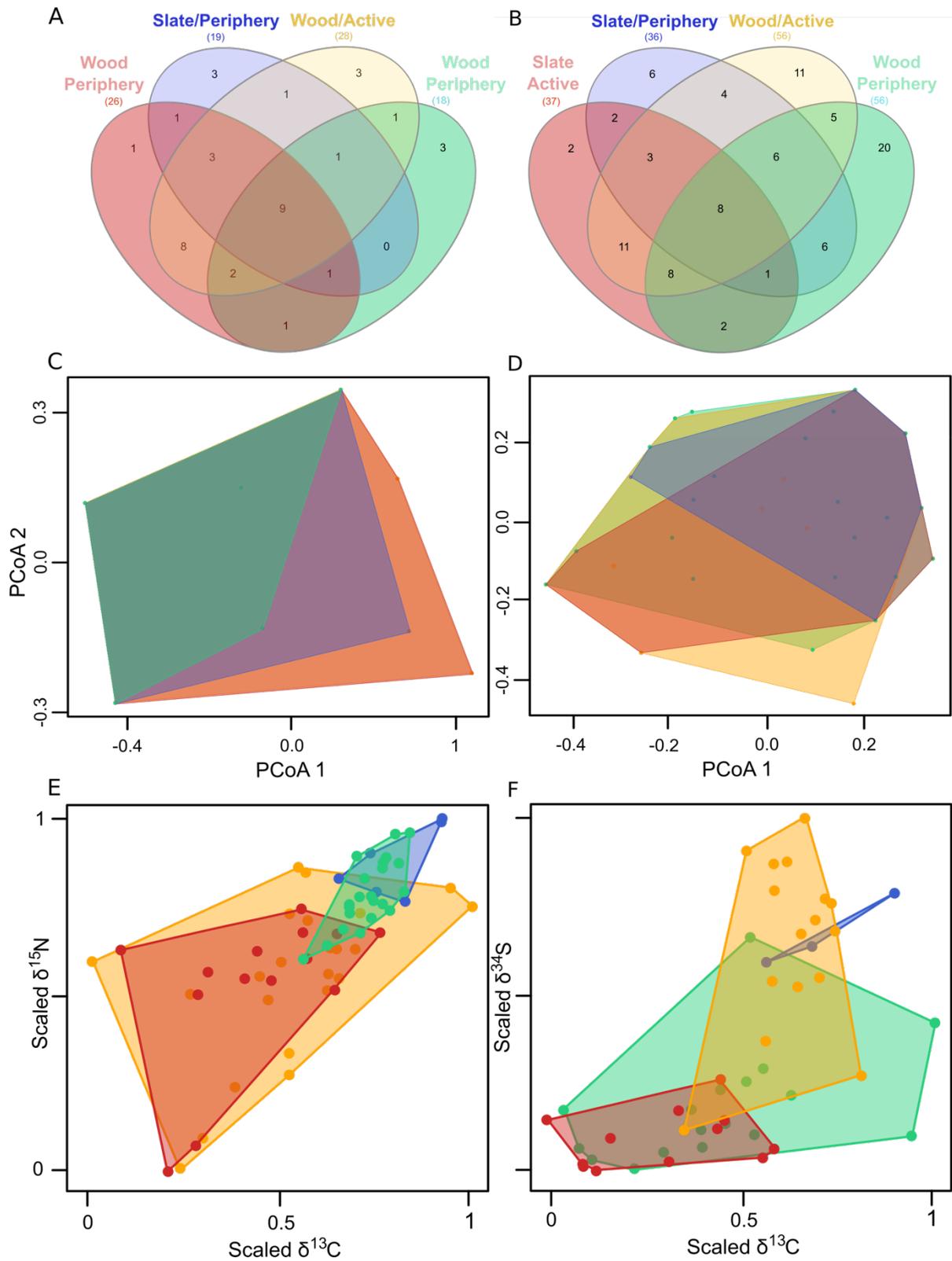
Figure 4.3. Species, functional and isotopic overlap. Meio- (A) and macrofaunal (B) species overlap among groups (substrata/condition). Values equal number of species. Functional space overlap among groups (substrata/condition) of meio- (C) and macrofauna (D). Isotopic space overlap of mqacrofauna among groups (substrata/condition) estimated with $\delta^{13}C$ and $\delta^{15}N$ (E) and $\delta^{13}C$ and $\delta^{34}S$ (F) isotopic spaces.

For functional β-diversity, nestedness rather than turnover was the main process leading dissimilarities in both faunal compartments (Appendix S4.6). Two main different patterns though were observed. Meiofauna in inactive conditions was completely nested with assemblages of active conditions as illustrated by the complete functional space overlap observed (Figure 4.3C and D, Appendix S4.6). Wood assemblages at periphery were especially dissimilar and completely nested to that of all other groups highlighting their low FEs richness. Dissimilarity was null in substrata in hydrothermally active conditions as highlighted by the complete niche overlap (Figure 4.3C). For macrofauna, slate substrata tend to be nested to wood substrata (Figure 4.3D). Only dissimilarity between slates in hydrothermally active and peripheral conditions was mainly driven by turnover. As in meiofauna, lower dissimilarities were found between woods and slates in active conditions. Interestingly, the highest dissimilarity was found between slate substrata in active conditions and woods in peripheral conditions, although the niche overlap was 56.44% (Figure 4.3D, Appendix S4.6). As in the case of species, this apparent contradiction was explained by the high exclusive FEs found on woods at the periphery. In inactive conditions, slates were almost entirely nested to woods, showing a 95% functional niche overlap (Figure 4.3D, Appendix S4.6). Either in meio- or in macrofauna compartments, woods in active conditions showed a great percentage of niche overlap with all other groups suggesting that, as observed for species composition, they are creating a hybrid functional environment (Figure 4.3C and D).

As for isotopic richness, isotopic similarity (Isim) and nestedness (Ines) varied depending on the isotopic space selected (Figure 4.3E and F, Appendix S4.6). For $\delta^{13}C$ and $\delta^{15}N$, substrata from each environmental condition (active/periphery) were more similar and showed a great niche overlap (Figure 4.3E, Appendix S4.6). Woods and slates at periphery were quite dissimilar from slate substrata in hydrothermally active conditions respectively showing no or a poor niche overlap (Figure 4.3E, Appendix S4.6). For $\delta^{13}C$ and $\delta^{34}S$, similarity was higher between wood substrata at periphery and slates and woods in active conditions with respectively 97 and 65% of their isotopic niches nested into wood periphery (Figure 4.3F). For $\delta^{13}C$ and $\delta^{34}S$, only 5% of the fauna on slates at periphery was nested into that of woods (Figure 4.3F, Appendix S4.6). In both isotopic spaces, wood substrata at active sites tend to show high isotopic niche overlaps with other groups as shown for species composition and trait functional spaces (Figure 4.3E and F).

Discussion

The relationships between the different facets of biodiversity analyzed in this study, namely species, functional and isotopic richness, elucidate distinct biodiversity patterns observed in this study. It is well known that environmental stress associated to hydrothermalism limit the colonization to a few well-adapted species leading to low-diversity assemblages in comparison to the diversity found at vent peripheries and deep-sea habitats in general (e.g., Gollner et al., 2015; Zeppilli et al., 2015; Plum et al., 2017). Although total species richness was similar between slate substrata placed in active and peripheral conditions for both faunal compartments, the mean species richness and

density per substrata was substantially higher in active conditions. Furthermore, as expected, total and mean functional richness was higher in slates in the active than in the peripheral conditions. In fact, as found in Chapter 3, null models of macrofauna revealed that FRic was only lower than expected by chance on slate substrata in periphery. This suggests that at the scale of our study, peripheral environments but not active vent or wood fall habitats may filter for certain traits limiting colonization on early community assembly (Chapter 3). High-energetic vent habitats may promote more functional strategies decreasing the effect of competition and allowing for a relatively high number of species to coexist in high densities in reduced spaces. Here, we further support this hypothesis by showing that isotopic richness on slates was higher in active than in peripheral conditions suggesting that the dense vent assemblages were benefiting from high-resource diversity supporting many ecological strategies (Fric) and boosting species richness.

Strikingly different biodiversity patterns were observed on woods at the periphery for meio- and macrofauna. Meiofauna in wood falls formed the least species and functional rich but the most abundant assemblages observed in this experiment. On the contrary, macrofauna formed the most abundant, species and functional rich assemblages. This suggests that the colonization of wood falls by meiofauna was restricted to few, albeit abundant, trait-specific species. Whether this pattern is related to environmental conditions or to biological interactions with macrofauna is unknown and could be addressed in a future study. Negative relationship between meio- and

macrofauna were observed in other organic falls (Debenham et al., 2004). On the contrary to active habitats, which benefit from diverse chemosynthetic resources, woods at the periphery where in a low-energy environment as suggested by the patterns observed on slates at the periphery. The question that arises is "How woods located at the periphery support denser, taxonomically and functionally richer assemblages in such spatially restricted environment"? The organic input provided by the substrata itself could be yclopo the rich assemblages however, insights from isotopic richness suggest that the multiple origins of energy were boosting functional richness allowing many different species to colonize wood falls.

When estimated with $\delta^{13}C$ and $\delta^{15}N$, the isotopic richness was higher in slates in hydrothermally active conditions. $\Delta^{13}C$ values may reflect several chemosynthetic pathways in this environment: values from -15‰ to -10‰ reflect methanotrophy, from -12.9 ± 3.4‰, the reductive tricarboxylic acid (rTCA) and from –36‰ to -30‰, the Calvin-Benson-Bassham (CBB) cycles (e.g., Reid et al., 2013; Portail *et al.* 2018). Nitrogen values reflected two large inorganic sources with very different signatures, i.e. nitrates ($\delta^{15}N=$ 5-7‰) and ammonium ($\delta^{15}N<0$‰) (Lee and Childress, 1994; Riekenberg et al., 2016). $\Delta^{34}S$ may exhibit very distinct values depending on its origin with values around and below 10‰ for organic matter of chemosynthetic origin and values around or over 19‰ for photosynthetic origin (e.g., Reid et al., 2013). Thus the high Iric $_{C:N}$ and low Iric $_{C:S}$ on substrata in active conditions compared to woods at the periphery should be interpreted as the reflection of the high diversity of resources from chemosynthetic pathways. On the

contrary, the very high Iric c:s values on woods in periphery reflect the diversity of origins of the resources, i.e., chemosynthetic and photosynthetic (wood itself). Certainly, woods at the periphery support chemosynthetic production as highlighted by the isotopic values of some "vent" inhabitant species colonizing them, such as the gastropod *Protolira valvatoides* ($\delta^{34}S$= 4.7‰) (see Appendix S4.3). Thus, at local scales, the multiple origins of resources rather than the diversity of resources of one single energy source likely explained the higher species and functional diversities observed in wood falls compared to vents.

Environmental stress inherent to vent habitats may play a role as well in reducing diversity compared to wood falls. Placing wood fall-like habitats in hydrothermally active conditions served as an experiment to test such hypotheses. Results showed that woods in active conditions supported higher species, FRic, Iric c:n and Iric c:s than slates in the active and peripheral conditions, and higher FRic and Iric c:n (but not Iric c:s) than woods at the periphery. Interestingly, the addition of resources that represent the wood substrata in active conditions attracted more vent species than on slates, but also few wood specialists, such as wood-boring bivalves as well as species only previously found at the periphery, e.g., amphipods and isopods, forming an "hybrid" community. Wood-boring bivalves, among others, exhibited a completely new functional strategy in the vent environment, expanding not only the functional but also the isotopic spaces and enhancing the functional and isotopic overlap with the rest of the groups. Thus, as

hypothesized for woods on the periphery, the addition of new resources boosts species and functional richness despite the presence of the vent "stressful" environment.

Our experiment revealed that the interactions between environmental conditions and the type of substratum significantly drive the species and functional structures of meio- and macrofaunal assemblages. As suggested by a previous experiment (Plum et al., 2016) and despite the peculiarities of wood, faunal assemblages tend to converge in species and functional entities independently of substratum type in hydrothermally active conditions. They were mainly dominated by typical vent inhabitants. This is supported by the lower species and functional β-diversity observed between slate and wood substrata compared to other groups, and the high functional and isotopic niche overlap of the fauna on the substrata in this environment. These patterns strongly suggest that the vent environment is the main factor structuring meio- and macroinvertebrate assemblages in hydrothermally active conditions at the temporal scale of our study (Cuvelier et al., 2014; Plum et al., 2017; Baldrighi et al., 2018). In contrast, in peripheral conditions, slate and wood substrata were mainly colonized by typical deep-sea inhabitants and wood-fall specialists, respectively, leading to different assemblages and showing both higher dissimilarities in species and functions. Due to the restricted spatial extent of our experiment (~500 m), dispersal had most likely a negligible role on colonization and rather eco-evolutionary processes linked to each habitat drove the becoming of community assembly of each group.

The eco-evolutionary relationships between vents and organic substrata have been a topic of debate ever since the discovery of vent fauna in whale remains (Smith et al., 1989). Discussions of overlapping fauna mainly involved vent chemosymbiotic and other large invertebrate species (e.g., Distel et al., 2000; Bienhold et al., 2013; Kiel, 2016). However, much remain unknown for the smaller faunal compartments, and the potential overlap of wood falls and background environments. Of special interest thus were the taxonomic, functional and isotopic relationships of assemblages on slates at active and peripheral conditions with those on woods in the periphery. Although, high species and functional dissimilarities were observed, ~50 and ~60% of the meio- and macroinvertebrate species found on slates in active and inactive conditions, respectively, were also found on wood substrata in periphery. This apparent contradiction may be explained by the high turnover originated from 1) the high number of exclusive taxa and FEs found on slates compared to woods in the meiofaunal compartment and 2) the high number of exclusive species (wood-fall specialists mainly) with exclusive FEs found on woods. Rather than turnover, nestedness was the main process driving the high functional dissimilarities for both compartments, meaning that functionally poorer assemblages were mainly subsets of the richer. The meiofauna found on woods was 100% functionally nested into that found on slates whereas the macrofauna found on slates was almost entirely nested to that found on woods. Similarly, despite the dissimilarity suggested by isotopic indices, we observed isotopic niche overlap between woods at the periphery and slates in active and peripheral conditions. As for functional diversity, the isotopic nestedness was higher but the observed relationships changed depending on the

isotopic space used, i.e., the $\delta^{13}C$ and $\delta^{15}N$ or $\delta^{13}C$ and $\delta^{34}S$ space. In the former, 20% of the isotopic space found on woods in periphery was nested to that on slates in active conditions whereas, in the latter, 97% of the isotopic niche of slates in active conditions was nested to that of woods in periphery. At the periphery, 56% of the $\delta^{13}C/\delta^{15}N$ isotopic niche on slates overlapped with that of woods whereas very little overlap was observed in the $\delta^{13}C$ and $\delta^{34}S$ space.

These findings confirm the role of woods in the deep-sea as hotspots of biodiversity and potential stepping stones for meio- and macrofauna, not only for "vent" inhabitants but also for other species such as those found on the periphery. Nevertheless, large dominant species, such as the ecosystem engineer mussel *Bathymodiolus azoricus* or *Amphisamytha lutzi*, were not supported at our wood falls outside the vents. Instead, a confamilial species of the mussel, *Idas* spp., was dominant. Size (the larger vs small) and feeding (symbiotic vs filter feeding) traits in vent and wood fall assemblages were mainly driven by the abundance of these two species. It is tempting to speculate about the result of an evolutionary process where *B. azoricus* has been able to cope with the stressful hydrothermal conditions, and have thus accessed higher energy resources allowing them to reach higher sizes (Duperron, 2008). Previous studies suggest that increasing wood-fall size would increase chemosynthetic production (Cunha et al., Sumida et al., 2016; McClain et al., 2016), which place the bases for future studies to test if increasing the wood size would contribute to enhance species and functional similarities or, alternatively, would create more dissimilar assemblages. This study constitutes an example of how the

analyses of multiple biodiversity facets integrated in a common conceptual framework may help to elucidate old and new questions of deep-sea ecology and other poorly known ecosystems.

References:

Adler, P. B., J. HilleRisLambers, and J. M. Levine. 2007. A niche for neutrality. Ecology Letters 10 :95–104.

Alfaro-Lucas, J., Shimabukuro, I. Ogata, Y. Fujiwara, and P. Sumida. 2018. Trophic structure and chemosynthesis contributions to heterotrophic fauna inhabiting an abyssal whale carcass. Marine Ecology Progress Series 596 :1–12.

Alfaro-Lucas, J. M., M. Shimabukuro, G. D. Ferreira, H. Kitazato, Y. Fujiwara, and P. Sumida. 2017. Bone-eating Osedax worms (Annelida : Siboglinidae) regulate biodiversity of deep-sea whale-fall communities. Deep Sea Research Part II : Topical Studies in Oceanography.

Ashford, O. S., A. J. Kenny, C. R. Froján, M. B. Bonsall, T. Horton, A. Brandt, G. J. Bird, S. Gerken, and A. D. Rogers. 2018. Phylogenetic and functional evidence suggests that deep-ocean ecosystems are highly sensitive to environmental change and direct human disturbance. Proceedings of the Royal Society B 285 :20180923.

Baco, A.R., Smith, C.R., Peek, A.S., Roderick, G.K., Vrijenhoek, R.C. 1999. The phylogenetic relationships of whale-fall vesicomyid clams based on mitochondrial COI DNA sequences. Marine Ecology Progress Series 182 :137–147.

Barreyre T, Escartin J, Sohn RA, Cannat M, Ballu V, Crawford WC. 2014 Temporal variability and tidal modulation of hydrothermal exit-fluid temperatures at the Lucky Strike deep-sea vent field, Mid-Atlantic Ridge. J. Geophys. Res. Solid Earth 119, 2543 – 2566

Baselga, A., and D. C. Orme. 2012. Betapart: an R package for the study of beta diversity. Methods in Ecology and Evolution 3:808–812.

Bearhop, S., C. E. Ada, S. Waldron, R. A. Fuller, and H. Macleod. 2004. Determining trophic niche width: a novel approach using stable isotope analysis. Journal of Animal Ecology 73:1007–1012.

Bernardino, A. F., C. R. Smith, A. Baco, I. Altamira, and P. Sumida. 2010. Macrofaunal succession in sediments around kelp and wood falls in the deep NE Pacific and

community overlap with other reducing habitats. Deep Sea Research Part I : Oceanographic Research Papers 57 :708–723.

Bienhold, C., P. Ristova, F. Wenzhöfer, T. Dittmar, and A. Boetius. 2013. How Deep-Sea Wood Falls Sustain Chemosynthetic Life. PloS ONE 8 :e53590.

Cadotte, M. W., and C. M. Tucker. 2017. Should Environmental Filtering be Abandoned ? Trends in Ecology & Evolution 32 :429–437.

Chapman, A. S., S. E. Beaulieu, A. Colaço, A. V. Gebruk, A. Hilario, T. C. Kihara, E. Ramirez-Llodra, J. Sarrazin, V. Tunnicliffe, D. J. Amon, M. C. Baker, R. E. Boschen-Rose, C. Chen, I. J. Cooper, J. T. Copley, L. Corbari, E. E. Cordes, D. Cuvelier, S. Duperron, C. Preez, S. Gollner, T. Horton, S. Hourdez, E. M. Krylova, K. Linse, P. LokaBharathi, L. Marsh, M. Matabos, S. Mills, L. S. Mullineaux, H. Rapp, W. D. Reid, E. (Goroslavskaya), T. A. Thomas, S. Southgate, S. Stöhr, P. J. Turner, H. Watanabe, M. Yasuhara, and A. E. Bates. 2019. sFDvent : A global trait database for deep-sea hydrothermal-vent fauna. Global Ecology and Biogeography 28 : 1538-1551.

Chase, J. M. 2010. Stochastic Community Assembly Causes Higher Biodiversity in More Productive Environments. Science 328 :1388–1391.

Chase, J. M., and M. A. Leibold. 2002. Spatial scale dictates the productivity–biodiversity relationship. Nature 416 :427–430.

Chesson, P. 2000. Mechanisms of maintenance of species diversity. Annual Review of Ecology and Systematics 31 :343–366.

Cucherousset, J., and S. Villéger. 2015. Quantifying the multiple facets of isotopic diversity : New metrics for stable isotope ecology. Ecological Indicators 56 :152–160.

Cunha, M. R., F. L. Matos, L. Génio, A. Hilário, C. J. Moura, A. Ravara, and C. F. Rodrigues. 2013. Are Organic Falls Bridging Reduced Environments in the Deep Sea ? Results from Colonization Experiments in the Gulf of Cádiz. PloS ONE 8 :e76688.

Cuvelier, D., J. Beesau, V. N. Ivanenko, D. Zeppilli, P.-M. Sarradin, and J. Sarrazin. 2014. First insights into macro- and meiofaunal colonisation patterns on paired wood/slate substrata at Atlantic deep-sea hydrothermal vents. Deep Sea Research Part I : Oceanographic Research Papers 87 :70–81.

Debenham, N. J., P. J. D. Lambshead, T. J. Ferrero, and C. R. Smith. 2004. The impact of whale falls on nematode abundance in the deep sea. Deep Sea Research Part I : Oceanographic Research Papers 51 :701–706.

Distel, D. L., A. R. Baco, E. Chuang, W. Morrill, C. Cavanaugh, and C. R. Smith. 2000. Marine ecology : Do mussels take wooden steps to deep-sea vents ? Nature 403 :725–726.

Feldman, R., Tank, Black, A. Baco, C. Smith, and R. Vrijenhoek. 1998. Vestimentiferan on a Whale Fall. The Biological Bulletin 194 :116–119.

Fujiwara, Y., M. Kawato, T. Yamamoto, T. Yamanaka, W. Sato-Okoshi, C. Noda, S. Tsuchida, T. Komai, S. Cubelio, T. Sasaki, K. Jacobsen, K. Kubokawa, K. Fujikura, T. Maruyama, Y. Furushima, K. Okoshi, H. Miyake, M. Miyazaki, Y. Nogi, A. Yatabe, and T. Okutani. 2007. Three-year investigations into sperm whale-fall ecosystems in Japan. Marine Ecology 28 :219–232.

Gaudron, F. Pradillon, M. Pailleret, S. Duperron, L. N. Bris, and F. Gaill. 2010. Colonization of organic substrates deployed in deep-sea reducing habitats by symbiotic species and associated fauna. Marine Environmental Research 70 :1–12.

Giere, O. 2009. Meiobenthology, The Microscopic Motile Fauna of Aquatic Sediments. Springer. Pp. 527.

Gollner, S., B. Govenar, P. Arbizu, S. Mills, N. Bris, M. Weinbauer, T. ank, and M. Bright. 2015a. Differences in recovery between deep-sea hydrothermal vent and vent-proximate communities after a volcanic eruption. Deep Sea Research Part I : Oceanographic Research Papers 106 :167–182.

Govenar, B. 2010. The Vent and Seep Biota, Aspects from Microbes to Ecosystems. Springer 33 :403–432.

Hall-Spencer, J. M., R. Rodolfo-Metalpa, S. Martin, E. Ransome, M. Fine, S. M. Turner, S. J. Rowley, D. Tedesco, and M.-C. Buia. 2008. Volcanic carbon dioxide vents show ecosystem effects of ocean acidification. Nature 454 :96.

HilleRisLambers, J., P. B. Adler, W. S. Harpole, J. M. Levine, and M. M. Mayfield. 2012. Rethinking Community Assembly through the Lens of Coexistence Theory. Ecology, Evolution, and Systematics 43 :227–248.

Hooper, D., F. Chapin, J. Ewel, A. Hector, P. Inchausti, S. Lavorel, J. Lawton, D. Lodge, M. Loreau, S. Naeem, B. Schmid, H. Setälä, A. Symstad, J. Vandermeer, and D. Wardle. 2005. Effects of biodiversity on ecosystem functioning: a consensus of current knowledge. Ecological Monographs 75:3–35.

Johnson, K. S., J. J. Childress, R. R. Hessler, C. kamoto-Arnold, and C. L. Beehler. 1988. Chemical and biological interactions in the Rose Garden hydrothermal vent field, Galapagos spreading center. Deep Sea Research Part A. Oceanographic Research Papers 35 :1723–1744.

Jones, W. J., Y.-J. Won, P. A. Y. Maas, P. J. Smith, R. A. Lutz, and R. C. Vrijenhoek. 2006. Evolution of habitat use by deep-sea mussels. Marine Biology 148 :841–851.

Judge, J., and J. P. Barry. 2016. Macroinvertebrate community assembly on deep-sea wood falls in Monterey Bay is strongly influenced by wood type. Ecology 97 :3031–3043.

Kalenitchenko, D., M. Dupraz, N. Bris, C. Petetin, C. Rose, N. J. West, and P. E. Galand. 2016. Ecological succession leads to chemosynthesis in mats colonizing wood in sea water. The ISME Journal 10 :2246.

Kalenitchenko, D., E. Péru, C. L. Pereira, C. Petetin, P. Galand, and L. N. Bris. 2018. The early conversion of deep-sea wood falls into chemosynthetic hotspots revealed by in situ monitoring. Scientific Reports 8 :907.

Kiel, S. 2016. A biogeographic network reveals evolutionary links between deep-sea hydrothermal vent and methane seep faunas. Proc. R. Soc. B 283 :20162337.

Kiel, S. 2017. Reply to Smith et al. : Network analysis reveals connectivity patterns in the continuum of reducing ecosystems. Proceedings of the Royal Society B 284 :20171644.

Kraft, N. J., P. ler, O. Godoy, E. C. James, S. Fuller, and J. M. Levine. 2015. Community assembly, coexistence and the environmental filtering metaphor. Functional Ecology 29 :592–599.

Laliberté, E. & P. Legendre. 2010. A distance-based framework for measuring functional diversity from multiple traits. *Ecology* **91,** 299–305

Lamanna, C., B. Blonder, C. Violle, N. J. Kraft, B. Sandel, I. Šímová, J. C. Donoghue, J.-C. Svenning, B. J. McGill, B. Boyle, V. Buzzard, S. Dolins, P. M. Jørgensen, A. Marcuse-Kubitza, N. Morueta-Holme, R. K. Peet, W. H. Piel, J. Regetz, M. Schildhauer, N. Spencer, B. Thiers, S. K. Wiser, and B. J. Enquist. 2014. Functional trait space and the latitudinal diversity gradient. Proceedings of the National Academy of Sciences 111:13745–13750.

Lee, R., and J. Childress. 1996. Inorganic N Assimilation and Ammonium Pools in a Deep-Sea Mussel Containing Methanotrophic Endosymbionts. The Biological bulletin 190:373–384.

Le Bris, N., M. Yücel, A. Das, S. evert, P. LokaBharathi, and P. R. Girguis. 2019. Hydrothermal Energy Transfer and Organic Carbon Production at the Deep Seafloor. Frontiers in Marine Science 5 :531.

Lorion, J., S. Kiel, B. Faure, M. Kawato, S. Y. Ho, B. Marshall, S. Tsuchida, J.-I. Miyazaki, and Y. Fujiwara. 2013. Adaptive radiation of chemosymbiotic deep-sea mussels. Proc. R. Soc. B 280 :20131243.

Luther III, G. W., T. F. Rozan, M. Taillefert, D. B. Nuzzio, C. Meo, T. ank, R. A. Lutz, and C. S. Cary. 2001. Chemical speciation drives hydrothermal vent ecology. Nature 410 :813.

McClain, C., and J. Barry. 2014. Beta-diversity on deep-sea wood falls reflects gradients in energy availability. Biology letters 10 :20140129.

McClain, C. R., J. P. Barry, D. Eernisse, T. Horton, J. Judge, K. Kakui, C. Mah, and A. Warén. 2016. Multiple processes generate productivity–diversity relationships in experimental wood-fall communities. Ecology 97 :885–898.

McClain, C. R., C. Nunnally, A. S. Chapman, and J. P. Barry. 2018b. Energetic increases lead to niche packing in deep-sea wood falls. Biology Letters 14 :20180294.

McGill, B. J., B. J. Enquist, E. Weiher, and M. Westoby. 2006. Rebuilding community ecology from functional traits. Trends in Ecology & Evolution 21 :178–185.

Micheli, F., and B. S. Halpern. 2005. Low functional redundancy in coastal marine assemblages. Ecology Letters 8:391–400.

Mittelbach, G. G., and D. W. Schemske. 2015. Ecological and evolutionary perspectives on community assembly. Trends in Ecology & Evolution 30 :241–247.

Mittelbach, G. G., C. F. Steiner, S. heiner, K. L. Gross, H. L. Reynolds, R. B. Waide, M. R. Willig, S. I. Dodson, and L. Gough. 2001. What is the observed relationship between species richness and productivity ? Ecology 82 :2381–2396.

Miyazaki, J.-I., L. de Martins, Y. Fujita, H. Matsumoto, and Y. Fujiwara. 2010. Evolutionary Process of Deep-Sea Bathymodiolus Mussels. PloS ONE 5 :e10363.

Montagna, P. A., J. G. Baguley, C. Hsiang, and M. G. Reuscher. 2017. Comparison of sampling methods for deep-sea infauna. Limnology and Oceanography : Methods 15 :166–183.

Mouchet, M. A., S. Villéger, N. W. Mason, and D. Mouillot. 2010. Functional diversity measures : an overview of their redundancy and their ability to discriminate community assembly rules. Functional Ecology 24 :867–876. Newsome, S. D., C. del Rio, S. Bearhop, and D. L. Phillips. 2007. A niche for isotopic ecology. Frontiers in Ecology and the Environment 5 :429–436.

Oksanen J., Blanchet F.G., Friendly M., Kindt R., Legendre P., McGlinn D., Minchin P.R., O'Hara R.B., Simpson G.L., Solymos P., Stevens M.H.H., Szoecs E., Wagner H. (2019). Vegan: Community Ecology Package. R package version 2.5-4. https ://CRAN.R-project.org/package=vegan

Petchey, O. L., and K. J. Gaston. 2006. Functional diversity : back to basics and looking forward. Ecology Letters 9 :741–758.

Plum, C., F. Pradillon, Y. Fujiwara, and J. Sarrazin. 2017. Copepod colonization of organic and inorganic substrata at a deep-sea hydrothermal vent site on the Mid-Atlantic Ridge. Deep Sea Research Part II : Topical Studies in Oceanography 137 :335–348.

Portail, M., C. Brandily, C. Cathalot, A. Colaço, Y. Gélinas, B. Husson, P.-M. Sarradin, and J. Sarrazin. 2018. Food-web complexity across hydrothermal vents on the Azores

triple junction. Deep Sea Research Part I : Oceanographic Research Papers 131 :101–120.

R Core Team (2019). R: A language and environment for statistical computing. R Foundation for Statistical Computing, Vienna, Austria. URL https://www.R-project.org/

Reid, W. D., C. J. Sweeting, B. D. Wigham, K. Zwirglmaier, J. A. Hawkes, R. A. McGill, K. Linse, and N. V. Polunin. 2013. Spatial Differences in East Scotia Ridge Hydrothermal Vent Food Webs : Influences of Chemistry, Microbiology and Predation on Trophodynamics. PloS ONE 8 :e65553.

Rigolet, C., E. Thiébaut, A. Brind'Amour, and S. F. Dubois. 2015. Investigating isotopic functional indices to reveal changes in the structure and functioning of benthic communities. Functional Ecology 29 :1350–1360.

Riekenberg, P., R. Carney, and B. Fry. 2016. Trophic plasticity of the methanotrophic mussel Bathymodiolus childressi in the Gulf of Mexico. Marine Ecology Progress Series 547:91–106.

Romano, C., J. R. Voight, J. B. Company, M. Plyuscheva, and D. Martin. 2013. Submarine canyons as the preferred habitat for wood-boring species of Xylophaga (Mollusca, Bivalvia). Progress in Oceanography 118 :175–187.

Smith, C. R., D. J. Amon, N. D. Higgs, A. G. Glover, and E. L. Young. 2017. Data are inadequate to test whale falls as chemosynthetic stepping-stones using network analysis: faunal overlaps do support a stepping-stone role. Proceedings of the Royal Society B 284:20171281.

Smith, C. R., A. G. Glover, T. Treude, N. D. Higgs, and D. J. Amon. 2015. Whale-Fall Ecosystems: Recent Insights into Ecology, Paleoecology, and Evolution. Annual Review of Marine Science 7:1–26.

Smith, C.R., Kukert, H., Wheatcroft, R.A., Jumars, P.A., Deming, J.W. 1989. Vent fauna on whale remains. Nature 341 :27–28.

Sumida, P. Y., J. M. Alfaro-Lucas, M. Shimabukuro, H. Kitazato, J. A. Perez, A. Soares-Gomes, T. Toyofuku, A. O. Lima, K. Ara, and Y. Fujiwara. 2016. Deep-sea whale fall fauna from the Atlantic resembles that of the Pacific Ocean. Scientific Reports 6 :22139.

Teixidó, N., M. Gambi, V. Parravacini, K. Kroeker, F. Micheli, S. Villéger, and E. Ballesteros. 2018. Functional biodiversity loss along natural CO_2 gradients. Nature Communications 9 :5149.

Thubaut, J., N. Puillandre, B. Faure, C. Cruaud, and S. Samadi. 2013. The contrasted evolutionary fates of deep-sea chemosynthetic mussels (Bivalvia, Bathymodiolinae). Ecology and Evolution 3 :4748–4766.

Tilman, D. 1982. Resource Competition and Community Structure. Princeton University Press, Princeton, NJ.

Tivey M, Bradley A, Terrence J, Kadco D. 2002 Insights into tide-related variability at seafloor hydrothermal vents from time-series temperature measurements. Earth Planet. Sci. Lett. 202, 693– 707

Turner, R. D. 1973. Wood-boring bivalves, opportunistic species in the deep sea. Science 180 : 1377–1379.

Van Dover, C., and R. A. Lutz. 2004. Experimental ecology at deep-sea hydrothermal vents: a perspective. Journal of Experimental Marine Biology and Ecology 300:273–307.

Van Dover, C., C. German, K. Speer, L. Parson, and R. Vrijenhoek. 2002. Evolution and Biogeography of Deep-Sea Vent and Seep Invertebrates. Science 295:1253–1257.

Vellend, M. 2010. Conceptual synthesis in community ecology. The Quarterly review of biology 85 :183–206.

Villéger, S., G. Grenouillet, and S. Brosse. 2013. Decomposing functional β-diversity reveals that low functional β-diversity is driven by low functional turnover in European fish assemblages. Global Ecology and Biogeography 22 :671–681.

Villéger, S., P. M. Novack-Gottshall, and D. Mouillot. 2011. The multidimensionality of the niche reveals functional diversity changes in benthic marine biotas across geological time. Ecology Letters 14 :561–568.

Voight, J. R. 2015. Xylotrophic bivalves : aspects of their biology and the impacts of humans. Journal of Molluscan Studies 81 :175–186.

Weiher, E., D. Freund, T. Bunton, A. Stefanski, T. Lee, and S. Bentivenga. 2011. Advances, challenges and a developing synthesis of ecological community assembly theory. Philosophical transactions of the Royal Society of London. Series B, Biological sciences 366 :2403–13.

Wiens, J. 1989. Spatial Scaling in Ecology. Functional Ecology 3:385.

Wolff, T. 2011. Magrofaunal utilization of plant remains in the deep sea. Sarsia 64:117–143.

Zeppilli, D., A. Vanreusel, F. Pradillon, S. Fuchs, P. Mandon, T. James, and J. Sarrazin. 2015. Rapid colonisation by nematodes on organic and inorganic substrata deployed at the deep-sea Lucky Strike hydrothermal vent field (Mid-Atlantic Ridge). Marine Biodiversity 45 :489–504.

Appendix S4.1
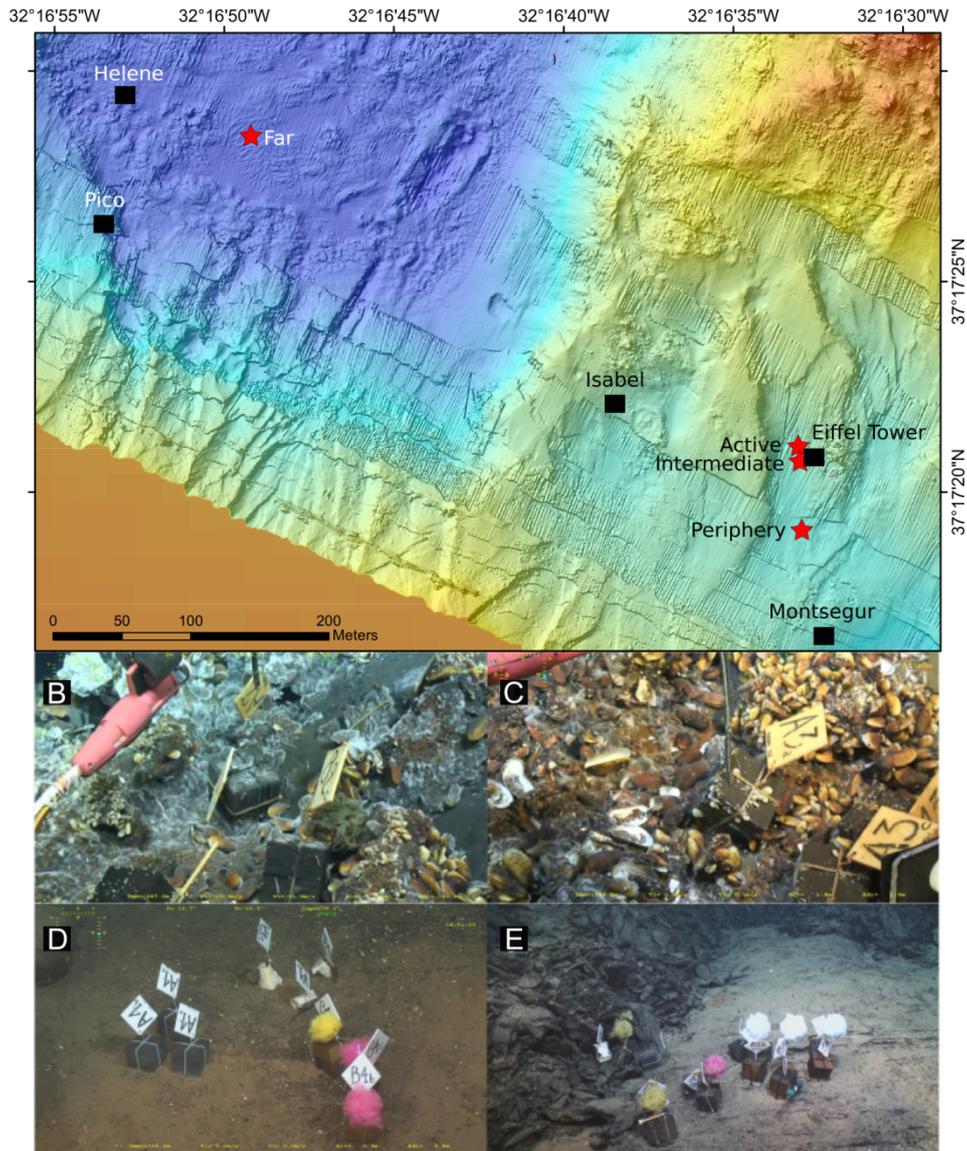
Figure S4.1.1. The southeast region of the Lucky Strike vent field located at 1700 m depth on the Mid-Atlantic Ridge, south of the Azores. A. Locations of the four deployment sites (red stars) and surrounding main active edifices (black squares). Note that the far site is located further west, in the fossil lava lake. Colonized substratum blocks at B. active, C. intermediate, D. periphery and E. far sites. Also visible in the photos are the other types of substratum used in parallel experiments.

Appendix S4.2

Table S4.2.1. Functional indexes used to measure functional diversity. Formulas for indices computation, indice relationships, properties and interpretations may be found in the given references.

Measure	Goal	Properties	Interpretation	References
Functional richness (FRic)	FRic measures the volume of functional space	FRic is very sensitive to the number of species and outliers. It does not consider species abundances.	High FRic values equal to high functional richness.	Villéger et al., 2008 ; Mouchet et al., 2010
Functional entities (FE)	FE measures the number of unique trait combinantions.	UTC is very sensitive to the number of species. It does not consider species abundances.	High UTC may equal to high functional richness.	Teixido et al., 2018
Functional evenness (Feve)	Feve measures the regularity of the distribution of species and abundances in the functional space.	Feve determines the distribution of species in the functional space independently of its volume. It considers species abundances. It is only weakly affected by species richness. Bounded between 0 and 1.	Feve is high when both species and abundances are regularly distributed in the functional space. Low values of Feve correspond to uneven species and abundances distributions in the functional space.	Villéger et al., 2008 ; Mouchet et al., 2010

Table S4.2.2. Species trait definitions for meio- and macrofaunal species.

Trait	Modalities	Definition	Rationale	References
Adult motility	1 (Sessile)	Non-mobile	This trait affects the ability of a species to access suitable habitat and nutritional sources. More mobile species may be less vulnerable to the environment stress and predation.	Bates et al. (2010)
	2 (Facultative)	Regularly non-mobile and only moving when necessary.		
	3 (Slow)	Regularly free slow swimmer, walker or crawler.		
	4 (Fast)	Regularly free fast swimmer and/or walker.		
Max adult body size	0	0,02 - <0,3 mm	Size is fundamentally related to energy flow and nutrient cycling. It affects the physiological tolerance of organisms (thermal mass, barriers to diffusion, and limits anatomical, physiological or behavioral options). It is also tightly related to dispersal and reproduction.	McGill et al. (2006) ; Gollner et al. (2015); McClain et al. (2018a)
	1	≥0,3 - <1 mm		
	2	≥1 - <5 mm		
	3	≥5 - <10 mm		
	4	≥10 - <15 mm		
	5	≥15 - <20 mm		
	6	≥20 mm		
Feeding mechanism	Symbiotic	Obtain energy from a symbiotic relationship	Feeding mechanisms are indicators of ecosystem productivity or energy availability. A diverse community will likely harbor species with diverse feeding mechanisms and trophic levels.	Post (2002) ; McClain et al. (2018b)
	Filter feeder	Obtain food particles mainly from filtering the water column		
	Deposit feeder	Mainly obtain food particles from the surface or buried food particles from the subsurface		
	Grazing	Scrap or nibble food from substrate.		
	Predator	Mainly capture animals capable of resistance.		

Table S4.2.3. Meiofaunal species and their functional traits.

Species	Mobility	Size	Feeding mechanisms	References
Halomonhystera sp.	3	0	deposit feeder	Wieser (1953); Zeppilli et al. (2015)
Oncholaimus dyvae	3	3	predator	Wieser (1953); Zeppilli et al. (2015)
Paracanthonchus sp.	3	0	predator	Wieser (1953); Zeppilli et al. (2015)
Microlaimus sp.	3	0	grazer	Wieser (1953); Zeppilli et al. (2015)
Cephalochetosoma sp.	2	0	deposit feeder	Wieser (1953); Zeppilli et al. (2015)
Chromadorita sp.	3	0	deposit feeder	Wieser (1953); Zeppilli et al. (2015)
Theristus sp.	3	0	deposit feeder	Wieser (1953); Zeppilli et al. (2015)
Epsilonema sp.	3	0	deposit feeder	Wieser (1953); Zeppilli et al. (2015)
Xylaridae sp.	3	0	deposit feeder	Wieser (1953); Zeppilli et al. (2015)
Desmoscolex sp.	3	0	deposit feeder	Wieser (1953); Zeppilli et al. (2015)
Nematoda sp. 1	3	0	deposit feeder	Wieser (1953); Zeppilli et al. (2015)
Tegastidae sp.	3	0	grazer	Heptner & Ivanenko (2002)
Smacigastes micheli	3	1	grazer	Heptner & Ivanenko (2002)
Hepterina confusa	4	1	grazer	Heptner & Ivanenko (2002), Limén et al. (2008), Gollner et al. (2015), Senokuchi et al. (2018)
Cyclopina sp.	4	1	grazer	Heptner & Ivanenko (2002), Limén et al. (2008), Gollner et al. (2015), Senokuchi et al. (2018)
yclopoid asp.	4	1	grazer	Heptner & Ivanenko (2002)
Calanoida sp.	4	1	grazer	Heptner & Ivanenko (2002)
Bathylaophonte azorica	3	1	grazer	Heptner & Ivanenko (2002)
Tisbidae sp. 1	4	0	grazer	Heptner & Ivanenko (2002)
Tisbidae sp. 2	4	1	grazer	Heptner & Ivanenko (2002)
Dorsiellinae sp.	3	1	grazer	Heptner & Ivanenko (2002)
Miraciidae sp.	3	1	grazer	Heptner & Ivanenko (2002)
Amereidae sp. 1	3	1	grazer	Heptner & Ivanenko (2002)
Ameiridae sp. 2	3	1	grazer	Heptner & Ivanenko (2002)
Amereidae sp. 3	3	0	grazer	Heptner & Ivanenko (2002)
Ameridae sp. 4	3	0	grazer	Heptner & Ivanenko (2002)
Dirivultidae sp. 1	4	0	grazer	Heptner & Ivanenko (2002), Limén et al. (2008), Gollner et al. (2015), Senokuchi et al. (2018)

Ectinosomatidae sp. 1	3	0	grazer	Heptner & Ivanenko (2002)
Ectinosomatidae sp. 2	3	1	grazer	Heptner & Ivanenko (2002)
Laophontidae sp.	3	0	grazer	Heptner & Ivanenko (2002)
Mesochra sp.	3	0	grazer	Heptner & Ivanenko (2002)
Aphotopontius sp.	4	1	grazer	Heptner & Ivanenko (2002), Limén et al. (2008), Gollner et al. (2015), Senokuchi et al. (2018)
Rimipontiussp.	4	1	grazer	Heptner & Ivanenko (2002), Limén et al. (2008), Gollner et al. (2015), Senokuchi et al. (2018)
cf. Ambilimbus? Sp.	3	0	grazer	Heptner & Ivanenko (2002)
cf. Kelliridae? Sp.	4	0	grazer	Heptner & Ivanenko (2002)
Thomontocypris excussa	4	1	grazer	Desbruyères et al. (2006) and references therein; Chapman et al. (2019); Tanaka pers. Obs.
Xylocythere sp.	4	1	grazer	Desbruyères et al. (2006) and references therein; Chapman et al. (2019); Tanaka pers. Obs.
Halacaridae sp.	3	1	predator	Desbruyères et al. (2006) ; Authors pers. Obs

Table S4.2.4. Macrofaunal species and their functional traits.

Species	Mobility	Size	Feeding	Reference
Bathymodiolus azoricus	2	6	symbiotic	Desbruyères et al. (2006) and references therein
Idas spp.	1	3	filter feeding	Rodrigues et al. (2015)
Xyloredo sp.	1	3	symbiotic	Voight (2015); authors pers. obs.
Xylophaga sp.	1	3	symbiotic	Voight (2015); authors pers. obs.
Lepetodrilus atlanticus	3	2	grazer	Desbruyères et al. (2006) and references therein
Pseudorimula midatlantica	3	3	grazer	Desbruyères et al. (2006) and references therein
Coccopigya spinigera	3	3	grazer	Jeffreys (1883);Dantart and Luque (1994)
Paralepetopspis ferrugivora	3	5	grazer	Desbruyères et al. (2006) and references therein
Protolira valvatoides	3	2	grazer	Desbruyères et al. (2006) and references therein
Lurifax vitreus	3	2	grazer	Desbruyères et al. (2006) and references therein
Xylodiscula analoga	3	2	grazer	Desbruyères et al. (2006) and references therein
Lirapex costellata	3	2	grazer	Desbruyères et al. (2006) and references therein

Divia briandi	3	3	grazer	Desbruyères et al. (2006) and references therein
Peltospira smaragdina	3	4	grazer	Desbruyères et al. (2006) and references therein
Laeviphitus debruyeris	3	2	grazer	Desbruyères et al. (2006) and references therein
Phymorhynchus sp.	3	6	predator	Van Dover (1995)
Amphisamytha lutzi	2	5	deposit feeder	Desbruyères et al. (2006) and references therein
Paramytha sp.	2	5	deposit feeder	Jumars et al. (2015); Shimabukuro pers. obs.
Glycera tesselata	3	4	predator	Desbruyères et al. (2006) and references therein
Sirsoe sp.	3	3	deposit feeder	Shimabukuro pers. obs.
Hesionidae sp. 3	3	2	deposit feeder	Shimabukuro pers. obs.
Hesionidae sp. 4	3	2	deposit feeder	Shimabukuro pers. obs.
Hesionidae sp. 5	3	2	deposit feeder	Shimabukuro pers. obs.
Pleijelius sp.	3	2	deposit feeder	Alfaro-Lucas et al. (2018)
Branchipolynoe seepensis	4	6	deposit feeder	Desbruyères et al. (2006) and references therein
Branchinotogluma sp. 1	4	3	predator	Jumars et al. (2015) ; authors pers. Obs.
Branchinotogluma sp. 2	4	4	predator	Jumars et al. (2015) ; authors pers. Obs.
Bathykermadeca sp.	4	4	predator	Jumars et al. (2015) ; authors pers. Obs.
Lepidonotopodium sp.	4	4	predator	Jumars et al. (2015) ; authors pers. Obs.
Harmothoe sp. 1	4	4	predator	Jumars et al. (2015) ; authors pers. Obs.
Harmothoe sp. 2	4	4	predator	Jumars et al. (2015) ; authors pers. Obs.
Malmgrenia sp.	4	4	predator	Jumars et al. (2015) ; authors pers. Obs.
Macelliphaloides sp.	4	2	predator	Jumars et al. (2015) ; authors pers. Obs.
Polynoid sp. 1	4	4	predator	Jumars et al. (2015) ; authors pers. Obs.
Prionospio unilamellata	2	5	deposit feeder	Desbruyères et al. (2006) and references therein
Laonice athecata	2	6	deposit feeder	Desbruyères et al. (2006) and references therein
Spionidae sp. 1	2	3	deposit feeder	Shimabukuro pers. obs.
Ophryotrocha cf. platykephale	3	2	grazer	Desbruyères et al. (2006) and references therein
Ophryotrocha sp. 2	3	2	grazer	Desbruyères et al. (2006) and references therein
Ophryotrocha fabriae	3	2	grazer	Desbruyères et al. (2006) and references therein
Dorvilleidae sp. 1	3	2	grazer	Jumars et al. (2015); Shimabukuro pers. obs.
Strepternos sp.	3	3	predator	Jumars et al. (2015); Shimabukuro pers. obs.
Capitella sp. 1	3	3	deposit feeder	Alfaro-Lucas et al. (2018); Shimabukuro pers. Obs.
Capitella sp. 2	3	4	deposit feeder	Alfaro-Lucas et al. (2018); Shimabukuro pers. Obs.
Phyllodocidae sp.	3	3	predator	Jumars et al. (2015) ; authors pers. Obs.
Acrocirridae sp.	3	3	deposit feeder	Jumars et al. (2015) ; authors pers. Obs.

Tomopteris sp. 1	4	2	predator	Jumars et al. (2015)
Tomopteris sp. 2	4	2	predator	Jumars et al. (2015)
Opheliidae sp.	3	3	deposit feeder	Jumars et al. (2015)
Nereididae sp.	4	3	predator	Jumars et al. (2015), Shimabukuro pers. obs.
Archinome sp.	3	3	predator	Desbruyères et al. (2006) and references therein
Flabelligeridae sp.	3	2	deposit feeder	Desbruyères et al. (2006) and references therein
Cnidaria sp.	2	2	predator	Desbruyères et al. (2006) and references therein
Mirocaris fortunata	4	6	predator	Desbruyères et al. (2006) and references therein
Alvinocaris sp.	4	6	predator	Desbruyères et al. (2006) and references therein
Luckia striki	3	3	deposit feeder	Desbruyères et al. (2006) and references therein
Liljeborgiidae sp.	3	3	deposit feeder	Authors pers. obs
Stegocephalidae sp.	3	3	deposit feeder	Authors pers. obs
Phoxocephalidae sp.	3	3	deposit feeder	Authors pers. obs
Bonnierella sp.	3	3	deposit feeder	Authors pers. obs
cf. Storthyngura sp.	3	3	deposit feeder	Desbruyères et al. (2006) and references therein
Heteromesus sp.	3	3	deposit feeder	Authors pers. obs
Asellota sp. 2	3	3	deposit feeder	Authors pers. obs
Assellota sp. 3	3	3	deposit feeder	Authors pers. obs
Asellota sp. 4	3	3	deposit feeder	Authors pers. obs
Haploniscidae sp.	3	2	deposit feeder	Desbruyères et al. (2006) and references therein
Obesutanais sigridae	2	2	deposit feeder	Desbruyères et al. (2006) and references therein
cf. Typhlotanais incognitus	3	2	deposit feeder	Desbruyères et al. (2006) and references therein
Thomontocypris sp.	4	1	grazer	Desbruyères et al. (2006) and references therein; Chapman et al. (2019); Tanaka pers. Obs.
Aphotopontius sp.	4	1	grazer	Heptner & Ivanenko (2002) ; Limén et al. (2008) ; Gollner et al. (2015), Senokuchi et al. (2018)
Rimipontius sp.	4	1	grazer	Heptner & Ivanenko (2002) ; Limén et al. (2008) ; Gollner et al. (2015), Senokuchi et al. (2018)
Siphonostomatoida sp.	4	1	grazer	Heptner & Ivanenko (2002) ; Limén et al. (2008) ; Gollner et al. (2015), Senokuchi et al. (2018)
Bathylaophonte azorica	3	1	grazer	Heptner & Ivanenko (2002)
Smacigastes micheli	3	1	grazer	Desbruyères et al. (2006) and references therein, Chapman et al. (2019)
Miraciidae sp.	3	1	grazer	Heptner & Ivanenko (2002)
Tisbe sp. 2	4	1	grazer	Heptner & Ivanenko (2002)
Ameiridae sp. 1	3	1	grazer	Heptner & Ivanenko (2002)
Ameiridae sp. 2	3	1	grazer	Heptner & Ivanenko (2002)
Lobopleura sp.	3	1	grazer	Heptner & Ivanenko (2002)

Haifameira sp.	3	1	grazer	Heptner & Ivanenko (2002)
Hepterina confusa	4	1	grazer	Heptner & Ivanenko (2002)
Ectinosomatidae sp. 2	3	1	grazer	Heptner & Ivanenko (2002)
Donsiellinae sp.	3	1	grazer	Heptner & Ivanenko (2002)
Cyclopina sp.	4	1	grazer	Heptner & Ivanenko (2002)
yclopoid asp.	4	1	grazer	Heptner & Ivanenko (2002)
Calanoida sp.	4	1	grazer	Heptner & Ivanenko (2002)
Cumacea sp.	4	4	deposit feeder	Authors pers. obs
Halacaridae sp.	3	1	predator	Desbruyères et al. (2006) ; Authors pers. Obs
Pycnogonida sp.	3	6	predator	Desbruyères et al. (2006) ; Authors pers. Obs
Ophiuroidea sp.	3	3	deposit feeder	Desbruyères et al. (2006) ; Authors pers. Obs
Oncholaimus dyvae	3	3	predator	Wieser (1953); Zeppilli et al. (2015)
Desmodora sp.	3	1	grazer	Wieser (1953); Zeppilli et al. (2015)
Chaetognatha sp.	2	3	predator	Authors pers. obs
Platyhelmintes sp.	3	2	predator	Authors pers. obs
Nemertea sp.	3	2	predator	Authors pers. obs

References:.

1. Chapman, A. S. *et al.* sFDvent: A global trait database for deep-sea hydrothermal-vent fauna. *Global Ecology and Biogeography* (2019). Doi:10.1111/geb.12975

2. Bates, A. E., Lee, R. W., Tunnicliffe, V. & Lamare, M. D. Deep-sea hydrothermal vent animals seek cool fluids in a highly variable thermal environment. *Nature Communications* **1,** ncomms1014 (2010).

3. Chapman, A. S., Tunnicliffe, V. & Bates, A. E. Both rare and common species make unique contributions to functional diversity in an ecosystem unaffected by human activities. *Diversity and Distributions* **24,** 568–578 (2018).

4. Dantart, L. & Luque, A. 1994. Cocculiniformia and Lepetidae (Gastropoda: Archaeogastropoda) from Iberian Waters. Journal of Molluscs Studies, 60: 277-313

5. Desbruyères, D. *et al.* Variations in deep-sea hydrothermal vent communities on the Mid-Atlantic Ridge near the Azores plateau. *Deep Sea Research Part I: Oceanographic Research Papers* **48,** 1325–1346 (2001).

6. Gollner, S., Govenar, B., Fisher, C. R. & Bright, M. Size matters at deep-sea hydrothermal vents: different diversity and habitat fidelity patterns of meio- and macrofauna. *Marine ecology progress series* **520,** 57–66 (2015).

7. Heptner & Ivanenko, 2002. Copepoda (Crustacea) of hydrothermal ecosystems of the World Ocean. Arthropoda Selecta 11:117-134

8. Jumars, P. A., Dorgan, K. M. & Lindsay, S. M. Diet of Worms Emended: An Update of Polychaete Feeding Guilds. *Annu Rev Mar Sci* **7,** 497–520 (2015).

9. Laliberté, E. & Legendre, P. A distance-based framework for measuring functional diversity from multiple traits. *Ecology* **91,** 299–305 (2010).

10. Levesque, C., Juniper, K. S. & Limén, H. Spatial organization of food webs along habitat gradients at deep-sea hydrothermal vents on Axial Volcano, Northeast Pacific. *Deep Sea Research Part I: Oceanographic Research Papers* **53,** 726–739 (2006).

11. McClain, C. R., Barry, J. P. & Webb, T. J. Increased energy differentially increases richness and abundance of optimal body sizes in deep-sea wood falls. *Ecology* **99,** 184–195 (2018).

12.   McGill, B. J., Enquist, B. J., Weiher, E. & Westoby, M. Rebuilding community ecology from functional traits. *Trends in Ecology & Evolution* **21,** 178–185 (2006).

13.   Mouchet, M. A., Villéger, S., Mason, N. W. & Mouillot, D. Functional diversity measures: an overview of their redundancy and their ability to discriminate community assembly rules. *Functional Ecology* **24,** 867–876 (2010).

14.   Senokuchi, R. *et al.* Chemoautotrophic food availability influences copepod assemblage composition at deep hydrothermal vent sites within sea knoll calderas in the northwestern Pacific. *Marine Ecology Progress Series* **607,** 37–51 (2018).

15.   Villéger, S. et al. New multidimensional functional diversity indices for a multifaceted framework in functional ecology. Ecology 89:2290-301. (2019).

16.   Wieser, W. (1953). Die Beziehung zwischen Mundhoehlengestalt, Ernaehrungsweise und Vorkommen bei freilebenden marinen Nematoden. Arkiv Zool 2, 439–484.

17.   Zeppilli, D. et al. Rapid yclopoid as by nematodes on organic and inorganic substrata deployed at the deep-sea Lucky Strike hydrothermal vent field (Mid-Atlantic Ridge). Marine Biodiversity 45, 489–504 (2015).

18.   Zeppilli D., Bellec, L., Cambon-Bonavita, M.A., Decraemer W., Fontaneto D., Fuchs S., Gayet N., Mandon P., Michel L.N., Portail M., Smol N., Sørensen M.V., Vanreusel A., Sarrazin J. (2019). Ecology and trophic role of Oncholaimus dyvae sp. nov. (Nematoda: Oncholaimidae) from the lucky strike hydrothermal vent field (Mid-Atlantic Ridge). BMC Zool 4: 6.

Appendix S4.3

Table S4.3.1. Stable isotopes of macrofaunal species.

Species	Site	Substrata	n	δ¹³C	sd δ¹³C	δ¹⁵N	sd δ¹⁵N	δ³⁴S	sd δ³⁴S
Amphisamytha lutzi	Active	Wood	12	-27.50	1.90	1.80	1.10	7.20	0.70
Bathymodiolus azoricus	Active	Wood	19	-31.50	1.00	-7.20	1.00	5.10	1.80
Branchipolynoe seepensis	Active	Wood	18	-31.00	1.40	-5.70	1.10	2.70	1.60
Glycera tesselata	Active	Wood	1	-24.90	NA	7.30	NA	6.20	NA
Lepetodrilus atlanticus	Active	Wood	1	-27.40	NA	2.80	NA	5.30	NA
Lepidonotopodium sp.	Active	Wood	3	-28.60	0.10	-3.70	0.50	3.00	0.30
Protolira valvatoides	Active	Wood	3	-25.50	0.10	2.60	0.20	5.60	0.10
Pseudorimula midatlantica	Active	Wood	1	-31.60	NA	0.40	NA	4.70	NA
Smacigastes micheli	Active	Wood	1	-36.27	NA	2.76	NA	NA	NA
Oncholaimus dyvae	Active	Wood	1	-25.45	NA	1.90	NA	NA	NA
Luckia striki	Active	Wood	2	-23.23	1.52	1.93	0.61	7.33	1.26
Nemertea sp.	Active	Wood	1	-22.32	NA	5.65	NA	7.99	NA
Laonice aseccata	Active	Wood	1	-25.32	NA	7.53	NA	NA	NA
Ophryotrocha fabriae	Active	Wood	1	-27.31	NA	2.47	NA	NA	NA
Xylophaga sp.	Active	Wood	3	-23.03	0.65	0.70	3.30	12.79	1.77
Amphisamytha lutzi	Intermediate	Wood	12	-19.80	1.50	2.40	2.00	5.80	1.00
Alvinocaris sp.	Intermediate	Wood	1	-22.20	NA	3.40	NA	NA	NA
Bathymodiolus azoricus	Intermediate	Wood	22	-31.50	1.60	-8.40	1.70	5.90	1.90
Branchipolynoe seepensis	Intermediate	Wood	19	-29.80	1.30	-6.80	1.30	4.10	1.60
Lepetodrilus atlanticus	Intermediate	Wood	2	-21.60	1.60	3.80	0.20	4.00	0.80
Lirapex costellata	Intermediate	Wood	2	-24.70	0.00	4.90	0.70	4.90	0.00
Lurifax vitreus	Intermediate	Wood	1	-31.00	NA	1.10	NA	3.80	NA
Mirocaris fortunata	Intermediate	Wood	5	-17.20	1.00	6.70	0.50	4.40	0.80
Paralepetopsis ferrugivora	Intermediate	Wood	1	-25.70	NA	-1.90	NA	3.90	NA
Protolira valvatoides	Intermediate	Wood	10	-26.30	0.70	2.70	0.30	5.40	0.80
Pseudorimula midatlantica	Intermediate	Wood	3	-25.90	0.80	2.50	0.70	3.40	0.70
Divia briandi	Intermediate	Wood	3	-16.00	0.60	5.70	0.50	8.80	1.50
Nemertea sp.	Intermediate	Wood	1	-21.60	NA	4.90	NA	4.10	NA
Aphotopontius sp.	Intermediate	Wood	1	-25.74	NA	-3.01	NA	NA	NA
Oncholaimus dyvae	Intermediate	Wood	1	-21.15	NA	4.95	NA	NA	NA
Luckia striki	Intermediate	Wood	1	-22.95	NA	1.81	NA	6.57	NA
Liljeborgiidae sp	Intermediate	Wood	1	-25.74	NA	5.22	NA	4.64	NA
Ophryotrocha fabriae	Intermediate	Wood	1	-26.43	NA	-0.91	NA	NA	NA
Xylophaga sp	Intermediate	Wood	3	-24.39	0.64	1.89	0.52	11.80	0.49

Strepternos sp.	Periphery	Wood	3	-19.90	0.40	7.60	0.10	9.60	1.40
Coccopygia spinifera	Periphery	Wood	3	-22.80	0.20	5.40	0.20	12.00	2.00
Idas spp.	Periphery	Wood	3	-21.10	0.30	5.80	0.20	12.10	1.40
Xyloredo sp.	Periphery	Wood	2	-24.50	0.10	1.30	0.50	14.40	2.50
Batylaophonte azorica	Periphery	Wood	1	-23.07	NA	4.22	NA	8.19	NA
Thomontocypris excussa	Periphery	Wood	2	-22.71	0.10	5.44	0.64	10.56	NA
Glycera tesselata	Periphery	Wood	1	-22.33	NA	7.92	NA	NA	NA
Phymorrinchus sp.	Periphery	Wood	1	-20.59	NA	5.18	NA	13.87	NA
Protolira valvatoides	Periphery	Wood	1	-23.80	NA	3.05	NA	NA	NA
Luckia striki	Periphery	Wood	1	-21.18	NA	4.01	NA	11.78	NA
Turbellaria sp.	Periphery	Wood	1	-22.20	NA	4.01	NA	15.28	NA
Capitella sp. 1	Periphery	Wood	3	-19.90	0.60	8.10	0.30	11.30	2.61
Paramytha sp.	Periphery	Wood	1	-21.40	NA	6.29	NA	17.03	NA
Laonice aseccata	Periphery	Wood	1	-21.49	NA	5.64	NA	NA	NA
Prionospio unilamellata	Periphery	Wood	1	-22.20	NA	5.83	NA	NA	NA
Capitella sp. 5	Periphery	Wood	1	-20.97	NA	5.51	NA	NA	NA
Hesionidae sp. 3	Periphery	Wood	1	-21.03	NA	7.96	NA	10.90	NA
Hesionidae sp. 4	Periphery	Wood	1	-20.98	NA	7.31	NA	NA	NA
Sirsoe sp.	Periphery	Wood	1	-19.02	NA	8.36	NA	6.84	NA
Lepidonotopodium sp.	Periphery	Wood	1	-20.30	NA	9.00	NA	13.60	NA
Ophryotrocha cf. *platykephale*	Periphery	Wood	1	-21.91	0.31	6.78	1.10	10.30	NA
Capitella sp. 1	Far	Wood	3	-21.98	0.67	7.09	0.94	14.65	2.59
Strepternos sp.	Far	Wood	6	-20.20	0.60	7.50	0.20	14.10	3.10
Coccopygia spinifera	Far	Wood	6	-22.70	0.30	5.30	0.40	16.80	1.00
Idas spp.	Far	Wood	3	-22.40	0.60	5.00	0.20	17.00	0.50
Macellicephaloides sp.	Far	Wood	1	-19.80	NA	6.00	NA	NA	NA
Protolira valvatoides	Far	Wood	1	-26.60	NA	2.10	NA	4.70	NA
Xyloredo sp.	Far	Wood	4	-23.70	0.50	4.40	0.50	16.30	1.00
Luckia striki	Far	Wood	1	-21.98	NA	5.50	NA	13.08	NA
Paramytha sp.	Far	Wood	1	-21.79	NA	5.49	NA	NA	NA
Sirsoe sp.	Far	Wood	1	-19.97	NA	9.87	NA	NA	NA
Hesionidae sp 3	Far	Wood	1	-20.56	NA	7.74	NA	10.52	NA
Amphysamitha lutzi	Active	Slate	12	-24.37	2.68	4.87	0.45	3.54	0.76
Bathymodiolus azoricus	Active	Slate	3	-32.09	0.28	-7.69	1.43	5.99	2.43
Branchipolynoe seepensis	Active	Slate	1	-29.34	NA	-7.05	NA	2.65	NA
Glycera tesselata	Active	Slate	1	-28.41	NA	7.18	NA	5.25	NA
Lepetodrilus atlantica	Active	Slate	1	-28.92	NA	1.76	NA	NA	NA
Protolira valvatoides	Active	Slate	2	-27.24	0.21	1.96	0.16	6.35	1.21

Pseudorimula midatlantica	Active	Slate	2	-31.92	0.67	0.81	1.31	4.21	NA
Smacigastes micheli	Active	Slate	1	-34.57	NA	3.24	NA	NA	NA
Oncholaimus dyvae	Active	Slate	1	-22.73	NA	5.02	NA	3.58	NA
Lirapex costellata	Active	Slate	1	-24.78	NA	4.11	NA	6.76	NA
Nemertea sp.	Active	Slate	1	-18.97	NA	4.83	NA	NA	NA
Prionospio unilamellata	Active	Slate	1	-27.24	NA	3.20	NA	NA	NA
Ophryotrocha fabriae	Active	Slate	1	-31.47	NA	3.38	NA	NA	NA
Amphysamitha lutzi	Intermediate	Slate	12	-24.79	0.77	0.75	1.46	6.71	1.14
Bathymodiolus azoricus	Intermediate	Slate	23	-32.01	1.30	-8.04	5.70	5.09	1.74
Branchipolynoe seepensis	Intermediate	Slate	18	-30.56	1.52	-6.65	1.50	3.40	1.45
Glycera tesselata	Intermediate	Slate	5	-24.18	0.63	4.95	0.32	4.74	0.13
Lepetodrilus atlantica	Intermediate	Slate	1	-26.94	NA	1.86	NA	3.55	NA
Protolira valvatoides	Intermediate	Slate	7	-26.25	0.38	1.60	0.24	5.31	0.91
Pseudorimula midatlantica	Intermediate	Slate	3	-29.46	1.35	1.08	0.57	2.82	0.49
Nemertea sp.	Intermediate	Slate	2	-21.39	1.06	3.72	1.06	4.05	NA
Aphotopontius sp.	Intermediate	Slate	1	-23.10	NA	1.23	NA	NA	NA
Ophryotrocha fabriae	Intermediate	Slate	1	-28.24	NA	0.90	NA	NA	NA
Oncholaimus dyvae	Intermediate	Slate	1	-23.30	NA	3.08	NA	3.82	NA
Liljeborgidae sp.	Periphery	Slate	1	-21.35	NA	8.33	NA	NA	NA
Lepidonotopodium sp.	Far	Slate	1	-17.39	NA	9.89	NA	14.03	NA
Luckia striki	Far	Slate	1	-20.89	NA	6.26	NA	11.91	NA
Storthyngura sp.	Far	Slate	1	-22.77	NA	6.94	NA	11.25	NA
Heteromesus sp.	Far	Slate	1	-19.32	NA	5.70	NA	NA	NA

Appendix S4.4

Table S4.4.1. Mean percentage abundance (± standard deviation) of meiofaunal taxa (<300->20 μm).

Phylum	Class	Order	Species	Slate/Active	Slate/Periph.	Wood/Active	Wood/Periph
Nematoda	Chromadorea	Monhysterida	*Halomonhystera* sp.	0.08±0.14	0	1.12±1.36	0
			Xyalidae sp.	0	0	0.16±0.39	0
			Theristus sp.	0	1.5±2.58	0.13±0.32	0.03±0.08
		Chromadorida	*Paracanthonchus* sp.	9.56±11.49	0	1.48±1.14	0
			Chromadorita sp.	6.37±7.45	0.88±2.15	3.63±2.89	0.74±1.24
		Desmodorida	*Cephalochaetosoma* sp.	17.91±19.09	0	24.94±13.83	0
			Microlaimus sp.	14.82±16.93	0.29±0.72	15.59±12.34	0.03±0.08
			Epsilonema sp.	0	0.19±0.46	0	0
		Desmoscolecida	*Desmoscolex* sp.	0	0	0	0.06±0.08
	Enoplea	Enoplida	*Oncholaimus dyvae*	4.71±4.01	0	0.71±1.01	0
		Unknown	Nematoda sp. 1	0	0	0	0.04±0.08
Arthropoda	Hexanauplia	Cyclopoida	yclopoid asp.	0	0	0	0.53±1.3
			Cyclopina sp.	0	0	3.11±4.93	0.22±0.32
			Heptnerina confusa	6.67±3.13	3.66±4.55	2.1±2.63	0
			cf. *Ambilimbus* sp.	0	0.93±2.27	0	0
			cf. Kelleriidae sp.	5.44±4.41	4.17±5.69	4.02±4.55	40.67±25.62
		Calanoida	Calanoida sp.	0.11±0.26	0	0	0.01±0.03
		Harpacticoida	Tegastidae sp.	4.26±7.42	3.73±6.36	9.81±11.65	1.11±1.13
			Smacigastes micheli	9.81±10.1	0	6.32±9.48	0.04±0.07
			Bathylaophonte azorica	3.19±6.31	4.36±6.78	0	8.85±7.07
			Tisbidae sp. 1	2.25±4.52	0.19±0.46	1.42±2.13	0.24±0.58
			Tisbidae sp. 2	0	0	0.58±0.91	0
			Donsiellinae sp.	0.16±0.32	0	2.8±1.53	0
			Miraciidae sp.	3.19±3.37	1.28±3.14	1.29±1.83	0
			Ameiridae sp. 1	1.16±1.99	32.22±16.13	17.22±16.76	12.79±13.9
			Ameiridae sp. 2	0.26±0.64	0	0.29±0.32	1.13±0.67
			Ameiridae sp. 3	0.32±0.79	11.25±17.25	0.05±0.12	0.02±0.05
			Ameiridae sp. 4	0.11±0.26	21.27±16.57	0	0
			Ectinosomatidae sp. 1	1.46±2.07	4.55±7.11	1.81±3.18	1.51±1.76
			Ectinosomatidae sp. 2	0	0.29±0.72	0.05±0.13	0
			Archesola typhlops	1.09±1.12	0	0.13±0.32	0

	Siphonostomatoida	*Mesochra* sp.	0.14±0.35	5.01±7.47	0.24±0.38	31.98±16.14
		Dirivultidae sp.	0	0	0.05±0.13	0
		Aphotopontius sp.	2.26±2.96	0	0.2±0.31	0
		Rimipontius sp.	0.22±0.38	0	0	0
Ostracoda	Podocopida	*Thomontocypris excussa*	0	3.18±4.31	0	0
		Xylocythere sp.	0.13±0.31	0	0.05±0.13	0
Arachnida	Trombidiformes	Halacaridae sp.	4.31±4.05	1.04±2.55	0.72±0.8	0

Table S4.4.2. Mean abundance (± standard deviation) of macrofaunal taxa (≥300 μm).

Phylum	Class	Order	Species	Slate/Active	Slate/Periph.	Wood/Active	Wood/Periph.
Mollusca	Bivalvia	Pteriomorphia	*Bathymodiolus azoricus*	427.17±400.67	0	320.83±263.44	0
			Idas spp.	0	0	0	299.17±129.64
		Heterodonta	*Xyloredo* sp.	0	0	0	48.33±48.65
			Xylophaga sp.	0	0	27.67±15.68	0
	Gastropoda	Vetigastropoda	*Lepetodrilus atlanticus*	25.33±20.31	0	48.67±48.35	1.5±2.35
			Pseudorimula midatlantica	15.33±11.18	0	10.5±14.8	0
		Cocculiniformia	*Coccopigya spinigera*	0	0	0.83±2.04	264.17±187.85
		Patellogastropoda	*Paralepetopsis ferrugivora*	0	0	1±1.26	0
		Vetigastropoda	*Protolira valvatoides*	72.5±58.12	0	147.5±108.63	2.67±2.34
		Heterobranchia	*Lurifax vitreus*	2±2.97	3.17±3.6	4.5±6.28	1.83±1.72
			Xylodiscula analoga	1.67±2.07	0	1.5±1.97	0.17±0.41
		Neomphalina	*Lirapex costellata*	1.17±1.17	0	4.83±11.84	0.17±0.41
		Neritimorpha	*Divia briandi*	0.83±1.6	0	3.5±8.57	0
		Neomphalina	*Peltospira smaragdina*	0	0	0.17±0.41	0
		Caenogastropoda	*Laeviphitus debruyeris*	3.17±4.67	0	0.17±0.41	0
			Phymorhynchus sp.	0	0	0	0.67±1.63
Annelida	Polychatea	Sedentaria	*Amphisamytha lutzi*	114±74.48	0	101.67±99.12	0
			Paramytha sp.	0	0	0	7.5±5.32
			Acrocirridae sp.	0.17±0.41	0.33±0.52	0	0
			Prionospio unilamellata	1±2	0	0.67±0.82	1±1.67
			Laonice asaccata	0.17±0.41	0	0.5±1.22	0.17±0.41
			Spionidae sp. 1	0	0.17±0.41	0	0
			Capitella sp. 1	0	0	0.17±0.41	88.67±35.46
			Capitella sp. 2	0	0	0	2.67±4.13
			Opheliidae sp.	0	0.17±0.41	0	0
			Flabelligeridae sp.	0	0.5±0.55	0.17±0.41	0.67±0.82
		Errantia	*Glycera tesselata*	8±6.6	1.33±1.21	2±1.41	3±3.41
			Sirsoe sp.	0	0	0	4.67±5.28
			Hesionidae sp. 3	0	0	0	204.33±90.04
			Hesionidae sp. 4	0	0	0	16.83±12.86
			Hesionidae sp. 5	0	0	0	11.5±12.21
			Pleijelius sp.	0	0	0	3.83±3.71

			Branchipolynoe seepensis	16.83±22.89	0	24.17±23.19	0
			Branchinotogluma sp. 1	0.67±1.63	0	1.5±3.67	0
			Branchinotogluma sp. 2	0	0	3.33±2.88	0
			Bathykermadeca sp.	0	0.33±0.82	0	1±1.26
			Lepidonotopodium sp.	0.17±0.41	0.17±0.41	0.5±0.84	0.17±0.41
			Harmothoe sp. 1	0	0	0	0.17±0.41
			Harmothoe sp. 2	0	0	0	0.33±0.82
			Malmgrenia sp.	0	0	0.17±0.41	0
			Macellicephala sp.	0.17±0.41	0	0	1.67±2.07
			Polynoidae sp. 1	0.33±0.82	0	1.33±1.51	0
			Ophryotrocha cf. *platykephale*	0	0	0	43.83±25.38
			Ophryotrocha sp. 2	0	0	0	1.17±1.83
			Ophryotrocha fabriae	29.67±20.26	0	12.5±13.44	0.17±0.41
			Dorvilleidae sp. 1	0	0	0	1.67±1.97
			Strepternos sp.	0	0	0.17±0.41	333.67±96.09
			Phyllodocidae sp.	0	0.17±0.41	0	0
			Tomopteris sp. 1	0.17±0.41	0	0	0
			Tomopteris sp. 2	0.17±0.41	0	0	0
			Nereididae sp.	0	0.33±0.52	0	0.33±0.52
			Archinome sp.	0	0	0.17±0.41	0.17±0.41
Cnidaria			Cnidaria sp.	0	1.67±4.08	0	5.33±13.06
Arthropoda	Malacostraca	Eumalacostraca	*Mirocaris fortunata*	0	0	1.17±1.94	0
			Alvinocaris sp.	0	0	0.17±0.41	0
			Luckia striki	17.33±17.31	1.83±1.72	117.67±58.44	138.67±130.05
			Liljeborgiidae sp.	0	1.67±2.25	1.83±3.6	0
			Stegocephalidae sp.	0	0.17±0.41	0	0.33±0.52
			Phoxocephalidae sp.	0	0	0.17±0.41	0
			Bonnierella sp.	0	0	0	0.17±0.41
			cf. *Storthyngura* sp.	0	0.67±1.21	0	0.33±0.52
			Heteromesus sp.	0	0.33±0.82	0	0
			Asellota sp. 2	0	1.17±1.17	0	4.5±4.64
			Assellota sp. 3	0	0	0	0.17±0.41
			Asellota sp. 4	0	0.17±0.41	0.17±0.41	0
			Haploniscidae sp.	0	0	1.17±2.04	0
			Obesutanais sigridae	0	0.17±0.41	9.67±18.44	0.17±0.41
			cf. *Typhlotanais incognitus*	0	0.17±0.41	0.5±0.84	0.17±0.41
			Cumacea sp.	13.83±15.14	3.33±4.89	36.17±65.09	878.67±734.82
	Ostracoda		*Thomontocypris excussa*	21.17±34.78	0.33±0.52	16.33±23.01	0
	Hexanauplia	Copepoda	*Aphotopontius* sp.	2.33±2.07	0	0.17±0.41	0
			Rimipontius sp.	0	0	0	3±5.93
			Siphonostomatoida sp.	0.67±1.21	0.83±0.75	0	185.5±148.45
			Bathylaophonte azorica	48±59.12	0	30.5±63.01	0
			Smacigastes micheli	4.17±3.6	0.17±0.41	2.83±5.53	0.17±0.41
			Miraciidae sp.	2.33±5.72	0.33±0.52	6.5±6.41	0.5±0.84
			Tisbe sp. 2	0	0.17±0.41	0.33±0.52	1.33±1.21
			Ameiridae sp. 1	0	0.17±0.41	0.5±0.55	0.5±1.22

			Ameiridae sp. 2	5.17±11.7	0.17±0.41	0	0
			Archesola typhlops	0	0.17±0.41	0	0
			Haifameira sp.	0.83±0.98	0.17±0.41	1.33±2.34	0
			Hepterina confusa	0	0	0.17±0.41	0
			Ectinosomatidae sp. 2	0.17±0.41	0	1±1.26	0
			Donsiellinae sp.	0	0.17±0.41	0.17±0.41	0
			Cyclopina sp.	0.67±0.52	0	0	0.33±0.82
			yclopoid asp.	0	0	0	0.33±0.52
			Calanoida sp.	0	0	0	0.17±0.41
	Arachnida	Acari	Halacaridae sp.	16.33±25.5	0.17±0.41	5.83±8.73	0.17±0.41
	Pycnogonida		Pycnogonida sp.	0	0	0.33±0.82	0
Echinodermata	Ophiuroidea		Ophiuroidea sp.	0	0.17±0.41	0.83±1.6	0.17±0.41
Nematoda	Enoplea	Enoplia	*Oncholaimus dyvae*	403.17±467.24	0	20.83±33.61	0.17±0.41
	Chromadorea	Chromadoria	Desmodora sp.	0	0.17±0.41	0	0
Chaetognatha			Chaetognatha sp.	0	0.33±0.82	0.17±0.41	0
Platyhelmintes			Turbellaria sp.	0	0	0.33±0.82	0.33±0.82
Nemertea			Nemerttea sp.	6.17±5.27	0.33±0.82	4.17±3.06	0

Table S4.4.3. Analyses of variance (Anova/Kruskal tests) of biodiversity indices. * P<0.01

	Macrofauna		Meiofauna	
	Mean difference	**P adj**	**Mean difference**	**P adj**
S				
Slate/active-Wood/active	1.45	0.88	0.33	1.00
Slate/periph-Wood/active	3.25	**0***	-7.17	**0.01**
Wood/periph –Wood/active	-0.53	1	-4.50	0.14
Slate/periph –Slate/active	1.8	0.4	-7.50	**0.01**
Wood/periph –Slate/active	-1.98	0.3	-4.83	0.10
Wood/periph –Slate/periph	-3.78	**0***	2.67	0.55
log(N)				
Slate/active-Wood/active	0.26	0.66	0.13	0.99
Slate/periph-Wood/active	-3.76	**0***	-1.83	**0***
Wood/periph –Wood/active	0.99	**0***	0.87	0.28
Slate/periph –Slate/active	-4.02	**0***	-1.95	**0***
Wood/periph –Slate/active	0.73	**0.02**	0.74	0.41
Wood/periph –Slate/periph	4.75	**0***	2.69	**0***
J				
Slate/active-Wood/active	-0.10	0.14	0.04	0.89
Slate/periph-Wood/active	0.25	**0***	0.14	0.09
Wood/periph –Wood/active	-0.02	0.98	-0.18	**0.02**
Slate/periph –Slate/active	0.35	**0***	0.10	0.30
Wood/periph –Slate/active	0.09	0.27	-0.21	**0***
Wood/periph –Slate/periph	-0.27	**0***	-0.31	**0***
sqrt(FRic)				
Slate/active-Wood/active	-2.45	**0***	1.16	0.06
Slate/periph-Wood/active	-5.93	**0***	-5.64	**0***
Wood/periph –Wood/active	-2.62	**0***	-6.64	**0***
Slate/periph –Slate/active	-3.48	**0***	-6.80	**0***
Wood/periph –Slate/active	-0.17	0.98	-7.80	**0***
Wood/periph –Slate/periph	3.31	**0***	-1.00	0.19
log(FE)			FE	
Slate/active-Wood/active	-0.20	0.06	-1.09	1.00
Slate/periph-Wood/active	-0.78	**0***	1.77	0.40
Wood/periph –Wood/active	-0.12	0.39	2.77	**0.03**
Slate/periph –Slate/active	-0.58	**0***	2.74	**0.04**
Wood/periph –Slate/active	0.08	0.69	3.86	**0***
Wood/periph –Slate/periph	0.66	**0***	0.71	1.00
log(Feve)			Feve	
Slate/active-Wood/active	0.01	0.9	0.05	0.82
Slate/periph-Wood/active	0.15	**0**	0.09	0.52
Wood/periph –Wood/active	-0.09	**0.03**	-0.1	0.32
Slate/periph –Slate/active	0.15	**0***	0.04	0.92
Wood/periph –Slate/active	-0.1	**0.02**	-0.15	0.07
Wood/periph –Slate/periph	-0.24	**0***	-0.19	**0.03**

Appendix S4.5
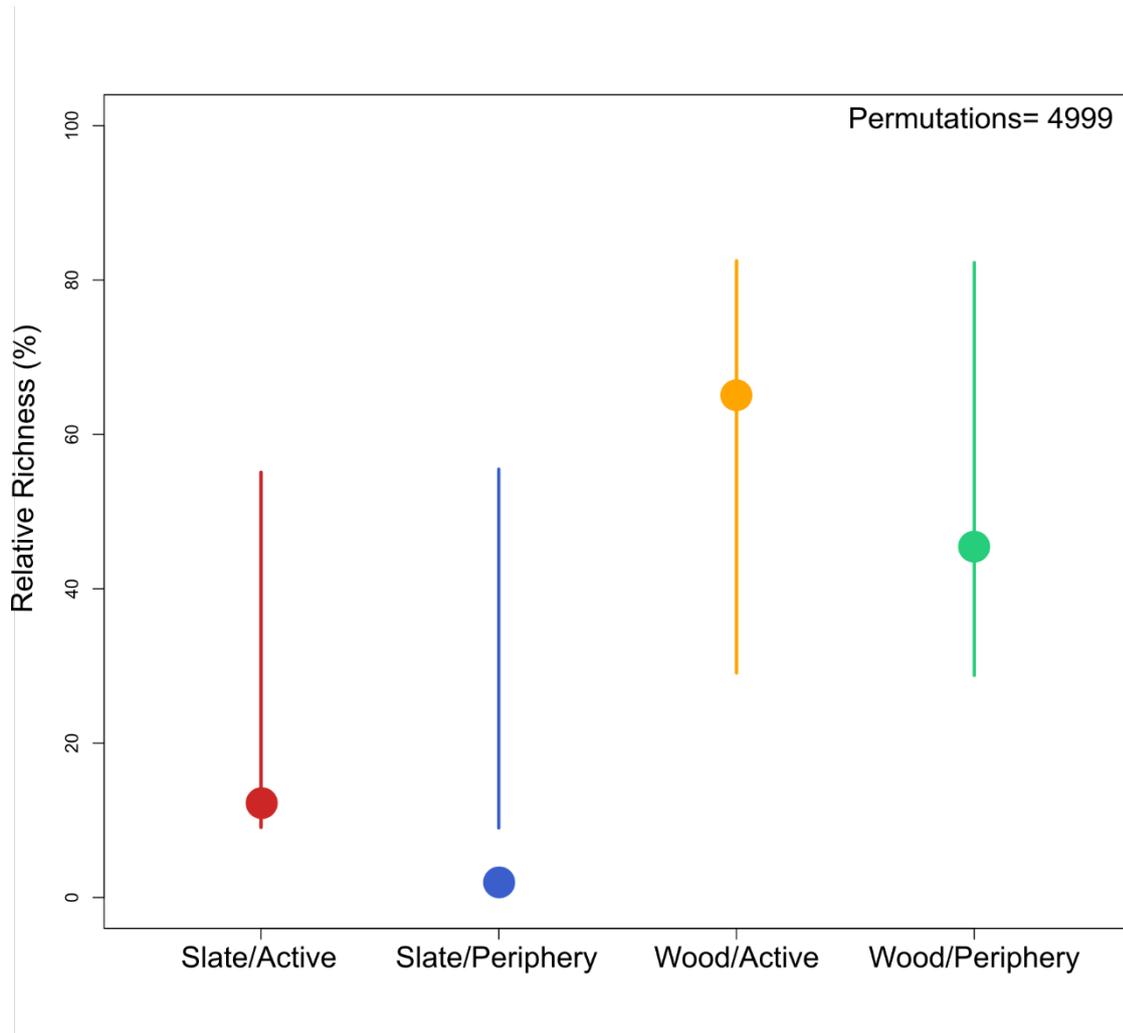
Figure S4.5.1. Null model of FRic (percentage volume of the total functional space) among sites for macroinvertebrates. Points are the observed values of FRic whereas bars represent the 95% confidence interval of expected values generated simulating a random sorting of the species from the total pool of functional entities (29 functional entities) while keeping the observed number of species at each site. Observed values within the bars provide evidence on that the functional richness does not deviate from null expectations. Null model was adapted from the script provided by Teixidó et al. (2018).
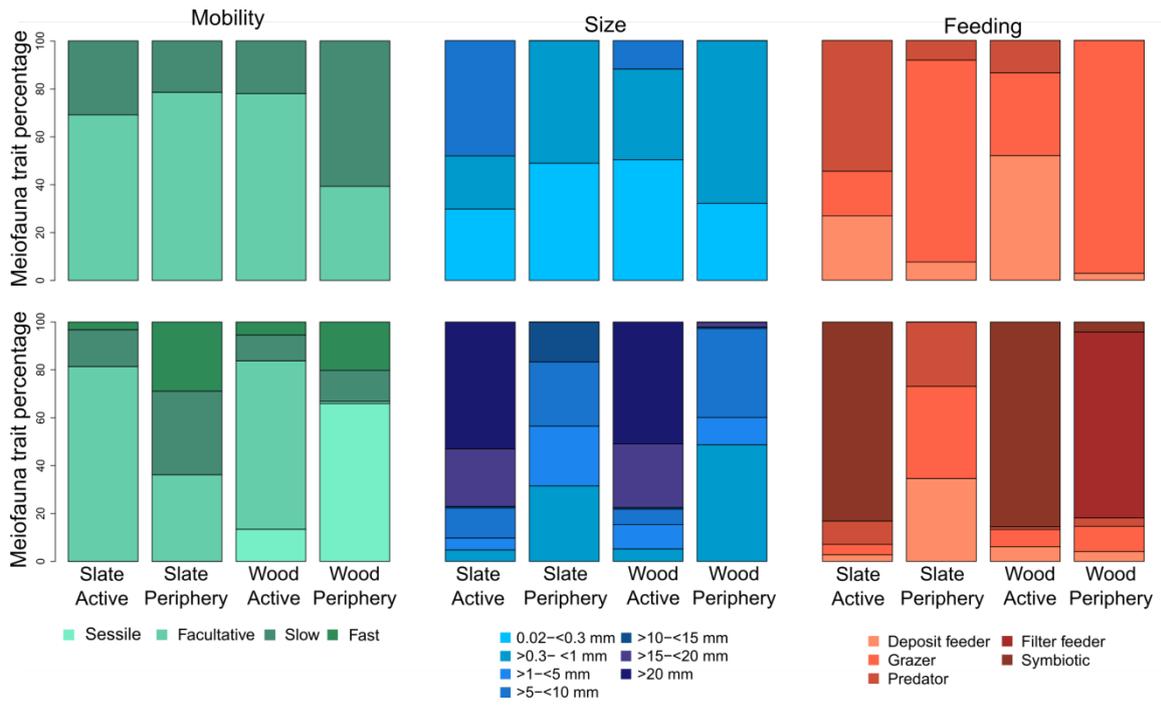
Figure S4.5.2. Percentage trait categories in meio- and macrofauna assemblages.

Appendix S4.6

Table S4.6.1. Species and functional β-diversity with contributions of the turnover and nestedness components for meio- and macrofauna assemblages, and isotopic similarity (Isim) and nestedness (Ines) indices for macrofauna assemblages estimated from the $\delta^{13}C$/ $\delta^{15}N$ (Iric C:N) and $\delta^{13}C$/ $\delta^{34}S$ (Iric C:S) isotopic space.

Species β-diversity	Meiofuana			Meiofuana		
Turnover	Slate/Active	Slate/Periph.	Wood/Active	Slate/Active	Slate/Periph.	Wood/Active
Slate/Periph.	0.76			0.42		
Wood/Active	0.32	0.59		0.27	0.42	
Wood/Periph.	0.65	0.59	0.68	0.43	0.56	0.43
Nestedness	Slate/Active	Slate/Periph.	Wood/Active	Slate/Active	Slate/Periph.	Wood/Active
Slate/Periph.	0.004			0.13		
Wood/Active	0.21	0.12		0.05	0.16	
Wood/Periph.	0.09	0.12	0	0.15	0.02	0.17
Total β-diversity	Slate/Active	Slate/Periph.	Wood/Active	Slate/Active	Slate/Periph.	Wood/Active
Slate/Periph.	0.76			0.55		
Wood/Active	0.52	0.70		0.31	0.58	
Wood/Periph.	0.74	0.70	0.68	0.58	0.58	0.61
Functional β-diversity						
Turnover	Slate/Active	Slate/Periph.	Wood/Active	Slate/Active	Slate/Periph.	Wood/Active
Slate/Periph.	0.67			0		
Wood/Active	0.31	0.05		0	0	
Wood/Periph.	0.08	0.06	0.29	0	0	0
Nestedness	Slate/Active	Slate/Periph.	Wood/Active	Slate/Active	Slate/Periph.	Wood/Active
Slate/Periph.	0.001			0.64		
Wood/Active	0.42	0.61		0	0.64	
Wood/Periph.	0.71	0.73	0.24	0.92	0.78	0.92
Total β-diversity	Slate/Active	Slate/Periph.	Wood/Active	Slate/Active	Slate/Periph.	Wood/Active
Slate/Periph.	0.67			0.64		
Wood/Active	0.73	0.67		0	0.64	
Wood/Periph.	0.79	0.79	0.53	0.92	0.78	0.92

Isotopic dissimilarity			
Isim cn	Slate/Active	Slate/Periph.	Wood/Active
Slate/Periph.	0		
Wood/Active	0.61	0.018	
Wood/Periph.	0.032	0.285	0.071
Iness C:N	Slate/Active	Slate/Periph.	Wood/Active
Slate/Periph.	0		
Wood/Active	0.99	0.29	
Wood/Periph.	0.2	0.56	0.72
Isim C:S	Slate/Active	Slate/Periph.	Wood/Active
Slate/Periph.	0		
Wood/Active	0.05	0.01	
Wood/Periph.	0.23	0	0.33
I Ness cs	Slate/Active	Slate/Periph.	Wood/Active

Slate/Periph.	0		
Wood/Active	0.16	0.62	
Wood/Periph.	0.97	0.05	0.65

Table S4.6.2. Species, functional and isotopic space overlap between groups.

	Macrofauna				Meiofauna			
Species	Slate/Active	Slate/Periphery	Wood/Active	Wood/Periphery	Slate/Active	Slate/Periphery	Wood/Active	Wood/Periphery
Slate/Active	100	38.9	53.57	33.9	100	73.68	78.57	72.22
Slate/Periphery	37.84	100	37.5	37.5	53.85	100	50	61.11
Wood/Active	81.1	58.33	100	48.21	84.61	73.68	100	72.22
Wood/Periphery	51.35	58.33	48.21	100	50	57.89	46.43	100
Functional space	Slate/Active	Slate/Periphery	Wood/Active	Wood/Periphery	Slate/Active	Slate/Periphery	Wood/Active	Wood/Periphery
Slate/Active	100	4.76	18.85	15.8	100	100	100	100
Slate/Periphery	25.25	100	3.37	5.1	41	100	41	100
Wood/Active	96.4	91.49	100	61.18	100	100	100	100
Wood/Periphery	56.44	95.73	42.72	100	6	16	6	100
Isotopic space C:N	Slate/Active	Slate/Periphery	Wood/Active	Wood/Periphery				
Slate/Active	100	0	60.38	2.32				
Slate/Periphery	0	100	1.91	34.88				
Wood/Active	99.21	29	100	69.67				
Wood/Periphery	20	56	72	100				
Isotopic space C:S	Slate/Active	Slate/Periphery	Wood/Active	Wood/Periphery				
Slate/Active	100	0	6.12	2.29				
Slate/Periphery	0	100	1	0.044				
Wood/Active	15.66	62.16	100	39.1				
Wood/Periphery	97.1	4.86	64.9	100				

General discussion, conclusions & perspectives

The objective of the present thesis was to better understand the early colonization processes structuring communities in vent habitats of the Lucky Strike vent field (Mid-Atlantic Ridge), from active hydrothermal areas on the Eiffel Tower to inactive poorly-sedimented and bare-basalt peripheries. Based on a conceptual model of the putative gradients found in deep-sea vents, linked to environmental stress and productivity, we applied a modern approach to explore biodiversity patterns during colonization process. This approach was based on three different facets, namely species richness, functional traits and stable isotopes.

This thesis was entirely based on a two-year colonizing experiment. Experiments using artificial substrata have a long history in vent ecology (e.g., Van Dover et al., 1988; Mullineaux et al., 1998; Micheli et al., 2000; Mullineaux et al., 2003; Hunt et al., 2004 ; Kelley and Metaxas, 2006, 2008; Kelly et al., 2007; Govenar et al., 2007 ; Cuvelier et al., 2014; Gollner et al., 2015; Zeppilli et al., 2015; Plum et al., 2017; Baldrighi et al., 2018; Nakamura et al., 2018). These studies have proven to be very useful for elucidating processes of colonization. This thesis also highlights that the use of colonizing substrata is not only an efficient method for performing manipulative experiments in the deep-sea but represents an efficient size-standardized sampling method, in an environment where quantitative sampling is still difficult to achieve (Gauthier et al. 2010). This is especially true for the fractions of fauna studied in this thesis which include meio- and macrofaunal groups. Indeed, substrata are easily placed and collected and the abundance of each taxa can be evaluated on a

standardized area, providing quantitative samples contrary to most deep-sea hard substratum faunal sampling tool (e.g., Gauthier et al. 2010; McClain et al., 2014). Substrata however, may not be that efficient for larger more-mobile taxa, such as crabs and shrimps.

Biodiversity at vent systems: active and peripheral habitats

Inherently to the global objective of this thesis was the determination of biodiversity in the studied area. The Eiffel Tower is arguably the most studied edifice on the entire Mid-Atlantic Ridge (e.g., Van Dover et al., 1996; Van Dover and Tusk, 2000; Desbruyeres et al., 2001; Cuvelier et al., 2009; Cuvelier et al., 2011; Cuvelier et al., 2014; Sarrazin et al., 2014; Sarrazin et al., 2015; Zeppilli et al., 2015; Plum et al., 2017; Baldrighi et al., 2018). After sampling on hydrothermally active areas, Sarrazin et al. (2015) as well as Husson et al. (2017) reported the highest number of species, a total of 70 and 79 species respectively (Chapter 3). In this thesis 116 species and/or morphospecies were identified in hydrothermally active and inactive conditions along and away from the edifice. Considering slate substrata only, a proxy of natural vent substrata, 77 taxa were identified in hydrothermally active and inactive conditions (Chapters 3 and 4). Species not recorded in this thesis include few large-mobile species, such as the crab *Segonzacia mesantlantica*, and some meiofaunal species, mainly within the copepod and nematode groups (Sarrazin et al., 2015; Zeppilli et al., 2015; Plum et al., 2016; Baldrighi et al., 2018). Author's taxonomic expertise and differences in site richness can explain the absence of these meiofauna species in the present study.

Species found in slates under the influence of hydrothermal activity were typical vent inhabitants, whereas species found in peripheral sites mostly belonged to faunal groups usually found on deep-sea hard substrata at Lucky Strike (Zeppilli et al., 205; Plum et al., 2016; Baldrighi et al., 2018, Chapters 3 and 4). Environmental conditions in both regimes were identified as main drivers structuring faunal assemblages in terms of species and traits. Of special relevance to vent ecology was the characterization of the poorly known fauna in peripheries of active areas. Studies at peripheries are scarce and usually focus on the megafaunal component of communities derived from image analyses (e.g., Sen et al., 2016; Gerdes et al., 2019). The megafauna associated to these habitats appears to be similar to those of other hard-bottom habitats, such as seamounts (Boschen et al., 2013). Indeed, the taxa mainly consist in long-lived sessile filter feeders, such as anemones, corals and sponges, or highly mobile scavengers and predators, such as fish, crabs and polynoids (Desbruyères et al., 2001; Boschen et al., 2013; Sen et al., 2016; Gerdes et al., 2019). Recent findings suggest that vent peripheries harbor distinct megafaunal assemblages compared to inactive sulfide habitats and background hard and soft deep-sea habitats (Gerdes et al., 2019). Studies reporting on the meiofauna at the vent periphery showed high diversity and low dominance of taxa (Gollner et al., 2010; Gollner et al., 2015; Zeppilli et al., 2015; Plum et al., 2016; Baldrighi et al., 2018). As observed in shallow water vents (Zeppilli and Danovaro, 2009), some generalist species become dominant in active environments, while sensitive "rare" species disappear. This is somehow opposed to what is observed for macrofauna in the deep sea, which increase in

dominance and density but also in its degree of specialization from periphery to active areas. Macrofaunal patterns in periphery are similar to those of meiofauna but due to the higher specialization of fauna inhabiting active habitats, there is substantially less overlap between active habitats (e.g., Gollner et al., 2015; Baldrighi et al., 2018).

This thesis adds to this body of bibliography and brings some other important findings. β-diversity analyses identified the periphery and far sites as contributing more than any other sites, both taxonomically and functionally, to the global dissimilarity for meio- and macrofauna (Chapter 3). Furthermore, some unique functional traits -not found in the hydrothermally active habitats- were found. Strikingly, the periphery and far sites were the most dissimilar in pairwise comparisons. This suggests that assemblages inhabiting distinct environments in the periphery may create a mosaic of quite unique taxonomic and functional assemblages around active habitats. Despite their uniqueness, these assemblages are not entirely independent, neither in composition nor energetically, from those found in hydrothermally active areas (Chapter 3). We quantified the overlap between active and peripheral assemblages in the Lucky Strike hydrothermal vent field (Figure 5.1). A higher overlap was observed in the smaller faunal compartment (<300 μm), as previously observed for assemblages in the Lucky Strike and other vent fields (e.g., Gollner et al., 2010; Gollner et al., 2015; Zeppilli et al., 2015; Plum et al., 2016; Baldrighi et al., 2018; Figure 5.1). Furthermore, based on stable δ^{34}S isotope values, this thesis showed that primary productivity of chemosynthetic origin is exported to and

consumed by peripheral assemblages (Chapter 3). Such links have been already
reported for large sessile filter feeding megafauna on inactive sulfide deposits
(Erickson et al., 2009) as well as on macrofauna at sedimented vents (Bell et al., 2016,
2017). Here, we extend these energetic relationships to the smaller faunal compartment
in basalt hosted vents.
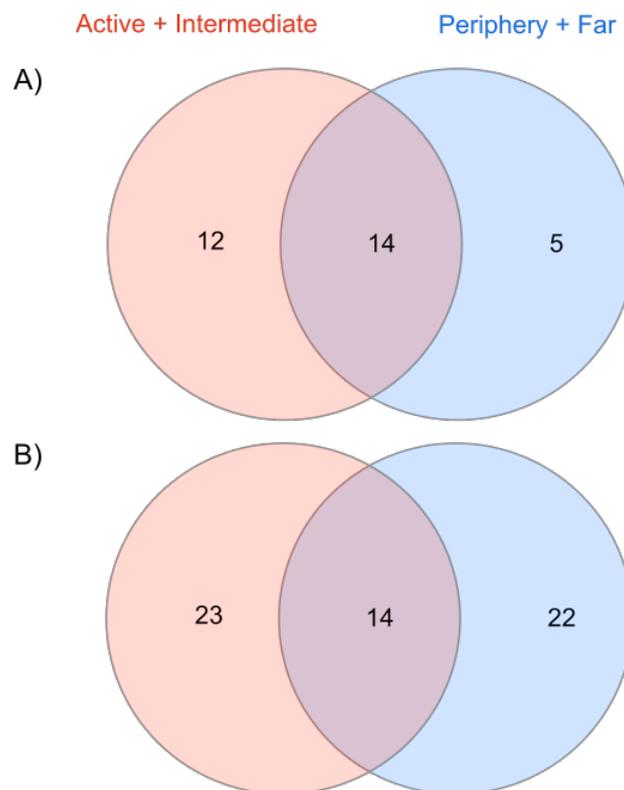
Figure 5.1. Venn diagram of exclusive and shared species founded in slate substrata in
hydrothermally active (active + intermediate sites) and peripheral (periphery + far sites)
conditions for A) <300 μm and B) >300 μm fauna. Although the number of species shared
between both conditions were the same between faunal compartments, this number was
proportionally higher for <300 μm fauna. Data derived from Chapter 3.

Functional richness in hydrothermal vent habitats

This thesis represents one of the first attempts to determine the functional richness along a deep-sea hydrothermal vent gradient for meio- and macrofaunal groups (but see similar approaches in Portail et al., 2018; Chapman et al., 2019). Thus, it provides a completely new perspective on vent ecology. Results obtained from the peripheral areas in this study revealed a low functional richness. On the top of that, and contrary to their shallow-water counterparts (Teixidó et al., 2018), deep-sea vents support functionally rich communities in active areas (Chapter 4). The great amount of energy provided by chemosynthesis is likely the driver of such a high functional diversity in comparison to the more stable, less-energetic inactive adjacent areas (Chapters 3 and 4). This hypothesis was supported by the observed distribution of functional traits among sites. Hydrothermally active sites support more energetically-expensive traits, such as large sizes and higher proportion of predator species. Vent communities thus are not only hotspots of biomass and abundance in the deep-sea but also of functional richness.

The relationship between species and functional richness: a matter of scale and a clue to the coexistence of dense faunal assemblages in vent habitats

It is important to highlight that the relationship between taxonomic and functional indices is scale dependent. Mean species and functional richness indices per substrata showed a higher richness in hydrothermally active environments than in

peripheral sites (Chapters 3 and 4; Figure 5.2A). This relationship was not observed in the total richness found at each site (Chapter 3) or within the different environmental conditions (Chapter 4; Figure 2B). For instance, in Chapter 3, the far site showed similar total species richness than those observed in the active or intermediate sites but much lower functional richness. In Chapter 4, slates in hydrothermally active conditions had only one more species than those at peripheral environments but almost six times more functional richness (Figure 5.2B). This is due to the presence of a large heterogeneity in species composition between the different substrata in peripheral environments. Each substrata presented similar low number of individuals but of distinct species. In other words, each substrata at hydrothermally active sites harbor the majority of species and mean values approximate are good representative of total values. On the contrary, each substrata in peripheral environments harbor few of the majority of species found at the periphery sites and the mean values were much lower than the total values (Chapters 3 and 4) (Figure 5.2).

These patterns highlight the long-recognized fact that hydrothermally active "harsh" environment limits colonization and filter for a suit of species that create dense assemblages that are in contrast with the low-abundance, high diversity communities found in background ecosystems. At small scales, such as at the "substrata scale" in this thesis, these differences are not observed. On the contrary as discussed above, substrata from active and intermediate sites have much higher mean species richness and abundance than substrata at the periphery and far sites (Figure 2A). Interestingly

functional diversity did not show such scale-dependent relationship. Both mean and total functional richness were higher at active sites than in periphery and far slate substrata (Figure 2A and B). In other words, functional richness was similarly higher in each of the slate substrata in hydrothermally active conditions than at each slate substrata in periphery. Compared to what was observed in species richness, functional diversity increases similarly with species richness when pooling slate substrata of active sites, whereas it increases much more slowly than species richness when pooling slates from the periphery. The average high mean functional richness may reflect the many ecological strategies of vent species, which may help to relax competition between species and allow high mean species richness and abundances to occur in reduced spaces. The low functional richness in peripheral sites was lower than expected by chance by the null models (see discussion below), which raises serious concerns regarding the potential imminent impacts of mining in deep-sea hydrothermal fields.
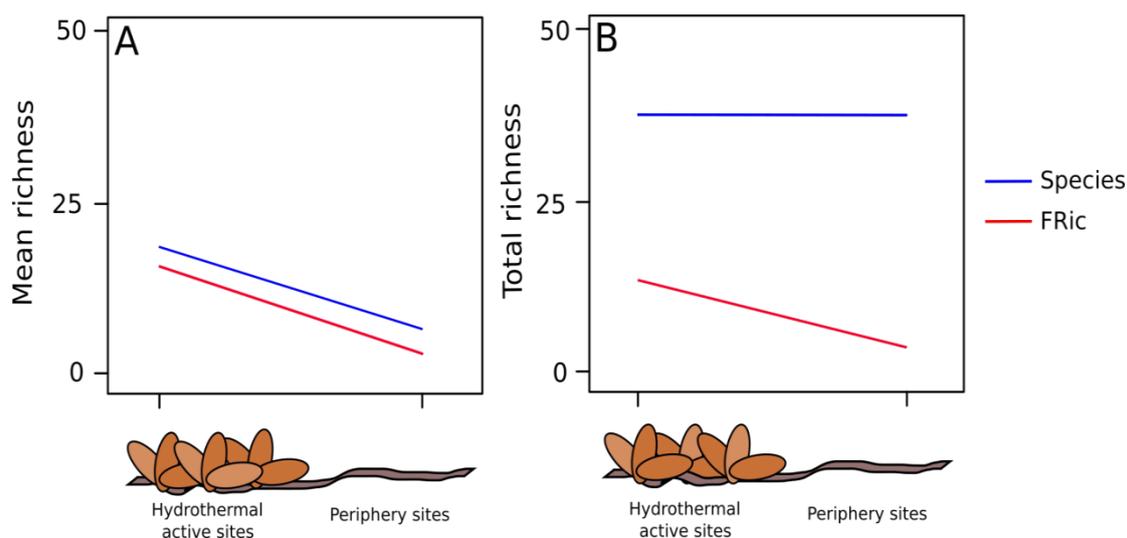
Figure 5.2. Species and functional richness relationship between hydrothermal active and peripheral sites as mean values (A) and total values (B) observed in this thesis. Values are based on mean and total richness indices of Chapter 3.

Functional richness in peripheral habitats

The extraction of mineral resources by the mining industry is one of the main impacts that hydrothermal vent habitats may face in the near future. This is especially true for the communities associated to inactive sulfide deposits which are the main mining targets for large-scale exploitation (Boschen et al., 2013; Van Dover, 2019). Aside direct habitat loss and faunal removal, the dispersal of unconsolidated sediment plume generated during mineral extraction will probably impact neighboring communities, i.e., active and peripheral habitats (reviewed in Boschen et al., 2013). Indeed, the generated plumes may extend as far as 10 km from mining sites and physically affect the environment by sediment deposition and release of heavy metals (Boschen et al., 2013). While the vent taxa associated to active areas are adapted to deal with very unstable physico-chemical conditions and exhibit behavioral and

physiological adaptations (Childress and Fisher, 1992; Govenar, 2010; Bates et al., 2010), those from periphery are more likely to be adapted to the quite stable environmental conditions of the deep-sea. The sessile filter feeding megafauna that includes sponges and corals is probably more sensitive to significant disturbances. Predictions are more difficult for the macro- and meiofauna due to the poor knowledge of hard substratum communities but some studies have already suggested that colonization after a disturbance may be considerably slow in vent peripheral habitats (Gollner et al., 2010). These results are in agreement to those obtained in studies performed in other deep-sea hard substrata habitats, such as polymetallic nodule fields (Miljuti et al., 2011).

In this colonizing experiment, values of functional diversity were lower than expected by chance at least in one of the 2 peripheral areas studied (Chapter 3, Far site). Results of Chapter 4, in which peripheral sites (periphery & far) were pooled, revealed the same trend suggesting that the "peripheral" assemblages may be strongly structured by the environment. The assemblages structured by the environment rather than by competitive biological interactions are considered to be more sensible to impacts (Didham et al., 2004; Ashford et al., 2018). Thus, based on these results, we suggest that the meio- and macrofauna found in the periphery of vent sites may be especially sensitive to impacts of mining. We further suggest that rather than the vision of two separate entities, peripheral and hydrothermally active areas should be considered as biologically and energetically connected areas (Chapter 3). This focus

will ensure the recognition and protection of these historically neglected habitats. Indeed, they represent important parts of the ecosystem as they harbor rich, diverse and unique taxonomic and functional assemblages that contribute to increase the β-diversity at vents and in the deep sea.

Biodiversity in wood falls and their relationships with vents

When placed in hydrothermally inactive regimes, wood substrata in our experiment yield a total of 56 species (>300 μm), which represent 19 to 20 more species than slates in hydrothermally active and peripheral conditions, respectively (Chapter 4). In other words, our artificially created wood falls harbor substantially more species than hydrothermal vent and peripheral assemblages on slates. Wood falls also harbor more individuals than slates in hydrothermally active and inactive conditions, ca. ~2 and ~120 times more, respectively. It is well known that wood in the deep sea, as well as other organic falls, creates hotspots of biodiversity in very restricted areas (Bienhold et al., 2013; Judge and Barry, 2016). Species rich communities are expected to be functionally rich because a diverse array of functional traits may facilitate coexistence (Petcheley and Gaston, 2006). Alternatively, functional redundancy may also promote the coexistence of species, especially in energy-rich habitats where competition may be released by the abundant resources (McClain et al., 2018). In concordance with the first hypothesis, the taxonomical richness correlates with functional richness in our experiment (Chapter 3). Thus, this thesis shows that wood falls not only create hotspots of taxonomical diversity but also of functional diversity in the deep sea.

The isotopic richness may reflect several axes of the functional, and more specifically, of the trophic niche occupied by species in assemblages (Rigolet et al., 2015). It is indeed considered as a proxy of the "realized" niche of species and is complementary to the functional niche, a proxy of the "potential" niche (Berhop et al., 2004; Layman et al., 2007; Rigolet et al., 2015). As argued above, the positive relationship between species and functional diversity may be translated into an expansion or, alternatively, in an increase in the density of the isotopic niche (Rigolet et al., 2014; Wlodarka-Kolwalczuck et al., 2019). Interestingly, values of isotopic richness in this thesis yielded very different results depending on the isotopes used (Chapter 3). The $\delta^{13}C$ and $\delta^{15}N$ isotopic richness in vents and peripheral conditions are mainly associated to distinct energetic pathways (methanotrophy, rTCA, CBB and photosynthesis) and N inorganic sources. The $\delta^{13}C$ and $\delta^{34}S$ isotopic richness mainly reflect distinct origin of energy sources: values of ≤ 10‰ for organic matter of chemosynthetic origin and values ≥19‰ for that of photosynthetic origin including wood (e.g., Reid et al., 2013; Portail et al., 2016, 2018).

When estimated with $\delta^{13}C$ and $\delta^{15}N$, the isotopic richness was high on slates in hydrothermally active conditions but low when estimated with $\delta^{13}C$ and $\delta^{34}S$, whereas wood in periphery showed the opposite patterns. The high isotopic diversity values estimated with $\delta^{13}C$ and $\delta^{34}S$ in wood falls highlight the dual energy pathways, i.e., chemosynthetic and photosynthetic. On the contrary, on slates in hydrothermally active conditions, isotopic values highlight that the high diversity of resources

identified from δ¹³C and δ¹⁵N values was derived mainly from a single energy pathway, i.e., chemosynthesis. Thus, our results suggest that the diverse energy pathways in woods likely promote many different ecological strategies (high functional richness) allowing species to exploit very different resources in the same habitat and relaxing competition. The fact that wood substrata in hydrothermally active conditions exhibit high isotopic richness values estimated either with δ¹³C and δ¹⁵N or δ¹³C and δ³⁴S support the idea that the dual energy pathway boosts species and functional richness (Chapter 4).

For the smaller faunal fraction (<300 μm), the story was quite different. Overall, main meiofaunal groups, such as nematodes and copepods, are very poorly known in organic falls (Debenham et al., 2004; Zeppilli et al., 2015; Plum et al., 2017; Amon et al., 2017). Here, wood falls harbored assemblages with the lowest meiofaunal species and functional richness, highest abundances, and lowest J' of the experiment (Chapter 4). Previous similar experiments at Lucky Strike have reported similar patterns. Zeppilli et al. (2015) found that nematodes were more specious in slate than in wood substrata in three out of four different environments along a gradient of hydrothermal activity, including one site in periphery. Similarly, Plum et al. (2017) found that copepods were more specious or as specious in slate as in wood substrata in four out of five environments, including two peripheral habitats. Despite their lower species richness in wood substrata, nematode assemblages in the single periphery site studied in Zeppilli et al. (2015) and copepods in the two peripheral sites of Plum et al. (2016)

showed higher abundance. Results of wood falls and whale falls in the Pacific showed very similar patterns. This thesis was build on the previous experiments undertaken in our laboratory (Cuvelier et al., 2014; Zeppilli et al., 2015; Plum et al., 2016) and support the assumptions that organic falls are not suitable habitats for meiofauna in general. Some authors have hypothesized that the species rich and abundant macrofaunal assemblages inhabiting woods may negatively affect meiofaunal richness due to competition or predation (Debenham et al., 2004).

For larger fauna, the wood-fall assemblages were largely dominated by wood-fall specialists already reported in assemblages of the North-West and South-West Atlantic Ocean (Table 5.1). The taxa reported here thus have important implications for the poorly known wood fall biogeography. Wood fall studies have largely been focused on specific taxa or assemblages, especially microorganisms and wood-boring bivalves due to their functional roles (e.g., Kalenitchenko et al., 2016, 2018; Fagervold et al., 2014; Romano et al., 2014; Amon et al., 2015; Voight et al., 2015; Voight et al., 2019), and few have examined the whole communities (Bernardino et al., 2010; Gaudron et al., 2012; Cunha et al., 2013; Bienhold et al., 2013; Judge and Barry, 2016; Saeedi et al., 2019). Results of this thesis suggest that several wood-fall specialists may have a wide-basin and even inter-basin distribution, at least at the genus level, as similarly observed for whale falls (Sumida et al., 2016; Table 1).

Table 5.1. Selected species highlighting the relationships between vents, wood falls and other cognate habitats.

Species	Location in this study	Previously found at wood falls?	Found at other habitats	References
Lepetodrilus atlanticus	Slate/Active and Wood/Periphery	No	N Atlantic whale falls (genus)	Desbruyères et al. (2006); Hilario et al., (2015)
Protolira valvatoides	Slate/Active and Wood/Periphery	Yes (genus)	Whale falls	Desbruyeres et al. (2006) and references therein
Lurifax vitreus	Slate/Active, Wood/Periphery, Slate/Periphery	No		Desbruyeres et al. (2006)
Xylodiscula analoga	Slate/Active and Wood/Periphery	Yes	N Atlantic whale falls	Desbruyeres et al. (2006); Hilario et al. (2015)
Lirapex costellata	Slate/Active and Wood/Periphery	No		Desbruyeres et al. (2006)
Glycera tesselata	Slate/Active, Wood/Periphery and Slate/Periphery	Yes		Desbruyeres et al. (2006); Gaudron et al. (2012)
Prionospio unilamellata	Slate/Active and Wood/Periphery	No	N Atlantic whale falls	Desbruyeres et al. (2006); Hilario et al. (2015)
Laonice aseccata	Slate/Active and Wood/Periphery	No		Desbruyeres et al. (2006)
Ophryotrocha fabriae	Slate/Active and Wood/Periphery	Yes (genus)	Whale falls, cold seeps and vents	Smith and Baco (2003); Levin et al. (2016)
Luckia striki	Slate/Active, Wood/Periphery and Slate/Periphery	No		Desbruyeres et al. (2006)

Thomontocypris excussa	Vents, Wood/Periphery and Slate/Periphery	Yes (genus)		Desbruyeres et al. (2006)
Idas spp.	Wood/Periphery	Yes	Mediterranean, SW and N Atlantic Whale falls	Gaudron et al. (2012); Rodrigues et al. (2014); Hilario et al. (2015) ; Saeedi et al. (2019)
Xyloredo sp.	Wood/Periphery	Yes	Mediterranean, SW and N Atlantic	Gaudron et al. (2012); Voight et al. (2015); Saeedi et al. (2019)
Coccopigya spinigera	Wood/Periphery	Yes	N Atlantic wood falls	Jeffreys (1883); Gaudron et al. (2012)
Sirsoe sp.	Wood/Periphery	Yes	Pacific and SW Atlantic whale and wood falls, Caribbean vents	Sumida et al. (2016); Saeedi et al. (2019); Shimabukuro et al. (2019)
Pleijelius sp.	Wood/Periphery	Yes	SW Atlantic whale falls	Sumida et al. (2016); Saeedi et al. (2019); Shimabukuro et al. (2019)
Strepternos sp.	Wood/Periphery	Yes	NW and SW Atlantic whale falls and wood falls	Watson et al. (1991); Saeedi et al. (2019)
Capitella spp.	Slate/Active and Wood/Periphery	Yes	SW Atlantic whale falls and wood falls	Silva et al. (2016); Saeedi et al. (2019)

Research on organic falls has been largely driven by the stepping-stone hypothesis after the discovery of vent fauna in whale remains (Smith et al., 1989). This hypothesis states that attracted by the partial chemosynthetic environment in organic falls, some vent and cold-seep fauna may colonize them allowing their dispersion to newly opened habitats located far away (Smith et al., 2015). Despite not universal (e.g., Kiel, 2016), this hypothesis has proven to hold true for some fauna, especially polychaetes (Feldman et al., 1998; Vrijenhoek et al., 2010; Smith et al., 2003; Smith et al., 2015; Smith et al., 2017; Sumida et al., 2016; Saeedi et al., 2019; Shimabukuro et al., 2019). This hypothesis may also apply to chemosynthetic-symbiont-bearing mussels and clams that invaded the deep sea from shallow waters likely using wood falls (e.g., Distel et al., 2000; Duperon, 2010). This thesis directly tackles the ecological facet of this hypothesis. Indeed, we show that even a small 10 cm^3 wood may present a ~50% compositional overlap with assemblages of hydrothermally active vents in the absence of dispersal barriers (Chapter 4; Figure 5.3). Nevertheless, iconic Lucky Strike vent fauna, such as its main foundation species, the mussel *B. azoricus*, the abundant polychaete *Amphisamytha lutzi* and some gastropods species, among others (Sarrazin et al. 2015, Husson et al. 2017), were absent of wood substrata at inactive sites.

Certainly, organic fall assemblages have long been recognized to harbor a mix of specialists, chemosymbiotic taxa, sulfide generalists and sulfide tolerant background fauna (Smith and Baco, 2003; Bernardiono et al., 2010; Bienhold et al., 2013). However, few studies compared the community composition and overlap of

organic falls and background environment due to the lack of information about the geographical location of these organic falls (but see Cunha et al., 2010; Lundsten et al., 2010; Gaudron et al., 2012). This thesis also focuses on the overlap of wood falls with vent inactive peripheral assemblages (Chapter 3) and shows that they harbor up to ~60% of the taxa found on slate substrata in the periphery of vents (Figure 5.3). Thus, wood falls may offer suitable habitats, not only for some active vent species, but also for peripheral species. Based on niche overlap analyzes, we hypothesized that, as for biodiversity patterns, the different origins of the resources (chemosynthetic versus photosynthetic) drive the observed functional and isotopic space overlap observed between wood and both hydrothermally active and peripheral habitats.
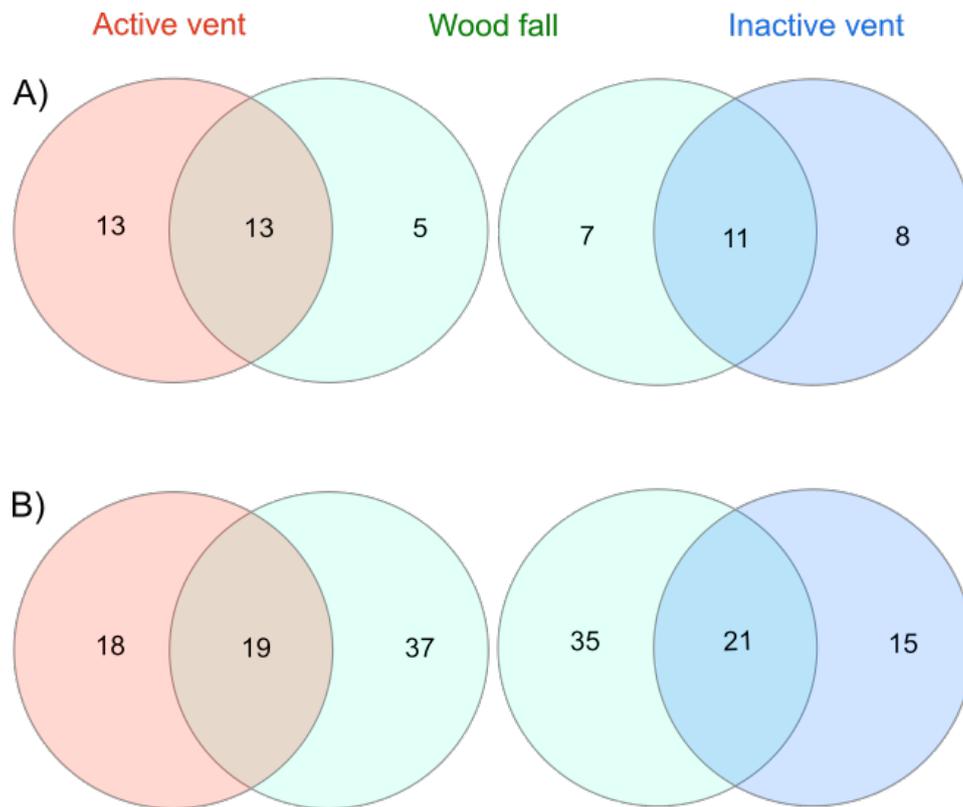
Figure 5.3. Venn diagram of shared and exclusive species found between slate substrata in hydrothermally active conditions (Active vent) and wood substrata in periphery (Wood fall) and between slate substrata in periphery (Periphery) wood substrata in periphery for A) <300 µm and B) >300 µm fauna. Approximately 50% of species of assemblages found on slates in hydrothermal active conditions were shared with wood falls for meio- (13 species) and macrofauna (19 species). Approximately 60 % of species found on slates in peripheral conditions were shared with wood falls for meio- (11 species) and macrofauna (21 species). Data derived from Chapter 4.

Perspectives

The findings and conclusions of this thesis pave the ground to future studies and represent a solid reference from where to derive ecological hypotheses to increase our understanding of chemosynthetic-based habitat ecology, deep-sea and community assembly in general. This thesis is based on the most extensive colonizing experiment

ever done at hydrothermal vents of the Atlantic Ocean. However, it was "restricted" to 4 different sites representing two main environments, i.e., hydrothermal active and peripheral sites, and two main habitats, vents and wood falls. It constitutes thus an appropriate experiment to compare biodiversity patterns in a dual fashion, hydrothermally active regimes (stressful and productive) and inactive peripheries (stable and unproductive), but more information is needed to characterize the finer scale relationship between species and functional richness and the different hydrothermal active regimes and microhabitats.

The productivity-stress-richness relationship in vents

Certainly, other hydrothermal active microhabitats should be studied with the same or similar approaches to the ones included in this thesis in order to complete the picture. For instance, high temperature anhydrite substrata on the Eiffel Tower is characterized by the almost absence of fauna, including *Bathymodiolus azoricus*, probably due to the extremely harsh environment and physical instability of the substrata (Cuvelier et al., 2009; Cuvelier et al., 2011; Cuvelier et al., 2014). On the contrary, colder microhabitats are colonized by small and medium sizes *B. azoricus* which harbor the richest assemblages within hydrothermally active habitats (Sarrazin et al., 2015; Husson et al., 2016). The two hydrothermally active sites studied in this thesis lay between these two vent extremes. I suggest that these anhydrite and colder microhabitats should be included in future studies as they are of main importance to

fully test the hypothesis related with the energy-stress-diversity framework applied and discussed in this thesis.

Although vents are one of the few habitats supporting local primary productivity in the deep-sea, the distribution of productivity rates along the hydrothermal vent gradient is not well understood (Le Bris et al., 2019). Knowledge is based on culture experiments in laboratories or energetic models (Le Bris et al., 2019). This is because primary producers at vents are microscopic and methods to properly sample and study them are not of easy implementation in the deep sea (Sievert and Vettriani, 2012). One of the most important conceptual contributions to vent ecology recently is the classification of chemosymbiotic foundation species as "holobionts" as corals are in reefs. Although primary productivity of free-living microorganisms should not be neglected, the biomass of holobionts may be considered a proxy for vent primary productivity as plant biomass is used in terrestrial ecology (Mittlebach et al., 2001). Due to the spatial distribution of foundations species, it may be hypothesized that productivity present a concave down relationship from most extreme to colder environments. This conceptual model is based on the trade-offs between the availability of chemically reduced compounds and oxygen (see thesis Introduction for a more detailed discussion). Some authors have already explored this approach (e.g., Husson et al., 2017) but results do not support theory. This may be due to the use of mean biomass values rather than total (Husson et al., 2017). Again, colonizing substrata, by providing a standardized surface area, would represent an ideal setting

for determining symbiotic species biomasses and relate them to environmental conditions as well as species and functional richness.

After the determination of primary productivity and its distribution, it would be of fundamental importance to assess the shape of the relationship between environmental conditions and both taxonomic and functional diversities. Studies in Mid-Atlantic Ridge and East Pacific Rise vents have reported an increase of species from extreme stressful active habitats to the colder end of the gradient (e.g., Gollner et al., 2015; Sarrazin et al., 2015). However, the exact shape of species richness and environment is not well determined and probably change between distinct faunal groups (Gollner et al., 2015; Zeppilli et al., 2015; Plum et al., 2016). Assuming that low or very low taxonomic and functional assemblages inhabit very extreme vent habitats, four main possible relationships between species, functional richness and environment within active vent regimes in the Atlantic can be hypothesized:

1. Species and functional richness increase linearly from anhydrite to colder *B. azoricus* assemblages (Figure 5.4A).

2. Species and functional richness present a concave-down relationship from anhydrite to colder *B. azoricus* assemblages (Figure 5.4C).

3. Species and functional diversity present different patterns from anhydrite to colder *B. azoricus* assemblages (Figure 5.4B and D).
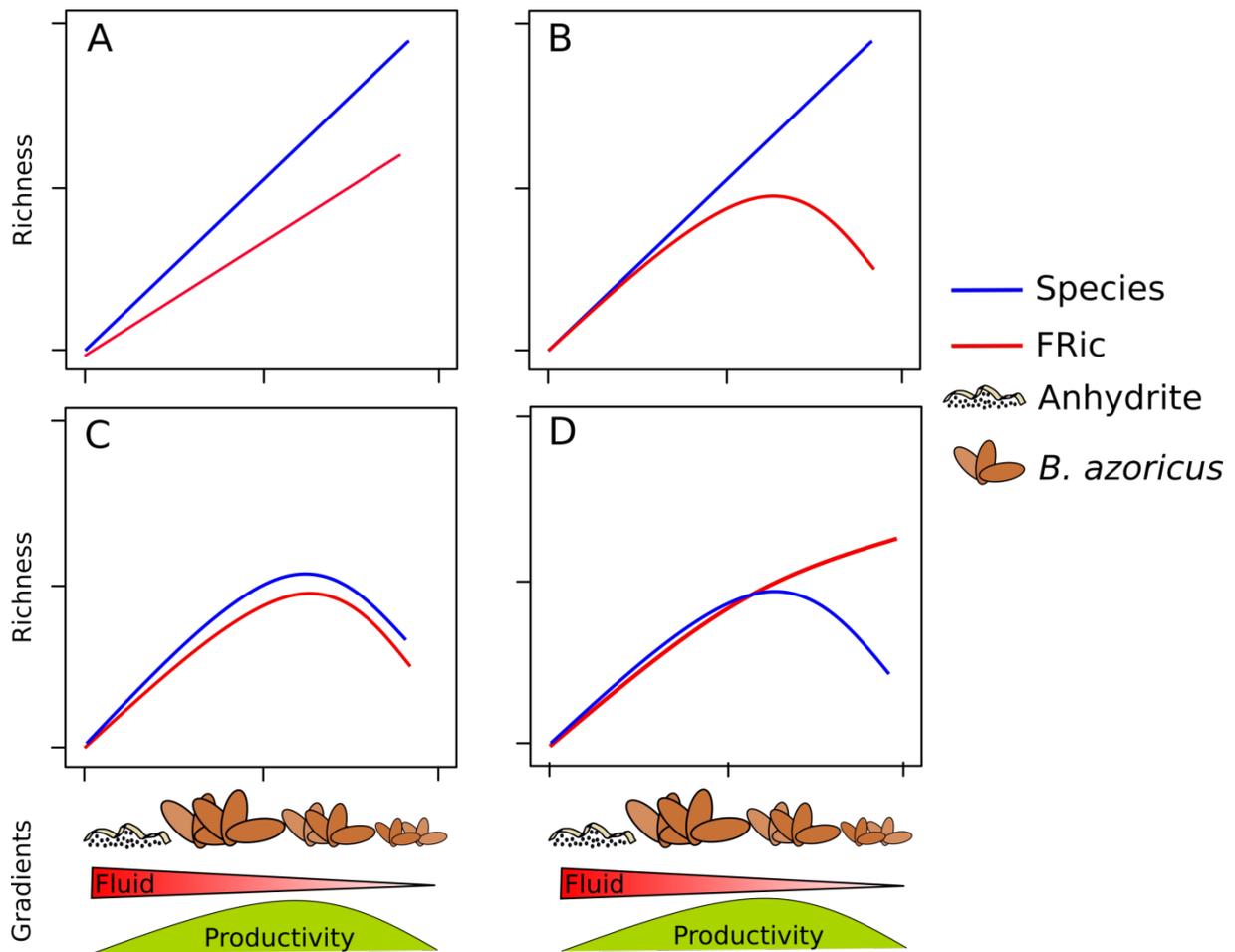
Figure 5.4. Hypothetical scenarios for patterns of species and functional richness along a hydrothermal vent gradient at the scale of microhabitats. A: Species and functional richness increase linearly from most stressful to least stressful habitats. B: Species but not functional richness increase linearly from most stressful to least stressful habitats. C: Species and functional richness present a concave-down relationship from most stressful to least stressful habitats. D: Functional but not species richness increase linearly from most stressful to least stressful habitats.

Why should we matter about the energy-stress-diversity relationship in hydrothermal vents? Indeed, this relationship has been one of the most debated questions in ecology and is still not well resolved (e.g., Mittlebach et al., 2001, see Introduction of this thesis). Although in the present study, only those theories related with smaller-scale processes have been superficially presented and discussed, others

relating to broad weather conditions and evolutionary history also participate in this large unresolved debate. Understanding the relationship and why it exists constitutes one of the most significant intellectual challenges to ecologists and biogeographers (Gaston et al., 2000). In practice, to understand the drivers and causes of biodiversity changes on Earth has also crucial implications for the management and protection of the ecosystems (e.g., Svensson et al., 2011).

This thesis showed that deep-sea vents may be considered as natural laboratories in which long-debated ecological questions may be tested. The advantage is that these tests may be done in relatively restricted areas characterized by steep gradients as in the intertidal zone. Vents are colonized by a restricted subset of species of a regional pool, highlighting the evolutionary history of these habitats. These species may present fine adaptations to very restricted microhabitats within active regimes (Luther III et al., 2001). Indeed, aside of the productivity and stress gradients, microhabitats at active sites exhibit contrasted physico-chemical conditions and extension at small spatial scales. These patterns may be considered analogous to those of climatic regions, elevation gradients or intertidal zones and their associated fauna on land and sea. To recognize such analogies may open the door to test for specific hypothesis related to the different facets of biodiversity, greatly expanding our knowledge of vent, deep-sea and ecology in general. Some of the most debated theories, some of them already tested in other deep-sea habitats (e.g., McClain et al.,

2016), are included in Table 5.2 with examples of derived predictions and specific tests for vent environments.

The experiment on which this thesis is based is not appropriate for testing these hypotheses because productivity was not measured and the limited spatial extent of the study. Nevertheless, it is possible to discuss some trends with the predictions derived from the different Productivity-Diversity hypotheses (Table 5.2). In order to discuss these trends I a) use the slate substrata (proxy of hydrothermal vent natural substrata), b) assume that as hypothesized in Figure 5.4 productivity peaks at intermediate hydrothermal regimes, c) focus at the scale of each site as in Chapter 2, i.e., not pooling the active with the intermediate and the periphery with the far site as in Chapter 3, and d) use the mean species richness (Table 3.2).

As found in other studies (e.g., McClain et al., 2016) patterns found in this thesis give mixed evidence for several theories. From the far to the active site there is an increase in species richness and abundance in meio- and macrofauna which is consistent with the predictions of both the More-individual hypothesis and the More-Specialization theory. The More-Specialization theory predicts that only some species increase abundance from less- to more-productive environments. As showed in Chapter 2 several species where found shared between hydrothermal active and inactive background habitats and these species where usually more abundant in active areas probably taking advantage of the higher productivity. Furthermore, as predicted

by the More-Specialization theory, different assemblages were founded in the different sites potentially matching different productivities. In this case, however, environmental stress caused by hydrothermal activity may have also played a role. The Resource competition theory predicts a positive humped relationship between species and productivity but it is especially difficult to discuss here due to the limited spatial extension of the study. The many feeding strategies and the high IRic found in hydrothermally active sites may support the Productive space hypothesis that states that there is an increase of species correlated with the number of trophic levels.

Table 5.2. Some hypotheses explaining different productivity-diversity relationships to be tested at vents, their predictions (for species and their abundances) and possible mechanisms. (1) The more-individual hypothesis states that higher energy contributes to increase diversity by sustaining more individuals; (2) The resource-competition theory departs from the assumption that no species is better in competing than others. Diversity would peak at intermediate productivities in areas where species from high and low-productive habitats coexist without excluding others; (3) The more-specialization theory states that at high productivities, resources may be abundant enough to allow a higher number of specialist species while preventing the exclusion of other species, whereas at low productivities, the resources are too scarce, lowering the number of specialist species; (4) The productive-space hypothesis departs from the assumption that energy-transfer efficiency is low between basal and higher trophic levels. A higher productivity promotes higher diversity by supporting more trophic levels; (5) the connectivity hypothesis assumes that if the exchange of species from high to low productivity habitats, or *vice-versa*, is high no diversity relationships may be observed. Predictions are largely, but not totally, based on McClain et al. (2016).

Hypothesis	References	Predictions		Specific tests
		Species (S)	**Abundance (N)**	
(1) More-individual hypothesis	Wright, 1983; Srivastava and Lawton, 1998; Storch et al., 2018	S increases matching productivity. S positively correlated with N.	N increases with S and productivity.	Significant relationship in N~productivity and S~N. A full model identifies N as best predictor variable for S.
(2) Resource competition theory	Tilman, 1982	Positive humped relationship of S partially decoupled from productivity.	No *a priori* prediction.	Significant quadratic relationship of S in space. MOS tests. Specific assemblages to each of the different productivity regimes.
(3) More-specialization theory	Schoener, 1976	S and rare species increase with productivity.	Only some species increase abundances from less-productive to more-productive microenvironments.	Significant relationship in rare species~productivity.
(4) Productive space hypothesis	Post, 2002	S increases with productivity. S positively correlated with n. trophic levels.	No *a priori* prediction.	Significant relationship in n. trophic levels~productivity and n. trophic levels~species. A full model identifies n. trophic levels as best predictor variable for S.
(5) Connectivity hypothesis	Chase and Ryberg, 2004	If only few shared species between active microhabitats, S increases match productivity; otherwise no clear pattern.	No *a priori* prediction.	Community compsition differes between microhabitats, i. e., few species are shared.

Other theories and hypotheses could be developed in order to add the effect of stress to the predictions. The Dynamic Equilibrium model of Huston (1979) and the vast literature derived (e.g., Svensson et al., 2011) may constitute a solid base. Furthermore, in future studies, the deployment of substrata dispatched across several edifices, each equipped with individual temperature probes would represent an ideal setting to test for such hypotheses. This would allow for a regression-like analysis instead of an Anova-like design as it is the case in this thesis. This new design would be appropriate to detect non-linear relationships potentially emerging with richness and productivity or other factors (Figure 5.4B, 5.4C and 5.4D). Also other approaches could help deriving functional traits more specifically related to energy or stress. Regarding stress, physiological and behavioral tests on species may bring important insights (e.g., Bates et al., 2010).

Ecology of vents

The hydrothermally active habitats included in this thesis were "restricted" to one single edifice. It has been long recognized that differences in physico-chemical factors even between edifices within the same vent field affect species composition contributing to increase β-diversity (reviewed in Mullineaux et al., 2017). Lucky Strike is not an exception (Desbruyères et al., 2001; Chavagnac et al., 2018). However, very few information is available for edifices others than Eiffel Tower at Lucky Strike. This vent field would represent an ideal site for future studies as it includes various edifices characterized by different chemistries (Chavagnac et al. 2018). Some work has already begun regarding species composition between different edifices of Lucky Strike but not

including functional richness (Sarrazin et al., *submitted*). The same logic can be extended to the scale of multiple fields within a region (e.g., Menez Gwen and Lucky Strike), basin (N Atlantic Ridge) and inter-basin (e.g., N Atlantic (slow-spreading center) vs East Pacific (fast spreading-center)). This thesis also highlights the poor knowledge of the fauna colonizing the peripheries of the vent habitats. More sampling is needed to extend experiments and to tests the proposed hypothesis. Future research should focus on determining the taxonomic and functional connectivity between peripheries at different vent sites, and between other adjacent habitats such as the large extensions of bare-mineral substrata along mid-ocean ridges and seamounts as well as soft-bottom habitats.

Although less used than the $\delta^{13}C$ and the $\delta^{15}N$, the analysis of the $\delta^{34}S$ yielded the most conclusive data on the export of organic matter of chemosynthetic origin to periphery habitats. This is because the values between photosynthetic- and chemosynthetic-derived organic matter greatly differ ($\leq$ 10‰ for organic matter of chemosynthetic origin and $\geq$19‰ for organic matter of photosynthetic origin (e.g., Reid et al., 2013; Portail et al., 2016, 2018). For the analysis of the $\delta^{34}S$ more tissue is needed than for the analyses of $\delta^{13}C$ and the $\delta^{15}N$, which is difficult to obtain for most size of most meio- and macrofauna. Nevertheless, the results of this thesis add to the body of literature showing that research aiming to study the "sphere of influence" of vents should include the analysis of $\delta^{34}S$ of at least some taxa.

A less clear aspect would be the temporal dynamics of vents, especially for those of the MAR. For instance, vents in the East Pacific show successional stages in which foundation species compete for resources, driving community structure and contributing to the increase of the regional richness (Mullineaux et al., 2017). It would be expected that functional diversity correlates to species dynamics, positively increasing functional β-diversity at the regional scale. Vents in the MAR only exhibit one foundation species and all of them belong to mussels of the genus *Bathymodilus*. Furthermore, the stability of Atlantic vents points towards a negligible role of succession in the increase of diversity at the field and regional scales. Thus, it is not known if successional dynamics, or similar processes, exists in Atlantic vents and so it remains difficult to speculate on the relationships of these processes with species and functional richness.

Biological interactions

Null models and the distribution of traits in our experiment strongly suggest that environment and not biological interactions is the main factor structuring colonizing assemblages in our substrata in hydrothermally inactive sites (periphery and far sites). (Chapter XXX and XXX). Null models showed that species were more similar between them than expected by chance suggesting that the low productivity and chemosynthetic fluid regime filters for certain species with similar ecological strategies. The higher diversity of traits in hydrothermally active sites suggest that despite the environmental stress imposed by the higher fluid fluxes productivity allow for many species to coexist in high abundances due to their different ecological strategies. These conclusions however

are based in the results obtained in a single time, i.e., after two years of colonization, and biological interactions ca not be excluded as important factors in structuring assemblages either in earlier nor in future stages. Furthermore, the null model chosen was specifically designed to test the filter effect of environment (Teixidó et al., 2018).

Engineer species in hydrothermal vents are known to increase species diversity by creating complex 3D habitats that provide new niches, shelter, and food (Governar, 2010). Similarly, in organic falls the ecosystem engineers also boost diversity by allowing new colonizers to access resources and adding physical complexity in the habitat (Alfaro –Lucas et al., 2017 and 2018). Currently, we are investigating the effect of xylophagids diversity and density in the species and functional diversity and the structure of communities (Romano et al., in prep.). A side of the engineering species, other processes such as dispersion may have had a deep effect on the colonization and thus on biodiversity in our experiment. Mulineaux et al. (2012) showed that the earlier colonization of vents by a species coming from afar after a catastrophic eruption change the succession of communities due to pioneer effects. In a previous experiment in the Eiffel Tower of one year of duration nematodes rapidly colonize substrata and were more diverse than in the present experiment (Zeppilli et al., 2015). The causes of these differences are unknown but it may be either due to pioneering effects or the effects or lately macrofaunal colonizers (competition, predation, etc.). Experiments specifically designed for testing the effects of biological interactions on vent biodiversity are needed

in order to fully disentangle the assembly of communities (e.g., Micheli et al., 2002; Mullineaux et al., 2003).

Relationships between vents, wood falls and other cognate habitats

This thesis constitutes a novel approach in the comparison of cognate chemosynthetic-based deep-sea habitats, namely vents and wood falls. Wood falls however are diverse and previous studies have shown that the type, physical structure and size of the wood deeply influence the composition and structure of the community (Judge and Barry, 2016; McClain et al., 2014; McClain et al., 2016).

Some wood types are denser than others and/or exhibit chemical defenses that affect not only the composition of the community but its longevity (Judge and Barry, 2016). Bigger wood log sizes, for instance, usually support more chemosynthetic primary productivity (e.g., McClain et al., 2016) and probably offer conditions that are more similar to those of vent and seep habitats than smaller logs (Cunha et al., 2010; Sumida et al., 2016). Wood and its colonization by microorganisms may create "sulfophilic" conditions relatively early (days) after its deposition on the seafloor (Kalmenitchenko et al., 2016; 2018). Colonization by wood-boring bivalves further accelerates the degradation of the wood. These organisms produce a "rain" of fecal pellets that boost chemosynthetic productivity rates (e.g., Bienhold et al., 2013, Voight et al., 2019). Thus, factors (type of wood, chemical defenses, etc) that may inhibit colonization by wood-boring bivalves may slow down chemosynthetic production. Similarly, "soft woods" may be degraded too

quick to allow the development of chemosynthetic production and thus colonization by vent and seep fauna.

Following the findings of this thesis, future studies should test the role of wood type and its implication for the stepping-stone hypothesis. It is known that small wood falls (as the ones in this thesis) may not support some iconic vent fauna due to the restricted chemosynthetic production. Testing if the increase of wood size creates a community more similar to the active vents than the one reported here or, on the contrary, create a more dissimilar community would be particularly interesting. Indeed, larger wood substrata may produce higher sulfide fluxes allowing the colonization of vent fauna not found in this study, such as *B. azoricus* or *A. lutzi*. On the contrary, they may not promote the colonization of more vent fauna but an increase in species abundances or colonization by other wood-fall specialists that would be only supported by larger wood falls.

This thesis, builts on the previous experiments undertaken by our laboratory, (Cuvelier et al., 2014; Zeppilli et al., 2015; Plum et al., 2016) and represents one of the few attempts to characterize meio- and macrofaunal groups in wood falls and thus constitutes a reference for future studies to compare community composition and derive ecological hypotheses. Future studies should also try elucidating why wood falls are more suitable for larger than smaller taxa. Moreover continuing on wood-size experiments, it would be interesting to test if the increase of wood size may support more meiofaunal species or,

alternatively, if larger wood substrata are as unsuitable habitats as smaller ones. The experimental exclusion of macrofauna, for instance with caged-experiments, could be an interesting approach and the first step to test if biological interactions or the nature of the habitat itself are the limiting factors for meiofaunal colonization. More broadly, the experimental approach of this thesis may be applied to other organic falls and other chemosynthetic habitats in general. Whales, or smaller carcasses, may be also deployed near vents. Many of the aspects discussed above affecting wood-fall colonization and its relationships with vents also concern carcasses (Smith et al., 2015; Sumida et al., 2016; Alfaro-Lucas et al., 2017, 2018) suggesting that many parameters and experiments may be tested and designed, respectively.

Concluding remarks

This thesis represents one of the few attempts to focus on vent ecology applying a contemporary community assemblage approach, including recently developed functional and β-diversity indices. Results of this thesis may have important implication for the understanding of vent and deep-sea ecosystems, the protection of vents from imminent industrial activities and long-debated questions about the relationships between vents and cognate habitats. More broadly, as suggested for shallow water vents (Hall-Spencer et al., 2008), this thesis highlights the potential of deep-sea vents as natural laboratories to test ecological hypotheses of global relevance.

General References

A

Adams, D., S. Arellano, and B. Govenar. 2012. Larval Dispersal: Vent Life in the Water Column. Oceanography 25:256–268.

Adler, P. B., J. HilleRisLambers, and J. M. Levine. 2007. A niche for neutrality. Ecology Letters 10:95–104.

Alfaro-Lucas, J., Shimabukuro, I. Ogata, Y. Fujiwara, and P. Sumida. 2018. Trophic structure and chemosynthesis contributions to heterotrophic fauna inhabiting an abyssal whale carcass. Marine Ecology Progress Series 596:1–12.

Alfaro-Lucas, J. M., M. Shimabukuro, G. D. Ferreira, H. Kitazato, Y. Fujiwara, and P. Sumida. 2017. Bone-eating Osedax worms (Annelida: Siboglinidae) regulate biodiversity of deep-sea whale-fall communities. Deep Sea Research Part II: Topical Studies in Oceanography.

Amon, D. J., A. Hilario, P. Arbizu, and C. R. Smith. 2016. Observations of organic falls from the abyssal Clarion-Clipperton Zone in the tropical eastern Pacific Ocean. Marine Biodiversity 47:311–321.

Amon, D. J., D. Sykes, F. Ahmed, J. T. Copley, K. M. Kemp, P. A. Tyler, C. M. Young, and A. G. Glover. 2015. Burrow forms, growth rates and feeding rates of wood-boring Xylophagaidae bivalves revealed by micro-computed tomography. Frontiers in Marine Science 2:10.

Anderson, M. J., T. O. Crist, J. M. Chase, M. Vellend, B. D. Inouye, A. L. Freestone, N. J. Sanders, H. V. Cornell, L. S. Comita, K. F. Davies, S. P. Harrison, N. J. Kraft, J. C. Stegen, and N. G. Swenson. 2011. Navigating the multiple meanings of β-diversity: a roadmap for the practicing ecologist. Ecology Letters 14:19–28.

Ardyna, M., L. Lacour, S. Sergi, F. d'Ovidio, J.-B. Sallée, M. Rembauville, S. Blain, A. Tagliabue, R. Schlitzer, C. Jeandel, K. Arrigo, and H. Claustre. 2019. Hydrothermal vents trigger massive phytoplankton blooms in the Southern Ocean. Nature Communications 10:2451.

Ashford, O. S., A. J. Kenny, C. R. Froján, M. B. Bonsall, T. Horton, A. Brandt, G. J. Bird, S. Gerken, and A. D. Rogers. 2018. Phylogenetic and functional evidence suggests that deep-

ocean ecosystems are highly sensitive to environmental change and direct human disturbance. Proceedings of the Royal Society B 285:20180923.

B

Baldrighi, E., D. Zeppilli, R. Crespin, P. Chauvaud, F. Pradillon, and J. Sarrazin. 2018. Colonization of synthetic sponges at the deep-sea Lucky Strike hydrothermal vent field (Mid-Atlantic Ridge): a first insight. Marine Biodiversity 48:89–103.

Baselga, A. 2010. Partitioning the turnover and nestedness components of beta diversity. Global Ecology and Biogeography 19:134–143.

Bates, A. E., R. W. Lee, V. Tunnicliffe, and M. D. Lamare. 2010. Deep-sea hydrothermal vent animals seek cool fluids in a highly variable thermal environment. Nature Communications 1:1014.

Bearhop, S., C. E. Ada, S. Waldron, R. A. Fuller, and H. MacLeod. 2004. Determining trophic niche width: a novel approach using stable isotope analysis. Journal of Animal Ecology 73:1007–1012.

Beaulieu, S. E., E. T. Baker, and C. R. German. 2015. Where are the undiscovered hydrothermal vents on oceanic spreading ridges? Deep Sea Research Part II: Topical Studies in Oceanography 121:202–212.

Bell, J. B., A. Aquilina, C. Woulds, A. G. Glover, C. T. Little, W. D. Reid, L. E. Hepburn, J. Newton, and R. A. Mills. 2016. Geochemistry, faunal composition and trophic structure in reducing sediments on the southwest South Georgia margin. Royal Society Open Science 3:160284.

Bell, J. B., W. D. Reid, D. A. Pearce, A. G. Glover, C. J. Sweeting, J. Newton, and C. Woulds. 2017. Hydrothermal activity lowers trophic diversity in Antarctic hydrothermal sediments. Biogeosciences 14:5705–5725.

Bergquist, D., J. Eckner, I. Urcuyo, E. Cordes, S. Hourdez, S. Macko, and C. Fisher. 2007. Using stable isotopes and quantitative community characteristics to determine a local hydrothermal vent food web. Marine Ecology Progress Series 330:49–65.

Bernardino, A. F., C. R. Smith, A. Baco, I. Altamira, and P. Sumida. 2010. Macrofaunal succession in sediments around kelp and wood falls in the deep NE Pacific and community overlap with other reducing habitats. Deep Sea Research Part I: Oceanographic Research Papers 57:708–723.

Bienhold, C., P. Ristova, F. Wenzhöfer, T. Dittmar, and A. Boetius. 2013. How Deep-Sea Wood Falls Sustain Chemosynthetic Life. PLoS ONE 8:e53590.

Boschen, R. E., A. A. Rowden, M. R. Clark, A. Pallentin, and J. Gardner. 2016. Seafloor massive sulfide deposits support unique megafaunal assemblages: Implications for seabed mining and conservation. Marine Environmental Research 115:78–88.

Brault, S., C. T. Stuart, M. C. Wagstaff, C. R. McClain, J. A. Allen, and M. A. Rex. 2013a. Contrasting patterns of α- and β-diversity in deep-sea bivalves of the eastern and western North Atlantic. Deep Sea Research Part II: Topical Studies in Oceanography 92:157–164.

Brault, S., C. T. Stuart, M. C. Wagstaff, and M. A. Rex. 2013b. Geographic evidence for source–sink dynamics in deep-sea neogastropods of the eastern North Atlantic: an approach using nested analysis. Global Ecology and Biogeography 22:433–439.

C

Cadotte, M. W., and C. M. Tucker. 2017. Should Environmental Filtering be Abandoned? Trends in Ecology & Evolution 32:429–437.

Campanyà-Llovet, N., P. Snelgrove, and C. C. Parrish. 2017. Rethinking the importance of food quality in marine benthic food webs. Progress in Oceanography 156:240–251.

Chapman, A. S., S. E. Beaulieu, A. Colaço, A. V. Gebruk, A. Hilario, T. C. Kihara, E. Ramirez-Llodra, J. Sarrazin, V. Tunnicliffe, D. J. Amon, M. C. Baker, R. E. Boschen-Rose, C. Chen, I. J.

Cooper, J. T. Copley, L. Corbari, E. E. Cordes, D. Cuvelier, S. Duperron, C. Preez, S. Gollner, T. Horton, S. Hourdez, E. M. Krylova, K. Linse, P. LokaBharathi, L. Marsh, M. Matabos, S. Mills, L. S. Mullineaux, H. Rapp, W. D. Reid, E. (Goroslavskaya), T. A. Thomas, S. Southgate, S. Stöhr, P. J. Turner, H. Watanabe, M. Yasuhara, and A. E. Bates. 2019. sFDvent: A global trait database for deep-sea hydrothermal-vent fauna. Global Ecology and Biogeography 28: 1538-1551.

Chapman, A. S., V. Tunnicliffe, and A. E. Bates. 2018. Both rare and common species make unique contributions to functional diversity in an ecosystem unaffected by human activities. Diversity and Distributions 24:568–578.

Chase, J. M. 2003. Community assembly: when should history matter? Oecologia 136:489–498.

Chase, J. M. 2010. Stochastic Community Assembly Causes Higher Biodiversity in More Productive Environments. Science 328:1388–1391.

Chase, J. M. 2014. Spatial scale resolves the niche versus neutral theory debate. Journal of Vegetation Science 25:319–322.

Chase, J. M., and W. A. Ryberg. 2004. Connectivity, scale-dependence, and the productivity–diversity relationship. Ecology Letters 7:676–683.

Chase, J. M., and M. A. Leibold. 2002. Spatial scale dictates the productivity–biodiversity relationship. Nature 416:427–430.

Chesson, P. 2000. Mechanisms of maintenance of species diversity. Annual Review of Ecology and Systematics 31:343–366.

Childress, J. and C. R. Fisher. 1992. The biology of hydrothermal vent animals: Physiology, biochemistry, and autotrophic symbioses. Oceanography and marine Biology 30:337:441.

Comtet, T., and D. Desbruyeres. 1998. Population structure and recruitment in mytilid bivalves from the Lucky Strike and Menez Gwen hydrothermal vent fields (37° 17′N and 37° 50′N on the Mid-Atlantic Ridge). Marine Ecology Progress Series 163:165–177.

Connell, J. H. 1978. Diversity in tropical rain forests and coral reefs. Science 199:1302–1310.

Coplen, T.B., 2010, Isotopic reference materials, in Beauchemin. D, and Matthews, D.E., eds., Elemental and Isotope Ratio Mass Spectrometry: The Encyclopedia of Mass Spectrometry, Gross, M. L. and Caprioli, R. M., series eds., Oxford, U.K., Elsevier, v. 5, p. 774-783.

Cordes, E. E., M. R. Cunha, J. Galéron, C. Mora, K. Roy, M. Sibuet, S. Gaever, A. Vanreusel, and L. A. Levin. 2010. The influence of geological, geochemical, and biogenic habitat heterogeneity on seep biodiversity. Marine Ecology 31:51–65.

Corliss et al., 1979. Submarine Thermal Springs on the Galápagos Rift. Science 203: 1073-1083.

Cucherousset, J., and S. Villéger. 2015. Quantifying the multiple facets of isotopic diversity: New metrics for stable isotope ecology. Ecological Indicators 56:152–160.

Cunha, M. R., F. L. Matos, L. Génio, A. Hilário, C. J. Moura, A. Ravara, and C. F. Rodrigues. 2013. Are Organic Falls Bridging Reduced Environments in the Deep Sea? Results from Colonization Experiments in the Gulf of Cádiz. PLoS ONE 8:e76688.

Cuvelier, D., J. Beesau, V. N. Ivanenko, D. Zeppilli, P.-M. Sarradin, and J. Sarrazin. 2014. First insights into macro- and meiofaunal colonisation patterns on paired wood/slate substrata at Atlantic deep-sea hydrothermal vents. Deep Sea Research Part I: Oceanographic Research Papers 87:70–81.

Cuvelier, D., P. Sarradin, J. Sarrazin, A. Colaço, J. T. Copley, D. Desbruyères, A. G. Glover, R. Santos, and P. A. Tyler. 2011a. Hydrothermal faunal assemblages and habitat characterisation at the Eiffel Tower edifice (Lucky Strike, Mid-Atlantic Ridge). Marine Ecology 32:243–255.

Cuvelier, D., J. Sarrazin, A. Colaço, J. Copley, D. Desbruyères, A. G. Glover, P. Tyler, and R. Santos. 2009. Distribution and spatial variation of hydrothermal faunal assemblages at Lucky Strike (Mid-Atlantic Ridge) revealed by high-resolution video image analysis. Deep Sea Research Part I: Oceanographic Research Papers 56:2026–2040.

Cuvelier, D., J. Sarrazin, A. Colaço, J. T. Copley, A. G. Glover, P. A. Tyler, R. Santos, and D. Desbruyères. 2011b. Community dynamics over 14 years at the Eiffel Tower hydrothermal edifice on the Mid-Atlantic Ridge. Limnology and Oceanography 56:1624–1640.

D

Danovaro, R., P. Snelgrove, and P. Tyler. 2014. Challenging the paradigms of deep-sea ecology. Trends in Ecology & Evolution 29:465–475.

Dayton, P., K., Hessler, R., R. 1972. The role of biological disturbance in maintaining diversity in the deep sea. DeepSea Research 19:199–208.

Debenham, N. J., P. J. D. Lambshead, T. J. Ferrero, and C. R. Smith. 2004. The impact of whale falls on nematode abundance in the deep sea. Deep Sea Research Part I: Oceanographic Research Papers 51:701–706.

De Busserolles, F., J. Sarrazin, O. Gauthier, Y. Gélinas, M. C. Fabri, P. M. Sarradin, and D. Desbruyères. 2009. Are spatial variations in the diets of hydrothermal fauna linked to local environmental conditions? Deep Sea Research Part II: Topical Studies in Oceanography 56:1649–1664.

Desbruyères, D., Segonzac, M., Bright M. 2006. Handbook of deep-sea hydrothermal vent fauna. Linz, Austria: Biologiezentrum der Oberösterreichischen Landesmuseen. 544 p.

Desbruyères, D., M. Biscoito, J.-C. Caprais, A. Colaço, T. Comtet, P. Crassous, Y. Fouquet, A. Khripounoff, L. N. Bris, K. Olu, R. Riso, P.-M. Sarradin, gonzac, and A. Vangriesheim. 2001. Variations in deep-sea hydrothermal vent communities on the Mid-Atlantic Ridge near the Azores plateau. Deep Sea Research Part I: Oceanographic Research Papers 48:1325–1346.

Didham, R. K., C. H. Watts, and D. A. Norton. 2005. Are systems with strong underlying abiotic regimes more likely to exhibit alternative stable states? Oikos 110:409–416.

Distel, D., L., A. R. Baco, E. Chuang, W. Morrill, C. Cavanaugh, and C. R. Smith. 2000. Marine ecology: Do mussels take wooden steps to deep-sea vents? Nature 403:725–726.

Dittel, A. I., Perovich, G., and Epifanio, C. E. (2008). Biology of the vent crab *Bythograea thermydron*: a brief review. Journal of Shellfish Research 27:63–77.

Du Preez, C., and C. R. Fisher. 2018. Long-Term Stability of Back-Arc Basin Hydrothermal Vents. Frontiers in Marine Science 5:54.

Durden, J., B. J. Bett, D. Jones, V. Huvenne, and H. A. Ruhl. 2015. Abyssal hills – hidden source of increased habitat heterogeneity, benthic megafaunal biomass and diversity in the deep sea. Progress in Oceanography 137:209–218.

E

Erickson, K. L., S. A. Macko, and C. L. Dover. 2009. Evidence for a chemoautotrophically based food web at inactive hydrothermal vents (Manus Basin). Deep Sea Research Part II: Topical Studies in Oceanography 56:1577–1585.

F

Fabricius, K., G. De'ath, S. Noonan, and S. Uthicke. 2014. Ecological effects of ocean acidification and habitat complexity on reef-associated macroinvertebrate communities. Proceedings of the Royal Society B: Biological Sciences 281:20132479.

Fagervold, S. K., P. E. Galand, M. Zbinden, F. Gaill, P. Lebaron, and C. Palacios. 2012. Sunken woods on the ocean floor provide diverse specialized habitats for microorganisms. FEMS 82:616–628.

Feldman, R., Tank, Black, A. Baco, C. Smith, and R. Vrijenhoek. 1998. Vestimentiferan on a Whale Fall. The Biological Bulletin 194:116–119.

Fujiwara, Y., M. Kawato, T. Yamamoto, T. Yamanaka, W. Sato-Okoshi, C. Noda, S. Tsuchida, T. Komai, S. Cubelio, T. Sasaki, K. Jacobsen, K. Kubokawa, K. Fujikura, T. Maruyama, Y. Furushima, K. Okoshi, H. Miyake, M. Miyazaki, Y. Nogi, A. Yatabe, and T. Okutani. 2007.

Three-year investigations into sperm whale-fall ecosystems in Japan. Marine Ecology 28:219–232.

Fukami, T. 2012. Historical Contingency in Community Assembly: Integrating Niches, Species Pools, and Priority Effects. Annual Review of Ecology, Evolution, and Systematics 46:1–23.

G

Garrard, S. L., C. M. Gambi, B. ipione, F. P. Patti, M. Lorenti, V. Zupo, D. M. Paterson, and C. M. Buia. 2014. Indirect effects may buffer negative responses of seagrass invertebrate communities to ocean acidification. Journal of Experimental Marine Biology and Ecology 461:31–38.

Gaston, K. J. 2000. Global patterns in biodiversity. Nature 405:220–227.

Gaudron, F. Pradillon, M. Pailleret, S. Duperron, L. N. Bris, and F. Gaill. 2010a. Colonization of organic substrates deployed in deep-sea reducing habitats by symbiotic species and associated fauna. Marine Environmental Research 70:1–12.

Gauthier, O., J. Sarrazin, D. Desbruyeres, D. 2010. Measure and mismeasure of species diversity in deep-sea chemosynthetic communities. Marine Ecology Progress Series 402:285-302.

Gerdes, K. H., M. P. Arbizu, S. Martin, R. Freitag, U. Schwarz-Schampera, A. Brandt, and T. C. Kihara. 2019. Megabenthic assemblages at the southern Central Indian Ridge: Spatial segregation of inactive hydrothermal vents from active-, periphery- and non-vent sites. Marine Environmental Research:104776.

German, C. R., E. Ramirez-Llodra, M. C. Baker, and P. A. Tyler. 2011. Deep-Water Chemosynthetic Ecosystem Research during the Census of Marine Life Decade and Beyond: A Proposed Deep-Ocean Road Map. PLoS ONE 6:e23259.

Gillman, L. N., and S. D. Wright. 2010. Mega mistakes in meta-analyses: devil in the detail. Ecology 91:2550–2.

Girguis, P. R., and R. W. Lee. 2006. Thermal Preference and Tolerance of Alvinellids. Science 312:231–231.

Goffredi, S. K., S. Johnson, V. Tunnicliffe, D. Caress, D. Clague, E. Escobar, L. Lundsten, J. B. Paduan, G. Rouse, D. L. Salcedo, L. A. Soto, R. Spelz-Madero, R. Zierenberg, and R. Vrijenhoek. 2017. Hydrothermal vent fields discovered in the southern Gulf of California clarify role of habitat in augmenting regional diversity. Proceedings of the Royal Society B 284:20170817.

Gollner, S., B. Govenar, P. Arbizu, S. Mills, N. Bris, M. Weinbauer, T. ank, and M. Bright. 2015a. Differences in recovery between deep-sea hydrothermal vent and vent-proximate communities after a volcanic eruption. Deep Sea Research Part I: Oceanographic Research Papers 106:167–182.

Gollner, S., B. Govenar, C. R. Fisher, and M. Bright. 2015b. Size matters at deep-sea hydrothermal vents: different diversity and habitat fidelity patterns of meio- and macrofauna. Marine ecology progress series 520:57–66.

Gollner, S., B. Riemer, P. Arbizu, N. Bris, and M. Bright. 2010. Diversity of Meiofauna from the 9°50′N East Pacific Rise across a Gradient of Hydrothermal Fluid Emissions. PLoS ONE 5:e12321.

Govenar, B. 2010. Shaping Vent and Seep Communities: Habitat Provision and Modification by Foundation Species. The Vent and Seep Biota, Aspects from Microbes to Ecosystems. Springer 33:403–432.

Govenar, B. 2012. Energy Transfer Through Food Webs at Hydrothermal Vents: Linking the Lithosphere to the Biosphere. Oceanography 25:246–255.

Govenar, B., L. N. Bris, S. Gollner, J. Glanville, Aerghis, S. Hourdez, and C. Fisher. 2005. Epifaunal community structure associated with Riftia pachyptila aggregations in chemically different hydrothermal vent habitats. Marine Ecology Progress Series 305:67–77.

Govenar, B., and C. R. Fisher. 2007. Experimental evidence of habitat provision by aggregations of Riftia pachyptila at hydrothermal vents on the East Pacific Rise. Marine Ecology 28:3–14.

Govenar, B., C. R. Fisher, and T. ank. 2015. Variation in the diets of hydrothermal vent gastropods. Deep Sea Research Part II: Topical Studies in Oceanography 121:193–201.

Grassle, J. F., Sanders, H. L. 1973. Life histories and the role of disturbance. Deep-Sea Research, 34:313–341.

H

Hall-Spencer, J. M., R. Rodolfo-Metalpa, S. Martin, E. Ransome, M. Fine, S. M. Turner, S. J. Rowley, D. Tedesco, and M.-C. Buia. 2008. Volcanic carbon dioxide vents show ecosystem effects of ocean acidification. Nature 454:96.

Hardin, G. 1960. The competitive exclusion principle. Science 131:1292–1297.

Hedges, J. I., and J. H. Stern. 1984. Carbon and nitrogen determination of carbonate-containing solids. Limnology and Oceanography 29:657-663.

Hessler, R. R., Sanders H. L. 1967. Faunal diversity in the deep sea. Deep-Sea Research, 14:65–78.

Hilario, A., M. R. Cunha, L. Génio, A. Marçal, A. Ravara, C. F. Rodrigues, and H. Wiklund. 2015. First clues on the ecology of whale falls in the deep Atlantic Ocean: results from an experiment using cow carcasses. Marine Ecology 36:82–90.

HilleRisLambers, J., P. B. Adler, W. S. Harpole, J. M. Levine, and M. M. Mayfield. 2012. Rethinking Community Assembly through the Lens of Coexistence Theory. Ecology, Evolution, and Systematics 43:227–248.

Hubbell, S. P. 2005. Neutral theory in community ecology and the hypothesis of functional equivalence. Functional Ecology 19:166–172.

Husson, B., P.-M. Sarradin, D. Zeppilli, and J. Sarrazin. 2017. Picturing thermal niches and biomass of hydrothermal vent species. Deep Sea Research Part II: Topical Studies in Oceanography 137:6–25.

Huston, M. A. 1979 A general hypothesis of species diversity. American Naturalist 113:81–101.

J

Johnson, K. S., J. J. Childress, C. L. Beehler, and C. M. Sakamoto. 1994. Biogeochemistry of hydrothermal vent mussel communities: the deep-sea analogue to the intertidal zone. Deep Sea Research Part I: Oceanographic Research Papers 41:993–1011.

Johnson, K. S., J. J. Childress, R. R. Hessler, C. kamoto-Arnold, and C. L. Beehler. 1988. Chemical and biological interactions in the Rose Garden hydrothermal vent field, Galapagos spreading center. Deep Sea Research Part A. Oceanographic Research Papers 35:1723–1744.

Johnson K., S., Beehler, C., L., Sakamotoarnold C., M., Childress, J., J. 1986. In situ measurements of chemical distributions in a deep-sea hydrothermal vent field. Science 231:1139–1141.

Jones, W. J., Y.-J. Won, P. A. Y. Maas, P. J. Smith, R. A. Lutz, and R. C. Vrijenhoek. 2006. Evolution of habitat use by deep-sea mussels. Marine Biology 148:841–851.

Judge, J., and J. P. Barry. 2016. Macroinvertebrate community assembly on deep-sea wood falls in Monterey Bay is strongly influenced by wood type. Ecology 97:3031–3043.

Jumars, P., A., Dorgan, K., M., Lindsay, S., M. 2015. Diet of Worms Emended: An Update of Polychaete Feeding Guilds. Annu Rev Mar Sci 7:497–520.

K

Kalenitchenko, D., M. Dupraz, N. Bris, C. Petetin, C. Rose, N. J. West, and P. E. Galand. 2016. Ecological succession leads to chemosynthesis in mats colonizing wood in sea water. The ISME Journal 10:2246.

Kalenitchenko, D., E. Péru, C. L. Pereira, C. Petetin, P. Galand, and L. N. Bris. 2018. The early conversion of deep-sea wood falls into chemosynthetic hotspots revealed by in situ monitoring. Scientific Reports 8:907.

Kark, S., and B. J. van Rensburg. 2013. Ecotones: Marginal or Central Areas of Transition? Israel Journal of Ecology & Evolution 52:29–53.

Kelly, N., and A. Metaxas. 2008. Diversity of invertebrate colonists on simple and complex substrates at hydrothermal vents on the Juan de Fuca Ridge. Aquatic Biology 3:271–281.

Kelly, N., A. Metaxas, and D. Butterfield. 2007. Spatial and temporal patterns of colonization by deep-sea hydrothermal vent invertebrates on the Juan de Fuca Ridge, NE Pacific. Aquatic Biology 1:1–16.

Kiel, S. 2016. A biogeographic network reveals evolutionary links between deep-sea hydrothermal vent and methane seep faunas. Proc. R. Soc. B 283:20162337.

Kiel, S. 2017. Reply to Smith et al.: Network analysis reveals connectivity patterns in the continuum of reducing ecosystems. Proceedings of the Royal Society B 284:20171644.

Kraft, N. J., P. ler, O. Godoy, E. C. James, S. Fuller, and J. M. Levine. 2015. Community assembly, coexistence and the environmental filtering metaphor. Functional Ecology 29:592–599.

Kroeker, K. J., F. Micheli, M. Gambi, and T. R. Martz. 2011. Divergent ecosystem responses within a benthic marine community to ocean acidification. Proceedings of the National Academy of Sciences 108:14515–14520.

L

Lawton, J. H. 1999. Are There General Laws in Ecology? Oikos 84:177.

Layman, C. A., M. S. Araujo, R. Boucek, C. M. Hammerschlag-Peyer, E. Harrison, Z. R. Jud, P. Matich, A. E. Rosenblatt, J. J. Vaudo, L. A. Yeager, D. M. Post, and S. Bearhop. 2012. Applying stable isotopes to examine food-web structure: an overview of analytical tools. Biological Reviews 87:545–562.

Layman, C. A., A. D. Arrington, C. G. Montaña, and D. M. Post. 2007. Can stable isotope ratios provide for community-wide measures of trophic structure? Ecology 88:42–48.

Le Bris, N., M. Yücel, A. Das, S. evert, P. LokaBharathi, and P. R. Girguis. 2019. Hydrothermal Energy Transfer and Organic Carbon Production at the Deep Seafloor. Frontiers in Marine Science 5:531.

Leduc, D., A. Rowden, D. Bowden, S. Nodder, P. Probert, C. Pilditch, G. Duineveld, and R. Witbaard. 2012. Nematode beta diversity on the continental slope of New Zealand: spatial patterns and environmental drivers. Marine Ecology Progress Series 454:37–52.

Lee, R., and J. Childress. 1996. Inorganic N Assimilation and Ammonium Pools in a Deep-Sea Mussel Containing Methanotrophic Endosymbionts. The Biological bulletin 190:373–384.

Legendre, P. 2014. Interpreting the replacement and richness difference components of beta diversity. Global Ecology and Biogeography 23:1324–1334.

Legendre, P., and M. Cáceres. 2013. Beta diversity as the variance of community data: dissimilarity coefficients and partitioning. Ecology Letters 16:951–963.

Lenihan, H., S. Mills, L. Mullineaux, C. Peterson, C. Fisher, and F. Micheli. 2008a. Biotic interactions at hydrothermal vents: Recruitment inhibition by the mussel Bathymodiolus thermophilus. Deep Sea Research Part I: Oceanographic Research Papers 55:1707–1717.

Levesque, C., K. S. Juniper, and H. Limén. 2006. Spatial organization of food webs along habitat gradients at deep-sea hydrothermal vents on Axial Volcano, Northeast Pacific. Deep Sea Research Part I: Oceanographic Research Papers 53:726–739.

Levin, L. A., A. R. Baco, D. A. Bowden, A. Colaco, E. E. Cordes, M. R. Cunha, A. W. Demopoulos, J. Gobin, B. M. Grupe, J. Le, A. Metaxas, A. N. Netburn, G. W. Rouse, A. R. Thurber, V. Tunnicliffe, C. Dover, A. Vanreusel, and L. Watling. 2016. Hydrothermal Vents and Methane Seeps: Rethinking the Sphere of Influence. Frontiers in Marine Science 3:72.

Levin, L. A., V. J. Orphan, G. W. Rouse, A. E. Rathburn, W. Ussler, G. S. Cook, S. K. Goffredi, E. M. Perez, A. Waren, B. M. Grupe, G. Chadwick, and B. Strickrott. 2012. A hydrothermal seep on the Costa Rica margin: middle ground in a continuum of reducing ecosystems. Proc. R. Soc. B 279:2580–2588.

Limen, H., C. Levesque, S.K. Juniper. 2007. POM in macro-/meiofaunal food webs associated with three flow regimes at deep-sea hydrothermal vents on Axial Volcano, Juan de Fuca Ridge. Marine Biology 153:129–139.

Lorion, J., S. Kiel, B. Faure, M. Kawato, S. Y. Ho, B. Marshall, S. Tsuchida, J.-I. Miyazaki, and Y. Fujiwara. 2013. Adaptive radiation of chemosymbiotic deep-sea mussels. Proc. R. Soc. B 280:20131243.

Lundsten, L., C. K. Paull, K. L. Schlining, M. McGann, and W. Ussler. 2010a. Biological characterization of a whale-fall near Vancouver Island, British Columbia, Canada. Deep Sea Research Part I: Oceanographic Research Papers 57:918–922.

Lundsten, L., K. L. Schlining, K. Frasier, S. B. Johnson, L. A. Kuhnz, J. Harvey, G. Clague, and R. C. Vrijenhoek. 2010b. Time-series analysis of six whale-fall communities in Monterey Canyon, California, USA. Deep Sea Research Part I: Oceanographic Research Papers 57:1573–1584.

Luther III, G. W., T. F. Rozan, M. Taillefert, D. B. Nuzzio, C. Meo, T. ank, R. A. Lutz, and C. S. Cary. 2001. Chemical speciation drives hydrothermal vent ecology. Nature 410:813.

M

Marcus, J., V. Tunnicliffe, and D. A. Butterfield. 2009. Post-eruption succession of macrofaunal communities at diffuse flow hydrothermal vents on Axial Volcano, Juan de Fuca Ridge, Northeast Pacific. Deep Sea Research Part II: Topical Studies in Oceanography 56:1586–1598.

Marsh, A. G., L. S. Mullineaux, C. M. Young, and D. T. Manahan. 2001. Larval dispersal potential of the tubeworm Riftia pachyptila at deep-sea hydrothermal vents. Nature 411:77–80.

Marsh, L., J. T. Copley, V. A. Huvenne, K. Linse, W. D. Reid, A. D. Rogers, C. J. Sweeting, and P. A. Tyler. 2012. Microdistribution of Faunal Assemblages at Deep-Sea Hydrothermal Vents in the Southern Ocean. PLoS ONE 7:e48348.

Mason, N., F. Bello, D. Mouillot, S. Pavoine, and S. Dray. 2013. A guide for using functional diversity indices to reveal changes in assembly processes along ecological gradients. Journal of Vegetation Science 24:794–806.

McCallum, A. W., S. Woolley, M. Błażewicz-Paszkowycz, J. Browne, S. Gerken, R. Kloser, G. C. Poore, D. Staples, A. Syme, J. Taylor, G. Walker-Smith, A. Williams, and R. S. Wilson. 2015. Productivity enhances benthic species richness along an oligotrophic Indian Ocean continental margin. Global Ecology and Biogeography 24:462–471.

McClain, C., and J. Barry. 2014. Beta-diversity on deep-sea wood falls reflects gradients in energy availability. Biology letters 10:20140129.

McClain, C. R., J. P. Barry, D. Eernisse, T. Horton, J. Judge, K. Kakui, C. Mah, and A. Warén. 2016. Multiple processes generate productivity–diversity relationships in experimental wood-fall communities. Ecology 97:885–898.

McClain, C. R., J. P. Barry, and T. J. Webb. 2018a. Increased energy differentially increases richness and abundance of optimal body sizes in deep-sea wood falls. Ecology 99:184–195.

McClain, C. R., C. Nunnally, A. S. Chapman, and J. P. Barry. 2018b. Energetic increases lead to niche packing in deep-sea wood falls. Biology Letters 14:20180294.

McClain, C. R., and M. A. Rex. 2015. Toward a Conceptual Understanding of β-Diversity in the Deep-Sea Benthos. Annual Review of Ecology, Evolution, and Systematics 46:623–642.

McClain, C. R., and T. A. Schlacher. 2015. On some hypotheses of diversity of animal life at great depths on the sea floor. Marine Ecology 36:849–872.

McGill, B. J., B. J. Enquist, E. Weiher, and M. Westoby. 2006. Rebuilding community ecology from functional traits. Trends in Ecology & Evolution 21:178–185.

Micheli, F., C. H. Peterson, L. S. Mullineaux, C. R. Fisher, S. W. Mills, G. Sancho, G. A. Johnson, and H. S. Lenihan. 2002. Predation structures communities at deep-sea hydrothermal vents. Ecological Monographs 72:365–382.

Miljutin, D., M., Miljutina, M., A., Arbizu, P., M., Galeron, J. 2011. Deep-sea nematode assemblage has not recovered 26 years after experimental mining of polymetallic nodules (ClarionClipperton Fracture Zone, Tropical Eastern Pacific). DeepSea Research Part I: Oceanographic Research Papers 58:885– 897.

Mittelbach, G. G., and D. W. Schemske. 2015. Ecological and evolutionary perspectives on community assembly. Trends in Ecology & Evolution 30:241–247.

Mittelbach, G. G., C. F. Steiner, S. heiner, K. L. Gross, H. L. Reynolds, R. B. Waide, M. R. Willig, S. I. Dodson, and L. Gough. 2001. What is the observed relationship between species richness and productivity? Ecology 82:2381–2396.

Miyazaki, J.-I., L. de Martins, Y. Fujita, H. Matsumoto, and Y. Fujiwara. 2010. Evolutionary Process of Deep-Sea Bathymodiolus Mussels. PLoS ONE 5:e10363.

Moalic, Y., D. Desbruyères, C. arte, A. F. Rozenfeld, C. Bachraty, and S. Arnaud-Haond. 2012. Biogeography Revisited with Network Theory: Retracing the History of Hydrothermal Vent Communities. Systematic Biology 61:127–137.

Montagna, P. A., J. G. Baguley, C. Hsiang, and M. G. Reuscher. 2017. Comparison of sampling methods for deep-sea infauna. Limnology and Oceanography: Methods 15:166–183.

Mouchet, M. A., S. Villéger, N. W. Mason, and D. Mouillot. 2010. Functional diversity measures: an overview of their redundancy and their ability to discriminate community assembly rules. Functional Ecology 24:867–876.

Mouillot, D., N. Graham, S. Villéger, N. Mason, and D. R. Bellwood. 2013. A functional approach reveals community responses to disturbances. Trends in Ecology & Evolution 28:167–177.

Mullineaux, L. S., D. K. Adams, S. W. Mills, and S. E. Beaulieu. 2010. Larvae from afar colonize deep-sea hydrothermal vents after a catastrophic eruption. Proceedings of the National Academy of Sciences 107:7829–7834.

Mullineaux, L. S., N. Bris, S. W. Mills, P. Henri, S. R. Bayer, R. G. Secrist, and N. Siu. 2012. Detecting the Influence of Initial Pioneers on Succession at Deep-Sea Vents. PLoS ONE 7:e50015.

Mullineaux, L. S., A. Metaxas, S. E. Beaulieu, M. Bright, S. Gollner, B. M. Grupe, S. Herrera, J. B. Kellner, L. A. Levin, S. Mitarai, M. G. Neubert, A. M. Thurnherr, V. Tunnicliffe, H. K. Watanabe, and Y.-J. Won. 2018. Exploring the Ecology of Deep-Sea Hydrothermal Vents in a Metacommunity Framework. Frontiers in Marine Science 5:49.

Mullineaux, L. S., S. W. Mills, and E. Goldman. 1998. Recruitment variation during a pilot colonization study of hydrothermal vents (9°50′N, East Pacific Rise). Deep Sea Research Part II: Topical Studies in Oceanography 45:441–464.

Mullineaux, L. S., C. H. Peterson, F. Micheli, and S. W. Mills. 2003. Successional mechanism varies along a gradient in hydrothermal fluid flux at deep-sea vents. Ecological Monographs 73:523–542.

Murcia, C. 1995. Edge effects in fragmented forests: implications for conservation. Trends in Ecology & Evolution 10:58–62.

Myers, J. A., J. M. Chase, I. Jiménez, P. M. Jørgensen, A. Araujo-Murakami, N. Paniagua-Zambrana, and R. Seidel. 2013. Beta-diversity in temperate and tropical forests reflects dissimilar mechanisms of community assembly. Ecology Letters 16:151–157.

N

Newsome, S. D., C. del Rio, S. Bearhop, and D. L. Phillips. 2007. A niche for isotopic ecology. Frontiers in Ecology and the Environment 5:429–436.

P

Pärtel, M., K. Zobel, L. Laanisto, R. Szava-Kovats, and M. Zobel. 2010. The productivity–diversity relationship: varying aims and approaches. Ecology 91:2565–2567.

Perronne, R., F. Munoz, B. Borgy, X. Reboud, and S. Gaba. 2017. How to design trait-based analyses of community assembly mechanisms: Insights and guidelines from a literature review. Perspectives in Plant Ecology, Evolution and Systematics 25:29–44.

Petchey, O. L., and K. J. Gaston. 2006. Functional diversity: back to basics and looking forward. Ecology Letters 9:741–758.

Plum, C., F. Pradillon, Y. Fujiwara, and J. Sarrazin. 2017. Copepod colonization of organic and inorganic substrata at a deep-sea hydrothermal vent site on the Mid-Atlantic Ridge. Deep Sea Research Part II: Topical Studies in Oceanography 137:335–348.

Portail, M., C. Brandily, C. Cathalot, A. Colaço, Y. Gélinas, B. Husson, P.-M. Sarradin, and J. Sarrazin. 2018. Food-web complexity across hydrothermal vents on the Azores triple junction. Deep Sea Research Part I: Oceanographic Research Papers 131:101–120.

Portail, M., K. Olu, E. Escobar-Briones, J. Caprais, L. Menot, M. Waeles, P. Cruaud, Prradin, A. Godfroy, and J. Sarrazin. 2015. Comparative study of vent and seep macrofaunal communities in the Guaymas Basin. Biogeosciences 12:5455–5479.

Post, D. M. 2002. The long and short of food-chain length. Trends in Ecology & Evolution 17:269–277.

Pradillon, F., N. Bris, B. Shillito, C. M. Young, and F. Gaill. 2005. Influence of environmental conditions on early development of the hydrothermal vent polychaete Alvinella pompejana. Journal of Experimental Biology 208:1551–1561.

Pradillon, F., M. Zbinden, L. N. Bris, S. Hourdez, A.-S. Barnay, and F. Gaill. 2009. Development of assemblages associated with alvinellid colonies on the walls of high-temperature vents at the East Pacific Rise. Deep Sea Research Part II: Topical Studies in Oceanography 56:1622–1631.

Q

Qiu, J. 2010. Death and rebirth in the deep. Nature 465:284–286

R

Ramirez-Llodra, E., A. Brandt, R. Danovaro, D. B. Mol, E. Escobar, C. German, L. Levin, M. P. Arbizu, L. Menot, P. Buhl-Mortensen, B. Narayanaswamy, C. Smith, D. Tittensor, P. Tyler, A. Vanreusel, and M. Vecchione. 2010. Deep, diverse and definitely different: unique attributes of the world's largest ecosystem. Biogeosciences 7:2851–2899.

Reid, W. D., C. J. Sweeting, B. D. Wigham, K. Zwirglmaier, J. A. Hawkes, R. A. McGill, K. Linse, and N. V. Polunin. 2013. Spatial Differences in East Scotia Ridge Hydrothermal Vent Food Webs: Influences of Chemistry, Microbiology and Predation on Trophodynamics. PLoS ONE 8:e65553.

Resing, J. A., P. N. Sedwick, C. R. German, W. J. Jenkins, J. W. Moffett, B. M. Sohst, and A. Tagliabue. 2015. Basin-scale transport of hydrothermal dissolved metals across the South Pacific Ocean. Nature 523:200.

Riekenberg, P., R. Carney, and B. Fry. 2016. Trophic plasticity of the methanotrophic mussel Bathymodiolus childressi in the Gulf of Mexico. Marine Ecology Progress Series 547:91–106.

Ries, L., and T. D. Sisk. 2004. A predictive model of edge effects. Ecology 85:2917–2926.

Rigolet, C., E. Thiébaut, A. Brind'Amour, and S. F. Dubois. 2015. Investigating isotopic functional indices to reveal changes in the structure and functioning of benthic communities. Functional Ecology 29:1350–1360.

Romano, C., J. R. Voight, J. B. Company, M. Plyuscheva, and D. Martin. 2013. Submarine canyons as the preferred habitat for wood-boring species of Xylophaga (Mollusca, Bivalvia). Progress in Oceanography 118:175–187.

Rodrigues, C. F., S. R. Laming, S. M. Gaudron, G. Oliver, N. Bris, and S. Duperron. 2015. A sad tale: has the small mussel Idas argenteus lost its symbionts? Biological Journal of the Linnean Society 114:398–405.

S

Saeedi, H., A. F. Bernardino, M. Shimabukuro, G. Falchetto, and P. Sumida. 2019. Macrofaunal community structure and biodiversity patterns based on a wood-fall experiment in the deep South-west Atlantic. Deep Sea Research Part I: Oceanographic Research Papers 145:73–82.

Sancho, G. C. R. Fisher, S. Mills, F. Micheli, G. A. Johnson, H. S. Lenihan, C. H. Peterson, and L. S. Mullineaux. 2005. Selective predation by the zoarcid fish Thermarces cerberus at hydrothermal vents. Deep Sea Research Part I: Oceanographic Research Papers 52:837–844.

Sanders, H. L, Hessler RR (1969) Ecology of the Deep-Sea Benthos. Science 163:1419–1424.

Sarrazin, J., P. Legendre, F. de Busserolles, M.-C. Fabri, K. Guilini, V. N. Ivanenko, M. Morineaux, A. Vanreusel, and P.-M. Sarradin. 2015. Biodiversity patterns, environmental drivers and indicator species on a high-temperature hydrothermal edifice, Mid-Atlantic Ridge. Deep Sea Research Part II: Topical Studies in Oceanography 121:177–192.

Sarrazin J, C. Levesque, S.K. Juniper, MK Tivey. 2002. Mosaic community dynamics of Juan de Fuca Ridge sulfide edifices: Substratum, temperature and implications for trophic structure. Cahiers de Biologie Marine 43:275–279.

Sarrazin, J., V. Robigou, K. Juniper, J. Delaney. 1997. Biological and geological dynamics over four years on a high-temperature sulfide structure at the Juan de Fuca Ridge hydrothermal observatory. Marine Ecology Progress Series 153:5–24.

Schoener, T. W. 1976. Alternatives to Lotka-Volterra competition: models of intermediate complexity. Theoretical Population Biology 10:309-333.

Scott, K., and C. R. Fisher. 1995. Physiological ecology of sulfide metabolism in hydrothermal vent and cold seep vesicomyid clams and vestimentiferan tube worms. American Zoologist 35:102–111.

Sen, A., S. Kim, A. J. Miller, K. J. Hovey, S. Hourdez, G. W. Luther, and C. R. Fisher. 2016. Peripheral communities of the Eastern Lau Spreading Center and Valu Fa Ridge: community composition, temporal change and comparison to near-vent communities. Marine Ecology 37:599–617.

Shank, T. M., D. J. Fornari, K. L. Damm, M. D. Lilley, R. M. Haymon, and R. A. Lutz. 1998. Temporal and spatial patterns of biological community development at nascent deep-sea hydrothermal vents (9°50′N, East Pacific Rise). Deep Sea Research Part II: Topical Studies in Oceanography 45:465–515.

Shillito, B., N. Bris, S. Hourdez, J. Ravaux, D. Cottin, J.-C. Caprais, D. Jollivet, and F. Gaill. 2006. Temperature resistance studies on the deep-sea vent shrimp Mirocaris fortunata. Journal of Experimental Biology 209:945–955.

Shimabukuro, M., O. Carrerette, J. Alfaro-Lucas, A. Rizzo, K. M. Halanych, and P. Sumida. 2019. Diversity, Distribution and Phylogeny of Hesionidae (Annelida) Colonizing Whale Falls: New Species of Sirsoe and Connections Between Ocean Basins. Frontiers in Marine Science 6:478.

Sievert, S., and C. Vetriani. 2012. Chemoautotrophy at Deep-Sea Vents: Past, Present, and Future. Oceanography 25:218–233.

Silva, C. F., M. Shimabukuro, J. M. Alfaro-Lucas, Y. Fujiwara, P. Sumida, and A. Amaral. 2016. A new Capitella polychaete worm (Annelida: Capitellidae) living inside whale bones in the abyssal South Atlantic. Deep Sea Research Part I: Oceanographic Research Papers 108:23–31.

Smith, C. R., D. J. Amon, N. D. Higgs, A. G. Glover, and E. L. Young. 2017. Data are inadequate to test whale falls as chemosynthetic stepping-stones using network analysis: faunal overlaps do support a stepping-stone role. Proceedings of the Royal Society B 284:20171281.

Smith, C.R., Glover, A.G., Treude, T., Higgs, N.D., Amon, D.J. 2015. Whale-fall ecosystems: recent insights into ecology, paleoecology, and evolution. Annual Review in Marine Science 7:571–596.

Smith, C. R., F. C. Leo, A. F. Bernardino, A. K. Sweetman, and P. Arbizu. 2008. Abyssal food limitation, ecosystem structure and climate change. Trends in Ecology & Evolution 23:518–528.

Smith C., R. and Baco A., R. 2003. Ecology of whale falls at the deep-sea floor. Oceanography and Marine Biology 41: 311–354.

Smith, C.R., Kukert, H., Wheatcroft, R.A., Jumars, P.A., Deming, J.W. 1989. Vent fauna on whale remains. Nature 341:27–28.

Snelgrove, P. V. R., and C. R. Smith. (2002). A riot of species in an environmental calm: the paradox of the species-rich deep sea. Oceanography and Marine Biology: An Annual Review, Volume 40.

Spasojevic, M. J., and K. N. Suding. 2012. Inferring community assembly mechanisms from functional diversity patterns: the importance of multiple assembly processes. Journal of Ecology 100:652–661.

Srivastava, D. S., and J. H. Lawton. 1998. Why More Productive Sites Have More Species: An Experimental Test of Theory Using Tree-Hole Communities. The American Naturalist 152:510–529.

Storch, D., E. Bohdalková, and J. Okie. 2018. The more-individuals hypothesis revisited: the role of community abundance in species richness regulation and the productivity–diversity relationship. Ecology Letters 21:920–937.

Stuart, C. T., S. Brault, G. T. Rowe, C. Wei, M. Wagstaff, C. R. McClain, and M. A. Rex. 2016. Nestedness and species replacement along bathymetric gradients in the deep sea reflect productivity: a test with polychaete assemblages in the oligotrophic north-west Gulf of Mexico. Journal of Biogeography 44:548–555.

Sumida, P. Y., J. M. Alfaro-Lucas, M. Shimabukuro, H. Kitazato, J. A. Perez, A. Soares-Gomes, T. Toyofuku, A. O. Lima, K. Ara, and Y. Fujiwara. 2016. Deep-sea whale fall fauna from the Atlantic resembles that of the Pacific Ocean. Scientific Reports 6:22139.

Svensson, R. J., M. Lindegarth, P. R. Jonsson, and H. Pavia. 2012. Disturbance–diversity models: what do they really predict and how are they tested? Proceedings of the Royal Society B: Biological Sciences 279:2163–2170.

T

Teixidó, N., M. Gambi, V. Parravacini, K. Kroeker, F. Micheli, S. Villéger, and E. Ballesteros. 2018. Functional biodiversity loss along natural CO_2 gradients. Nature Communications 9:5149.

Thubaut, J., N. Puillandre, B. Faure, C. Cruaud, and S. Samadi. 2013. The contrasted evolutionary fates of deep-sea chemosynthetic mussels (Bivalvia, Bathymodiolinae). Ecology and Evolution 3:4748–4766.

Turner. R., D. 1973. Wood-boring bivalves, opportunistic species in the deep sea. Science 180: 1377–1379.

V

Van Dover, C. 2019. Inactive Sulfide Ecosystems in the Deep Sea: A Review. Frontiers in Marine Science 6:461.

Van Dover, C., C. J. Berg, and R. D. Turner. 1988. Recruitment of marine invertebrates to hard substrates at deep-sea hydrothermal vents on the East Pacific Rise and Galapagos spreading center. Deep Sea Research Part A. Oceanographic Research Papers 35:1833–1849.

Van Dover, C., and R. A. Lutz. 2004. Experimental ecology at deep-sea hydrothermal vents: a perspective. Journal of Experimental Marine Biology and Ecology 300:273–307.

Van Dover, V. C., C. German, K. Speer, L. Parson, and R. Vrijenhoek. 2002. Evolution and Biogeography of Deep-Sea Vent and Seep Invertebrates. Science 295:1253–1257.

Van Dover, C., and J. Trask. 2000. Diversity at deep-sea hydrothermal vent and intertidal mussel beds. Marine Ecology Progress Series 195:169–178.

Van Dover, C., D. Desbruyères, M. Segonzac, T. Comtet, L. Saldanha, A. Fiala-Medioni, and C. Langmuir. 1996. Biology of the Lucky Strike hydrothermal field. Deep Sea Research Part I: Oceanographic Research Papers 43:1509–1529.

Vellend, M. 2010. Conceptual synthesis in community ecology. The Quarterly review of biology 85:183–206.

Villéger, S., G. Grenouillet, and S. Brosse. 2013. Decomposing functional β-diversity reveals that low functional β-diversity is driven by low functional turnover in European fish assemblages. Global Ecology and Biogeography 22:671–681.

Villéger, S., P. M. Novack-Gottshall, and D. Mouillot. 2011. The multidimensionality of the niche reveals functional diversity changes in benthic marine biotas across geological time. Ecology Letters 14:561–568.

Villéger2008. New multidimensional functional diversity indices for a multifaceted framework in functional ecology. Ecology .

Violle, C., Z. Pu, and L. Jiang. 2010. Experimental demonstration of the importance of competition under disturbance. Proceedings of the National Academy of Sciences 107:12925–12929.

Vizzini, S., B. Martínez-Crego, C. Andolina, A. Massa-Gallucci, S. Connell, and M. Gambi. 2017. Ocean acidification as a driver of community simplification via the collapse of higher-order and rise of lower-order consumers. Scientific Reports 7:4018.

Vrijenhoek, R. C. 2010. Genetic diversity and connectivity of deep-sea hydrothermal vent metapopulations. Molecular Ecolology 19:4391–4411.

Voight, J. R. 2015. Xylotrophic bivalves: aspects of their biology and the impacts of humans. Journal of Molluscan Studies 81:175–186.

W

Wagstaff, M., K. Howell, B. Bett, D. Billett, S. Brault, C. Stuart, and M. Rex. 2014. β-diversity of deep-sea holothurians and asteroids along a bathymetric gradient (NE Atlantic). Marine Ecology Progress Series 508:177–185.

Watson-Russell, C. 1991. *Strepternos didymopyton* Watson Russell In: Bhaud, M., Cazaux, C., 1987 (Polychaeta: Chrysopetalidae) from experimental wooden panels in deep waters of the western North Atlantic. Ophelia, supplement 5 (Systematics, Biology and Morphology of World Polychaeta), pp. 283–294.

Webb, C. O., D. D. Ackerly, M. A. McPeek, and M. J. Donoghue. 2002. Phylogenies and community ecology. Annual Review of Ecology and Systematics 33:475–505.

Webb, T. J., J. P. Barry, and C. R. McClain. 2017. Abundance–occupancy relationships in deep sea wood fall communities. Ecography 40:1339–1347.

Wei, C.-L., and G. T. Rowe. 2009. Faunal zonation of large epibenthic invertebrates off North Carolina revisited. Deep Sea Research Part II: Topical Studies in Oceanography 56:1830–1833.

Wei, C.-L., G. T. Rowe, E. Escobar-Briones, A. Boetius, T. Soltwedel, J. M. Caley, Y. Soliman, F. Huettmann, F. Qu, Z. Yu, R. C. Pitcher, R. L. Haedrich, M. K. Wicksten, M. A. Rex, J. G. Baguley, J. Sharma, R. Danovaro, I. R. MacDonald, C. C. Nunnally, J. W. Deming, P. Montagna, M. Lévesque, J. Weslawski, M. Wlodarska-Kowalczuk, B. S. Ingole, B. J. Bett, D.

Billett, A. Yool, B. A. Bluhm, K. Iken, and B. E. Narayanaswamy. 2010. Global Patterns and Predictions of Seafloor Biomass Using Random Forests. PLoS ONE 5:e15323.

Weiher, E., D. Freund, T. Bunton, A. Stefanski, T. Lee, and S. Bentivenga. 2011. Advances, challenges and a developing synthesis of ecological community assembly theory. Philosophical transactions of the Royal Society of London. Series B, Biological sciences 366:2403–13.

Whittaker, R. J. 2010a. Meta-analyses and mega-mistakes: calling time on meta-analysis of the species richness-productivity relationship. Ecology 91:2522–33.

Whittaker, R. J. 2010b. In the dragon's den: a response to the meta-analysis forum contributions. Ecology 91:2568–2571.

Wiens, J. 1989. Spatial Scaling in Ecology. Functional Ecology 3:385.

Włodarska-Kowalczuk, M., M. Aune, L. N. Michel, A. Zaborska, and J. Legeżyńska. 2019. Is the trophic diversity of marine benthic consumers decoupled from taxonomic and functional trait diversity? Isotopic niches of Arctic communities. Limnology and Oceanography 64:2140–2151.

Wright, D. H. 1983. Species-energy theory: An extension of species-area theory. Oikos 41:496-506.

Woolley, S. N., D. P. Tittensor, P. K. Dunstan, G. Guillera-Arroita, J. J. Lahoz-Monfort, B. A. Wintle, B. Worm, and T. D. O'Hara. 2016. Deep-sea diversity patterns are shaped by energy availability. Nature 533:393.

Z

Zeppilli, D., A. Vanreusel, F. Pradillon, S. Fuchs, P. Mandon, T. James, and J. Sarrazin. 2015. Rapid colonisation by nematodes on organic and inorganic substrata deployed at the deep-sea Lucky Strike hydrothermal vent field (Mid-Atlantic Ridge). Marine Biodiversity 45:489–504.

The End

Titre : **Rôle de l'activité hydrothermale et de la nature du substrat sur les processus de colonisation de la faune en milieu marin profond**

Mots clés : sources hydrothermales ; assemblages des communautés ; diversité fonctionnelle

Resumé : Quatre décennies après leur découverte, nous savons maintenant que les sources hydrothermales sont répandues, diversifiées et dynamiques et qu'elles interagissent avec d'autres écosystèmes des grands fonds marins. Face aux potentiels impacts anthropiques qui pèsent sur les environnements hydrothermaux, il devient essentiel d'avoir une meilleure compréhension des processus qui façonnent la biodiversité de ces écosystèmes et de leurs interactions avec d'autres écosystèmes. Les processus structurant l'élaboration des communautés et contrôlant les interactions entre les habitats actifs, la périphérie et les communautés liées aux bois, ont été étudiés grâce à une vaste expérience de colonisation à 1700 m de profondeur sur le champ hydrothermal Lucky Strike (nord de la dorsale médio-Atlantique). Un cadre d'analyse moderne et multi-facettes, basé sur la richesse spécifique, les traits fonctionnels et les isotopes stables, a été appliqué. Les résultats ont montré que les sites actifs supportent une richesse fonctionnelle plus élevée que les habitats périphériques.

En outre, la diversité spécifique et fonctionnelle des habitats périphériques était très hétérogène, ce qui suggère qu'ils pourraient être particulièrement vulnérables aux impacts liés à l'exploitation minière. Les redondances fauniques et les liens énergétiques observés suggèrent que, plutôt que d'être des entités séparées, les habitats actifs et périphériques semblent être interconnectés. Les conditions environnementales et la présence de différentes ressources ont été identifiées comme étant les principaux facteurs influençant la biodiversité et la structure des communautés. Le rôle des bois en tant que potentielles « pierres de gué » pour la dispersion de la méio- et la macrofaune, non seulement pour les habitants des sources hydrothermales mais aussi pour ceux de la périphérie, est validé. Les résultats de cette thèse améliorent significativement notre compréhension des processus qui structurent les communautés associées aux sources hydrothermales et aux autres écosystèmes chimiosynthétiques dans les grands fonds marins et pourraient avoir des implications importantes dans l'élaboration de stratégies de protection dans le cadre d'éventuelles activités industrielles.

Title: **Influence of hydrothermal activity and substrata nature on faunal colonization processes in the deep sea**

Keywords: Hydrothermal vents; community assembly; functional diversity

Abstract: Four decades after their discovery, we know now that deep-sea hydrothermal vents are widespread, diverse and dynamic, and interact with other chemosynthetic-based and background ecosystems. In the face of potential imminent anthropogenic impacts, more than ever the understanding of the processes that shape vent biodiversity, in its multiple facets, and the interactions with other systems is of paramount importance. The early processes driving community assembly and interactions between hydrothermally active habitats, vent periphery and cognate communities, namely wood falls, were investigated with an extensive colonizing experiment at 1700 m depth on the Lucky Strike vent field (northern Mid-Atlantic Ridge). A modern multifaceted framework of community assembly based on species richness, functional traits and stable isotopes was applied.

Results showed that vent ecosystems support higher functional richness that background peripheral habitats. The latter were highly heterogeneous and unique in species and functions suggesting that they may be especially vulnerable to impacts, such as deep-sea mining. The observed faunal overlap and energy links suggest that rather than being separate entities, active and peripheral habitats may be considered as interconnected. Environmental conditions and the presence of different resources at vent, periphery and wood habitats, were identified as main drivers of biodiversity patterns and community structure. The role of woods in the deep-sea as potential stepping stones for meio- and macrofauna, not only for "vent" but for periphery inhabitants, is validated. The results of this thesis significantly improve our understanding of vent and chemosynthetic communities and may have implications for their protection from industrial activities.